UNIVERSITEIT VAN PRETORIA
UNIVERSITY OF PRETORIA
YUNIBESITHI YA PRETORIA

SUBCELLULAR EFFECTS OF PAVETAMINE ON RAT CARDIOMYOCYTES

By

CHARLOTTE ELIZABETH ELLIS

Submitted in partial fulfilment of the requirements for the degree of Doctor of Philosophy in the Department of Paraclinical Sciences, Faculty of Veterinary Science, University of Pretoria

Date submitted: April 2010

UNIVERSITEIT VAN PRETORIA
UNIVERSITY OF PRETORIA
YUNIBESITHI YA PRETORIA

SUBCELLULAR EFFECTS OF PAVETAMINE ON RAT CARDIOMYOCYTES

By

CHARLOTTE ELIZABETH ELLIS

Submitted in partial fulfilment of the requirements for the degree of Doctor of Philosophy in the Department of Paraclinical Sciences, Faculty of Veterinary Science, University of Pretoria

Date submitted: April 2010

SUMMARY

SUBCELLULAR EFFECTS OF PAVETAMINE ON RAT CARDIOMYOCYTES

By

CHARLOTTE ELIZABETH ELLIS

Promoter: Professor C.J. Botha
Department: Department of Paraclinical Sciences, Faculty of Veterinary Science, University of Pretoria

Co-promoter: Professor R.A. Meintjes
Department: Department of Anatomy and Physiology, Faculty of Veterinary Science, University of Pretoria
Degree: PhD

The aim of this study was to investigate the mode of action of pavetamine on rat cardiomyocytes. Pavetamine is the causative agent of gousiekte ("quick-disease"), a disease of ruminants characterized by acute heart failure following ingestion of certain rubiaceous plants. Two *in vitro* rat cardiomyocyte models were utilized in this study, namely the rat embryonic cardiac cell line, H9c2, and primary neonatal rat cardiomyocytes.

Cytotoxicity of pavetamine was evaluated in H9c2 cells using the MTT and LDH release assays. The eventual cell death of H9c2 cells was due to necrosis, with LDH release into the culture medium after exposure to pavetamine for 72 h. Pavetamine did not induce apoptosis, as the typical features of apoptosis were not observed. Electron microscopy was employed to study ultrastructural alterations caused by pavetamine in H9c2 cells. The mitochondria and sarcoplasmic reticula showed abnormalities after 48 h exposure of the cells to pavetamine. Abundant secondary lysosomes with electron dense material were present in treated cells.

Numerous vacuoles were also present in treated cells, indicative of autophagy. During this exposure time, the nuclei appeared normal, with no chromatin condensation as would be expected for apoptosis. Abnormalities in the morphology of the nuclei were only evident after 72 h exposure. The nuclei became fragmented and plasma membrane blebbing occurred. The mitochondrial membrane potential was investigated with a fluorescent probe, which demonstrated that pavetamine caused significant hyperpolarization of the mitochondrial membrane, in contrast to the depolarization caused by apoptotic inducers. Pavetamine did not cause opening of the mitochondrial permeability transition pore, because cyclosporine A, which is an inhibitor of the mitochondrial permeability transition pore, did not reduce the cytotoxicity of pavetamine significantly.

Fluorescent probes were used to investigate subcellular changes induced by pavetamine in H9c2 cells. The mitochondria and sarcoplasmic reticula showed abnormal features compared to the control cells, which is consistent with the electron microscopy studies. The lysosomes of treated cells were more abundant and enlarged. The activity of cytosolic hexosaminidase was nearly three times higher in the treated cells than in the control cells, which suggested increased lysosomal membrane permeability. The activity of acid phosphatase was also increased in comparison to the control cells. In addition, the organization of the cytoskeletal F-actin of treated cells was severely affected by pavetamine.

Rat neonatal cardiomyocytes were labelled with antibodies to detect the three major contractile proteins (titin, actin and myosin) and cytoskeletal proteins (F-actin, desmin and β-tubulin). Cells treated with pavetamine had degraded myosin and titin, with altered morphology of sarcomeric actin. Vacuoles appeared in the β-tubulin network, but the appearance of desmin was normal. F-actin was severely disrupted in cardiomyocytes treated with pavetamine and was degraded or even absent in treated cells. Ultrastructurally, the sarcomeres of rat neonatal cardiomyocytes exposed to pavetamine were disorganized and disengaged from the Z-lines, which can also be observed in the hearts of ruminants that have died of gousiekte

It is concluded that the pathological alteration to the major contractile and cytoskeleton proteins caused by pavetamine could explain the cardiac dysfunction that characterizes gousiekte. F-actin is involved in protein synthesis and therefore can play a role in the inhibition of protein synthesis in the myocardium of ruminants suffering from gousiekte. Apart from inhibition of protein synthesis in the heart, there is also increased degradation of cardiac proteins in an animal with gousiekte. The mitochondrial damage will lead to an energy deficiency and possibly to generation of reactive oxygen species. The sarcoplasmic reticula are involved in protein synthesis and any damage to them will affect protein synthesis, folding and post-translational modifications. This will activate the unfolded protein response (UPR) and sarcoplasmic reticula-associated protein degradation (ERAD). If the oxidizing environment of the sarcoplasmic reticula is disturbed, it will activate the ubiquitin-proteasome pathway (UPP) to clear aggregated and misfolded proteins. Lastly, the mitochondria, sarcoplasmic reticula and F-actin are involved in calcium homeostasis. Any damage to these organelles will have a profound influence on calcium flux in the heart and will further contribute to the contractile dysfunction that characterizes gousiekte.

Keywords

Actin, cardiotoxicity, cytoskeleton, F-actin, gousiekte, H9c2 cell line, lysosome, mitochondria, myosin, necrosis, pavetamine, polyamine, protein synthesis, rat neonatal cardiomyocytes, sarcoplasmic reticula, titin.

ACKNOWLEDGEMENTS

I wish to thank the following people and institutions that helped me to peep into the fascinating world of God's cell:

- Ms Anitra Schultz and Dr Dharmarai Naicker, project team members of the Division of Toxicology (ARC-OVI).
- Prof Christo Botha (Department of Paraclinical Sciences, Faculty of Veterinary Science, University of Pretoria) as promoter and Prof Roy Meintjes (Department of Anatomy and Physiology, Faculty of Veterinary Science, University of Pretoria) as co-promoter of this study.
- Mr Alan Hall (Laboratory for Microscopy and Microanalysis, University of Pretoria) for the laser scanning confocal microscopy analyses.
- The South African National Biodiversity Institute (SANBI) for the distribution maps of gousiekte plants in South Africa.
- Ms Erna van Wilpe and Ms Lizette du Plessis for the electron microscopy analyses (Electron Microscopy Unit, Faculty of Veterinary Science, University of Pretoria).
- The computer centre at ARC-OVI.
- Funding provided by the Gauteng Province (Department of Agriculture, Conservation and Environment) and the North-West Province (Department of Agriculture, Conservation, Environment and Tourism).
- Family, friends and colleagues.
- Ms Nettie Engelbrecht for proof-reading this thesis.
- Lastly, a special friend, adv. David le Roux.

DECLARATION

I hereby declare that this study was my own work**,** except that pavetamine was purified by Ms Karen Basson.

Candidate: C Ellis

TABLE OF CONTENTS

ultrastructural changes in H9c2(2-1) cells treated with pavetamine, a novel polyamine. *Toxicon*, 22: 12-19.

APPENDIX II. ELLIS, C.E., NAICKER, D., BASSON, K.M., BOTHA, C.J., MEINTJES, R.A. AND SCHULTZ, R.A. 2010. A fluorescent investigation of subcellular damage in H9c2 cell caused by pavetamine, a novel polyamine. *Toxicology in Vitro*, 24: 1258-1265.

APPENDIX III. ELLIS, C.E., NAICKER, D., BASSON, K.M., BOTHA, C.J., MEINTJES, R.A. AND SCHULTZ, R.A. 2010. Damage to some contractile and cytoskeleton proteins of the sarcomere in rat neonatal cardiomyocytes after exposure to pavetamine. *Toxicon*, 55: 1071-1079.

LIST OF FIGURES

LIST OF TABLES

LIST OF ABBREVIATIONS

ACTN	Actinin
AIF	Apoptosis-inducing factor
AJ	Adhering junction
AMP	Adenosine monophosphate
ANT	Adenine nucleotide transporter
ARs	Adrenergic receptors
ATF	Activating transcription factors
ATG	Autophagy-related protein
ATP	Adenosine triphosphate
ATPase	ATP hydrolysing enzyme
β-MHC	β-Myosin heavy chain
BECN1	Beclin-1
BCl-1/2	B-cell leukemia/lymphoma ½
BSA	Bovine serum albumin
Ca^{2+}	Calcium

cAMP	3',5'-Cyclic adenosine monophosphate
CapZ	Protein that caps the barbed end of actin to the Z-band
CARP	Cardiac ankyrin-repeat protein
Cas	Crk-associated substrate
Caspase	Cytosolic aspartate residue-specific cysteine protease
CaR	Calcium-sensing receptor
CH	Cardiac hypertrophy
CHAPS	3[(3-Cholamidopropyl)dimethylammonio]-propanesulphonic acid
CHO	Chinese hamster ovary
CICR	Ca^{2+}-induced Ca^{2+} release
CLSM	Confocal laser scanning microscopy
CMA	Chaperone-mediated autophagy
CrP	Creatine phosphate
CsA	Cyclosporin A
CytoD	Cytochalasin D
DAG	Diacylglycerol
DAPI	4',6-Diamidino-2-phenylindole
DMEM	Dulbecco's modified Eagle's medium
DMSO	Dimethyl sulfoxide
DTT	Dithiothreitol
EC_{50}	Half maximum effective concentration
ER	Endoplasmic reticulum
ERAD	ER-associated degradation
F-actin	Filamentous actin
FAK	Focal adhesion kinase
FCS	Foetal calf serum
FHL	Four and a half LIM domain
FITC	Fluorescein isothiocyanate
G-actin	Globular actin
GDP	Guanosine diphosphate
GJ	Gap junctions
GPCRs	G protein-coupled receptors

GTP	Guanosine triphosphate
HBSS	Hank's balanced salt solution
H9c2	A clonal cell line derived from embryonic rat ventricle
H_2O_2	Hydrogen peroxide
HEPES	4-(2-hydroxyethyl)-1-piperazineethanesulphonic acid
HSP	Heat shock protein
$I_{Ca\text{-}L}$	L-type calcium channel
ID	Intercalated disk
IF	Intermediate filament
IκB	NF-κB inhibitor
IP_3	Inositol 1,4,5-triphosphate
I/R	Ischaemia/reperfusion
IRE	Inositol-requiring enzyme-1
JC-1	5,5′,6,6′-Tetrachloro-1,1′,3,3′-tetraethyl-imidacarbocyanine iodide
JNK	c-Jun NH_2-terminal protein kinase
K^+	Potassium
kDa	Kilo dalton
LC3	Light chain 3
LDH	Lactate dehydrogenase
LSCM	Laser scanning confocal microscopy
LVEDP	Left ventricular end diastolic pressure
MADS	Consists of genes with a conserved region of approximately 182 bp that codes for a DNA binding domain-the MADS-box
MAPK	Mitogen-activated protein kinase
MAPKKKs	MAP kinase kinases
MARP	Muscle ankyrin-repeat protein
mDa	Mega dalton
$\Delta\Psi_m$	Mitochondrial membrane potential
MHC	Myosin heavy chain
MLC1	Myosin light chain 1
MLP	Muscle LIM protein
3MA	3-Methyladenine

MPTP	Mitochondrial permeability transition pore
mTOR	Mammalian target of rapamycin
MTT	3-(4,5-Dimethyl-2-thiazolyl)-2,5-diphenyl-2H-tetrazolium bromide
MURF	Muscle-specific ring finger protein
MyBP-C	Myosin-binding protein C
NAD^+	Nicotinamide adenine dinucleotide
NEC-1	Necrostatin 1
NCX	Na^+/Ca^{2+} exchanger
NF-κB	Nuclear factor kappa beta
NO	Nitric oxide
OXPHOS	Oxidative phosphorylation
PAK1	p21-Activated kinase
PARP	Poly(ADP-ribose) polymerase
PBS	Phosphate-buffered saline
PERK	Protein kinase R-like ER kinase
PEVK	Proline (P), glutamate (E), valine (V) and lysine (K) region
Pi	Inorganic phosphate
PIK3	Phosphatidylinositol 3-kinase
PKA	Protein kinase A
PKB/Akt	Serine/threonine protein kinase
PKC	Protein kinase C
PLC	Phospholipase C
PP2A	Protein phosphatase 2A
PQC	Protein quality control
PSV	Polyamine-sequestering vesicles
RIP1	Receptor-interacting protein 1
RNCM	Rat neonatal cardiomyocytes
ROCK	Rho-dependent kinase
ROS	Reactive oxygen species
RYR	Ryanodine receptor
S100A1	S100 calcium binding protein A1
SER	Serine

SERCA	Sarcoplasmic reticulum Ca^{2+}-ATPase
siRNA	Silencing RNA
SR	Sarcoplasmic reticulum
SRF	Serum response factor
T-cap	Telethonin
TEM	Transmission electron microscopy
THR	Threonine
TMRM	Tetramethylrhodamine methyl ester perchlorate
TN	Troponin
TNF	Tumor necrosis factor
TNT	Troponin T
TPM	Tropomyosin
UPR	Unfolded protein response
UPS	Ubiquitin-proteasome system

CHAPTER 1
PATHOGENESIS OF GOUSIEKTE

1.1 Introduction

Livestock losses due to poisoning by the 600-odd toxic plant species in South Africa alone is estimated to number more than 37,000 head of cattle and 250,000 small stock each year (Kellerman *et al*. 1996). Therefore, the prevention of intoxication by plants remains relevant for commercial and rural farmers (Kellerman *et al*. 2005).

Gousiekte ("quick disease") is rated one of the six most important plant poisonings of livestock in southern Africa and causes the death of about 7,000 head of livestock annually (Kellerman *et al*. 1996, Kellerman *et al*. 2005). It is a disease of ruminants characterized by acute heart failure, without any premonitory signs, four to eight weeks after the initial ingestion of certain rubiaceous plants (Kellerman *et al*., 2005). Six plant species have been implicated thus far, namely *Pachystigma pygmaeum* (Fig. 1.1), *Pachystigma thamnus*, *Pachystigma latifolium*, *Pavetta schumanniana* (Fig. 1.2), *Pavetta harborii* (Fig. 1.3) and *Fadogia homblei* (Fig. 1.4). In South Africa, gousiekte occurs in Gauteng, North-West, Limpopo, Mpumalanga and KwaZulu-Natal (Fig. 1.5-1.8). However, gousiekte-inducing plants are also distributed in Botswana, Zimbabwe, Namibia and Mozambique.

Figure 1.1 *Pachystigma pygmaeum*.

Figure 1.2 *Pavetta schumanniana*.

Figure 1.3 *Pavetta harborii*.

Figure 1.4 *Fadogia homblei*.

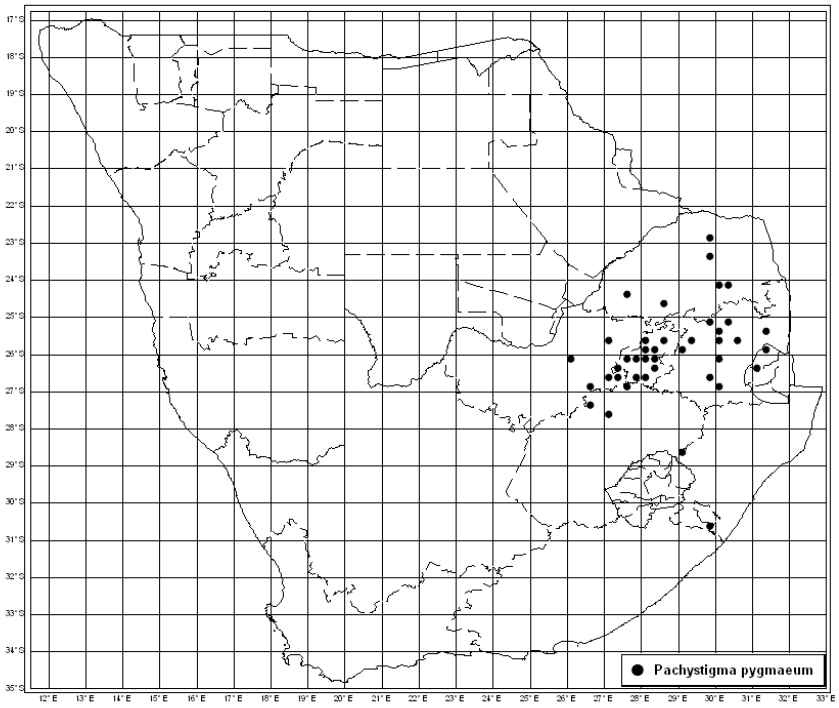

Figure 1.5 Distribution of *Pachystigma pygmaeum*.

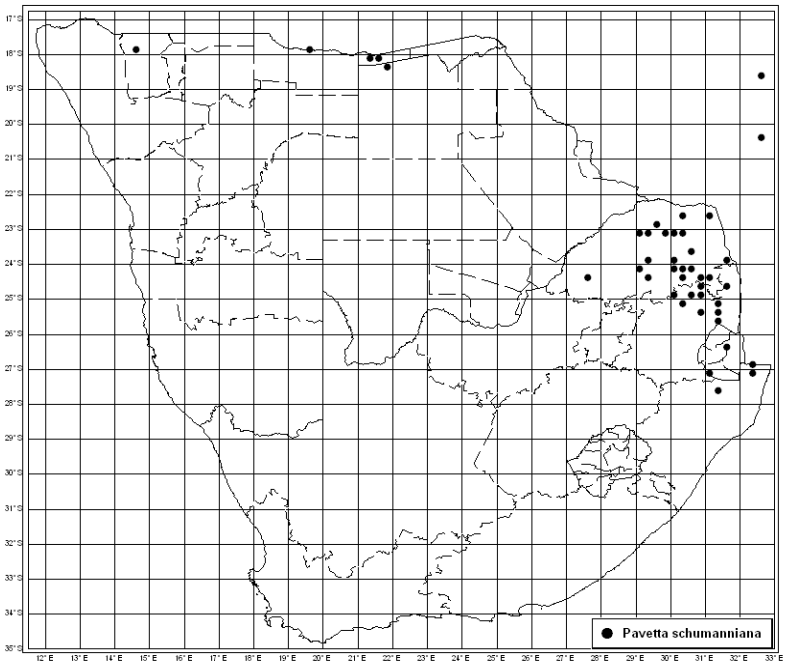

Figure 1.6 Distribution of *Pavetta schumanniana*.

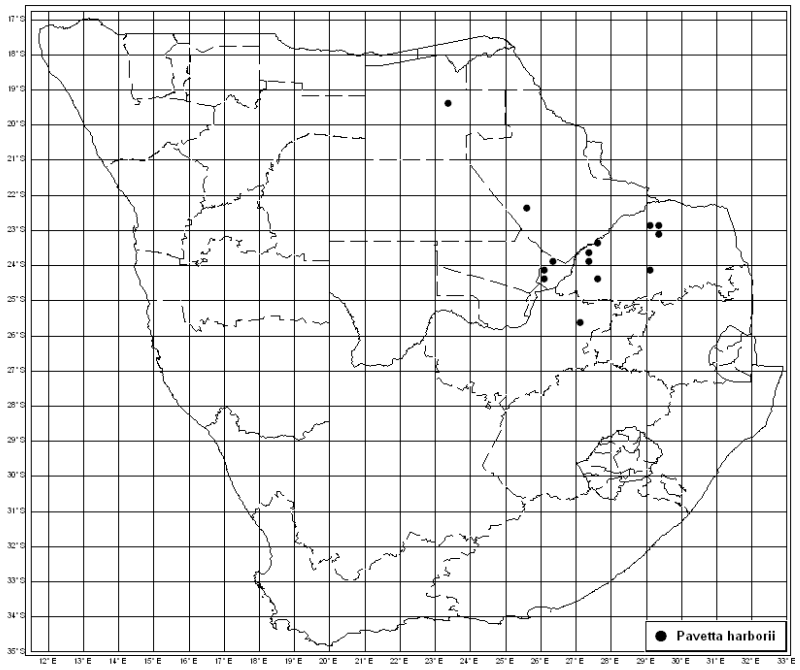

Figure 1.7 Distribution of *Pavetta harborii*.

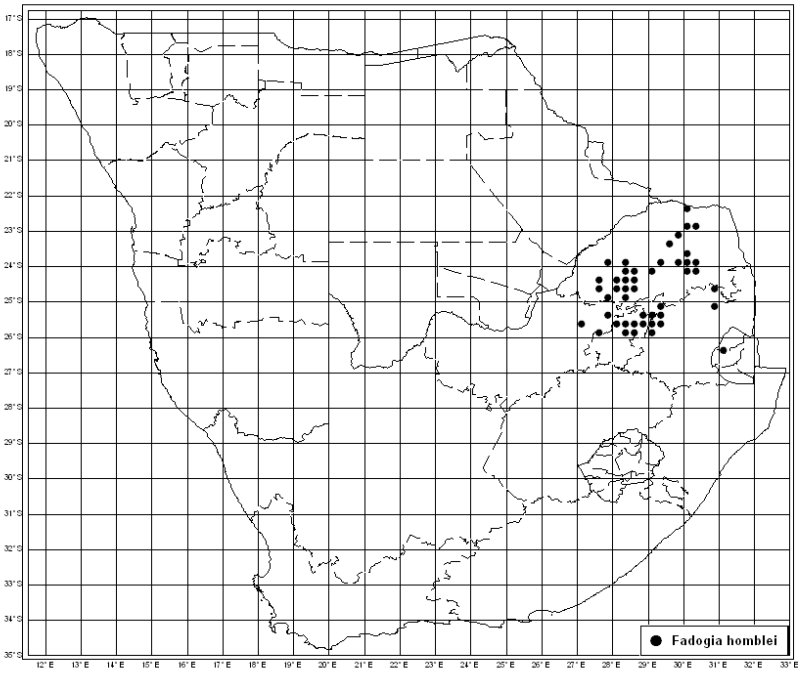

Figure 1.8 Distribution of *Fadogia homblei*.

The toxin that causes gousiekte was first isolated from *Pavetta harborii* and given the trivial name pavetamine (Fourie *et al*., 1995). The structure of pavetamine was elucidated (Fig 1.9). It belongs to the polyamine group and is similar to spermidine, spermine and putrescine (Bode *et al*., 2010). The structure of spermidine ($C_7H_{19}N_3$) is the closest to that of pavetamine, however, pavetamine has a ten carbon backbone and, in addition, four hydroxyl groups.

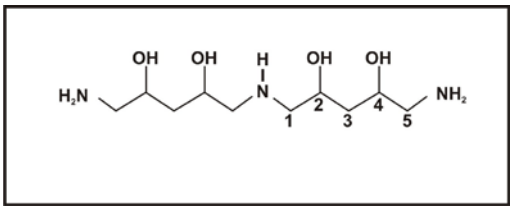

Figure 1.9 Structure of pavetamine

Studies evaluating the clinical pathology parameters and cardiodynamics of gousiekte in ruminants revealed that notable changes appeared terminally, i.e. in the last two weeks of intoxication (Pretorius *et al*., 1973a, van der Walt *et al.*, 1977, van der Walt *et al*., 1981, Fourie *et al*., 1989). Cardiac failure occurs with the following aberrations: systolic murmurs, gallop rhythms, QRS amplitude alterations, bundle branch blocks, dulling of the first heart sound and decreased myocardial contractility (Pretorius *et al.*, 1973a).

Electron micrographs of the myocardium of sheep intoxicated with *Pachystigma pygmaeum*, showed a lack of register in individual and adjacent myofibres (Prozesky, 2008). The myofibres became disintegrated and had a frayed appearance accompanied by replacement fibrosis. There was a significant increase in intercalated disc length due to the development of complex folds (Schutte *et al*., 1984, Kellerman *et al.*, 2005, Prozesky *et al*., 2005). Furthermore, transmission electron microscopy (TEM) of sections of the hearts of sheep dosed with gousiekte-inducing plants, showed abnormalities of the mitochondria and sarcoplasmic reticula. The mitochondria varied in size, number and shape and demonstrated

the formation of concentric cristae as well as rupture of swollen cristae. The sarcoplasmic reticula were also dilated and proliferated. Pretorius and colleagues (1973b) reported a reduced uptake of Ca^{2+} by sarcoplasmic reticula fragments isolated from the hearts of ruminants with gousiekte. The cardiac muscle of sheep with gousiekte had reduced levels of ATP and creatine phosphate (CrP), and reduced oxygen uptake by isolated mitochondria (Snyman *et al*., 1982).

Figure 1.10 Transmission electron micrograph of a gousiekte sheep heart, demonstrating damaged Z-lines and the presence of numerous vacuoles. V, vacuoles that have the appearance of white empty vesicles; Z, disturbed Z-line. (Prozesky *et al*., 2005; Prozesky, 2008).

Rats were affected when extracts prepared from a gousiekte-inducing plant, *Pavetta harborii,* were administered subcutaneously (Hay *et al.*, 2001) or when pavetamine was administered intraperitoneally (Schultz *et al.*, 2001). Several cardiodynamic parameters were determined in rats exposed to *Pavetta harborii* extracts and compared to control rats (Hay *et al.*, 2001).

The contractility (reflected in stroke volume) was reduced by more than 50 % and the cardiac output (product of heart rate and stroke volume) by 40 %. The left ventricle end diastolic pressure (LVEDP) was about seven times higher than the control group, which is indicative of inefficient pumping of blood by the ventricles (Hay *et al*., 2001). Another study was conducted to evaluate whether purified pavetamine had the same cardiodynamic effects

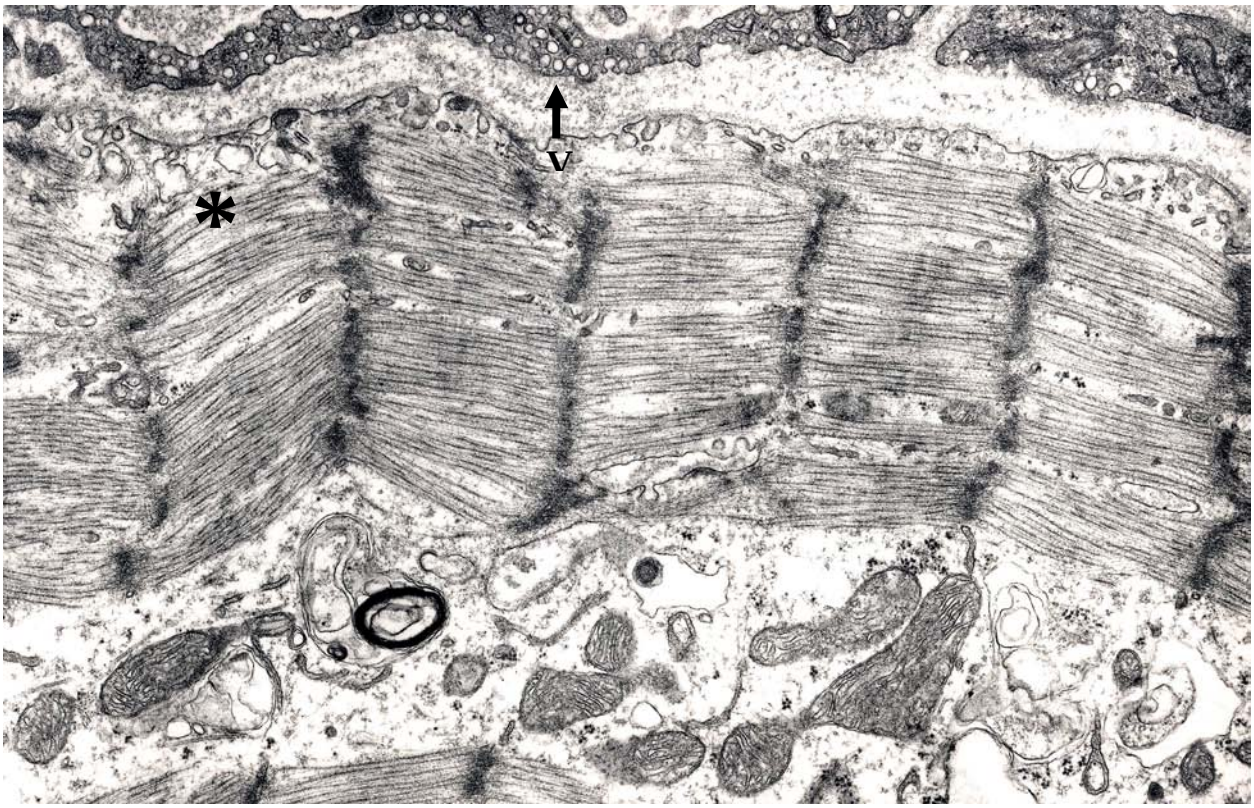

Figure 1.11 Transmission electron micrographs of gousiekte sheep hearts, demonstrating disordered myofibres. V, vacuoles that have the appearance of white empty vesicles; *, disorganized myofibres (Prozesky *et al*., 2005; Prozesky, 2008).

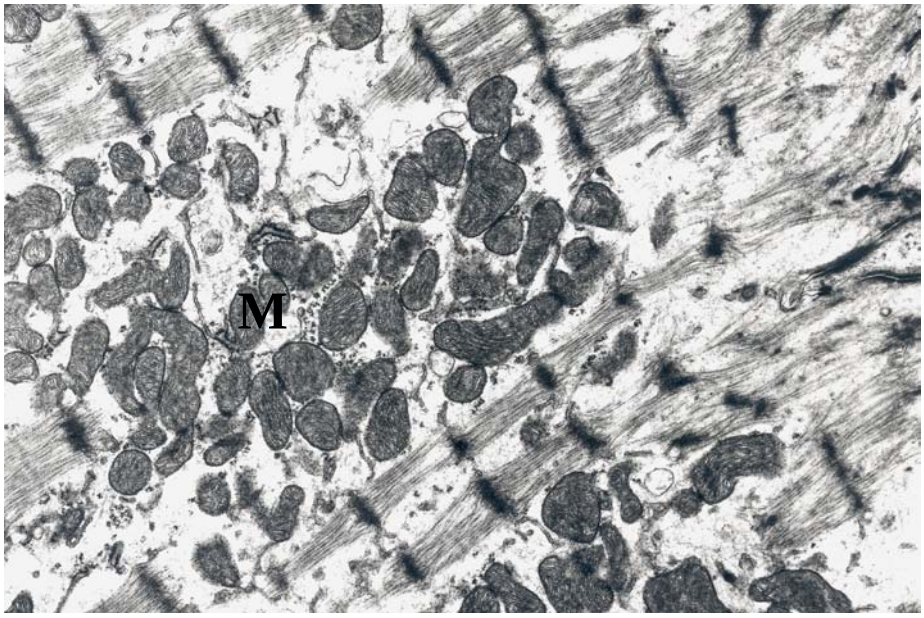

Figure 1.12 Transmission electron micrographs of affected mitochondria (M) in gousiekte sheep hearts. The mitochondria are proliferated and intermingled with the myofibres (Prozesky *et al*., 2005; Prozesky, 2008).

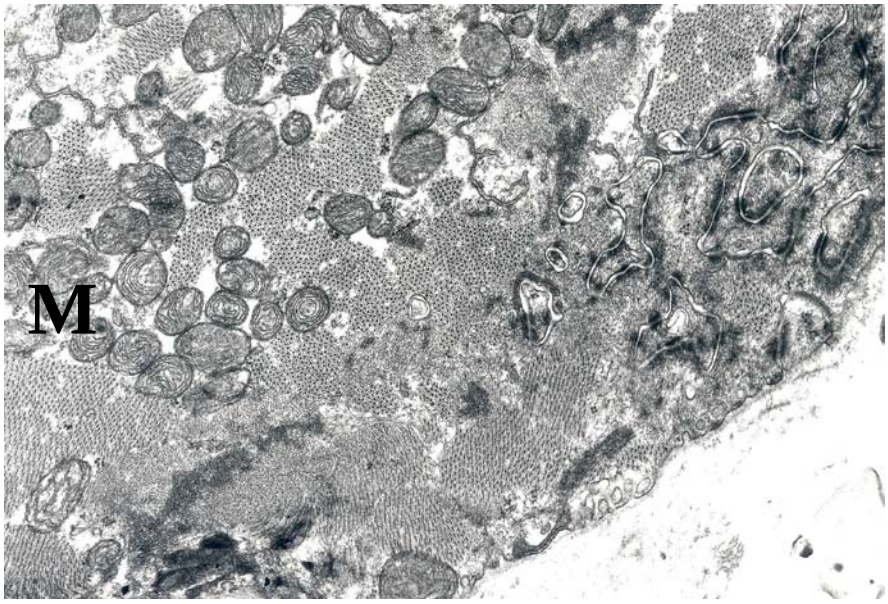

Figure 1.13 Transmission electron micrographs of gousiekte sheep hearts with swollen mitochondrial cristae. M, swollen mitochondrial cristae (Prozesky *et al*., 2005; Prozesky, 2008).

in rats (Hay *et al*., 2008). Pavetamine administered to rats reduced systolic function significantly, but not the diastolic function and heart rate (Hay *et al*., 2008). These authors concluded that the rats were not in an advanced stage of congestive heart failure (high LVEDP and compensatory tachycardia), possibly due to a sub-optimal dose of pavetamine and/or a trial period that was too short.

Schultz and co-workers (2001) investigated the effect of pavetamine on protein synthesis in selected rat tissue. Four hours post exposure of rats to pavetamine, protein synthesis in the heart, liver and kidney was less than 66 %, compared to control rats, but skeletal muscle was not affected. Protein synthesis in the liver and kidney returned to base line levels 24 to 48 h post exposure, while protein synthesis in the heart remained suppressed at 48 h after exposure to the toxin. The authors speculated that depending on the half-life of the cardiac protein, a point will be reached where breakdown of tissues exceeds synthesis, resulting in functional disturbances and abnormal intracellular proteins and organelles.

CHAPTER 2
LITERATURE REVIEW

During the foetal and early perinatal phase, cardiac cells divide by mitosis (Rumyantsev, 1977). However, mature cardiomyocytes are terminally differentiated cells and are not able to proliferate, due to their exit from the cell cycle (Tam *et al*., 1995). In the failing heart, pressure and volume overload leads to cardiac hypertrophy, through activation of a multigene programme in cardiomyocytes. This is accompanied by biogenesis of mitochondria and synthesis of proteins resulting in enlargement of the cardiomyocytes (Morgan *et al*., 1987; Lorell & Carabello, 2000; Hannan, *et al*., 2003). In addition, the efficient functioning of cardiac muscle is dependent upon the proper alignment of myofibrils, microtubules, and intermediate filaments (Gregorio *et al*., 2005).

2.1 Components of the cardiomyocytes

2.1.1 Myofibrillar contractile proteins

A muscle fibre contains myofibrils and is divided into contractile units *viz*. sarcomeres. Each sarcomere contains amongst other proteins, thick and thin filaments, and titin (Fig. 2.1).

2.1.1.1 Titin

Titin, previously called connectin, is a giant macromolecule of 3.0-3.7 mDa, and it spans the length of half a sarcomere to form a third filament system in vertebrate striated muscle. Titin molecules run from the Z-line through the I-band and A-band to the M-band, thereby linking the different sarcomeric regions to one another (Fürst *et al*., 1988). A shorter, stiffer N2B isoform (3.0 mDa) and a longer more compliant N2BA isoform (3.2-3.7 mDa) have been identified (Granzier & Labeit, 2004; Krüger & Linke, 2009). The protein is encoded by one gene with 363 exons, and these different isoforms are the product of alternative gene splicing (Lahmers *et al*., 2004). Decreased myocardial stiffness is often seen in heart failure patients with dilated cardiomyopathy and involves isoform switching of titin (Nagueh *et al*., 2004). The total titin concentration between heart failure patients and controls was the same, but the

N2BA:N2B expression ratio was significantly increased in the heart failure group, which showed significantly lower diastolic stiffness (Nagueh *et al*., 2004).

Titin in the I-band exhibits elastic behaviour upon sarcomeric stretch, contributing to the passive tension of cardiac muscle (Fig. 2.1). The extensible I-band region of titin has multiple segments: the tandemly arranged Ig (immunoglobulin-like) segments, N2B, N2A and the PEVK region, so called because it is rich in proline (P), glutamate (E), valine (V) and lysine (K) (Labeit & Kolmerer, 1995). The PEVK region of titin binds to actin, a reaction which is Ca^{2+}-dependent, involving the S100 Ca^{2+} binding protein A1 (S100A1) (Yamasaki *et al*., 2001). The COOH-terminus of titin is cross-linked to the myosin heavy chain (MHC) and with the myosin-binding protein of the M-band, myomesin (Agarkova & Perriard, 1995). The NH_2-terminus of titin is integrated through telethonin (T-cap) and α-actinin, its Z-line ligands (Gregorio *et al*., 1998). α-Actinin interacts with a number of proteins, two of which are titin and nebulette (Pyle & Solaro, 2004). The C-terminus of titin attaches to the M-line of the sarcomere. The Ig-domain, 14, just inside the I-band titin region, interacts with calpain 1 (Coulis *et al*., 2008). Communication between titin and Z-line proteins provide a mechanism for the cardiac myocyte to sense strain. Multiple phosphorylation sites reside on titin and thus play a role in signalling cascades. The C-terminus domain of titin has protein kinase activity (Yamasaki *et al*., 2002). The titin kinase domain is activated by phosphorylation of tyrosine residues, with subsequent binding of Ca^{2+}/calmodulin (Mayans *et al*., 1998).

The cardiac-specific N2B in the I-band binds two isoforms of the four-and-a half-LIM-domain proteins, FHL1 and FHL2 (Lange *et al*., 2002; Sheikh *et al*., 2008). These proteins act as transcriptional co-activators in the nucleus (Scholl *et al*., 2000) and interact with mitogen-activated protein kinases (MAPKs), especially the extra-cellular-signal-regulated kinase-2 (ERK2) (Sheikh, 2008). The N2A domain in the I-band binds to muscle ankyrin-repeat proteins (MARPs), cardiac ankyrin-repeat protein (CARP), diabetes-related ankyrin-repeat protein and ankyrin-repeat domain protein-2 (Miller *et al*., 2003). These MARPS shuttle between their I-band location and the nucleus, where they act as transcriptional regulators (Kojic *et al*., 2004). Titin also binds to the small ankyrin-1, a protein of the sarcoplasmic reticulum (SR) membrane to position the SR near the Z-line region (Kontrogianni-Konstantopoulos & Bloch, 2003).

2.1.1.2 Myosin

Myosin, the thick filament of the contractile apparatus, is composed of two myosin heavy chains (MHC) and two pairs of light chains, the essential light chain and the regulatory light chain. In the heart, two varieties of the light chains are expressed: the atrial and the ventricular light chains. The portion of MHC closest to the N-terminus is called the head or motor domain and hydrolyses ATP (Palmer, 2005). Myosin head portions cross-bridge with the actin filament in the sarcomere to promote movement during contraction.

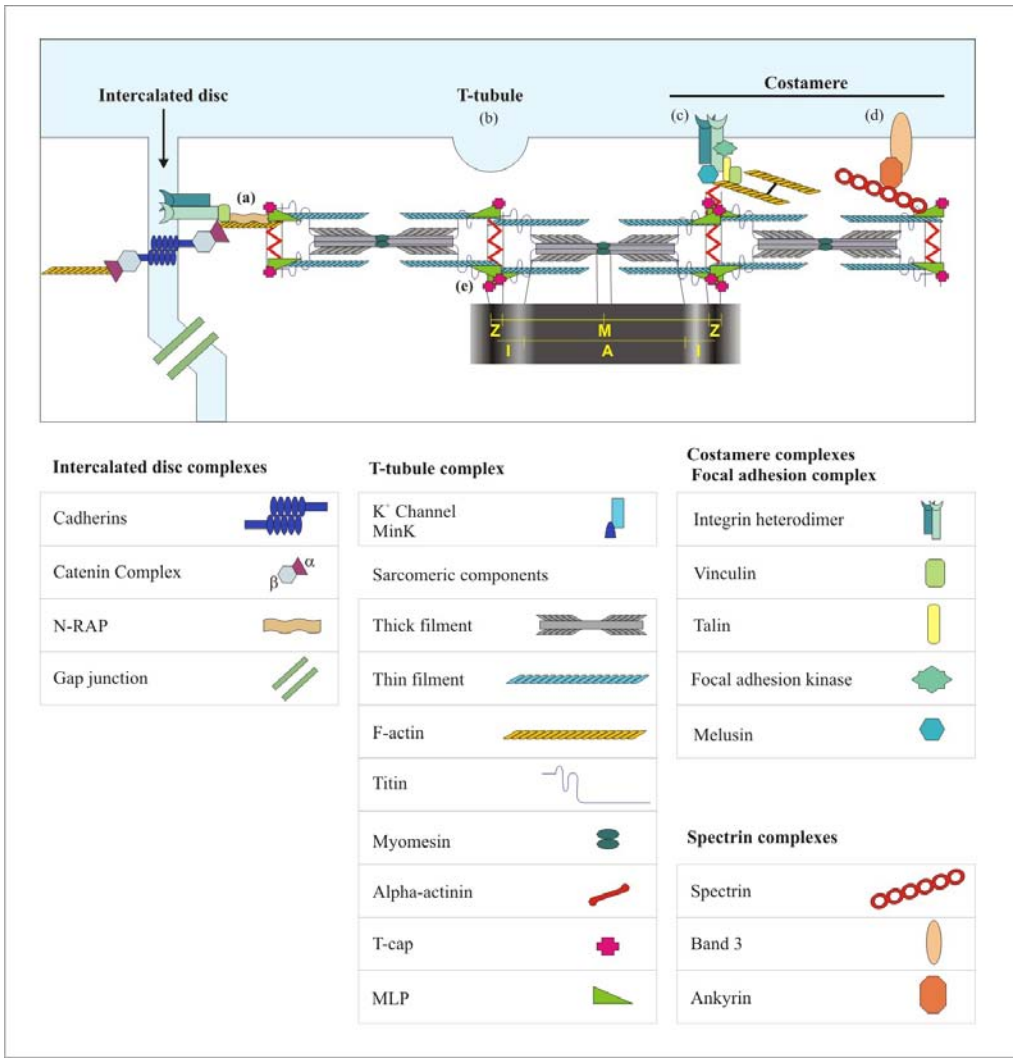

Figure 2.1 Composition of the contractile machinery in the heart (Miller *et al*., 2004). The thick filament is myosin and the thin filament is actin.

Two isoforms exist for myosin heavy chains namely the α-MHC and β-MHC (Xie *et al*., 2003). The thick filament is connected from the M-line to the Z-line by titin and the myosin-binding protein C (MYBP-C) connects myosin with actin (Granzier, *et al*., 2004).

2.1.1.3 Thin filament (actin) and thin filament regulatory proteins (troponin, tropomyosin)

Actin is one of the most conserved eukaryotic proteins and actin isoforms show greater than 90 % overall sequence homology, except in their 18 N-terminal residues (Lessard, 1988). The main actin in the heart is α-actin. The thin filament proteins tropomyosin (TPM) and the globular Ca^{2+}-binding troponins (TNC) regulate the interaction between actin and the myosin head (Ebashi & Ebashi, 1964) (Fig. 2.2). Troponin consists of three subunits: TNT, TNI and TNC. TNC functions as a Ca^{2+} receptor, TNI (the inhibitory subunit) inhibits actomyosin ATPase and binds actin (Xing *et al*., 2008), and TNT links the entire troponin complex to tropomyosin (TPM) (Greaser & Gergely, 1971). Phosphorylation plays an important part in the regulation of thin filaments. Multiple phosphorylation sites exist on TNI and TNT that affects maximum Ca^{2+} activation, kinetics of the cross-bridge cycle and sensitivity to Ca^{2+}, pH and sarcomere length (Solaro 2001; Wolska *et al*., 2001; Konhilas *et al*., 2003). The level of phosphorylation of TNI and TNT is determined by the following kinases: protein kinase A (PKA), protein kinase C (PKC), protein kinase D (PKD), protein kinase G (PKG), p21-activated kinase (PAK1) and Rho-dependent kinase (ROCK) (Vahebi *et al*., 2005). PAK1 isoform activates protein phosphatase 2A (PP2A) and is a major phosphatase in the heart (Ke *et al*., 2004). Thin filaments also interact with proteins in the Z-line network, which connects to the cytoskeleton and nucleus (Vahebi *et al*., 2005). The barbed ends of the thin filaments are linked to the Z-line through α-actinin and CapZ (Hart & Cooper, 1999).

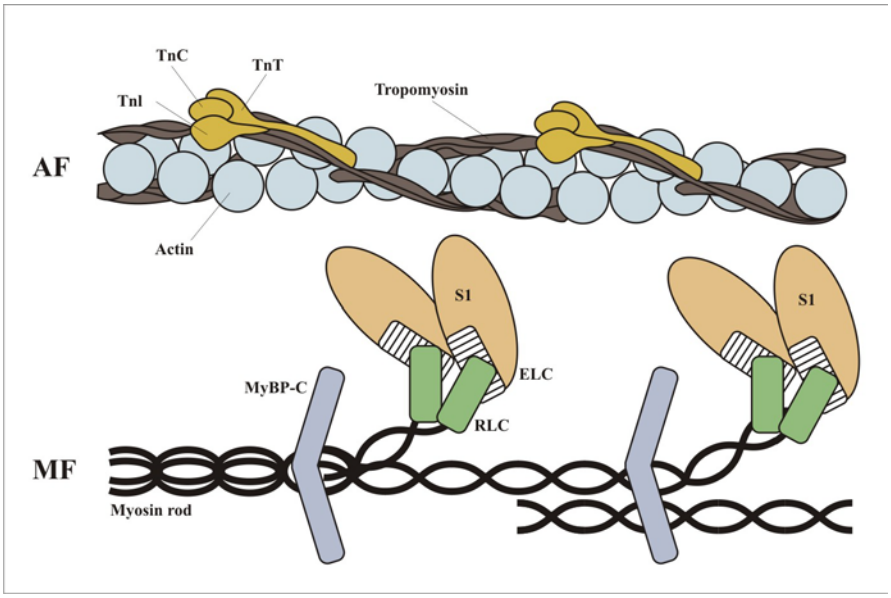

Figure 2.2 The troponin complex. AF: thin actin filament, MF: thick myosin filament, TNI: inhibitory troponin, TNC: Ca^{2+}-binding troponin, TNT: tropomyosin-binding troponin, S1: myosin subfragment-1 (myosin head portion), ELC: essential myosin light chain, RLC: regulatory myosin light chain and MyBP-C: hypothetical localization of the myosin binding protein-C. The M-line is to the left and the Z-line is to the right (Schaub *et al*., 1998).

2.1.2 Z-disc complex

Z-lines cross-link the myofilaments and have a unique position at the interface of the sarcomere, the cytoskeleton, the SR and the sarcolemma (Pyle & Solaro, 2004). The Z-line proteins anchor actin, titin and nebulin filaments. Z-lines are responsible for force transmission, signal transduction and nuclear translocation (Knöll, *et al*., 2002). The following proteins are located at the Z-line: α-actinin (ACTN), muscle LIM protein (MLP), four and a half LIM domain proteins (FHL), enigma factor, actinin-associated LIM protein, FATZ family, myopalladin, telethonin (titin cap or T-cap) and muscle-specific ring finger protein (MURF) (Knöll, *et al*., 2002) (Fig. 2.3). The FATZ family is an acronym for filamin, alpha-actinin and telethonin-binding protein of the Z-disc. The barbed end of actin filaments is capped by CapZ, to anchor sarcomeric actin to the Z-line (Hart & Cooper, 1999).

α-Actinin cross-links sarcomeric actin and plays a role in reversing the polarity of the actins on either side of the Z-line. α-Actinin is a member of the dystrophin superfamily and is capable of cross-linking actin and titin filaments from neighbouring sarcomeres (Djinovic-Carugo *et al*., 1999). ACTN2 is the isoform present in cardiac cells. α-Actinin is critical in stabilizing the cytoskeleton when contraction begins (Fyrberg *et al*., 1998).

Nebulette, the cardiac homologue of skeletal muscle protein nebulin, also resides in the Z-line and is associated with the thin filaments (Moncman & Wang, 1999). Nebulette is composed of four domains: an acidic N-terminal domain, a large central repeat domain (nebulin modules), a terminal linker and a SH3 domain (Moncman & Wang, 2002). The SH3 domain is a Src homology-3 (SH3) domain, a family of small globular domains of 60 amino acids and serves as a mediator of protein-protein interactions in signalling pathways (Mayer, 2001) The linker and SH3 domain interact with a number of Z-line associated proteins, namely CapZ, Z-line titin, α-actinin and myopalladin (Bonzo *et al*., 2008). The nebulin modules of the repeat domain interact with tropomyosin, actin, filamin C and desmin (Bonzo *et al*., 2008). Myopalladin acts as a scaffold to regulate the actin cytoskeleton (Otey *et al*., 2005).

Muscle LIM protein (MLP) belongs to a superfamily of proteins that have one or several LIM domains, which are characterized by a cysteine-rich consensus domain. The four and a half LIM domain proteins (FHL) behave as transcriptional co-activators and enhance the transcriptional activity of the androgen receptor (Müller *et al*., 2000). The enigma family of proteins contain an amino-terminal PDZ domain and one to three carboxy-terminal LIM domains (Guy *et al*., 1999). Actinin-associated LIM protein is concentrated at the intercalated disc, which forms the junction between neighbouring cardiomyocytes (McKoy *et al*., 2000). It co-localizes with vinculin, desmin, α-actinin and γ-catenin. Actinin-associated LIM proteins are in part responsible for sarcomeric organization and enhances the ability of α-actinin to cross-link F-actin filaments (Pashmforoush, *et al*., 2001). Myopalladin is enriched at sites of

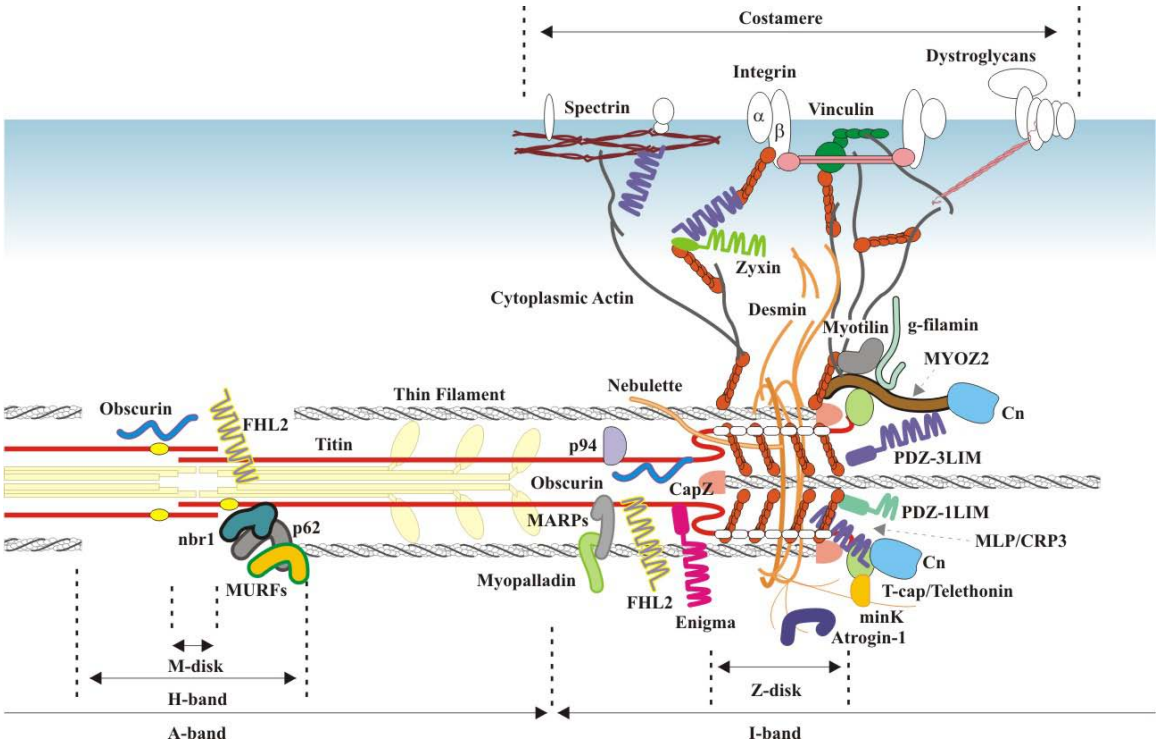

Figure 2.3 Cardiac Z-disc complex**.** MYOZ2: myozenin 2 (carsarin 1), Cn,: calcineurin, PDZ-3LIM: one-PDZ and three-LIM domain protein, PDZ-1LIM: one-PDZ and one-LIM domain protein, MLP/CRP3: muscle-specific LIM protein/cysteine-rich protein 3, FHL2: four-and-a-half LIM protein 2, MAPRs: muscle ankyrin repeat proteins and MURFs, muscle-specific ring finger proteins (Hoshijima, 2006).

actin filament anchorage (Bang *et al*., 2001). In cardiac cells myopalladin interacts with nebulette via its proline-rich domain and with cardiac ankyrin repeat protein (CARP) via its amino-terminal domain. This interaction suggests a link between myofibrillar organization and gene expression, as CARP is a nuclear protein involved in gene expression (Zou *et al*., 1997). CARP down-regulates expression of cardiac genes for TNC, MLC2 and atrial natriuretic peptide (Jeyaseelan *et al*., 1997).

Telethonin (T-cap or titin cap) anchors titin within Z-lines and is phosphorylated during myofibrillogenesis by titin kinase (Mayans, *et al*., 1998). Telethonin interacts with the potassium channel beta-subunit (minK), suggesting a link in the potassium flux and the Z-line

(Furukawa *et al*., 2001). Muscle-specific ring finger protein 3 (MURF-3) is a cytoskeletal protein that is located at the Z-line and at the M-line (Gregorio *et al*., 2005)

Telethonin, muscle LIM protein, calsarcin-1 and calcineurin can respond in the Z-disc to passive titin-generated tension and belong to the stretch-sensor (Le Winter *et al*., 2007). T-cap is an important link via calcineurin, a phosphatase, between mechanical stretch signals and local Ca^{2+} concentrations. Calsarcin-1 has an inhibitory role on calcineurin (Frey *et al*., 2000). Calcineurin dephosphorylates nuclear factor of activated T-cell, which then enters into the nucleus and promotes transcription (Frey *et al*., 2000). Recently identified proteins residing at the Z-lines include myotilin, S100A1 Ca^{2+}-binding protein and myomaxin (Cox *et al*., 2008). Myotilin, a thin filament-associated protein, binds to F-actin and is responsible for the efficient cross-linking of actin filaments, and prevention of induced disassembly of filaments (Moza *et al*., 2007). Disturbances in the Z-line complex may have catastrophic consequences. These proteins are indirectly involved in the progression of heart failure due to their association with intracellular signalling molecules, protein kinase C (PKC) and calcineurin (Molkentin *et al*., 1998).

2.1.3 M-band proteins

The M-band is situated in the centre of the A-band, where the thick filaments are interconnected in the middle of the sarcomere (Hornemann *et al*., 2003). Its function is to provide physical stability between thick filaments during contraction. The components of the M-band are myosin, a 185 kDa myomesin, a 165 kDa M-protein and the C-terminal region of titin (Obermann *et al*., 1996). Myomesin is the principal cross-linking protein of the thick filament, a role similar to α-actinin in the Z-line. Myomesin is expressed at a fixed ratio to myosin (Agarkova *et al*., 2004). The myomesin-related M-protein is only present in fast skeletal muscle fibres and cardiomyocytes (Hornemann *et al*., 2003). Muscle-type creatine kinase is bound to the M-band and is an intramyofibrillar ATP-regenerating system for the actin-activated myosin ATPase located nearby on both sides of the M-band (Wallimann *et al*., 1992; Hornemann *et al*., 2003). Spectrin, ankyrin and obscurin might be involved in the lateral connection of M-bands to the sarcolemma (Bagnato *et al*., 2003). The affinity of

myomesin to titin is regulated by phosphorylation and interaction with myofibrillogenesis regulator-1 (Obermann *et al*., 1997; Li *et al*., 2004). Obscurin senses the stress between the myofibrils and the sarcolemma, which activates Ca^{2+}-mediated and Rho GTPase-regulated signalling in the sarcomere (Young *et al*., 2001).

2.1.4 Costameres

Between the extracellular matrix, the sarcolemma and the Z-disc, the costameres form a centre of communication (Ervasti, 2003) (Fig. 2.4a). Costameres transmit contractile force from the myofibrils across the sarcolemma to the extracellular matrix and maintain the alignment of the myofibrils, a prerequisite for contraction (Quach & Rando, 2006). Costameres are rich in the focal adhesion proteins vinculin, integrins, talin, paxillin and Crk-associated substrate (Cas) (Quach & Rando, 2006) (Fig. 2.4b). Vinculin transmits stretch signals from the sarcolemma to actin/α-actinin in the sarcomere (Heling *et al*., 2000). Talin and vinculin link the cytoplasmic domains of integrins to the Z-disc (Heling *et al*., 2000). Integrins connect components of the extracellular matrix with the actin cytoskeleton (Cox *et al*., 2008). Integrins interact with adaptor proteins like filamin, α-actinin, tensin and talin (Bershadsky *et al*., 2003). Integrins also interact with signalling proteins such as focal adhesion kinase (FAK), src-family tyrosine kinases, melusin, integrin-linked kinase and small GTPases (Ervasti, 2003). Focal adhesion kinase plays an essential role in integrin-mediated signal transduction (Cox *et al*., 2008). Melusin, another signalling protein, is located at the costameres near the Z-disc, where it binds to the intracytoplasmic tail of β1-integrin (Brancaccio *et al*., 1999). Integrin-linked kinase directly interacts with β1-integrin (Hannigan *et al*., 1996). Paxillin binds to many proteins involved in the organization of the actin cytoskeleton (Turner, 2000). FAK, Cas and paxillin are localized in the sarcomeric Z-line (Kovacic-Milivojević *et al*., 2001). Laminin-2, collagens and fibronectin, all of which are extracellular matrix proteins, bind to specific integrins and align the costameres (Quach & Rando, 2006).

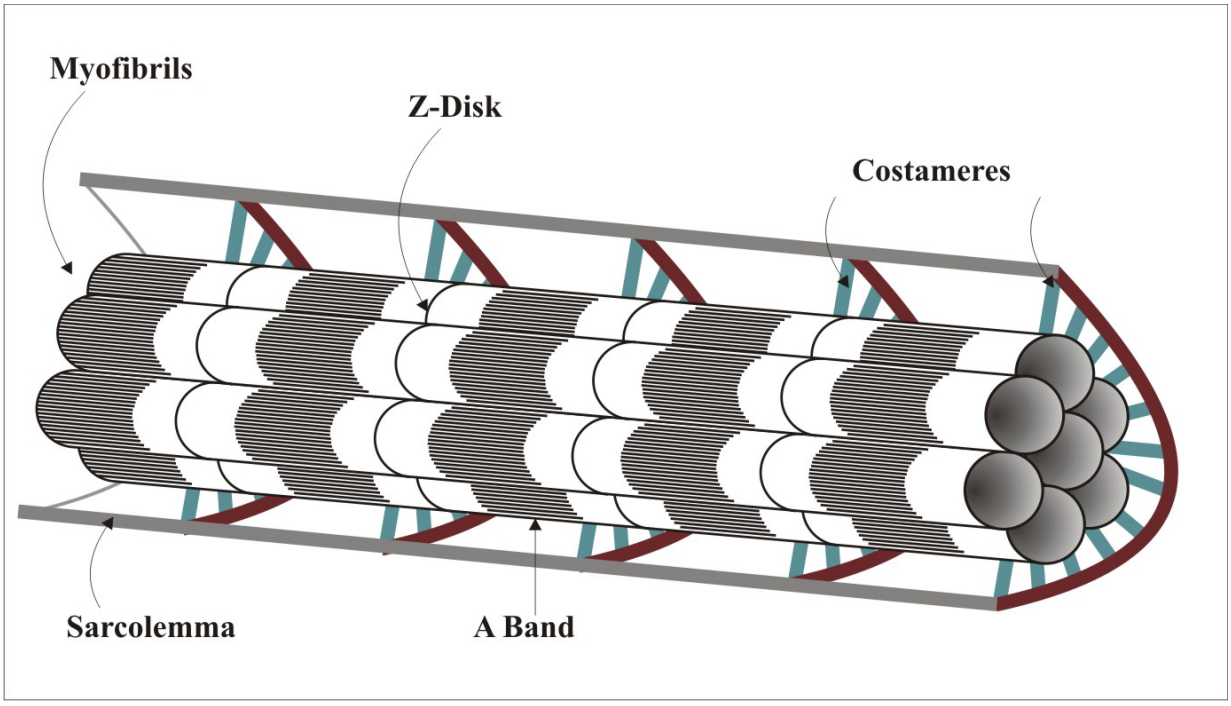

Figure 2.4a Structure of costamere and Z-disc (Ervasti, 2003).

2.1.5 Intercalated discs

The intercalated discs (IDs) between individual cardiomyocytes ensure mechanical coupling and propagation of electrical impulses throughout the heart (Fig. 2.5) (Noorman *et al*., 2009). The IDs consist of three protein complexes: the adherens junctions (AJs) (Fig. 2.5a), desmosomal junctions (Fig. 2.5b) and gap junctions (GJs) (Fig. 2.5c). The adherens junctions (AJs) are unique to cardiac cells in that they connect the cardiomyocytes with each other at the intercalated discs (ID), as well as the conductive Purkinje fibre cells (Franke *et al*., 2006). The AJs mechanically link the cardiomyocytes with the actin cytoskeleton (Niessen, 2007). AJs are also the anchor-point for cardiomyocyte attachment, ensuring transmission of contractile force from cell to cell. Cadherins are transmembrane proteins that form complexes with cytosolic α-, β-, γ-plakoglobin and p120 catenin, thereby establishing the connection to the actin cytoskeleton (Niessen, 2007; Noorman *et al*., 2009).

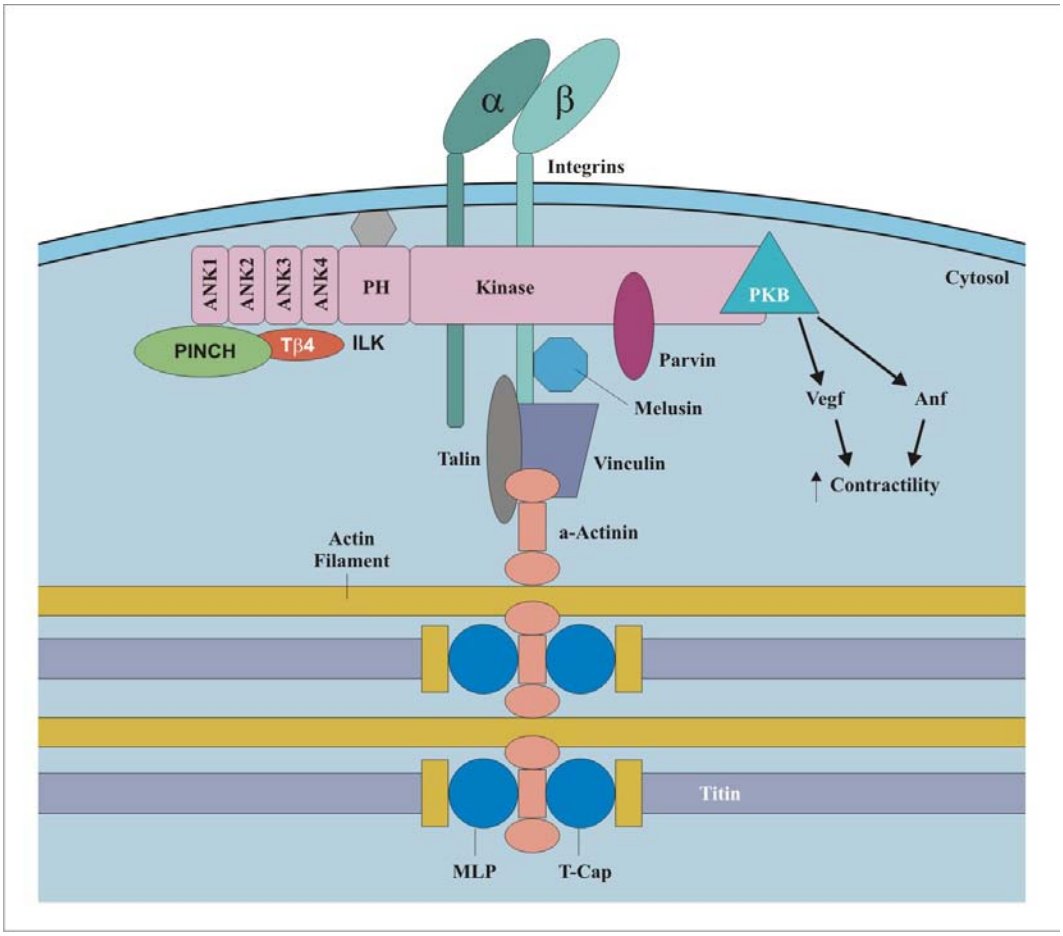

Figure 2.4b Components of the costameres (Srivastava & Yu., 2006). ANF, atrial natriuretic factor; ANK1, ankyrin; ILK, integrin-linked kinase; MLP, muscle LIM domain protein; PH, plekstrin homology domain of ILK; PINCH, particularly interesting Cys-His-rich protein; PKB, protein kinase B; PKC, protein kinase C; T-CAP, thelethonin of titin cap; Tβ4, thymosin β4; VEGF, vascular endothelial growth factor

The desmosomes or desmosomal junctions provide support between myocytes via their interaction with the intermediate filament (IF) cytoskeleton (Noorman, *et. al*., 2009). Desmoplakin, plakoglobin (γ-catenin) and plakophilin 2 (in the intracellular environment) mediate the linkage between the IF and the desmosomal catherins, desmocollin and desmoglein, in the intercellular part of the cell (Garrod & Chidgey, 2008). The desmosomes give mechanical strength to tissues because they form adhesive bonds in a network.

The gap junctions (GJs) mediate direct communication between adjacent cells (Noorman *et al*., 2009). Passive diffusion of various compounds, metabolites, water and ions up to a mass of 1000 Da occur through these intercellular ion channels, that links the cytoplasm of neighbouring cells (Elfgang *et al*., 1995). GJ channels consist of twelve connexin subunits, six of which are contributed by each cell. These six connexion subunits form a hemi-channel in the sarcolemma (Noorman *et al*., 2009). Connexin43 is the most important isoform in the ventricular myocardium (Beyer *et al*., 1987). A common feature during cardiac remodelling and heart failure is changes in GJ expression and distribution, with levels of connexin43 reduced and migration from the ID to the lateral sides of the cell (Noorman *et al*., 2009). Molecules at the intercalated disc also serve as mechanical stress sensors (Hoshijima, 2006). One molecule to perform this function is nebulin-related anchoring protein, which binds muscle LIM protein (MLP) (Ehler *et al*., 2001), actin, vinculin and talin (Luo *et al*., 1999).

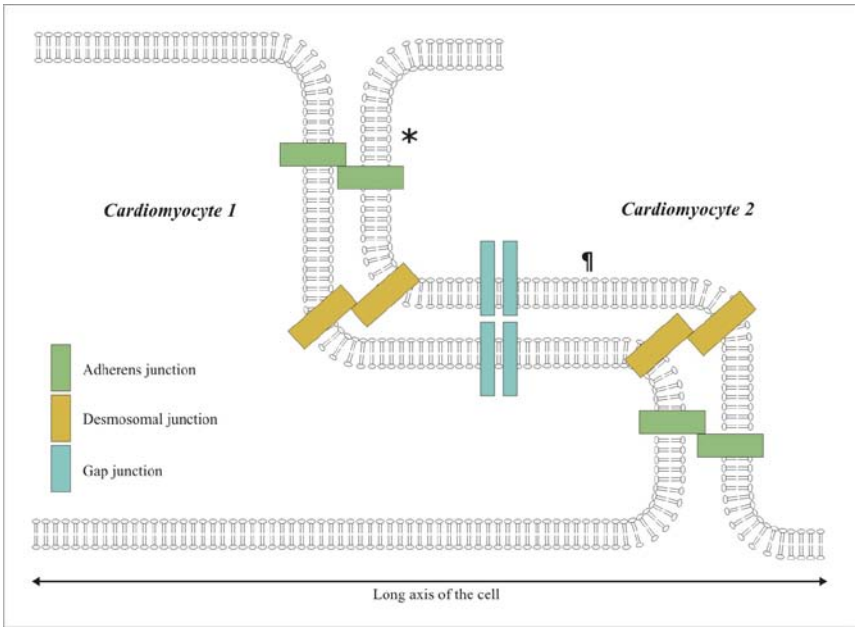

Figure 2.5a The intercalated discs consist of the adherens junctions, desmosomes and the gap junctions (Noorman *et al*., 2009).

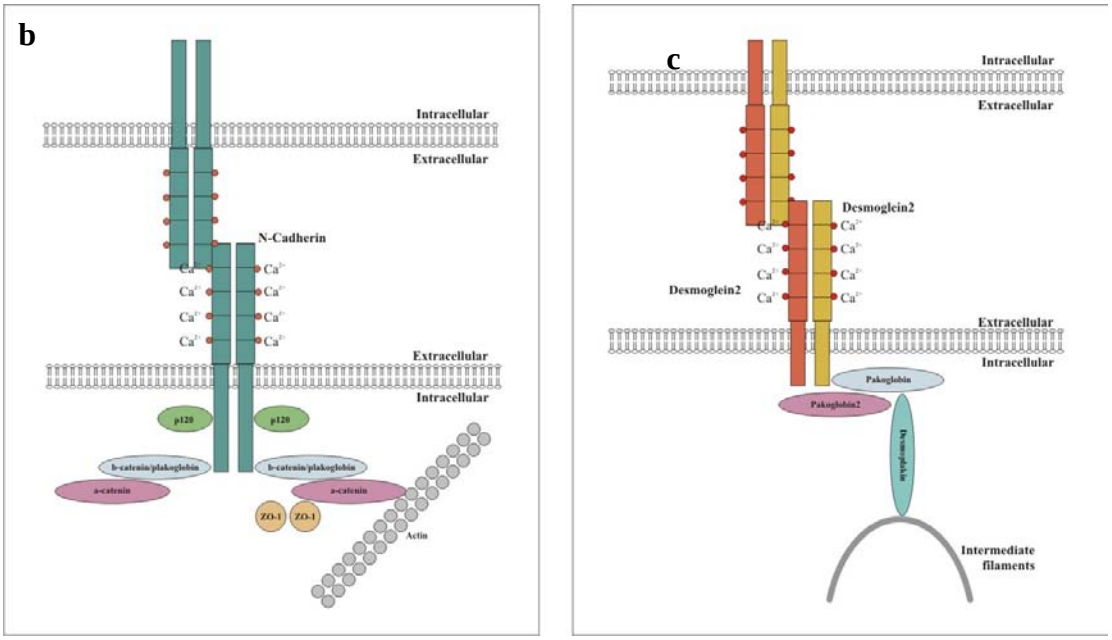

Figure 2.5b Adherens junctions connect adjoining cells to each other through N-cadherin (Noorman *et al.*, 2009). The adherens junction protein α-catenin binds to the actin cytoskeleton. ZO-1, scaffolding protein zonula occludens-1. **Figure 2.5c** Desmosomes connect neighbouring cells to each other. The extracellular part consists of two desmosomal cadherins: desmoglein-2 and desmocollin-2. The cadherins are linked to the intermediate filaments.

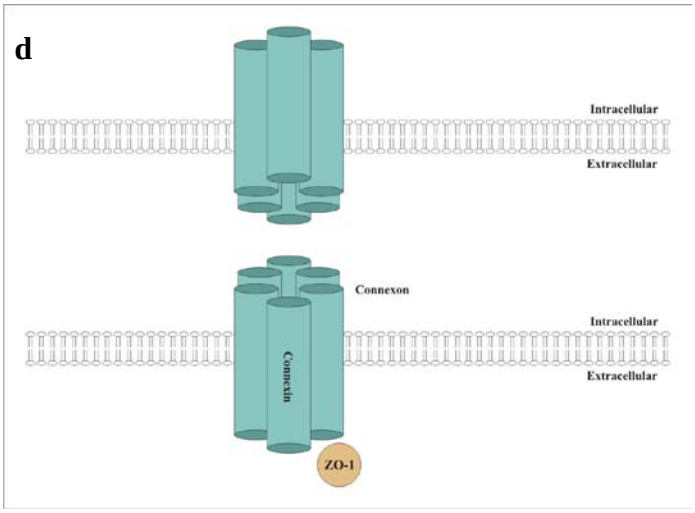

Figure 2.5d Gap junctions consist of two connexons, one of each delivered by each cell (Noorman *et al.*, 2009).

2.1.6 Cardiac extramyofibrillar cytoskeleton proteins: F-actin, microtubules and intermediate filaments

The cytoskeleton gives mechanical support to the cell and mediates cell motility, organelle movement, cytokinesis, muscle contraction and plays a role in protein synthesis, intracellular trafficking and organelle transport within the cell (Rogers & Gelfand, 2000). The cytoskeleton proteins include the microfilaments (actins), microtubules (tubulins) and the intermediate filaments (desmin).

2.1.6.1 F-actin

Filamentous actin (F-actin) is formed by the assembly of monomeric actin, also called globular-actin (G-actin) (Fig. 2.6). G-actin is polar, thus F-actin is also polar with a barbed end (plus end) and a pointed end (minus end) (Kustermans *et al*., 2008). F-actin is organized into complex structures. Actin filaments can be arranged in parallel as in filopodia or organized into orthogonal, net-like meshworks as in lamellipodia (Revenu *et al*., 2004). Anti-parallel actin filaments are found in stress-fibres. Actin monomers bind ATP and ADP. After incorporation of monomeric actin into a filament, the enzymatic activity of actin will in turn hydrolyze the bound ATP to ADP and Pi. The dynamics of actin (the coordinated assembly and disassembly of actin filaments in response to cellular signalling) are regulated by actin-binding proteins. Capping proteins regulate the length of actin filaments by either stabilizing an actin filament or promoting disassembly. Two compounds, phalloidin and jasplakinolide, favour the polymerization of actin, while cytochalasin D (Schliwa, 1982) and latrunculin B (Spector *et al*., 1983) inhibit actin polymerization.

The small Rho GTPases (RHO, RAC and CDC42) are actin dynamics-regulating proteins (Jaffe & Hall, 2005). RHO A activation of fibroblasts leads to the formation of actin stress fibres and focal adhesion complexes (Ridley & Hall, 1992). Actin polymerization is facilitated by activation of RAC 1 at the cell periphery to produce lamellipodia and membrane ruffling (Ridley *et al*., 1992). Activation of CDC42 induces filopodia (Nobes & Hall, 1995).

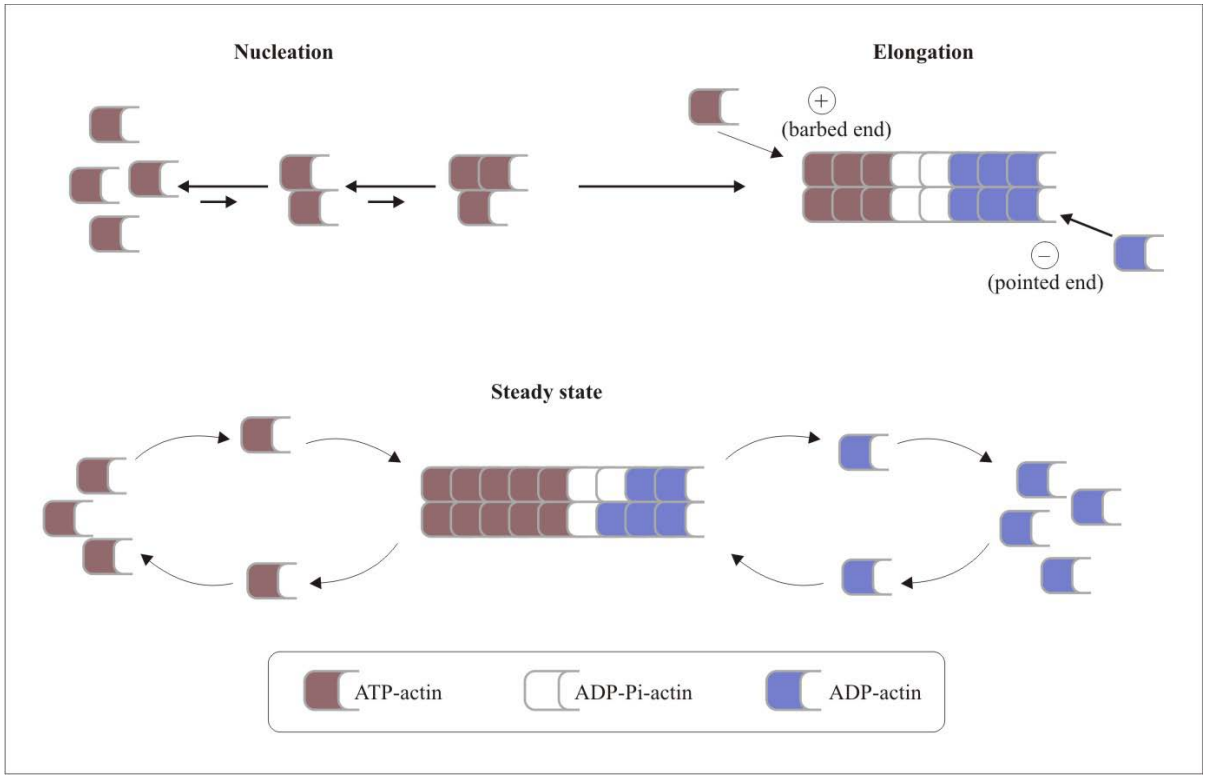

Figure 2.6 Monomeric G-actin is polymerized to form F-actin with a barbed end (plus end) and pointed end (minus end) (Kustermans *et al*., 2008).

Additional functions of the RHO subfamily are their ability to regulate cell polarity, gene transcription and cell cycle progression (Jaffe & Hall, 2005).

G protein-coupled receptors (GPCRs) can activate small GTPases, RHO A and RAC 1 in Swiss 3T3 cells (Ridley & Hall, 1992). Activation of RHO-associated coiled-coil containing protein kinase (ROCK), a downstream mediator of RHO A GTPase, leads to cardiac hypertrophy and remodeling (Kobayashi & Matsuoka, 2002). Activation of ROCK during apoptosis, results in increased myosin activity, bundling of F-actin, actin-myosin contractile force generation and membrane blebbing (Song *et al*., 2002). ROCK acts as a negative regulator of the PI3-kinase/AKT pathway, a pro-survival pathway functioning in endothelial cells during ischemia-reperfusion (Van Der Heijden *et al*., 2008). p21-Activated kinase 1 (PAK1), the predominant isoform in the heart, is activated by the small GTPases CDC42 and RAC-1 (Manser & Lim, 1999). PAK1 is involved in diverse cellular functions, such as cytoskeleton reorganization and proliferation (Sheehan *et al*., 2007). PAK1 forms a signalling

complex with protein phosphatase 2A (PP2A), that modulates the myofilament Ca^{2+} sensitivity and intracellular Ca^{2+} fluxes (Sheehan *et al*., 2007).

The cardiac L-type calcium channels ($I_{Ca\text{-}L}$) are anchored to F-actin by stabilizing proteins that control the activity of these channels (Lader *et al*., 1999). Activation of the L-type Ca^{2+} channels, that involves F-actin, increases the mitochondrial membrane potential ($\Delta\Psi_m$) (Viola *et al*., 2009). Cytoskeletal proteins regulate the subcellular distribution of mitochondria and the L-type Ca^{2+} channels regulate mitochondrial function via the cytoskeleton (Viola, *et al*., 2009).

Disturbances in the structure of F-actin by cold shock reduce protein synthesis in Chinese hamster ovary (CHO) cells (Stapulionist *et al*., 1997). Several authors have demonstrated that F-actin is involved in chromatin remodeling, transcription, RNA processing and nuclear export (Miralles & Visa, 2006; Vartiainen *et al*., 2007; Farrants, 2008; Vartiainen, 2008; Ye *et al*., 2008; Gieni & Hendzel, 2009). Nuclear actin is required for efficient transcription by all three classes of RNA polymerases (Fomproix & Percipalle, 2004; Hofmann *et al*., 2004; Hu *et al*., 2004). NM1, a myosin isoform, is also present in the nucleus and interacts with actin to execute specific nuclear functions (Ye *et al*., 2008). These authors also reported that for efficient transcription to occur, actin must be in the polymeric form, as drugs that inhibit actin polymerization e.g. cytochalasin D and latrunculin B, significantly decreased pre-rRNA synthesis. Serum response factor (SRF), a MADS-box transcription factor, is sensitive to the state of actin polymerization (Kuwahara *et al*., 2005). G-actin inhibits serum response factor (SRF) activity, while polymerization of actin, as a result of serum stimulation and RHO A signalling, stimulates SRF activity (Sotiropoulos *et al*., 1999).

2.1.6.2 Microtubules

Microtubules of the cardiomyocyte cytoskeleton are involved in protein synthesis, intracellular trafficking and intracellular signalling (Rogers & Gelfand, 2000). This network is dynamic through self-association of α,β-tubulin dimers. Microtubules are in a constant state of depolymerization and repolymerization. This dynamic state and their abundance may

change the stiffness of the cytoskeleton, which influences the contractility of the cardiomyocytes (Ishibashi *et al*., 2003). In pressure-overload cardiac hypertrophy, there is an increase in the microtubule network, which causes the contractile dysfunction (Tsutsui *et al*., 1993). Gómez and colleagues (1999) reported that microtubule depolarization by colchicine increased Ca^{2+} current and SR Ca^{2+} release of excitation-contraction coupling. Thus, besides a mechanical role, the microtubules are important modulators of cardiac function through Ca^{2+} signalling. Microtubules are unbranched tubular structures with their polar plus ends orientated towards the cell periphery and minus ends focused at the perinuclear region (Moss & Lane, 2006).

2.1.6.3 Intermediate filaments (IF)

The intermediate filaments (IF) of muscle cells contain several proteins namely desmin, vimentin, nestin, synemin, syncoilin, lamins and cytokeratins (Carlsson & Thornell, 2001). Of these, desmin is the major muscle-specific IF protein. It is located mainly in the Z-disc of striated muscle and plays an essential role in maintaining the cytoarchitecture as well as connecting the entire sarcomere to the sarcolemma, T-tubules, mitochondria and the nuclei (Conover *et al*., 2009). Skeletal and cardiac muscle of desmin knock-out mice (Des-/-) had misaligned sarcomeres and disintegrated myofibrils, and accumulated mitochondria (Conover *et al*., 2009). The network formed by IFs is involved in functions such as mechanical integration of all contractile actions, cellular integrity, force transmission, mechanical signalling and integration of organelle structure and function (Capetanaki *et al*., 2007). Desmin filaments extend from the Z-discs towards the nuclear pores, leading to *de novo* gene activity (Tolstonog *et al*., 2002). Desmin also plays a significant role in mitochondrial morphology, positioning and respiratory function in cardiac and skeletal muscle (Milner *et al*., 2000).

2.2 The role of mitochondria in the heart

The heart has a high energy demand and reduced energy generation leads to dysregulation of processes critical for cardiac pump function, including Ca^{2+} handling and contractile function.

There is a strong interrelationship between coronary blood flow, myocardial oxygen consumption and contractile performance. Energy metabolism is linked to gene expression, enzyme regulation and contractile function. The immediate response to a decrease in blood flow affects the transfer of substrates for ATP synthesis. Long-chain fatty acids are the major energy source for the heart, which are metabolized to acetyl coenzyme A, which is then metabolized in the Krebs cycle. When the levels of these fatty acids are low, the heart utilizes glucose for oxidative metabolism. Intracellular accumulation of protons, inorganic phosphate, sodium and calcium, is the result of ATP hydrolysis and lactate production during anaerobic energy metabolism (Depre *et al.*, 2006). ATP synthesis is carried out in the mitochondria through oxidative phosphorylation (OXPHOS). Three metabolic processes are involved in ATP production namely glycolysis, the Krebs cycle (also called the citric acid cycle) and the electron transport chain (ETC). Long-chain fatty acid oxidation generates the coenzymes NADH and FADH for entry into the electron transport chain.

2.2.1 Generation of energy in the mitochondria

Complex I (NADH dehydrogenase or NADH:quinone oxidoreductase) is the first enzyme of the mitochondrial electron transport chain. Complex I translocates 4 protons across the inner membrane per molecule of oxidized NADH to coenzyme Q, helping to establish the electrochemical potential used to produce ATP (Hatefi *et al*., 1959). Rotenone is an inhibitor of complex I activity (Lindahl & Oberg, 1961). Complex II (succinate-ubiquinone oxidoreductase), bound to the inner membrane, catalyzes the oxidation of succinate to fumarate with the reduction of ubiquinone (Q) to ubiquinol (QH_2) (Ziegler & Doeg, 1962). Complex III (ubiquinone-cytochrome *c* oxidoreductase), catalyzes the reduction of cytochrome *c* by oxidation of coenzyme Q (CoQ) and the concomitant pumping of 4 protons from the mitochondrial matrix to the intermembrane space (Green & Burkhard, 1961). Antimycin is an inhibitor of complex III (Alexandre & Lehninger, 1984). Complex IV (cytochrome *c* oxidase) receives an electron from each of four cytochrome *c* molecules, and transfers them to one oxygen molecule, converting molecular oxygen to two molecules of water. In the process, it binds four protons from the inner aqueous phase to produce water, and in addition translocates four protons across the membrane, helping to establish a transmembrane difference of proton electrochemical potential that the ATP synthase then uses

to synthesize ATP (Warburg, 1926). Cyanide is an inhibitor of complex IV (Slater, 1950). Complex V (F1-ATP synthase) synthesizes adenosine triphosphate (ATP) from adenosine diphosphate (ADP) and inorganic phosphate (Boyer, 2002). This energy is often in the form of protons moving down an electrochemical gradient from the inter-membrane space into the matrix in mitochondria. See Fig. 2.7 for an illustration of the reactions in OXPHOS.

Reactive oxygen species (ROS) are free radicals with one unpaired electron and are derived from molecular oxygen. Superoxide anion (O_2^-) is the precursor of most other ROS. Oxidative stress occurs when there is an imbalance between production and detoxification of ROS. Defects in oxidative phosphorylation (OXPHOS) lead to decreased energy production, as well as increased formation of superoxide, hydrogen peroxide (H_2O_2), peroxynitrite and hydroxyl radicals (Koopman, *et al.*, 2005). Accumulation of ROS results in DNA damage, protein oxidation and lipid peroxidation.

2.2.2 Mitochondrial membrane potential ($\Delta\Psi_m$)

The electrochemical potential is generated by the respiratory chain enzymes in the inner mitochondrial membrane (Fig. 2.7). Energy is provided by transfer of electrons from substrates to oxygen for pumping protons across the membrane and thus generates an electrochemical potential ($\Delta\mu_{H+}$):

$$(\Delta\mu_{H+}) = -2.3RT\Delta pH + F\Delta\Psi_m,$$

where ΔpH is the pH difference, R is the universal gas constant, T is the absolute temperature, F is the Faraday constant and $\Delta\Psi_m$ is the mitochondrial membrane potential

across the mitochondrial membrane, with the negative charge inside the mitochondria (Labajova *et al.*, 2006). The $\Delta\Psi_m$ is expressed in milliVolt units (mV). Lipid-soluble cations and anions are widely used for measurement of the $\Delta\Psi_m$. Popular fluorescent probes include rhodamine 123 and tetramethylrhodamine methyl ester (JC-1).

Apoptosis leads to dissipation or depolarization of the $\Delta\Psi_m$. Valinomycin is a K^+-selective ionophore which uncouples OXPHOS, thereby causing collapse of the $\Delta\Psi_m$ (Furlong *et al.*,

1998). Dissipation (depolarization) of the $\Delta\Psi_m$ leads to autophagic degradation of mitochondria, suggesting that autophagy is a house-keeping function (Twig *et al*., 2008). Mitochondrial autophagy is termed mitophagy (Elmore *et al*., 2001).

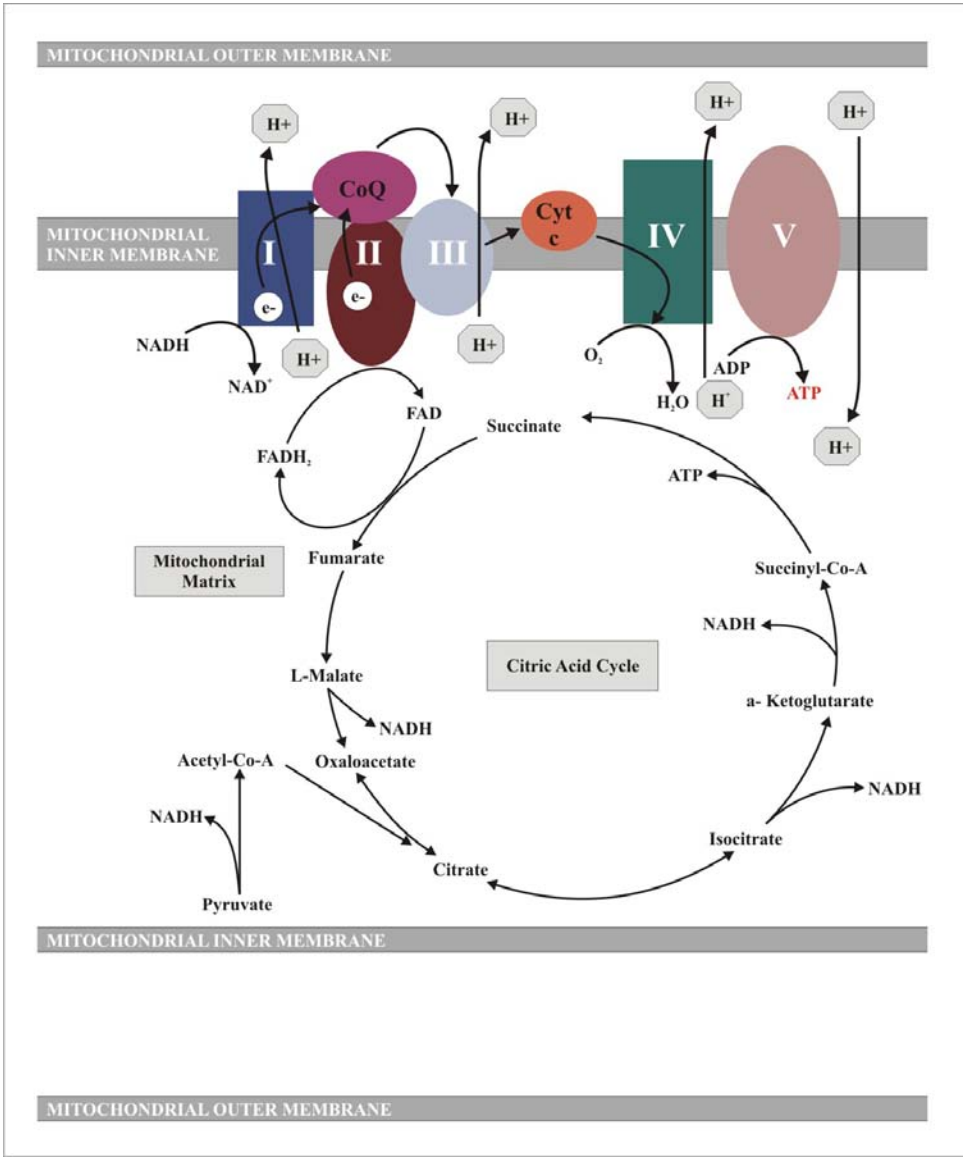

Figure 2.7 Diagrammatic scheme for oxidative phosphorylation in the mitochondria and its link to the citric acid cycle (Cognitive Enhancement Research Institute; http://www.ceri.com/mitobox.htm).

2.2.3 The mitochondrial permeability transition pore (MPTP)

The MPTP is a polyprotein complex of about 600 kDa in size situated between the outer- and inner mitochondrial membrane. It is involved in the regulation of the mitochondrial matrix homeostasis (Clerk *et al*., 2003). Three essential proteins form part of the MPTP *viz*. (1) the adenine nucleotide transporter (ANT), situated in the inner mitochondrial membrane and maintaining the proton gradient required for energy production; (2) Cyclophilin D, known as a mitochondrial peptidyl-prolyl *cis-trans* isomerase and (3) the mitochondrial phosphate carrier (PiC) (Halestrap & Pasdois, 2009). Previously, it was proposed that the voltage activated anion channel was also involved in the MPTP, but was later eliminated as a component of the MPTP (Halestrap & Pasdois, 2009). The MPTP opens with pathological increases in Ca^{2+}, adenine nucleotide depletion, high inorganic phosphate (Pi) and oxidative stress. Opening of the MPTP leads to dissipation of the proton motive force, the pH gradient and the $\Delta\Psi_m$. After opening of the pore, mitochondria can not synthesize ATP via OXPHOS and ATPase activity reverses and starts to break down the ATP, leading to an energy collapse. When the MPTP is opened, mitochondrial swelling and rupture of the outer mitochondrial membrane also occurs, leading to the release of cytochrome *c*. The MPTP is a non-selective pore, permeable to any molecule less than 1.5 kDa. Cyclosporin A (CsA) inhibits opening of the MPTP, where it blocks the association of cyclophilin D and ANT (Crompton *et al.*, 1988; Crompton, 1999).

2.3 Calcium homeostasis

Calcium plays an important role as second messenger in cellular processes such as muscle contraction, secretion, cell division, cell cycle progression, energy production and gene transcription (Maco, *et al.*, 2001). The excitation-contraction coupling of the heart is tightly controlled by the regulated release and uptake of intracellular Ca^{2+} between the SR and the cytoplasm (Fig. 2.8). Contraction is initiated when Ca^{2+} enters the cell via the L-type Ca^{2+} channels (dihydropyridine receptors; DHPRs) in the sarcolemma. This in turn releases a larger amount of Ca^{2+} from the SR, called Ca^{2+}-induced Ca^{2+} release (CICR), via the SR Ca^{2+}

release channels, called the ryanodine receptor (RYR). This raises the free intracellular Ca^{2+} concentration ($[Ca^{2+}]_i$) and binds to troponin C. Binding of calcium to troponin C, switches on the contractile machinery. Calcium must dissociate from troponin C in order for relaxation to occur, requiring that calcium must be transported out of the cytosol. Transport of calcium out of the cytosol is mediated by four pathways: SR Ca^{2+}-ATPase (SERCA) for re-uptake of Ca^{2+} by the SR, sarcolemmal Na^+/Ca^{2+} exchange, sarcolemmal Ca^{2+}-ATPase or mitochondrial Ca^{2+} uniport (Bers, 2002).

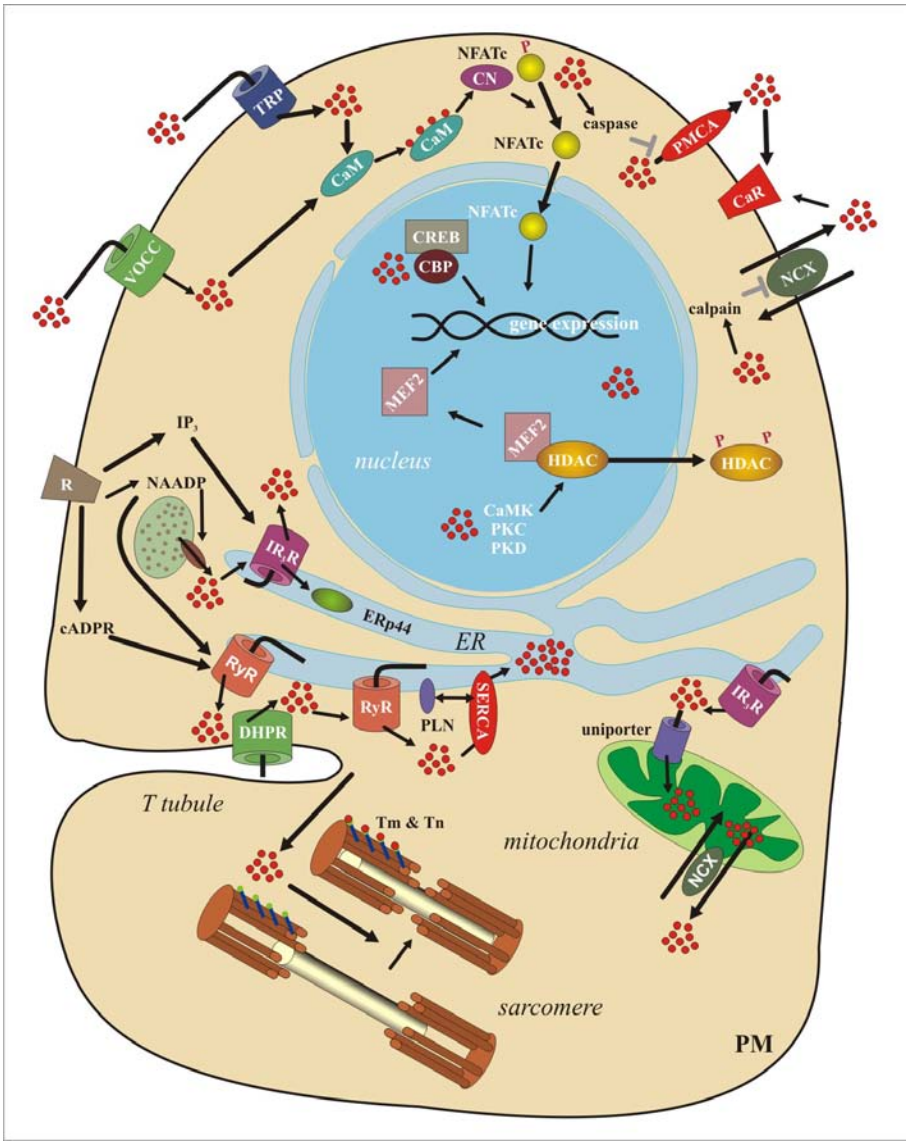

Figure 2.8. Components of Ca^{2+} signalling and organelles involved in Ca^{2+} homeostasis (Montell, 2005). Ca^{2+} ions being presented by red dots; cADPR, cyclic ADP-ribose; CaM,

calmodulin; CaMK, calmodulin dependent protein kinase; CaR, extracellular calcium-sensing receptor; CN, calcineurin; CREB, cAMP response element binding protein; DHPR, dihydropyridine receptor; HDAC, histone deacetylase; IP3, inositol triphosphate; IP3R, IP3 receptor; MEF2, myocyte transcription factor 2; NAADP, nicotinic acid adenine dinucleotide phosphate; NCX, Na^+/Ca^{2+} exchanger; NFAT, nuclear factor of activated T cells; PKC, protein kinase C; PKD, protein kinase D; PLN, phospholamban; PM, plasma membrane; PMCA, plasma membrane Ca^{2+} ATPase; RyR, ryanodine receptor; SERCA, sarcoplasmic and endoplasmic reticulum calcium ATPase; TM, tropomyosin; TN, troponin; TRP, transient receptor protein; VOCCs, voltage operated Ca^{2+} channels**.**

The expression of the calcium-sensing receptor (CaR), a G protein-coupled receptor, in cardiac tissue and cardiomyocytes was discovered by Wang and colleagues (2003). It is a key regulator for sensing calcium homeostasis, salt, water balance and osmotic regulation (Nearing *et al*., 2002). The main ligand for activation of CaR is Ca^{2+}, but it can also be activated by other cations (Handklogten *et al*., 2000). Physiological polyamine concentrations activate CaR and the efficacy is related to the number of positive charges, with spermine (4 positive charges) being more potent than spermidine (3 positive charges) in human embryonic kidney cells (HEK-293) (Quinn *et al*., 1997). Activation of CaR modulates a wide variety of proteins, including G proteins and phospholipase C, which in turn activates inositol 1,4,5-triphosphate production (IP_3). IP_3 subsequently increases intracellular Ca^{2+} release from the SR through the IP_3 receptor (Tfelt-Hansen, 2003). An increase in intracellular Ca^{2+} concentration in cardiomyocytes leads to increased cardiac activity but calcium overload also leads to apoptosis in cardiac I/R (Zhang & Xu, 2009).

Calmodulin is a Ca^{2+}-binding protein that regulates RYR opening by binding to it. The pump activity of SERCA is regulated by phospholamban (PLB) in an inhibitory manner. The SERCA2a isoform plays a central role in the heart for excitation-contraction coupling. Defects in the SERCA lead to altered contractile function (Periasamy & Huke, 2001).

S100 Ca^{2+}-binding protein A1 (S100A1), predominantly present in the heart, is associated with the sarcolemma, junctional and longitudinal SR, sarcomere, intercalated disc and mitochondria of ventricular cardiomyocytes (Schaub & Heizmann, 2008). Abnormal S100A1

gene expression leads to cardiomyopathy. At the molecular level, S100A1 interacts in a Ca^{2+}-dependent way with the ryanodine receptor (RYR2), SERCA2a, phospholamban, titin and the mitochondrial F1-ATP synthase (complex V). Stimulation of RYR2 by S100A1 increases CICR from the SR and by enforcing closure of the RYR2 channel, S100A1 reduces Ca^{2+} release from the SR. S100A1 binds to the N2B (or N2BA) isoforms and PEVK regions of titin in a Ca^{2+}-dependent manner. The N2B and PEVK elements bind to actin and this contributes to passive tension as it resists filament sliding during contraction. S100A1 is also involved in the mitochondrial energy production, by interacting with F1-ATP synthase. Increased concentrations of S100A1 increase the levels of ATP, and *vice versa* (Schaub & Heizmann, 2008).

2.4 The role of polyamines in mammalian cells

The polyamines (spermine, spermidine and putrescine), present in millimolar concentrations, play important roles in the cell. They are essential for normal cell growth, proliferation and differentiation, but can also cause neoplastic transformation and cell death (Janne *et al*., 1991). Polyamines are thus Janus-faced regulators that, depending on cell type and environmental signals, can promote growth or death. Abnormal expression of polyamines results in tumorigenesis, altered gene expression and induction of apoptosis (Cohen, 1998). Due to their cationic nature, polyamines interact with polyanions. Polyamines can interact with DNA and protect DNA from ROS (Pedreño *et al*., 2005). They also interact with RNA, nucleotide triphosphates, ion channels and other acidic substances (Igarashi & Kashiwagi, 2000).

Polyamine levels in cells are regulated by their biosynthesis, degradation, uptake and excretion (Igarashi & Kashiwagi, 2010). Putrescine is formed from ornithine by ornithine decarboxylase (Fig. 2.9). Decarboxylated S-adenosylmethionine is synthesized from S-adenosylmethionine by S-adenosylmethionine decarboxylase. These two enzymes are the rate-limiting enzymes in the synthesis of polyamines (Igarashi & Kashiwagi, 2010). Spermidine is synthesized from putrescine by spermidine synthase and spermine from spermidine by spermine synthase. In addition, spermidine is also formed from spermine by

spermine oxidase. Spermidine/spermine N-acetyltransferase and acetylpolyamine oxidase convert spermine to spermidine and spermidine to putrescine. A unique protein, antizyme, regulates the cellular polyamine content. It inhibits ornithine decarboxylase and aids in its degradation. Antizyme also inhibits polyamine uptake and enhances the excretion of polyamines (Mitchell *et al*., 1994).

Polyamine oxidases regulate the levels of mono- and polyamines by oxidative deamination, to generate H_2O_2, aminoaldehydes and ammonia. Acrolein (CH_2=CH-CHO) is then spontaneously formed between aminoaldehyde (from spermidine) and aminodialdehyde (from spermine) (Yoshida *et al.*, 2009). Hydrogen peroxide induces cell death due to oxidative stress (Toninello *et al.*, 2004). Mitochondrial monoamine oxidase acts as a scavenger of other amines with different chemical structures, e.g. catecholamines and serotonin.

Although mammalian cells posses a tightly-regulated biosynthetic pathway for synthesis of polyamines, there exists an active polyamine uptake system in the extracellular medium, the polyamine transport system (Cullis *et al*., 1999). This polyamine transporter was tested with a considerable range of polyamine analogues and they inhibit the uptake of spermidine (Cullis *et al*., 1999). It seemed that the number of positive charges were a major determinant of binding to the polyamine receptor. This transport system can, in addition to natural polyamines, take up a wide range of substrates (Phanstiel *et al*., 2000). Ghani and colleagues (2009) used polyamines as a vector to transport two toxic agents, 9-anthracenylmethyl-butanediamine and N1-anthracenylmethyl-4,4-triamine, to human leukemia cancer cells (HL-60). They observed a significant depletion of polyamines after treatment for 48 h and found that the toxicity of the two compounds increased when polyamine depletion occurred. Soulet and colleagues (2004) followed polyamine transport in CHO cells with a Spd-C_2-BODIPY probe (*N*-(4,4-difluoro-5,7-dimethyl-4-bora-3a,4a-diaza-s-indacene-3-propionyl),*N*'-(*S*-[spermidine{N^4-ethyl}]thioacetyl)ethylenediamine). Their proposed model included import of polyamines by a plasma membrane carrier and sequestration into pre-existing polyamine-sequestering vesicles (PSV). These PSVs co-localized with acidic vesicles of the late endocytic compartment, which involves H^+ exchange through vacuolar-ATPase activity, and the *trans* Golgi network.

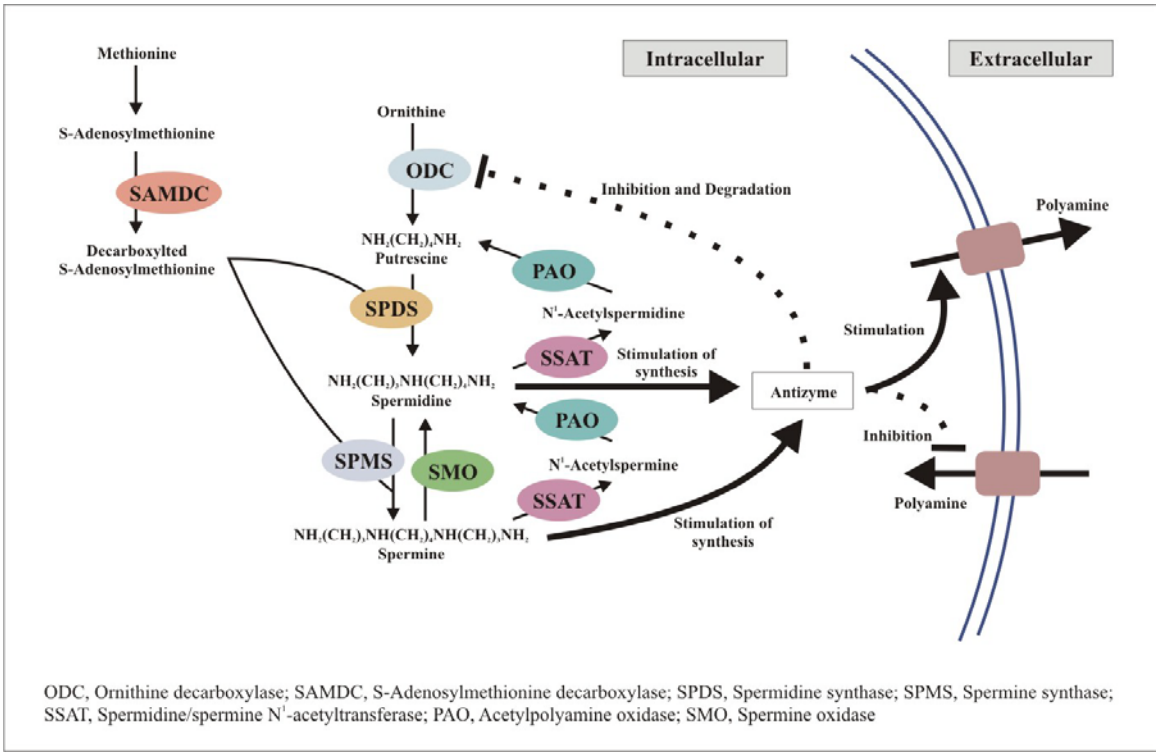

Figure 2.9 Synthesis and catabolism of the polyamines (Igarashi & Kashiwagi, 2009).

Polyamines induce muscle F-actin polymerization (Oriol-Audit, 1978). The chain length of polyamines determines the degree of F-actin polymerization, with maximum polymerization occurring with spermidine and spermine (Oriol-Audit, 1978). The dynamics of the cytoskeleton during cell proliferation and transformation were regulated by polyamines and ornithine decarboxylase, one of the rate-limiting enzyme of polyamine synthesis (Mäkitie *et al*., 2009). The activity of RHO A, a key modulator of actin cytoskeleton, was regulated by transglutaminase-catalyzed polyamination and the polyamination status of RHO A crucially influenced the progress of the cell cycle and rate of transformation in rat fibroblasts infected with viral sarcoma (v-src), a proto-oncogenic tyrosine kinase (Mäkitie *et al*., 2009).

The exact role of the polyamines in the heart has not yet been elucidated. It is now known that cardiac hypertrophy and simulated ischemia are characterized by an increase in

polyamine levels and are coupled with excessive apoptosis (Diez *et al.*, 1998; Tantini *et al.*, 2006). Spermine causes a dose-dependant decrease in ventricular contraction which follows the release of ATP in the effluent during heart perfusion studies (Guevara-Balcázar *et al.*, 2003). Polyamines, especially spermine, interact with myofibrillar proteins to reduce Ca^{2+} binding affinity (Harris *et al.*, 2000). Polyamines bind weakly and reversibly to the mitochondrial membrane at specific sites. This allows for their transport into the matrix and interaction with Ca^{2+} transporters. In addition, spermine plays an important role in Ca^{2+} homeostasis (Salvi & Toninello, 2004). Spermine increased intracellular Ca^{2+} in rat cardiomyocytes from adult hearts due to activation of the calcium-sensing receptor (CaR) (Wang *et al.*, 2003). Furthermore, polyamines present in cardiac muscle act as permeable cationic channel blockers of the ryanodine receptors (Uehara *et al.*, 1996).

Spermine is an inhibitor of MPTP in cardiomyocyte mitochondria (Lapidus & Sokolove, 1992). Spermine, at 10-100 µM, induces the release of cytochrome *c* from isolated rat heart mitochondria and is more potent than spermidine in this respect (Stefanelli *et al.*, 2000). The release of cytochrome *c* is not blocked by CsA, an inhibitor of the MPTP. Thus, the release of cytochrome *c* is not a consequence of opening of the MPTP. Maccarrone *et al*. (2001) reported that the release of cytochrome *c* from the mitochondria by spermine is paralleled by depolarization of $\Delta\Psi_m$, and thus disruption of the mitochondrial membrane integrity. They further reported that with the addition of pargyline, an inhibitor of amine oxidases, or catalase, an enzyme that converts H_2O_2 to water and oxygen, they abolished the release of cytochrome *c* and dissipation of the $\Delta\Psi_m$. They speculated that it was the polyamine oxidation products, rather than the polyamines themselves, that disrupted mitochondrial integrity.

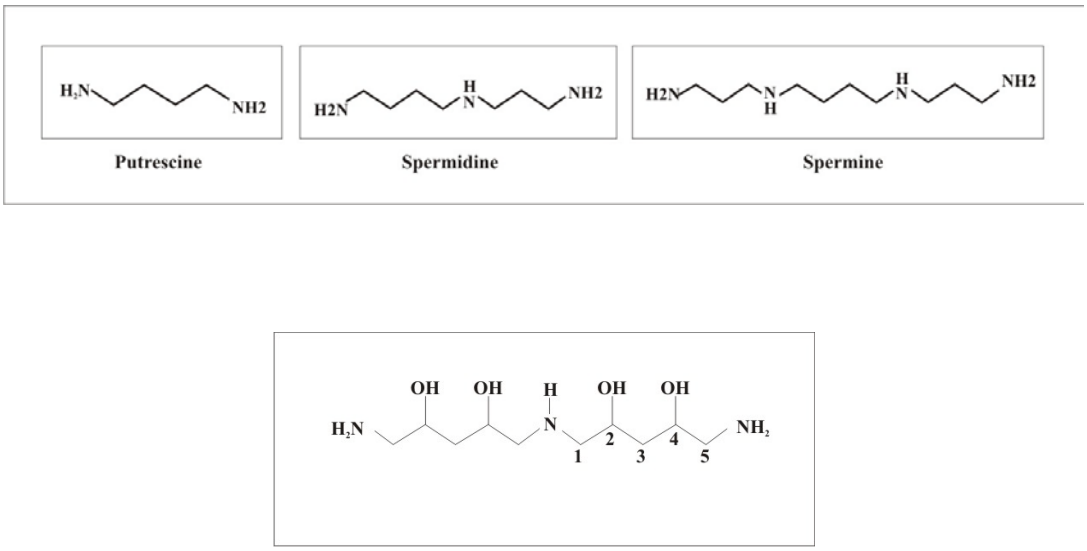

Figure 2.10 Structure of the natural polyamines and pavetamine (Bode *et al*., 2010).

2.5 Death of cardiomyocytes: apoptosis, autophagy and necrosis

Three types of programmed cell death are described in the literature: apoptosis, autophagy and necrosis (Table 2.1). Many studies reported on apoptotic cell death but necrosis was regarded as accidental cell death. Only recently, it became known that necrosis is also an organized cell death pathway. All three death pathways are interlinked and the final outcome may depend on the type of insult, its duration, as well as intracellular metabolic capacity (Loos & Engelbrecht, 2009). Complex interactions exist between autophagy and apoptosis (Levine & Yuan, 2005). Beclin-1 (BECN1), participates in autophagosome formation, but it also interacts with the anti-apoptotic protein, Bcl-2 and thus prevents autophagy (Pattingre *et al*., 2005). The death decision of cells is a complex process, as "cross-talk" between different cell death pathways exists (Lockshin & Zakeri, 2004). Therefore, it seems that autophagy promotes cell survival by avoiding a metabolic crisis and delays the onset of apoptosis and necrosis (Loos & Engelbrecht, 2009). However, it has been reported that intracellular ATP concentrations determine the eventual type of cell death (Leist *et al*., 1997).

2.5.1 Apoptosis

Apoptosis (programmed cell death I) is an active gene-directed process (Ohno *et al*., 2008). There exist two pathways for apoptosis: the extrinsic or death receptor pathway and the intrinsic or mitochondrial pathway (Skommer *et al*., 2007). Mitochondria are closely involved in the process of apoptosis. Several stress signals affect the mitochondria, namely reactive oxygen species (ROS), nitric oxide (NO), altered redox state, as well as increases in Ca^{2+} concentrations (Green & Leeuwenburgh, 2002). The MPTP opens during apoptosis, permitting the influx and efflux of molecules with a molecular weight of less than 15 kDa (Zoratti & Szabo, 1995) and consequentlythe $\Delta\Psi_m$ depolarizes (Kroemer & Reed, 2000).

Apoptotic cell death is characterized by cell shrinkage, pre-lytic DNA fragmentation (ladder pattern on gel electrophoresis), chromatin condensation (pyknosis) and chromatin fragmentation (karyorrhexis), exposed phosphatidyl serine (PS), cytochrome *c* release from the mitochondria into the cytoplasm and activation of the caspase family of proteases (cytosolic aspartate residue-specific cysteine proteases) (Kunapuli *et al.*, 2006). Apoptosis is characterized by an intact plasma membrane and requires ATP (Leist, *et al*., 1997). Caspase-activated DNAase induces DNA fragmentation of 200 base pairs (Van Wijk & Hageman, 2005). Caspase-independent apoptosis can proceed via translocation of an apoptosis-inducing factor (AIF), a mitochondrial intermembrane protein, to DNA and can induce large-scale DNA fragments of 50 base pairs (Kim *et al.*, 2006). AIF inhibits protein synthesis by interaction with the eukaryotic translation initiation factor 3 subunit p44 (dIF3g) (Kim *et al*., 2006). The end stage of heart failure (due to coronary artery disease, hypertension, valvular heart disease, myocarditis and diabetes) is death of the myocytes (Regula *et al*., 2003). Apoptosis was demonstrated in many experimental models of heart failure such as ischemia, ischemia-reperfusion (I/R), hypoxia, Ca^{2+} excess, oxidative stress, rapid pacing, gene induction, sustained stretching and doxorubicin use (Kunapuli *et al.*, 2006).

2.5.2 Autophagy

Long-lived proteins, macromolecules, membranes and whole organelles are degraded by autophagy via the lysosomes, thereby controlling the rate of turnover (Levine & Klionsky, 2004). Autophagy is activated during stress conditions such as amino acid starvation, unfolded protein response or viral infection, as part of the cell's survival. Autophagy is responsible for organelle turnover and occurs in four distinct steps: induction, formation of autophagosome, autophagosome docking and fusion with the lysosome or vacuole, as well as autophagic body breakdown (Kunapuli *et al*., 2006). Knaapen and co-workers (2001) demonstrated that cardiomyocytes preferentially undergo caspase-independent autophagic cell death during heart failure. However, as discussed above under the modes of cell death, various factors determine the eventual cell death fate and the availability of ATP which is a key determinant. Autophagy is a well regulated process, where under normal circumstances, growth factors activate class I phosphatidylinositol-3 kinase (PIK3) proteins. In turn, these then activate the mammalian target of rapamycin (mTOR) through the serine/threonine protein kinase (PKB/AKT) pathway (Abeliovich, 2004). Active mTOR inhibits an autophagy-related protein, ATG1, a key regulator of autophagy induction. During starvation, mTOR is not activated and ATG1 is able to form an ATG1 protein-kinase autophagy-regulatory complex that induces autophagy (Abeliovich, 2004). Small decreases in ATP lead to activation of AMP-activated protein kinase, which inhibits mTOR and protein synthesis (Meijer & Dubbelhuis, 2004). 3-Methyladenine is a specific inhibitor of autophagy, through inhibition of PIK3 (Seglen & Gordon, 1982).

The golden standard for assessing autophagy, is through the use of electron microscopy. This method shows the typical features of autophagy which include swollen SR and mitochondria, double-membraned autophagosomes/vacuoles, with the absence of chromatin condensation (Herrera *et al*., 2006). The microtubule-associated protein 1 light chain 3 (LC3) is a biomarker for autophagy, as it forms part of a structural component during autophagosome formation (Martinet *et al*., 2007). LC3 is lipidated during autophagosome formation and this LC3-phospholipid conjugated (LC3-II) is localized on autophagosomes. Beclin-1 has also been used to detect autophagy (Yan *et al*., 2005). The typical characteristics of autophagy have been reported in heart failure and the incidence of autophagy in heart failure has been

found to be greater than the incidence of apoptosis (Martinet *et al*., 2007). Autophagy has been described in heart failure caused by dilated cardiomyophathy (Kostin *et al*., 2003), valvular and hypertensive heart disease (Hein *et al*., 2003), chronic ischemia (Yan *et al*., 2005) and in human hibernating myocardium (Elsässer *et al*., 2004). A hibernating myocardium is described as a state of persistently impaired myocardial contractile function at rest due to reduced coronary blood flow (Rahimtoola, 1989).

2.5.3 Necrosis

Initially it was thought that necrosis is accidental cell death, but lately it has been shown that necrosis is an organized cell death pathway (Festjens *et al*., 2006). If the classic apoptotic cell death fails, other caspase-independent cell death pathways can occur, such as necrosis or autophagy (Festjens *et al*., 2006). Necrosis is characterized by cytoplasmic swelling, dilatation of cytoplasmic organelles-especially the mitochondria, irreversible plasma membrane damage and post-lytic random DNA digestion (smear pattern on gel electrophoresis) (Grooten *et al*., 1993). Necrosis is not accompanied by the typical apoptotic features such as internucleosomal DNA cleavage and nuclear condensation or by features of autophagy (Hitomi *et al*., 2008). Goldstein and Kroemer (2006) described the sequence of intracellular events for necrosis as follows: early signs of mitochondrial dysfunction, namely production of ROS and mitochondrial swelling, ATP depletion, Ca^{2+} overload, perinuclear clustering of organelles, activation of proteases (in particular calpains and cathepsins), lysosomal rupture and ultimately plasma membrane rupture. Necrotic cell death can be induced by ligands that bind to plasma membrane receptors, like tumor necrosis factor α (TNF α), which is an inflammatory cytokine (Goossens *et al*., 1995). Apoptosis can be triggered by partial selective lysosomal permeabilization, but a massive breakdown of lysosomes will result in unregulated necrosis (Bursch, 2001). Necrosis is characterized by ATP depletion, ion disregulation, mitochondrial and cellular swelling (Marx *et al*., 2006), as well as activation of cysteine proteases, Ca^{2+}-activated calpain, cathepsin and caspases (Yamashima, 2000).

Table 2.1 Comparison of typical features of cell death by the three programme cell death pathways

Type of cell death	Morphology of cells	Reference
Apoptosis	Cell shrinkage Pre-lytic DNA fragmentation (ladder pattern on gel electrophoresis) Chromatin condensation (pyknosis) and chromatin fragmentation (karyorrhexis) Exposed phosphatidyl serine (PS) Cytochrome *c* release from the mitochondria into the cytoplasm Activation of the caspase family of proteases (cytosolic aspartate residue-specific cysteine proteases) Requires ATP	Kunapuli *et al.*, 2006
Autophagy	Swollen SR and mitochondria Double-membraned autophagosomes/vacuoles No chromatin condensation Presence of microtubule-associated protein 1 light chain 3 (LC3) Beclin-1 expression Generates ATP	Yan *et al*., 2005; Martinet *et al*., 2007, Loos & Engelbrecht, 2009.
Necrosis	Cytoplasmic swelling Dilatation of cytoplasmic organelles, especially the mitochondria Irreversible plasma membrane damage Post-lytic random DNA digestion (smear pattern on gel electrophoresis) LDH leakage ATP depletion	Grooten *et al*., 1993

2.6 Cardiac hypertrophy

During cardiac hypertrophy, the immediate early gene family (c-JUN, c-FOS and early growth response gene 1) is activated and is then followed by reactivation of the expression of certain foetal genes like β-myosin heavy chain (β-MHC) and the natriuretic peptides *viz*. atrial natriuretic peptide, brain natriuretic peptide and C-type natriuretic peptide (Purcell *et al*., 2001; Gardner, 2003). The C-terminal peptides bind to the natriuretic peptide receptors (guanylyl cyclase receptors). This binding converts guanosine triphosphate (GTP) to the second messenger 3´,5´-cyclic guanosine monophosphate, which activates intracellular protein kinases and inhibits hypertrophy (Gardner *et al*., 2007). An increase in the expression of the β-MHC isoform decreases the ATPase activity, which then lowers the contraction rate, which is an important adaptation to altered workload (Lowes *et al*., 1997).

2.7 Important signalling pathways in the heart

2.7.1 Mammalian target of rapamycin (mTOR)/phosphoinositide 3-kinase/Akt signalling

The key regulator of protein synthesis for cell growth, is the mammalian target of rapamycin mTOR (Wang & Proud, 2006). mTOR stimulates protein synthesis by activating p70 ribosomal S6 kinase and by inhibiting eukaryotic translation initiating factor 4E-binding protein 1, which is a repressor of translation initiation (Sarbassov *et al*., 2005). mTOR senses the availability of amino acids and ATP levels (Chen & Fang, 2002). Rapamycin is an anti-tumor drug that prevents protein synthesis and arrests the cell cycle in the G1 phase (Asnaghi *et al*., 2004). Rapamycin is also a strong inducer of autophagy (De Meyer & Martinet, 2009). mTOR belongs to the phosphoinositide 3-kinase (PI3K) pathway and is activated by tyrosine kinase growth factor receptors such as epidermal growth factor receptor (EGFR) and insulin-like growth factor-1 receptor (IGF-1R), cell adhesion molecules such as integrins, G-protein-coupled receptors (GPCRs), and oncogenes such as Ras. (Vogt, 2001; LoPiccolo *et al*., 2008) (Fig. 2.11 for this pathway). An upstream regulator of mTOR is the serine/threonine protein kinase B (PKB)/AKT (Nave *et al*., 1999). mTOR controls the transcription activator, signal transducer and activator of transcription 3 (Yokogami, *et al*., 2000). Phosphoinositide 3-

kinase (PIK3) is involved in cell growth, proliferation, survival, migration, metabolism and other biological responses (Foukas & Okkenhaug, 2003). PIK3 exerts cardioprotective effects in the heart through activation of key proteins, including Akt. Activated Akt prevents apoptosis induced by different kind of insults (Fujio *et al*, 2000). Three isoforms of Akt exist, namely Akt 1 (PKBα), Akt 2 (PKBβ) and Akt 3 (PKBγ) (Matsui & Rosenzweig, 2005). Regulation of Akt is accomplished by protein phosphatase 2A. Akt phosphorylates the Forkhead transcription factor, leading to reduced transcription of pro-apoptotic molecules (Brunet *et al*., 1999).

2.7.2 Nuclear factor kappa beta (NF-κB)

The redox-sensitive inducible transcription factor NF-κB plays a central role in immune responses, inflammation, cell survival, differentiation and proliferation (Xiao, 2004). Nuclear factor kappa beta is retained in an inactive form in the cytoplasm by the inhibitor of NF-κB (IκB). The activation of the IκB kinase results in IκB phosphorylation, triggering its ubiquitination and proteasomal degradation. Free NF-κB translocates to the nucleus where it binds to target sequences. This promotes or inhibits transcription through co-activator or co-repressor recruitment (Hayden & Ghosh, 2008).

2.7.3 MAPK signalling

Other pathways that are involved in cardiac hypertrophy (CH) are the mitogen-activated protein kinase (MAPKs) and AKT pathways (Hayata *et al*., 2008). The MAPKs are a family

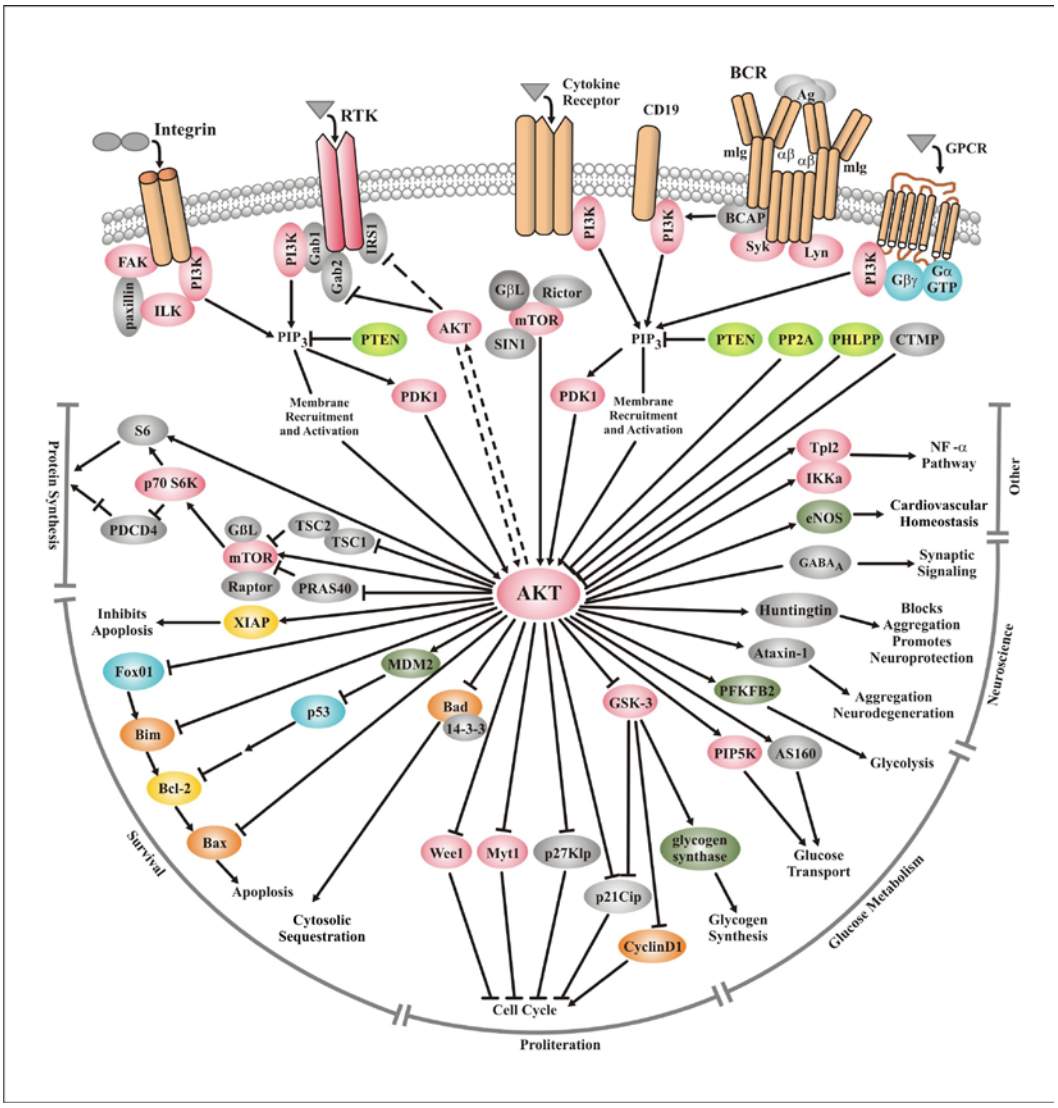

Figure 2.11 Schematic diagram of PI3K/Akt/mTOR signalling pathway (http://www.cellsignal.com/pathways/akt-signaling.jsp).

AS160, a substrate of Akt, Bax, Bcl-2-associated X protein, BCAP, B cell adaptor for PI3K, Bcl-2, B-cell lymphoma 2, BCR, B cell receptor, Bim, proapoptotic protein of the Bcl-2 family, CTMP, carboxyl-terminal modulator protein, eNOS, endothelial nitric oxide synthase, FAK, focal adhesion kinase, Foxo1, transcription factor, $GABA_A$, gamma aminobutyric acid, GSK-3, glycogen synthase kinase 3, IKKα, IκB kinase alpha, ILK, integrin-linked kinase, IRS1, Insulin receptor 1, Jak1, Janus kinase, Lyn, Src-related tyrosine kinase, MDM2, ubiquitin ligase, Myt1, myelin transcription factor, p53, p53 tumor suppressor protein, PDCD4, programmed cell death 4, PDK1, pyruvate dehydrogenase kinase 1, $PFKFB_2$, 6-

phosphofructo-2-kinase/fructose-2,6-biphosphatase 2, PHLPP, PH domain and leucine rich repeat protein phosphatase, PIP_3, phosphatidylinositol 3,4,5-trisphosphate, PIP5K, phosphatidylinositol 4-phosphate 5-kinase, PP2A, protein phosphatase 2, PRAS40, proline-rich Akt/PKB substrate 40 kDa, PTEN, phosphatase and tensin homolog, Raptor, regulatory associated protein of mTOR, Rictor, rapamycin insensitive companion of, mTOR, RTK, receptor tyrosine kinase, SIN1, SAPK-interacting protein 1, Syk, spleen tyrosine kinase, Tpl2, oncoprotein kinase, TSC1/2, tuberous sclerosis complex, Wee1, protein kinase, XIAP, X-linked inhibitor of apoptosis

of serin-threonine kinases that are activated via a variety of stimuli. Extracellular signal-related protein kinase, p38-MAPK and c-JUN NH_2-terminal protein kinase (JNK) are three major MAPKs, activated during ischemia and reperfusion (I/R) in the heart (Bogoyevitch *et al*., 1996; Knight & Buxton, 1996; Pearson *et al*., 2001). Activated MAPKs interact with protein kinases (i.e. mitogen- and stress-activated protein kinase, MSK1), cytoskeletal proteins , transcription factors and αB-crystallin (Aggeli, *et al*., 2008). The p38-MAPK in the heart is involved in cardiac gene expression, inflammation, energy metabolism, contractility, proliferation and apoptosis (Baines & Molkentin, 2005; Engel, 2005; Clerk & Sugden, 2006). Activated p38-MAPK has an influence on a number of transctiption factors, including myocyte enhancer factor 2, activating transcription factors (ATF-2 and ATF-6), NF-ĸB and E-26-like protein 1 (Kerkelä, 2003). Myocyte enhancer factor 2 is a transcription factor that is expressed in cardiac muscle and is required for cardiogenesis (Ren *et al*., 2007). JNKs and p38 kinases are called the stress-activated protein kinases because they function as transducers of stress or injury responses (Liang & Molkentin, 2003). p38-MAPK is involved in ischemic injury (Liu *et al*., 2005). Activators of p38-MAPK include MAPK kinase 3 (MKK3) and MAPK kinase 6 (MKK6), which are activated by phosphorylation on Ser/Thr residues by MAPK kinase kinase (MAPKKKs). These MAPKKKs are partly activated in response to oxidative stress, heat shock, UV irradiation, hypoxia, ischemia, and pro-inflammatory cytokines, interleukin 1 and tumor necrosis factor (TNF). (Rainaud *et al*., 1996). MAPK-activated protein kinase 2 phosphorylates heat shock protein 27, lymphocyte-specific protein 1 and cAMP response element-binding protein (Bassi *et al*., 2008). Activation of the p38-MAPK during myocardial ishaemia can be lethal, but under other

circumstances, activation of p38-MAPK can protect the heart (Bassi *et al*., 2008). Dual-specific MAPK phosphatases (MKPs) deactivate p38-MAPK (Keyse, 1999).

2.7.4 G protein-coupled receptors (GPCRs)

The GPCRs are dedicated to cell-cell communication. They regulate second messengers and ion channel activity. GPCRs are activated by their ligands, which lead to a conformational change. This change causes the GPCR to interact with heterotrimeric G proteins (Bockaert *et al*., 2004). A GDP to GTP transition occurs within the G protein and the Gα-GTP and Gβγ subunits. GPCRs also interact with GPCR interacting proteins (Bockaert *et al*., 2004). GPCRs are crucial in cardiovascular function and the adrenergic receptors (ARs) are GPCRs that are involved in the hypertrophic response (Barry *et al*., 2008). α-Adrenergic receptors activate phospholipase C (PLC) that hydrolyses α-Adrenergic receptors activate phospholipase C (PLC) that hydrolyses phosphoinositol 4,5-biphosphate to inositol 1,4,5-triphosphate and diacylglycerol (DAG) (Arimoto *et al*., 2006). DAG activates protein kinase C (PKC), which is part of the development of concentric hypertrophy (Takeishi *et al*., 2000). β-Adrenergic receptors that are coupled to the $G_{\alpha s}$ subunit of the heterodimeric G protein, activate adenyl cyclase, causing accumulation of cAMP and consequently activation of protein kinase A (PKA). This results in the phosphorylation of various proteins involved in cardiac contraction: L-type calcium channels ($I_{Ca\text{-}L}$), ryanodine receptors (RYRs), phospholambin (PLB) and troponin (TN) (Marian, 2006). It is interesting to note that polyamines stimulate G proteins in peritoneal mast cells through phospholipase C (PLC) (Bueb *et al*., 1992).

2.8 Protein quality control (PQC)

Cellular protein synthesis occurs in cytosolic free ribosomes, but depending on cell type can occur in the rough endoplasmic reticulum (ER). Membrane proteins and proteins for secretion are synthesized in the ER, where proper folding must take place (Blobel, 2000). The ER-associated protein quality control supports protein refolding, prevents unfolded proteins from aggregating and selectively removes misfolded polypeptides (Wang *et al*., 2008). In cardiomyocytes, myofibrillar proteins occupy more than 80 % of the cell volume and the PQC of these cells is not a function of the ER. In order for proper folding to take place, chaperones

are synthesized to prevent proteins from misfolding (Willis *et al*., 2009). Targeted proteolysis of misfolded proteins is accomplished by the ubiquitin-proteasome system (UPS) (Wang & Robbins, 2006).

Chaperones assist unfolded polypeptides to fold correctly. For each subcellular compartment (e.g. mitochondria, the ER, the nucleus, and the cytosol) there is a different set of chaperones. Chaperones serve as sensors for misfolded polypetides, bind them and prevent aggregation. In stressed cardiomyocytes, there is an increase in the synthesis of chaperones to handle increased protein misfolding. The heat shock proteins (HSP) are induced in cardiomyocytes during stress. Some of these HSP chaperones are capable of refolding the proteins that have been denatured under stress, while others escort terminally misfolded proteins for degradation. The most studied chaperones in the heart are HSP90, HSP70, carboxyl terminus of HSP70-interacting protein, HSP20 and αβ-crystallin. In a number of cardiac pathologies, the PQC is inadequate, resulting in congestive cardiac failure. The formation of protein aggregates can impair the UPS and activate autophagy (Rubinsztein, 2006). Although autophagy is a death signalling pathway, it also plays a crucial role in PQC, especially in pathological conditions. Autophagy is capable of degrading excessive or defective organelles and there is a link between autophagy and ER-associated degradation (ERAD).

2.9 The unfolded protein response (UPR)

The protein folding machinery, including numerous chaperones, proteins and factors, ensures efficient nascent protein folding. Any disturbance of this folding machinery will lead to accumulation of misfolded proteins, which will trigger events to augment folding capacity. The UPR is activated by stresses that impair the protein folding in the rough ER (McMillan *et al*., 1994). Optimal protein folding depends on the following factors: the correct redox state in the ER, suitable levels of glycosylation substrates and glycosylation enzymes, SR Ca^{2+} and chaperones (Glembotski, 2008). When ER protein folding is impaired, the accumulation of misfolded, dysfunctional proteins signals the initiation of ER stress (Chang *et al*., 1987). The proximal ER transmembrane effectors of the UPR are: protein kinase R-like ER kinase (PERK) (Shi *et al*., 1998), activating transcription factor-6 (ATF6) (Zhu *et al*., 1997) and

inositol-requiring enzyme-1 (IRE-1) (Mori *et al*., 1993). With efficient ER protein folding, the ER luminal domains of these three effectors are bound to the ER-resident chaperone, glucose-regulated protein 78, thereby keeping these effectors inactive (Lee, 2001). However, when misfolded proteins begin to accumulate, glucose-regulated protein 78 translocates to the misfolded proteins to aid in folding. Activated PERK phosphorylates eukaryotic initiation factor 2α, leading to decreased translation of most cellular mRNAs (Bertolotti *et al*., 2000). Upon ER-stress, IRE-1 exhibits a novel endoribonuclease activity, which cleaves the mRNA of active X-box binding protein-1. This splicing event generates a new transcript that encodes for an active form of X-box binding protein-11, a transcription factor that induces numerous ER stress response genes (Calfon *et al*., 2002). ATF6 translocates to the Golgi apparatus, upon ER stress. Here ATF6 is cleaved by two proteases, and the cytosolic region of ATF6 translocates to the nucleus, leading to the transcriptional regulation of ER stress response genes (Ye *et al*., 2000). The genes that are induced upon ER stress, encode proteins that improve the folding of nascent proteins in the ER lumen and enable the degradation of misfolded proteins. This degradation is performed by the ER-associated protein degradation (ERAD). ERAD causes retrotranslocation of the unfolded polypeptide into the cytosol followed by ubiquitination and proteasomal degradation, or targeting parts of the ER to lysosomes through autophagy (Kincaid & Cooper, 2007).

2.10 The ubiquitin-proteasome system (UPS)

The UPS system is a non-lysosomal, ATP-requiring system responsible for the degradation of ubiquitinated proteins that is recognized by the 26S proteasome (Glickman & Ciechanover, 2002). The barrel-shaped 20S proteasome forms the proteolytic core of the 26S proteasome. Three major peptidase activities have been assigned to the 20S proteasome: chymotrypsin-like, trypsin-like and caspase-like activities (Wang *et al*., 2006; Willis & Patterson, 2006). Damaged and misfolded proteins are degraded by the UPS, as well as intracellular proteins (Hochstrasser, 1995). The C-terminus of ubiquitin is covalently attached to the ε-amino group of specific lysine residues in the substrate protein. This ubiquitination of target proteins involves three enzyme families: E1, an activating enzyme; E2, a conjugating enzyme that carries the ubiquitin; and E3, a ligase that recognizes the target protein and transfer of

ubiquitin from E2 (Balasubramanian *et al*., 2006). The extent of ubiquitination determines the fate of target proteins. The 26S proteasome recognizes substrates with at least 4 poly-ubiquitin chains linked to their lysine 48 which is a signal for degradation (Willis & Patterson, 2006). Mono-ubiquitination of lysine residues or ubiquitination at Lys63, may signal for a non-proteolytic fate for modified proteins. This can result in the internalization and sorting of ion channels, receptors and junctional complexes to the endocytic environment (Bonifacino & Traub, 2003). Histone modification, transcription and DNA repair are modulated by mono-ubiquitination (Hicke, 2001). In the heart, the UPS regulates cardiac membrane channels and receptors, β2-adrenergic signalling, signal transduction and transcription factors (Willis & Patterson, 2006). In cardiac I/R injury, the proteasome is inhibited with accumulation of ubiquitinated proteins (Powell *et al*., 2005). Activation of caspases inhibits proteasome function and leads to apoptosis (Sun *et al*., 2004). The UPS is activated during cardiac hypertrophy (Depre *et al*., 2006). Muscle-specific ring finger proteins (MURFs) MURF-1, MURF-2 and MURF-3 are a subfamily of E3 ubiquitin ligases, expressed in cardiac and skeletal muscle (Spencer *et al*., 2000). MURF-1 is a microtubule-associated protein (Spencer *et al*., 2000) and interacts with titin at the M-band of the sarcomere (McElhinny *et al*., 2002). MURF-1 and MURF-2 interact with titin, nebulin, TNI and TNT, myotilin and T-cap (Witt *et al*., 2005). MURF-3 interacts with four and a half LIM domain protein (FHL2) and γ–filamin, and therefore controls their degradation (Fielitz *et al*., 2007a). Fielitz *et al.* (2007b) demonstrated that MURF-1 and MURF-3 interact with β/slow MHC and MHCIIa and play a central role in the maintenance of skeletal and cardiac structure and function. A proteomic study was undertaken to identify the ubiquitinated proteins in the mouse heart by way of a transgenic mouse model expressing a plasmid with an ubiquitin tag (Jeon *et al*., 2007). The cytosolic proteins identified in this manner included components of the contractile fibres, namely MHC α and β, TPM, titin, MYBPC, desmin and actinin 2 and 4. These findings underline the importance of the UPS in the turnover of the cardiac contractile and cytoskeletal proteins.

During myocardial ischemia, oxidation of proteins occurs, which can be measured by an increase in protein carbonyls and mixed disulfides after perfusion of isolated heart (Park *et al*., 1991). The proteasome plays a significant role in the removal of oxidized proteins during myocardial ischemia in an ubiquitin-independent manner (Divald & Powell, 2006). A

transgenic mouse model was also used to investigate the role of the UPS in the cardiotoxicity of doxorubicin therapy (Kumarapeli *et al*., 2005). These authors reported that doxorubicin enhanced UPS function in the heart and cultured cardiomyocytes.

2.11 Other proteases in cardiomyocytes: calpains, cathepsins and caspases

Lysosomal proteases, such as cathepsin D, are activated during the initial phase of ischemia and require an acidic pH for activity (Wildenthal, *et al*., 1978). A number of myofilament proteins, namely actin, myosin, TPM and troponin, are reported to be degraded in ischaemic human left ventricles (Hein *et al*., 1995). Protein degradation and loss were studied in rat hearts subjected to ischemia and ischemia/reperfusion (I/R) (Van Eyk *et al*., 1997). During ischemia, there was an increased loss and degradation of α-actinin and troponin I. During I/R, degradation of MLC1 was also found. These authors concluded that the changes involved in myocardial function associated with I/R is an altered response of the myofilaments to Ca^{2+}. The degradation and loss of some of these proteins was attributed to Ca^{2+}-dependent proteases, which were activated during the Ca^{2+} overload after I/R (Gross *et al*., 1999). Calpain, which is located near the Z-line, is one of the Ca^{2+}-dependent proteases that play a role in ischemia (Goa *et al*., 1997). In an immunohistochemical study using human hearts with dilated cardiomyopathy, the intensity of titin fluorescence was reduced, frequently disorganized or almost completely absent (Hein *et al*., 1994). These authors concluded that the loss of titin, myosin and the thin filament complex correlated with the reduction in cardiac function. Multimeric complexes of sarcomeric proteins cannot be degraded by the proteasome (Solomon & Goldberg, 1996). Calpain-1 is needed to dissociate sarcomeric proteins from the myofibril before the UPS is able to degrade those (Galvez *et al*., 2007). The SR plays a central role in cardiac contractility due to its ability to regulate intracellular Ca^{2+} (Bers, 2002). In an I/R rat heart model, it was demonstrated that the SR function and gene expression was altered (Temsah *et al*., 1999). SR Ca^{2+}-cycling and SR regulatory proteins were shown to be a target for calpain action (Singh *et al*., 2004). Upon leupeptin treatment, an inhibitor of calpain, there was a recovery of the major SR Ca^{2+}-handling proteins, RYR and SERCA2a, and its regulator phospholambin.

Myofibrillar proteins are degraded by the lysosomal proteases. TNT is being degraded by cathepsin H, while cathepsin B hydrolases MHC, TNT, TNI and TPM (Bechet *et al*., 2005). Most of the myofibrillar proteins are degraded by cathepsin L, except TNC and TPM (Matsukura *et al*., 1981).

2.12 Lysosomotropism

Lysosomes are vesicles that contain high concentrations of acid hydrolases which are active in an acidic pH of 4-5 (Kirschke & Barrett, 1987). The vacuolar (V)-type ATPase proton pump maintains the acidic pH of the lysosome. The accumulation of basic/cationic compounds inside acidic organelles, like the late endosome or lysosome, are termed lysosomotropism (De Duve *et al*., 1974). Several cell types form multiple and large vacuoles when treated with concentrated amine drugs, like procaine, procainamide, nicotine and atropine (Morisette *et al*., 2008). Bafilomycin A1, a V-ATPase inhibitor, completely prevented vacuole formation by diverse amine drugs (Morisette *et al*., 2004). Monoamines and diamines, because of their weak basic lipophilic character, are commonly employed to study vacuolar acidification (Millot *et al*., 1997). In their neutral form, these compounds are membrane-permeant, but once protonated, they would accumulate in acidic vesicles and become membrane-impermeant. Leakage of lysosomal enzymes can cause apoptosis or necrosis (Wang *et al*., 2006). Oxidative stress, accumulation of redox-active iron and lipid peroxidation cause lysosomal rupture (Parent *et al*., 2009). Pronounced lysosomal leakage and rupture result in necrosis, while moderate lysosomal leakage induces apoptosis (Bursch, 2001).

2.13 Justification for this study and hypothesis

The ultimate aim of this gousiekte research project is to develop preventative or treatment options for gousiekte. In order to achieve this, the mechanism of toxicity of pavetamine must first be clarified. Polyamines, present in millimolar quantities, play essential roles in cells, but the function of polyamines in cardiac cells is still largely unknown. Polyamines can promote cell growth or cell death, they can influence gene expression and are involved in Ca^{2+} homeostasis. During the catabolism of polyamines by polyamine oxidases, H_2O_2 is generated

and can cause extensive damage to the cell. The generation of ROS cause protein oxidation, thus forming protein aggregates, which are degraded by the UPS. Multimeric complexes of sarcomeric proteins must first be degraded by calpain 1 before the UPS can further digest them. Pavetamine can possibly interfere with the metabolism of polyamines, their biosynthesis and with their transport. Polyamines change the Ca^{2+} affinity of contractile proteins. Pavetamine can behave like other amine-containing compounds, such as NH_4Cl, chloroquine and methylamine, where it gets trapped inside acidic vesicles, causing multiple and large vacuoles, so called lysosomotropism.

In summary, the following cellular effects have been reported for pavetamine:

- It damages the mitochondria in the heart of rats and sheep and ATP levels are reduced (Snyman *et al*., 1982; Prozesky *et al*., 2005).
- It damages the SR in the hearts of sheep and rats and causes reduced uptake of calcium by the sarcoplasmic reticulum (Pretorius *et al*., 1973b; Prozesky *et al*., 2005).
- Ultrastructurally, myofibrillar loss and degeneration are typically observed in hearts of sheep and rats exposed to pavetamine (Schutte *et al*., 1984; Kellerman *et al*., 2005; Prozesky *et al*., 2005; Prozesky, 2008).
- Pavetamine also causes inhibition of protein synthesis in rat hearts (Schultz *et al*., 2001).

The working heart has a high rate of energy utilization to enable rhythmic contraction. Impaired ATP production will hamper contractility. Damaged mitochondria and SR are degraded in the lysosomes by autophagy. This is recognized as a cell survival mechanism. Autophagy can also be activated during starvation in order to generate ATP. However, defective autophagy can cause cell death. Interference in the Ca^{2+} homeostasis will also interfere with cardiac contraction. Increased intracellular Ca^{2+} concentration in cardiac cardiomyocytes will activate the Ca^{2+}-activated protease, calpain, which in turn will degrade the cardiac proteins. Up to thirty five percent of protein synthesis occurs at the ribosomes associated with the SR, called the rough SR. Any damage or alteration to the SR will influence protein synthesis and SR stress will lead to misfolded, dysfunctional proteins (Chang *et al*., 1987).

2.14 Objectives

The objectives of this study were:

1. To investigate the mode of cell death (apoptosis, autophagy and necrosis) caused by exposure of H9c2 cells to pavetamine.
2. To perform a transmission electron microscopy (TEM) study of H9c2 cells exposed to pavetamine.
3. To conduct mitochondrial studies in H9c2 cells evaluating the:
    a. Mitochondrial membrane potential.
    b. Cytochrome *c* release.
    c. Cyclosporin A inhibition of the mitochondrial permeability transition pore (MPTP).
4. To study the effect of pavetamine on the subcellular organelles of H9c2 cells with fluorescent probes.
5. To label rat neonatal cardiomyocytes (RNCM) with antibodies to some contractile and cytoskeleton proteins.

CHAPTER 3
MODE OF CELL DEATH AND ULTRASTRUCTURAL CHANGES IN H9C2 CELLS TREATED WITH PAVETAMINE, A NOVEL POLYAMINE

3.1 Introduction

Gousiekte, a cardiotoxicosis of ruminants, is characterized by acute heart failure without any premonitory signs four to eight weeks after the initial ingestion of certain rubiaceous plants (Theiler *et al*., 1923; Pretorius & Terblanche, 1967; Kellerman *et al*., 2005). The causative plants include *Pachystigma pygmaeum* Schltr., *Pachystigma thamnus* Robyns, *Pavetta harborii* S.Moore, *Pavetta schumaniana* F.Hoffm and *Fadogia homblei* Robyns (Kellerman *et al*., 2005). Electron micrographs of the myocardium of sheep intoxicated with *P. pygmaeum*, showed the myofibrils became disintegrated and had a frayed appearance accompanied by replacement fibrosis (Schutte *et al*., 1984; Kellerman *et al*., 2005; Prozesky *et al*., 2005). TEM of the hearts of sheep dosed with gousiekte-inducing plants, showed abnormalities of the mitochondria and SR (Prozesky *et al*., 2005).

Rats were susceptible to *P. harborii* extracts when administered subcutaneously (Hay *et al*., 2001). Cardiac contractility was reduced by more than 50% and the cardiac output (heart rate x stroke volume), an indication of the myocardial oxygen requirement, by 40% when compared to control rats (Hay *et al*., 2001). The novel toxin that causes gousiekte was isolated from *P. harborii* and called pavetamine (Fourie *et al*., 1995). The structure of pavetamine was elucidated and was identified to belong to the polyamine group, similar to spermidine, spermine and putrescine (R. Vleggaar, unpublished data 1997). Polyamines are essential for normal cell growth, proliferation and differentiation but can also cause neoplastic transformation and cell death (Janne *et al*., 1991). Schultz and co-workers (2001) reported that pavetamine, administered intraperitoneally to rats, inhibits protein synthesis in the heart. Synthesis of proteins in the liver and kidney was initially also reduced, but returned to normal after 48 h. Other muscle tissue was not affected. Purified pavetamine from *P. harborii* caused significantly reduced systolic function in rats (Hay *et al*., 2008).

Cardiac cells are post-mitotic and changes to the work load of the heart cause altered expression of the contractile proteins, as a compensatory mechanism (Samarel & Engelmann, 1991). In addition, damaged proteins and organelles are eliminated by pathways like autophagy, but can likewise cause cell death. Three pathways exist for cell death *viz.* apoptosis (programmed cell death I), autophagy (programmed cell death II) and necrosis (programmed cell death III). Apoptotic cell death is characterized by pre-lytic DNA fragmentation (ladder pattern on gel electrophoresis), chromatin condensation, cytochrome *c* release from the mitochondria into the cytoplasm and activation of the caspase family of proteases (Kunapuli *et al*., 2006). Apoptotic signals cause opening of the MPTP with influx of H^+ ions and loss of the mitochondrial membrane potential (Regula *et al*., 2003). Autophagy is responsible for organelle turnover (Klionsky & Emr, 2000) and occurs in four distinct steps: induction, formation of an autophagosome, autophagosome docking and fusion with the lysosome and autophagic body breakdown (Kunapuli *et al*., 2006). Excessive autophagy can destroy major portions of the cytoplasm and organelles, especially the mitochondria and endoplasmic reticula, leading to cell death. Necrosis causes disruption of the plasma membrane (Robiolo & Vega, 2008), leading to LDH leakage from the cells.

The clonal cell line H9c2, a permanent cell line, was derived from embryonic BDIX rat ventricular heart tissue and retained some of the properties of cardiac muscle (Kimes & Brandt, 1976). This cell line is being used as an *in vitro* model for cardiac muscle, as it resembles the biochemical and electrophysiological properties of adult cardiomyocytes (Hescheler *et al*., 1991; Green & Leeuwenburgh, 2002; Zordoky & El-Kadi, 2007; Aggeli *et al*., 2008).

The purpose of this study was to characterize the cytotoxicity and mode of cell death caused by pavetamine in a rat embryonic H9c2 cell line. Cytotoxicity of pavetamine was determined with the MTT (3-(4,5-dimethyl-2-thiazolyl)-2,5-diphenyl-2H-tetrazolium bromide) assay and the LDH release assay. Ultrastructural changes caused by pavetamine treatment of cells were evaluated with TEM. Changes in the mitochondrial membrane potential, caused by pavetamine, were investigated utilizing two fluorescent probes, JC-1 (5,5′,6,6′-Tetrachloro-1,1′,3,3′-tetraethyl-imidacarbocyanine iodide) and TMRM (tetramethylrhodamine methyl

ester perchlorate). Pavetamine was tested in the presence of CsA, an inhibitor of the MPTP, in H9c2 cells for reduced cytotoxicity. Apoptotic features were evaluated with activation of caspase 3, DNA fragmentation, DAPI staining of nuclei and cytochrome *c* release from the mitochondria into the cytoplasm.

3.2 Materials and Methods

3.2.1 H9c2 cell line

The H9c2 cell line (Kimes & Brandt, 1976) was obtained from the American Type Culture Collection (Manassas, USA). The cells were placed in Dulbecco's Modified Eagle's Medium (DMEM) (Sigma, St Louis) supplemented with 10% foetal calf serum (Gibco, Carlsbad, California), 100 U/ml penicillin and 100 µg/ml streptomycin sulphate (Gibco, Carlsbad, California). The cells were incubated in a humidified atmosphere of 5 % CO_2 at 37 °C.

3.2.2 Purification of pavetamine

Pavetamine was extracted and purified from the leaves of *P. harborii* S. Moore according to the method described by Fourie *et al*. (1995).

3.2.3 Cytotoxicity of pavetamine

Twelve well plates were incubated overnight until 80 % confluent. Fifty microliters of 10-fold serial dilutions of pavetamine (0.02; 0.2; 2; 20 and 200 µM) were added to each well, in duplicate. Untreated cells were used as controls. The cells were exposed for 24, 48 and 72 h. The results represent the average of three independent experiments.

3.2.3.1 MTT assay

The MTT assay (Sigma, St. Louis, MO), a measurement for viable cells, was used to measure the cytotoxicity of pavetamine in H9c2 cells (Mossman, 1983). This is a colorimetric assay for the quantification of cell toxicity, based on the conversion of yellow MTT to the water-insoluble purple formazan crystals by dehydrogenases of viable cells, which is impermeable to cell membranes. The crystals are solubilised by the addition of detergents and read in a spectrophotometer. The number of surviving cells is directly proportional to the amount of formazan formed. In this study, cells were exposed for the indicated times to the above-mentioned concentrations of pavetamine, after which the medium was replaced with fresh medium, containing 0.6 mM MTT (3-(4,5-dimethyl-2-thiazolyl)-2,5-diphenyltetrazolium bromide). The plates were incubated in a 5 % CO_2 incubator at 37 °C for 4 h. Five hundred microliters DMSO were added to each well to solubilize the formazan crystals. After incubation at 37 °C for 1 h in a 5 % CO_2 incubator, 100 µl were transferred to a 96-well plate and the absorbance was read at 570 nm.

3.2.3.2 LDH assay

The LDH cytotoxicity detection kit (Roche Diagnostics GmbH, Mannheim, Germany) is a colorimetric assay for the quantification of cell death and cell lysis, based on the determination of LDH activity released from the cytosol of damaged cells into the medium, thus indicating cell membrane damage, a feature of necrosis. After the end of a cell culture experiment, 200 µl cell culture medium was removed and added to a 96 well plate. One hundred microliters of the reaction mixture (250 µl of a Diaphorase/NAD^+ mixture, premixed with 11.25 ml of iodotetrazolium chloride/sodium lactate) was added to each well and the plate was incubated for 30 min at room temperature, protected from light. The absorbance was then measured at 492 nm.

3.2.4 Transmission electron microscopy

The TEM studies were conducted after exposure of H9c2 cells to 20 µM pavetamine for 24, 48 and 72 h. Staurosporine (Roche, USA) was used as a positive inducer of apoptosis (Yue,

et al., 1998). The cells were fixed in 2.5 % glutaraldehyde in Millonig's buffer for 5 min before scraping the cells off the bottom of the flask, removing cells and fixative from the flask into an Eppendorf tube and then additional fixing for another hour. The cells were post-fixed in 1 % osmium tetroxide in Millonig's buffer, washed in buffer and then dehydrated through a series of graded alcohols, infiltrated with a mixture of propylene oxide and an epoxy resin, and embedded in absolute resin at 60 ºC. The cells were pelleted after each step by centrifugation at 3000 rpm for 3 min. After curing overnight, ultra-thin sections were prepared and stained with lead citrate and uranyl acetate. The sections were then viewed in a Philips CM10 transmission electron microscope operated at 80 kV.

3.2.5 Mitochondrial analyses

3.2.5.1 Measurement of the electrochemical proton gradient of the inner mitochondrial membrane with JC-1 and TMRM

The ΔΨm was measured according to the manufacturer's instruction with JC-1 (Sigma, St. Louis, MO). The fluorescence was measured at an excitation: emission of 485/538 for green monomers and at an excitation: emission of 485/590 for red aggregates with a Fluoroscan Ascent FL fluorometer (Thermo Electron Corporation, Waltham, MA). Valinomycin, a potassium ionophore, was used at a concentration of 0.1 µM (Sigma, St. Louis, MO) as a positive control for depolarization of the mitochondrial membrane. Tetramethylrhodamine methyl ester perchlorate (TMRM) (Sigma, St. Louis, MO), another ΔΨm-dependent fluorescence dye (Yoon, *et. al*., 2003), was used at a concentration of 1 µM to stain H9c2 cells that had been exposed to 20 µM pavetamine for 24 h, followed by laser scanning confocal microscopy (LSCM). The microscope that was used for the LSCM was a model ZEISS LSM 510 (Jena, Germany).

3.2.5.2 Inhibition of mitochondrial permeability transition pore (MPTP)

The mitochondrial permeability transition pore is sensitive to CsA, by blocking the opening of this pore. As pavetamine causes swelling of the mitochondria, CsA was tested as a potential antagonist of pavetamine-induced mitochondrial damage. Cyclosporine A (Sigma, St. Louis, MO) at a concentration of 1 µM was used to pre-treat cells for 30 min to inhibit the MPTP,

before cells were exposed to 20 µM pavetamine for 48 h. Cell viability was determined with the MTT assay.

3.2.6 Evaluation of apoptosis

3.2.6.1 Activation of caspase 3

The kit for measurement of caspase 3 was obtained from Sigma (St. Louis, MO). The substrate, Ac-DEVD-pNA, was dissolved in 1.2 ml DMSO (20 mM) and stored at -20 °C. Just before use, the substrate was diluted to 2 mM with assay buffer. Staurosporine (Roche, USA) was used as positive control. The medium was removed and the cells were trypsinated. The cells were pelleted at 600 x g for 5 min at 4 °C. The supernatants were removed and the cells washed twice with PBS. The cells were suspended in 100 µl lysis buffer (50 mM HEPES (4-(2-hydroxyethyl)-1-piperazine-ethanesulfonic acid), pH 7.4, 5 mM CHAPS (3[(3-cholamidopropyl)dimethylammonio]-propanesulfonic acid), 5 mM DTT (dithiothreitol). The cells were incubated on ice for 20 min, after which the lysed cells were centrifuged at 13,000 rpm for 10 min at 4 °C. The supernatants were transferred to new Eppendorf microcentrifuge tubes. Thereafter, five µl were aliquoted into each well of a 96-well plate, 85 µl assay buffer was added followed by 10 µl substrate. The plates were incubated overnight at 37 °C. The absorbance was read at 405 nm in a Wallac Victor^2 1420 multilabel counter. For activation of caspase 3, pavetamine was tested at a concentration of 200 µM, doxorubicin at 2.5 µM and staurosporine at 0.6 µM for the indicated exposure times.

3.2.6.2 DNA fragmentation

DNA was purified from H9c2 cell cultures with a QIAGEN Genomic DNA kit (Qiagen, Germany). Cells from a 75 cm^2 cell culture flask were harvested with trypsin and washed with PBS. Cells were then suspended in 0.5 ml phosphate-buffered saline (PBS). One volume of ice-cold Buffer C1 and 3 volumes of ice-cold distilled water were added to each tube. The tubes were inverted several times and incubated on ice for 10 min. The lysed cells were centrifuged at 4 °C for 15 min at 1300 x g and the supernatants were discarded. Again 0.25 ml ice-cold buffer C1 and 0.75 ml ice-cold distilled water were added. The pelleted nuclei were resuspended by vortexing. The centrifugation step was repeated. One milliliter of buffer G2

was added and vortexed for 30 sec. Proteinase K digestion was performed by adding 25 µl of Proteinase K stock solution and the tubes incubated at 50 °C for 30-60 min. The samples were applied to an equilibrated QIAGEN Genomic-tip and allowed to enter the resin by gravity flow. The tips were then washed 3 times with 1 ml Buffer QC. The genomic DNA was eluted with 1 ml buffer QF. The DNA was then precipitated after the addition of 1.4 ml isopropanol. After mixing, the DNA was centrifuged at 5000 x g for 15 min at 4 °C. After removal of the supernatant, the pellet was washed with 1 ml 70 % ethanol. The centrifugation step was thereafter repeated. The final pellet was air-dried for 5-10 min and resuspended in 50 µl buffer TE. The concentration of the purified DNA was measured with a Nanodrop spectrophotometer (Thermoscientific, USA). The DNA was then visualized on a 1 % agarose gel, containing 1.25 µg/ml ethidium bromide. Pavetamine was tested at a concentration of 333 µM, doxorubicin at a concentration of 2.5 µM and staurosporine at a concentration of 0.75 µM.

3.2.6.3 DAPI staining of nuclei

DAPI (4',6-diamidino-2-phenylindole) is a fluorescent probe that forms complexes with double-stranded DNA (Kubista *et al*., 1987). The nuclei of H9c2 cells were stained with DAPI after exposure to 20 µM pavetamine or 1 µM rotenone for 72 h. Untreated and pavetamine-treated H9c2 cells were washed twice with PBS and then fixed with acetone for 10 min at -20 °C. Following two washes with PBS, the cells were stained with 3 µM DAPI (Sigma, St. Louis, MO) in PBS for 15 min at 37 °C. The cells were washed twice afterwards with PBS, mounted with ProLong Gold antifade mounting solution (Invitrogen, USA) and visualized with a Zeiss confocal laser scanning microscope, model ZEISS LSM 510 (Jena, Germany). Pavetamine was tested at a concentration of 20 µM and rotenone at a concentration of 1 µM.

3.2.6.4 Release of cytochrome *c* from the mitochondria into the cytoplasm

I) Isolation of mitochondria

A Q-proteome mitochondria isolation kit (Qiagen, Germany) was used to purify mitochondria from cell cultures. Cells were collected by trypsination and centrifuged at 500 x g for 10 min at 4 °C. The cells were washed with 1 ml 0.9 % NaCl. The cells were resuspended in ice-cold lysis buffer, with added protease inhibitor. The cells were chilled on ice for 10 min. The lysate was centrifuged at 1000 x g for 10 min at 4 °C. The supernatant, which contained the cytosolic proteins, was removed and kept at -70 °C for analysis later. The cell pellet was resuspended in 1.5 ml ice-cold disruption buffer and disrupted in a Dounce homogenizer. The lysate was centrifuged at 1000 x g for 10 min at 4 °C and the supernatant carefully transferred to a new 15 ml tube. The supernatant was then centrifuged at 6000 x g for 10 min at 4 °C. The final pellet was resuspended in the mitochondrial storage buffer and kept at -70 °C until further analysis with Western blot.

II) Western blot analysis of mitochondria to stain cytochrome *c*

Cytosolic and mitochondrial fractions were separated on a 12 % SDS Page gel and then transferred to Immobilon P membranes with a Semi-phor Western blotter (Hoefer Scientific Instruments, USA) for 1 h at 80 mA. The membrane was blocked for 1 h with 10 % non-fat milk powder in PBS. The membrane was rinsed with PBS that contained 0.1 % Tween 20 (Merck, Germany). The membrane was incubated for 1 h with shaking in the primary antibody solution, which was a monoclonal antibody to cytochrome *c* (Biomol International, USA) at a concentration of 2 µg/ml. The membrane was then washed 4 times for 5 min each with PBS containing 0.1 % Tween 20. The membrane was then incubated for 1 h with shaking in the conjugate solution which was goat anti-mouse HRP conjugate at a concentration of 1.2 µg/ml (Sigma, St. Louis, MO). The substrate which was used to develop the signals, was Supersignal West Pico chemilumenescent substrate (Pierce, USA).

Statistical analysis

The results were expressed as the mean ± SEM. The Student's *t*-test was used for statistical analyses of the data, with p values of <0.05 considered as significant.

3.3 Results

3.3.1 Cytotoxicity of pavetamine in H9c2 cell culture

Death of H9c2 cells exposed to pavetamine was time- and concentration-dependent. Exposure of H9c2 cells to the highest concentration of pavetamine, 200 µM, induced 27.47 % ± 5.59 cell death after 24 h, as measured by the MTT assay. Exposure of the H9c2 cells for longer periods (48 to 72 h) at a dose of 200 µM, led to about 50 % cell death (Fig. 3.1a). The percentage of dead cells almost doubled from 24 h to 48 h at concentrations of 2 µM, 20 µM and 200 µM. In contrast, cell death increased by only about 5 % after exposing the cells for another 24 h-72 h. Staurosporine at a concentration of 0.6 µM caused 85 % ± 0.002 cell death in 24 h. Pavetamine is thus a slower acting toxin than staurosporine, with a much higher EC_{50}. The percentage cell death of the cells exposed to pavetamine for 72 h correlated with the release of LDH (Fig. 3.1b). Maximum release of LDH (absorbance values between 2 and 2.25) was measured at concentrations of 20 µM and 200 µM pavetamine, respectively, which caused between 40 and 50 % cell death. No release of LDH into the medium was observed after exposing the cells for 24 h or 48 h at the above-mentioned concentrations of pavetamine (results not shown).

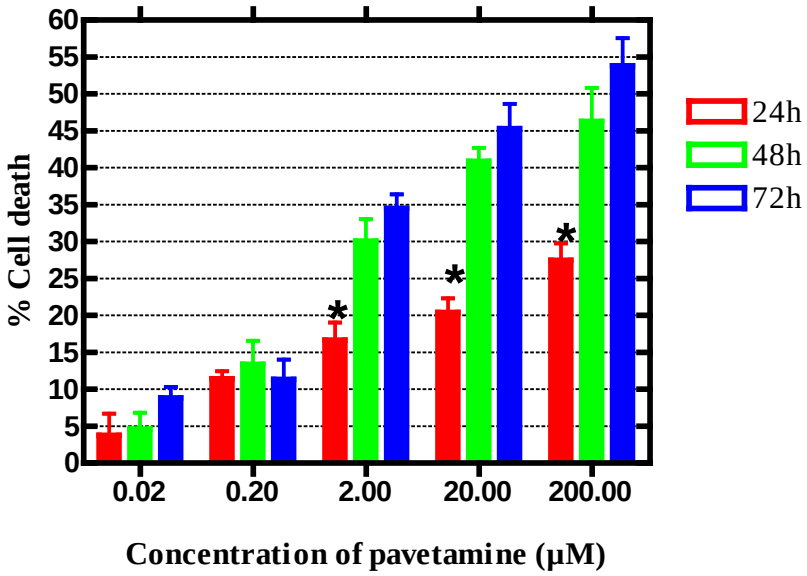

Figure 3.1a The cytotoxicity of pavetamine was measured in H9c2 cells over a period of 3 days, and the percentage cell death, compared to the untreated cells, was measured with the MTT assay. The Student's *t*-test (unpaired, two-tailed) was used to analyze the data *p < 0.05, significant difference between 24 h *versus* 48 h and 24 h *versus* 72 h. No significant difference between 48 h *versus* 72 h. The results represent the average of three independent experiments.

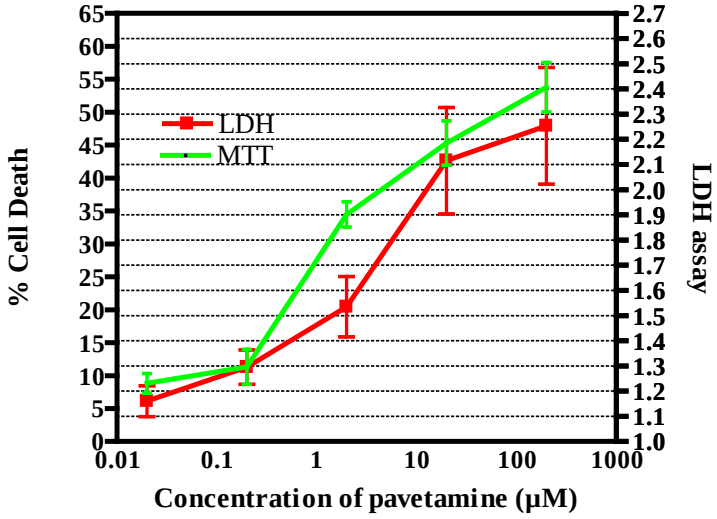

Figure 3.1b Comparison of the percentage cell death and LDH release into the medium in H9c2 cells exposed for 72 h to pavetamine at a concentration of ten-fold serial dilutions. The results represented the average of three independent experiments.

3.3.2 Ultrastructural changes of H9c2 cells induced by pavetamine

H9c2 cells exposed for 24 h, showed abnormal mitochondria (Fig. 3.2c), compared to the untreated cells (Fig. 3.2b). The cristae of the mitochondria were swollen and in some instances lysed, however, the nucleus appeared normal (Fig. 3.2d). Exposure of H9c2 cells to pavetamine for 48 h caused formation of vacuoles (Fig. 3.2e). Lysosomes were present and contained cellular matter, most likely secondary lysosomes. The nuclear membranes were indented and chromatin marginization also occurred (Fig. 3.2f). H9c2 cells exposed to pavetamine for 72 h had numerous empty vacuoles, nucleus fragmentation and abnormal mitochondria (Fig. 3.2g). Membrane blebbing and externalization of cell contents occurred after 72 h (Fig. 3.2g). Untreated H9c2 cells grown for 72 h had none of these features (Fig. 3.2a and 3.2b). H9c2 cells exposed to 0.6 µM staurosporine for 6 h, resulted in the typical crescent moon-shaped chromatin condensation, typical of apoptotic cell death, and swollen rough sarcoplasmic reticula (Fig. 3.2h).

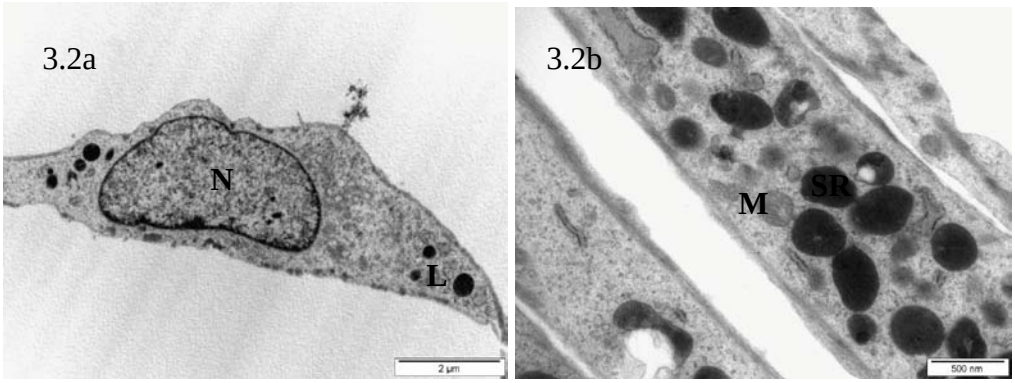

Figure 3.2a and 3.2b Transmission electron micrograph of control H9c2 cells.
SR: sarcoplasmic reticulum. M: mitochondria. L: lysosome. N: nucleus

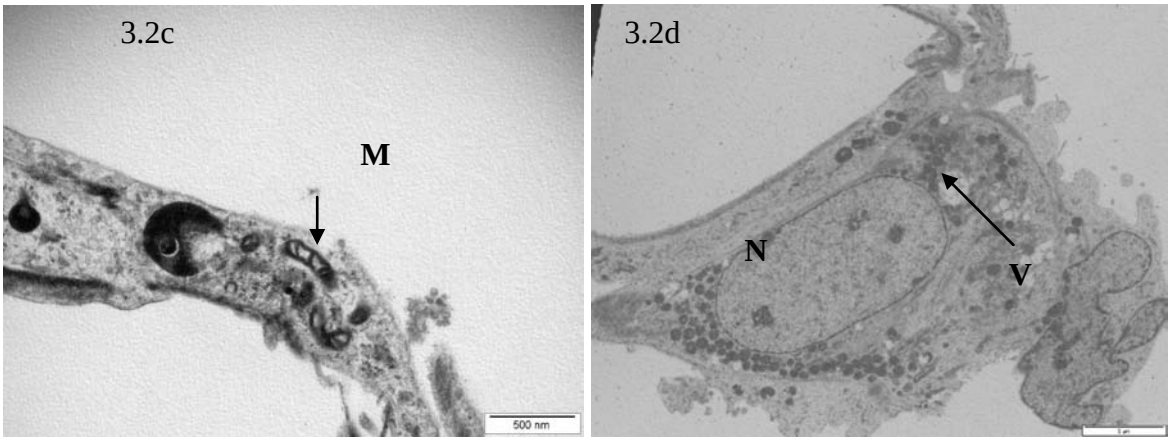

Figure 3.2c and 3.2d Transmission electron micrograph of H9c2 cells treated for 24 h with 20 µM pavetamine. The mitochondria (M) appeared abnormal in shape; the cristae were grossly swollen and lysed. The nucleus (N) appeared normal. Some vacuoles (V) appeared.

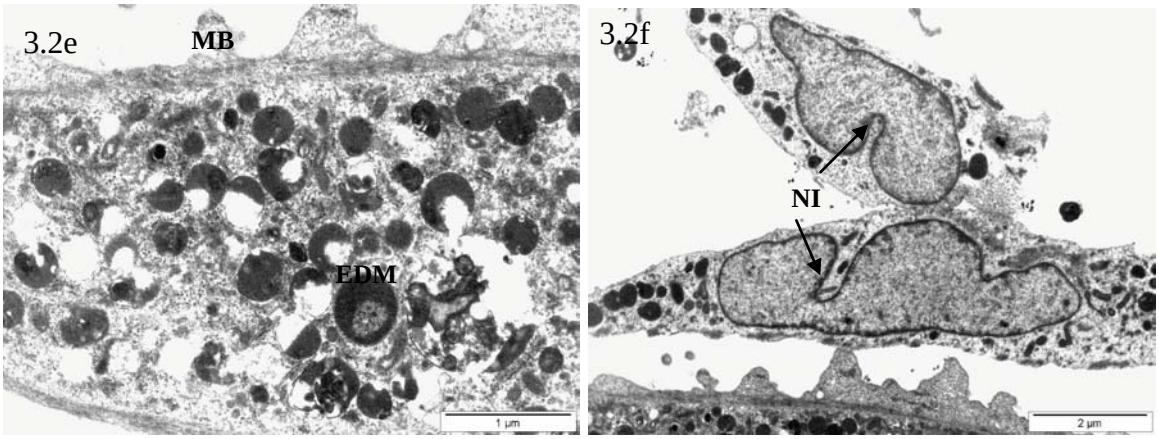

Figure 3.2e Transmission electron micrograph of H9c2 cells treated for 48 h with 20 µM pavetamine. Vacuoles (V) had formed, some containing electron dense material (EDM). Membrane blebbing (MB) also occurred. **Figure 3.2f** The nuclear membrane was indented (NI), but no chromatin condensation occurred.

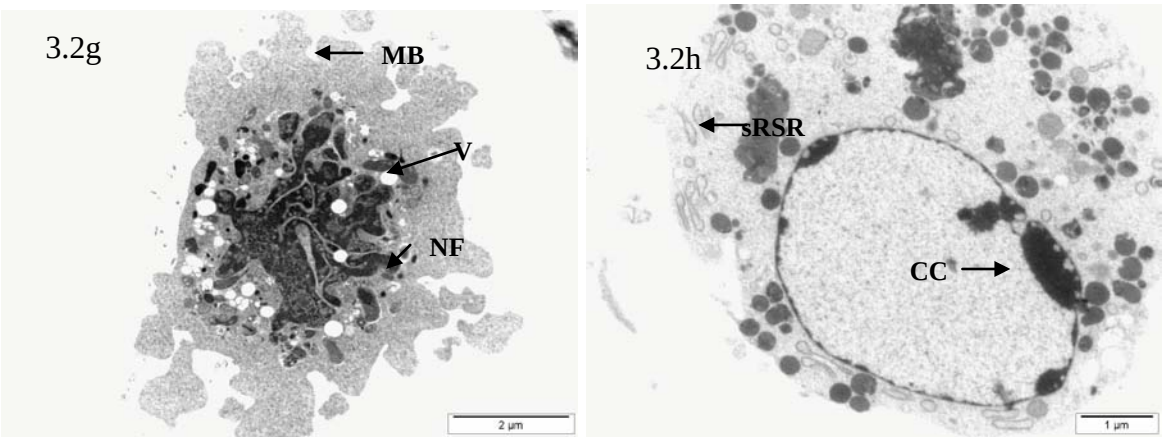

Figure 3.2g Transmission electron micrograph of H9c2 cells treated for 72 h with 20 µM pavetamine. Numerous vacuoles (V) were formed, the nucleus became fragmented (NF) and membrane blebbing (MB) occurred. **Figure 3.2h** Transmission electron micrograph of H9c2 cell exposed to 0.6 µM staurosporine for 6 h. Staurosporine caused chromatin condensation (CC) and the sarcoplasmic reticula became swollen (sRSR).

3.3.3 Mitochondrial analyses

3.3.3.1 Measurement of mitochondrial membrane potential of the inner mitochondrial membrane with JC-1 and TMRM

JC-1 is a dual fluorescent probe and at low ΔΨm potential JC-1 is a green fluorescent monomer. At higher ΔΨm JC-1 forms red fluorescent J-aggregates. Exposure of H9c2 cells to 20 µM pavetamine for 24 h caused significant hyperpolarization of the mitochondrial ΔΨm, as measured with the JC-1 probe, with an average ratio of red to green fluorescence of 17.12 ± 0.97, compared to untreated cells, which had a ratio of 12.4 ± 0.40 (Fig. 3.3a). Valinomycin caused significant depolarization or collapse of the mitochondrial membrane potential, as compared to untreated cells. The average red to green fluorescence for cells treated with valinomycin was 0.52 ± 0.13. As can be seen in Fig. 3.3b, pavetamine caused an increase in the intensity of stained mitochondria with TMRM, compared to untreated H9c2 cells, thus confirming that pavetamine causes hyperpolarization of the mitochondrial membrane potential, irrespective of the plasma membrane potential.

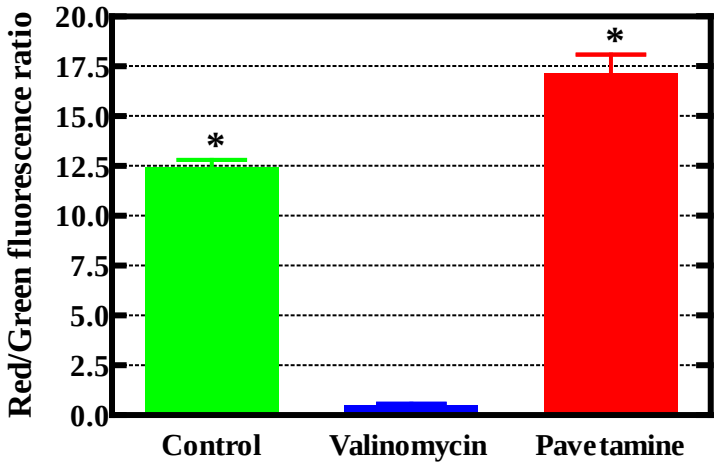

Figure 3.3a Mitochondrial membrane potential of H9c2 cells exposed to 20 µM pavetamine for 24 h. The mitochondrial membrane potential was determined with the fluorescent probe JC-1. The results represent the average of three independent experiments. The difference between the control and pavetamine-treated cells was significant with the unpaired, two-tailed Student's *t*-test (* $p<0.05$).

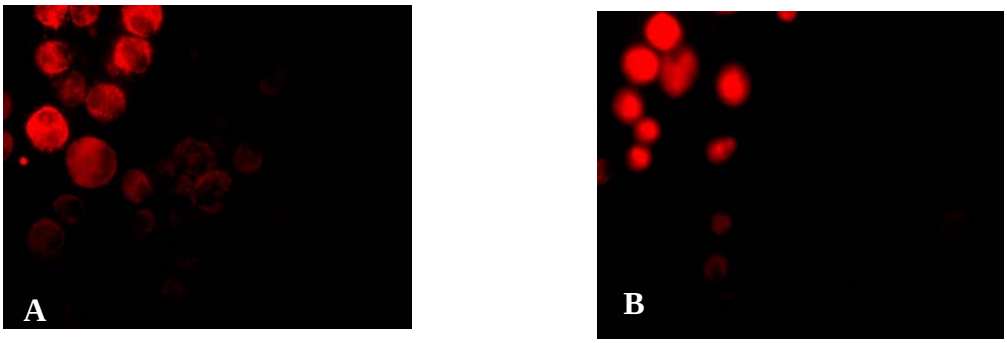

Figure 3.3b Measurement of mitochondrial membrane potential with tetramethylrhodamine methyl ester perchlorate (TMRM).A: untreated cells that served as control; B: H9c2 cells 24 h post-exposure to 20 µM pavetamine.

3.3.3.2 Cytotoxicity of pavetamine in the presence of cyclosporine A, an inhibitor of the mitochondrial permeability transition pore

The mean percentage cell survival of cells exposed to pavetamine was 70.24 % ± 1.84 (n=12), compared to the untreated cells, while the mean percentage survival of cells treated with pavetamine and cyclosporin A was 73.05 % ± 1.82 (n=12) (Fig. 3.4). This difference was not significant.

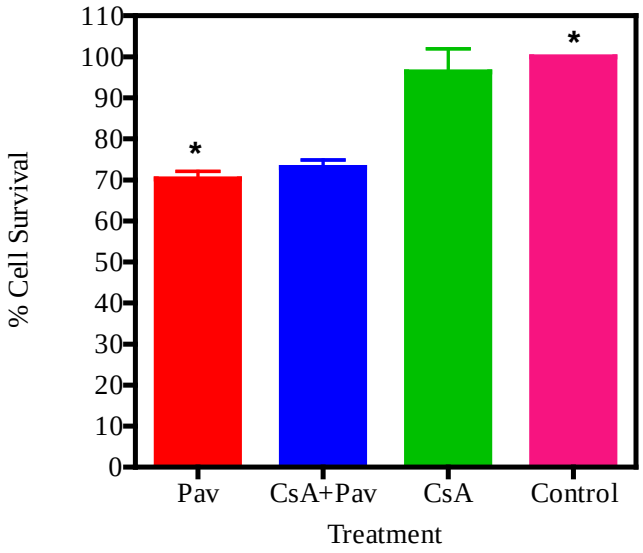

Figure 3.4 Cytotoxicity of 20 µM pavetamine in the presence or absence of 1 µM CsA. The cells were exposed for 48 h to 20 µM pavetamine. No significant difference was observed between pavetamine-treated cells and pavetamine-treated cells in the presence of CsA. Significant differences *($p<0.05$) with the Student's *t*-test were observed between cells treated with pavetamine only and untreated cells that served as controls. Pav: pavetamine; CsA: cyclosporin A.

3.3.4 Evaluation of apoptosis

Pavetamine at a concentration of 200 µM did not cause a significant increase in caspase 3 activity in H9c2 cells exposed for 6 h (Fig. 3.5a). However, staurosporine caused a significant

increase in caspase 3 activity in H9c2 cells exposed for 6 h. Longer exposure of H9c2 cells to pavetamine, *inter alia* 48 to 72 h, did not significantly activate caspase 3 (Fig. 3.5b).

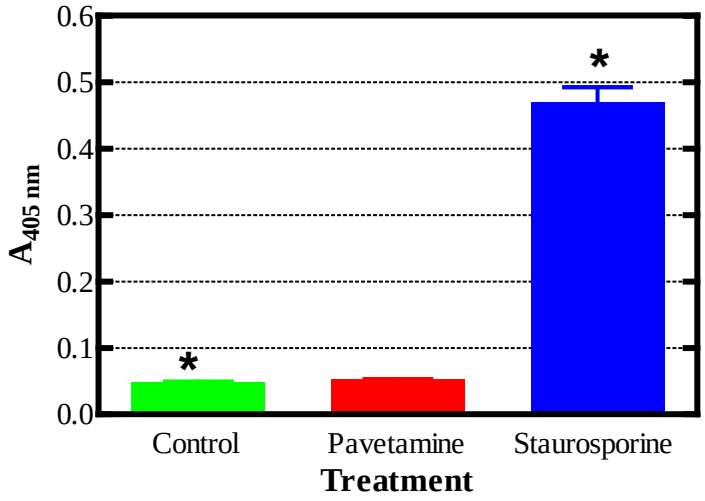

Figure 3.5a Caspase 3 activity studied after 6 h exposure. Pavetamine was tested at a concentration of 200 µM, while staurosporine was tested at a concentration of 0.6 µM.
* significant different from control, $p < 0.05$.

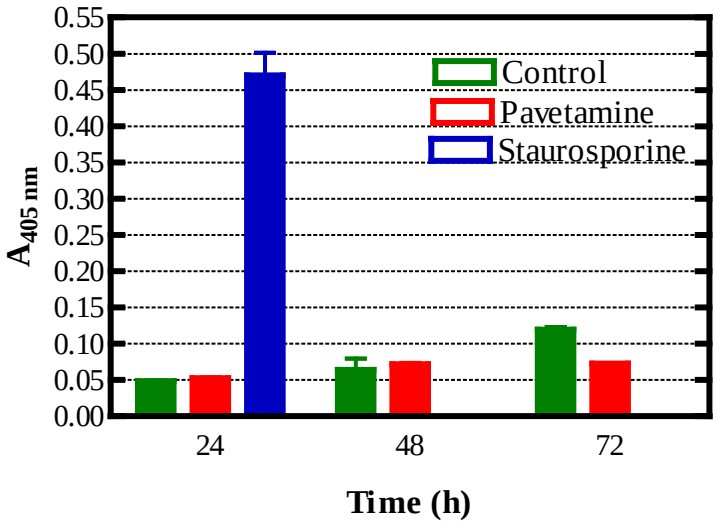

Figure 3.5b Caspase activation after 24, 48 and 72 h exposure to pavetamine and 24 h exposure to staurosporine.

Cells undergoing apoptosis have the typical DNA fragmentation or laddering features. H9c2 cells exposed to 333 µM pavetamine, 2.3 µM doxorubicin or 0.75 µM staurosporine for 24 h, were analysed for DNA laddering (Fig. 3.6). Genomic DNA was isolated and analysed with agarose gel electrophoresis. Neither pavetamine nor doxorubicin caused DNA laddering in H9c2 cells exposed for the indicated time periods. Staurosporine caused the typical apoptotic DNA laddering or fragmentation with fragments ranging in size from 10 kbp to less than 0.5 kbp (Fig. 3.6).

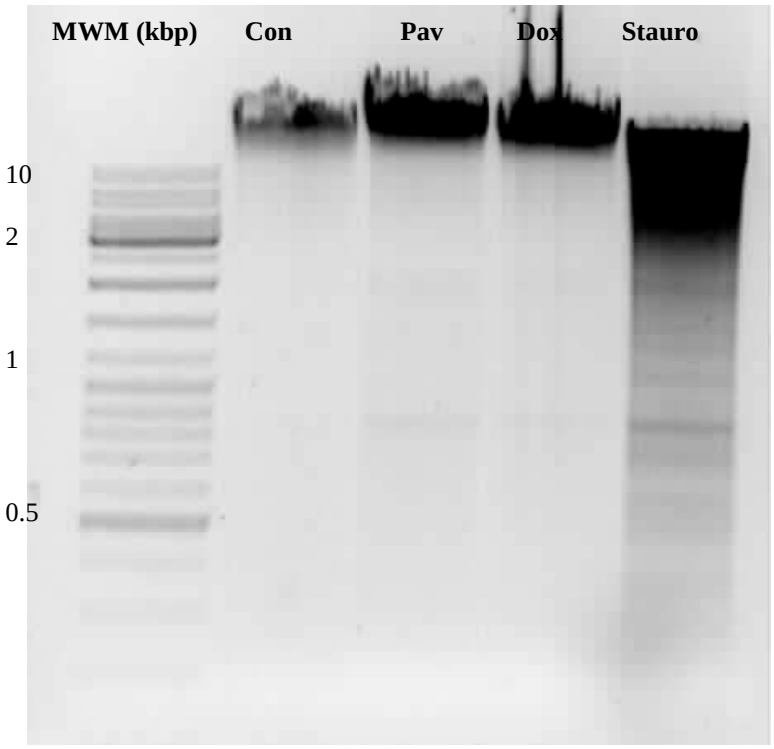

Figure 3.6 DNA fragmentation of H9c2 cells treated with pavetamine, doxorubicin and staurosporine for 24 h. Con, control cells; Pav, 333 µM pavetamine; Dox, 2.3 µM doxorubicin; Stauro, 0.75 µM staurosporine.

DAPI staining was performed on H9c2 cells that were treated with 20 µM pavetamine and 1 µM rotenone for 48 h. Rotenone-treated cells had typical fragmented nuclei. The nuclei of cells treated with pavetamine were elongated. In one image a fragmented nucleus was observed (arrow) (See arrow in Fig. 3.7).

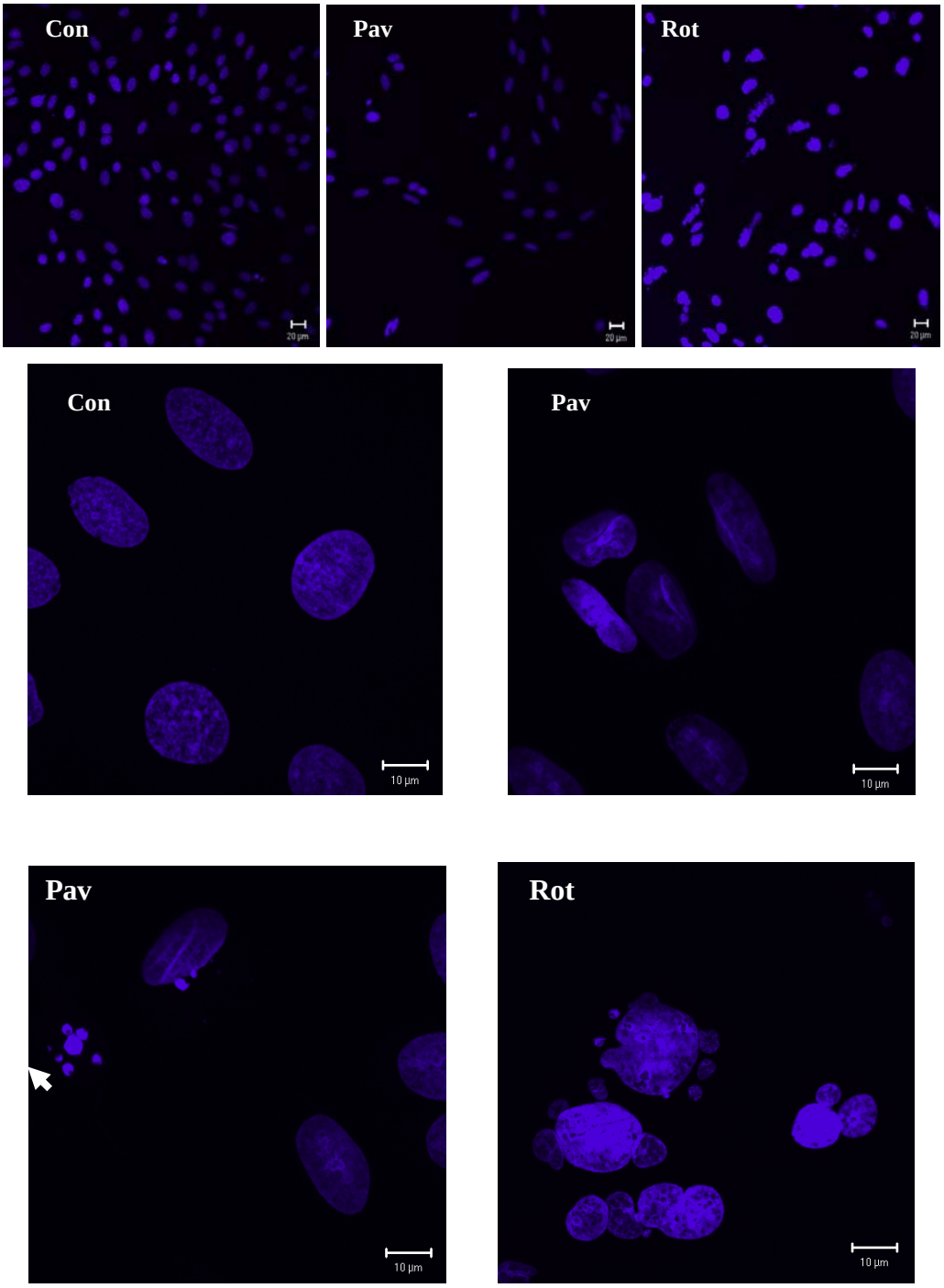

Figure 3.7 Fluorescent staining of nuclei with DAPI of cells exposed to 20 µM pavetamine (Pav) for 48 h. Untreated cells (Con) served as controls. Rotenone (Rot) was used as an apoptotic inducer.

As clearly seen in Fig. 3.8, some of the pavetamine-treated cells had an indented nucleus (star), disintegrated nuclei (dotted arrow) or pores in the nuclei (arrow).

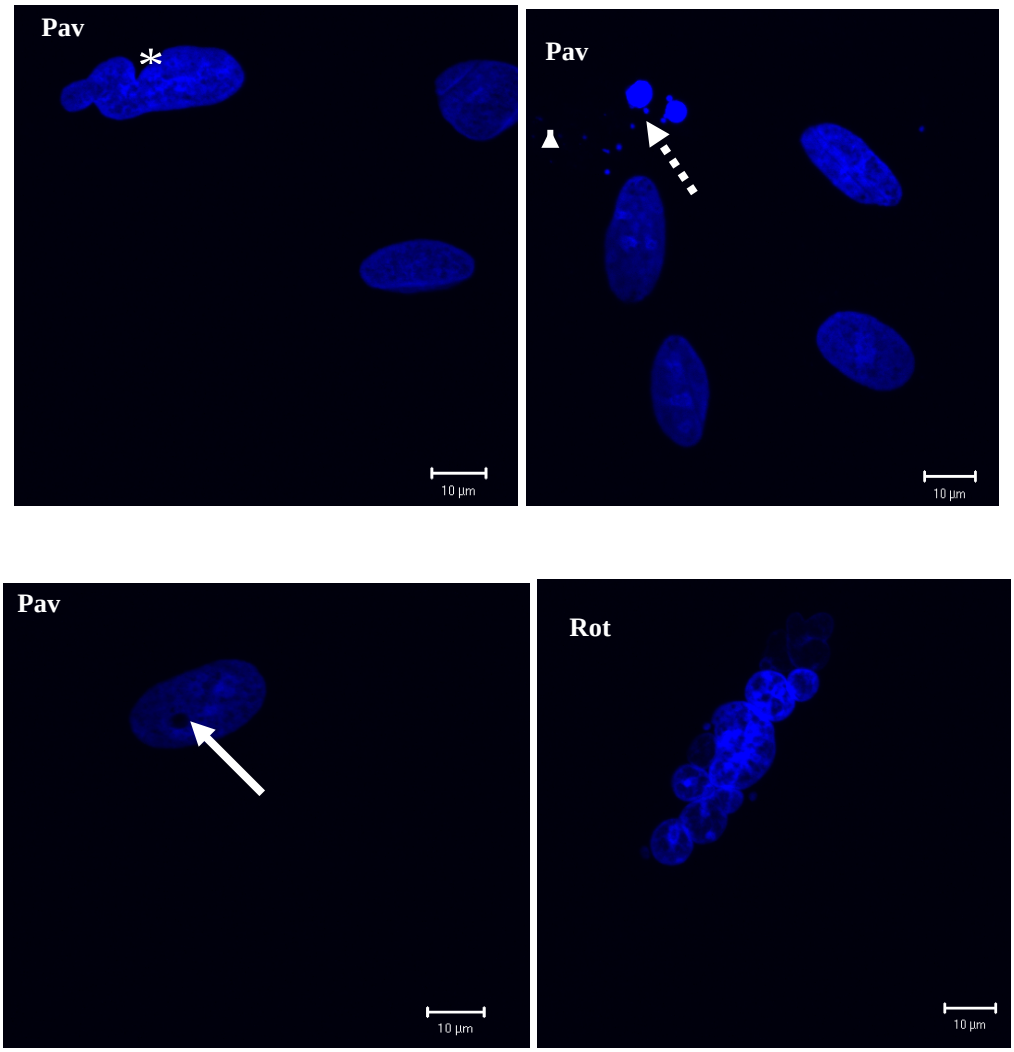

Figure 3.8 Nuclei of H9c2 cells visualised with DAPI, after exposure to 20 µM pavetamine (Pav) or 1 µM rotenone (Rot) for 72 h.

For cytochrome *c* release into the cytoplasm, H9c2 cells, in 75 cm^2 cell culture flasks, were exposed to 666 µM pavetamine and 4.7 µM doxorubicin for 24 h. Cytoplasmic and mitochondrial fractions of untreated and treated H9c2 cells were prepared and analysed with Western blot analyses with a monoclonal antibody to cytochrome *c*. The molecular weight of

cytochrome *c* is 12.4 kDa. Treatment of H9c2 cells with pavetamine did not release cytochrome *c* into the cytoplasm (Fig. 3.9, lane 4). Surprisingly, doxorubicin also did not release cytochrome *c* into the cytoplasm.

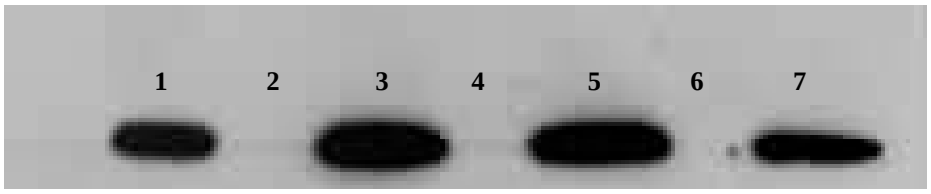

Figure 3.9 Western blot analysis of cytochrome *c* release from mitochondria. 1) Control mitochondrial fraction, 2) control cytosolic fraction, 3) control mitochondrial fraction, 4) cytosolic fraction of cells treated with pavetamine, 5) mitochondrial fraction of cells treated with pavetamine, 6) cytosolic fraction of cells treated with doxorubicin, 7) mitochondrial fraction of cells treated with doxorubicin.

3.4 Discussion

An interesting feature of gousiekte is the long latent period following ingestion of the causative rubiaceous plants, before ruminants eventually succumb due to heart failure. In the cardiac cell line H9c2, used as an *in vitro* model in this study, maximal cell death occurred 72 h post-exposure of the cells to pavetamine at concentrations of 20 µM and 200 µM, as determined by the MTT and LDH assays. The cause of death of these H9c2 cells 72 h after exposure to pavetamine, is necrosis, as maximal release of LDH (a hallmark of necrotic cell death) into the medium occurred at this time. Features of apoptosis were investigated, but apoptosis was not induced by pavetamine. H9c2 cells treated with pavetamine and other compounds were tested for activation of caspase 3, DNA fragmentation and cytochrome *c* release from the mitochondria, all features of apotptotic cell death. Known apoptotic inducers include doxorubicin, staurosporine and rotenone. Doxorubicin intercalates with DNA (Box, 2007) and was previously thought to form reactive oxygen species (ROS) (Horenstein *et al*., 2000) but Bernuzzi *et al.* (2009) suggested that doxorubicin down-regulates the anti-apoptotic protein haeme oxygenase-1. Staurosporine is a potent inhibitor of protein kinase C and

activates caspase 3 (Yue *et al*., 1998). Rotenone, a plant chemical used as insecticide and pesticide, inhibits complex I (NADH dehydrogenase) of the electron transfer chain in mitochondria (Lindahl & Oberg, 1961). Inhibition of complex I by rotenone produces O_2^- and causes lipid peroxidation (Koopman *et al*., 2005). Pavetamine did not cause caspase 3 activation nor DNA fragmentation. Nuclei of pavetamine-treated cells, stained with DAPI, were mostly intact and did not exhibit the features of rotenone-treated cells with typical fragmented nuclei. Release of cytochrome *c* was neither observed for pavetamine nor for doxorubicin. Two possible explanations are offered: either the Western blots lack adequate sensitivity to detect low levels of cytochrome *c* in the cytoplasm, or doxorubicin has auto-oxidized, which may explain the lack of DNA laddering. These results are thus inconclusive as to whether or not pavetamine causes cytochrome *c* release.

Mitochondria in H9c2 cells, exposed to pavetamine for 24 h were extensively damaged. It caused hyperpolarization of the mitochondrial membrane potential, swollen cristae and in some instances lysis of cristae. Although mitochondrial uptake of JC-1 can be limited by the plasma membrane potential ($\Delta\Psi p$) (Rottenberg & Wu, 1998), the TMRM is a sensitive probe for measuring the mitochondrial membrane potential and the uptake of this dye is independent of the plasma membrane potential. For this reason TMRM was also employed to verify the increase in the mitochondrial membrane potential. Opening of the MPTP leads to depolarization of the mitochondrial membrane potential, with an influx of H^+ ions, release of cytochrome *c* and consequently apoptotic cell death (Leung & Halestrap, 2008). When cyclosporin A binds to cyclophilin D, i.e. part of the MPTP, it causes inhibition of the MPTP and therefore prevents apoptosis (Crompton *et al*., 1988). The addition of CsA did not contribute significantly to a reduction in the cytotoxicity of pavetamine, thus eliminating the MPTP opening as a mechanism of cell toxicity.

Pavetamine-containing plants (*P. pygmaeum*, *F. homblei*, *P. harborii*) induced dilatation and proliferation of the SR in sheep (Prozesky *et al*., 2005). Pretorius and colleagues (1973) reported reduced uptake of Ca^{2+} by the SR of sheep treated with pavetamine-containing plants (*P. pygmaeum* and *P. harborii*). It was originally thought that the MTT assay measures enzyme activities in the mitochondria (Johnston *et al*., 1993), but it has recently been proven that enzymes in the endoplasmic reticulum are responsible for the reduction of MTT

(Berridge *et al*., 1996). The MTT cytotoxicity assay for pavetamine in the H9c2 cells thus measured the activity of the SR enzymes. The cytosolic free ribosomes are the site where protein synthesis occurs, but depending on cell type, up to 35 % of protein synthesis can actually take place in the endoplasmic reticulum (Glembotski, 2008). After proteins are synthesized, they must be correctly folded. Any disturbances in this folding process, will lead to the accumulation of misfolded proteins, which in turn will activate the ubiquitin-proteasome pathway (Glembotski, 2007). The unfolded protein response (UPR) is the SR-associated protein quality control in the cell, together with the cytosolic protein quality control system (Glembotski, 2008). It has now been ascertained that pavetamine caused inhibition of protein synthesis in rat hearts as early as 4 h after administration of pavetamine intraperitoneally at a concentration of 8-10 mg/kg live mass (Schultz *et al*., 2001). There is also the possibility of increased degradation of cardiac proteins by the UPS, as speculated by these authors.

Two systems exist in the cell for protein and organelle turnover, namely autophagy for damaged organelle turnover, especially the mitochondria and the SR (Klionsky & Emr, 2000), and the ubiquitin-proteasome pathway for oxidized and misfolded proteins (Glembotski, 2007). The late-endosomes, autophagosomes and molecular chaperones fuse with the lysosome where degradation of damaged constituents occurs (Buja & Vela, 2008). Autophagy is characterized by the formation of vacuoles in the absence of nuclear chromatin condensation with mitochondrial and endoplasmic reticular swelling as studied with TEM (Gozuacik & Kimshi, 2004; Martinet *et al*., 2007). H9c2(2-1) cells, treated for 48 h, had numerous vacuoles, possibly indicative of autophagy.

In conclusion, pavetamine caused damage to the mitochondria and caused SR aberrations in H9c2 cells. It is therefore surmised that this could either be by inhibition of one or more enzymes of Complex I-V, or by the production of ROS and/or interference with Ca^{2+} homeostasis. Damaged organelles were degraded, possibly by autophagy and misfolded or oxidized proteins, degraded by the ubiquitin-proteasome pathway, followed by necrosis as the eventual cell death pathway.

CHAPTER 4
A FLUORESCENT INVESTIGATION OF SUBCELLULAR DAMAGE IN H9C2 CELLS CAUSED BY PAVETAMINE, A NOVEL POLYAMINE

4.1 Introduction

Gousiekte ("quick disease") is a disease of ruminants characterized by acute heart failure without any premonitory signs four to eight weeks after the initial ingestion of certain rubiaceous plants (Theiler *et al*., 1923; Pretorius & Terblanche, 1967). The toxic compound, pavetamine, causing gousiekte was isolated from *Pavetta harborii* (Fourie *et al*., 1995). Ultrastructural changes were observed in the heart of sheep, intoxicated with extracts of *Pachystigma pygmaeum* as well as dried plants known to cause gousiekte. Disintegration of the myofibres, which appeared frayed, was accompanied by replacement fibrosis (Schutte *et al*., 1984; Kellerman *et al*., 2005; Prozesky *et al*., 2005). In addition, mitochondria varied in shape and size, with ruptured swollen cristae, and the SR were dilated and proliferated (Prozesky *et al*., 2005). Schultz and co-workers (2001) reported that pavetamine, administered intraperitoneally to rats, inhibits protein synthesis in the heart, but not in the liver, kidney, spleen, intestine and muscle. Exposure of H9c2 cells (derived from embryonic rat cardiac cells) to pavetamine, caused damage to mitochondria and SR, as demonstrated by TEM (Ellis *et al*., 2010). Eventual death of H9c2 cells after exposure to 20 µM pavetamine for 72 h was attributed to necrosis, with membrane blebbing and lactate dehydrogenase (LDH) release into the medium (Ellis *et al*., 2010).

Cardiomyocytes, performing vigorous mechanical work for an entire lifetime, have elegant mechanisms for protein quality control (PQC) (Wang *et al*., 2008). Protein synthesis occurs on cytosolic free ribosomes, and depending on cell type, in the rough SR (Blobel, 2000). In the SR, numerous chaperones, other proteins and factors ensure efficient protein folding, as part of the SR-associated PQC. For efficient protein folding during protein synthesis, the correct redox status is required for protein disulfide bond formation (Glembotski, 2008). ER stressors, namely dithiothreitol, thapsigargin and calcium levels, impair proper folding of proteins and lead to the accumulation of mis-folded and dysfunctional proteins, thereby

triggering the unfolded protein response (UPR) (Kozutsumi *et al*., 1988). Cardiomyocytes, in which the myofibrillar proteins occupy more than 80 % of the cell volume, have an SR-independent PQC, namely the UPS (Wang *et al*., 2008). Target proteins are ubiquitinated by ubiquitin E3 ligases and degradation occurs on the 26S proteasome. Proteolysis in cardiomyocytes can also occur via calpains and caspases.

The cytoskeleton of cardiomyocytes consists of actin microfilaments, microtubules and intermediate filaments (Kustermans *et al*., 2008). Actin has several essential roles, namely cell motility, membrane dynamics, endocytosis, exocytosis, vesicular trafficking and cytokinesis (Lanzetti, 2007; Kustermans *et al*., 2008). G-actin (globular-actin) exists as a monomer and is bound to ATP, whereas F-actin (filamentous actin) is a linear polymer (Kustermans *et al*., 2008). Many actin-binding proteins regulate the dynamics of actin polymerization (the coordinated assembly and disassembly of actin filaments in response to cellular signalling) (Kustermans *et al*., 2008). Actin is also found in the nucleus and is an important regulator of transcription, chromatin remodeling and transcription factor activity (Vartiainen, 2008). Furthermore, cardiac L-type calcium channel regulation is tightly controlled by actin filament organization (Lader *et al*., 1999; Rueckschloss & Isenberg, 2001).

The purpose of this study was to determine the effect of pavetamine on the structure of the mitochondria, SR, lysosomes and the F-actin cytoskeleton in the H9c2 cell line, a subclone derived from embryonic rat heart tissue, using fluorescent probes.

4.2 Materials and Methods

4.2.1 Chemicals

Cytochalasin D (CytoD), thapsigargin, digitonin, Dulbecco's modified Eagle's medium (DMEM), fast red violet LB, magnesium chloride ($MgCl_2$), naphthol phosphate AS-BI, phalloidin-FITC, *p*-nitrophenyl-*N*-acetyl-β-D-glucosaminide and thapsigargin were purchased from Sigma-Aldrich (St. Louis, MO, USA). Foetal calf serum (FCS) and penicillin-streptomycin were purchased from Gibco (Grand island, NY, USA). ER-Tracker Green dye, MitoTracker Green FM dye, Lysosensor Green DND-189 probe and ProLong Gold antifade reagent were purchased from Invitrogen (Eugene, OR, U.S.A.). DAPI (4',6-diamidino-2-

phenylindole) was purchased from Roche Diagnostics (Mannheim, Germany) and *N′*-*N′*-dimethylformamide was obtained from BDH Chemicals Ltd. (Poole, England).

4.2.2 H9c2 cell line

The H9c2 cell line (Kimes & Brandt, 1976) was obtained from the American Type Culture Collection (cat no: CRL-1446^{TM}, Manassas, USA). The cells were grown on sterile glass coverslips in DMEM, supplemented with 10 % FCS and 100 U/ml penicillin-100 µg/ml streptomycin sulphate.

4.2.3 Purification of pavetamine

Pavetamine was extracted and purified from the leaves of *P. harborii* S.Moore, collected near Ellisras (23°32´S, 27°42´E) in the Limpopo province, South Africa, by staff at the ARC-OVI Toxicology department according to the method described by Fourie *et al*., 1995. The yield during 2007 to 2008 was 2.7 mg pavetamine per kg dried material.

4.2.4 Treatment of H9c2 cells

H9c2 cells were treated with 20 µM pavetamine and untreated cells served as controls. In addition, they were also exposed to 3 µM thapsigargin, an ER stressor. In a previous study using TEM, pavetamine caused damage to the mitochondria and SR of H9c2 cells after 24 h of exposure, and secondary lysosomes only appeared after 48 h of exposure to pavetamine (Ellis *et al*., 2009). For this reason, the H9c2 cells were stained after 24 h and 48 h exposure periods to detect organelle damage, and only stained after 48 h exposure to determine lysosomal defects. Cells were incubated in a humidified atmosphere of 5 % CO_2 at 37 °C.

4.2.5 Fluorescent staining

Labeling of H9c2 cells was done with probes to stain subcellular organelles. The images in the figures are derived from three independent experiments with the aim being to study qualitative differences between control cells and H9c2 cells treated with pavetamine.

4.2.5.1 Staining of the sarcoplasmic reticulum

After 24 h and 48 h exposure periods, the cells were washed twice for 5 min each with Hank's balanced salt solution (HBSS), containing 1 % FCS. They were then fixed in 100 % acetone for 10 min at -20 °C, followed by staining with 20 µM ER-Tracker Green dye for 30 min at 37 °C and two final 5 min washes with HBSS/1 % FCS.

4.2.5.2 Staining of mitochondria

After 24 h and 48 h exposure periods, the cells were washed twice for 5 min at a time with DMEM/1 % FCS, stained with 0.2 µM MitoTracker Green FM dye for 45 min at 37 °C and washed twice for 5 min with DMEM/1 % FCS.

4.2.5.3 Staining of lysosomes

After a 48 h exposure period, the cells were washed twice for 5 min each with PBS/1 % FCS, stained with 1 µM Lysosensor Green DND-189 probe for 30 min at 37 °C, followed by two final washes for 5 min each time with PBS/1 % FCS.

4.2.5.4 Staining of F-actin cytoskeleton

After pavetamine exposure for 24 h or 48 h, the F-actin of H9c2 cells was stained with phalloidin-FITC. Cytochalasin D (CytoD), a cell-permeable mycotoxin and an inhibitor of actin polymerization, were included as a positive control. H9c2 cells were exposed to 12 µM CytoD for 10 min. Briefly, the cells were washed with PBS for 5 min, followed by fixation in 100 % ice-cold acetone at -20 °C for 10 minutes. They were then washed twice with PBS for

5 min and stained with phalloidin-FITC (diluted to 1 µg/ml in PBS) for 30 min at 37 °C. The washing was repeated and the nuclei were then stained with 1.3 µg/ml 4',6-diamidino-2-phenylindole (DAPI) for 15 min at 37 °C, followed by two 5 min washes in PBS.

4.2.5.5 Fluorescence microscopy

After staining and washing, the coverslips were mounted on microscopy glass slides using ProLong Gold antifade reagent. Fluorescence imaging was performed using a confocal laser scanning microscope (CLSM) (Model LSM 510, ZEISS, Germany).

4.2.6 Determination of lysosomal hexosaminidase activity

The hexosaminidase activity was determined according to the method described by Theodossiou *et al*. (2006), with a few modifications. Untreated H9c2 cells and H9c2 cells exposed for 48 h with 20 µM pavetamine, were harvested by trypsinization. Cells were washed with PBS and resuspended in 1200 µl PBS. Thereafter, 500 µl of the cell suspensions were transferred to 1.5 ml microcentrifuge tubes and centrifuged for 1 min at 720 x g. The supernatants were removed and the cell pellets resuspended in 500 µl of 5 µM digitonin in 0.1 M citric acid (pH 4.5), and incubated for 20 min at room temperature. The cells were then centrifuged at 5000 x g for 1 min and the supernatants collected. An amount of 500 µl of each supernatant was added to 500 µl of 3.75 mM *p*-nitrophenyl-*N*-acetyl-β-D-glucosaminide (in 0.1 M citric acid (pH 4.5) and incubated at 37 °C for 2 h. The reactions were stopped by the addition of 500 µl of 0.1 M carbonate buffer, pH 10.0. The absorbance values were measured at a wavelength of 404 nm in a UV-160A UV/visible spectrophotometer (Shimadzu, North America). The protein content was determined with a Bio-Rad protein assay reagent (Bio-Rad Laboratories, California, USA). The results were expressed as the mean ± standard error of the mean (SEM). The Student's *t*-test was used for statistical analysis of the data, with p values of <0.05 considered to be significant.

4.2.7 Determination of acid phosphatase activity

The activity of acid phosphatase was determined according to the method of Malagoli *et al*. (2006). Briefly, H9c2 cells cultured on coverslips, were treated with 20 µM pavetamine for 48 h in a humidified 5 % CO_2 incubator. For the acid phosphatase activity assay, both control and pavetamine-treated cells were incubated for 4 h at 37 °C in a 0.1 N sodium acetate–acetic acid buffer (pH 5.0) containing 0.01% naphthol phosphate AS-BI, 2 % *N′*-*N′*-dimethylformamide 0.06 % fast red violet LB and 0.5 mM $MgCl_2$. Light microscopy images were acquired using a microscope (Leica, Model CTR6000, Germany) fitted with a digital camera system (Leica, DFC490, Germany).

4.3 Results

The SR of 20 µM pavetamine treated H9c2 cells (Fig. 4.1B) differered in appearance from that of the control cells (Fig. 4.1A). The SR of treated cells was less compact than those of the control cells and appeared more granular (Fig. 4.1B-F), or even collapsed (Fig. 4.1C). The SR in Fig. 4.1D appeared more abundant, compared to the control cells (Fig. 4.1A). After exposure to pavetamine for 48 h, the SR accumulated around the nuclei (Fig. 4.1E-F). In Fig. 4.1G-H, cells treated with 3 µM thapsigargin demonstrated more numerous and denser SR, compared to the control cells (Fig. 4.1A).

Staining of H9c2 cells exposed to 20 µM pavetamine using MitoTracker Green FM dye revealed abnormal mitochondria (Fig. 4.2B-D). In the control cells (Fig. 4.2A), the mitochondria were evenly distributed around the nucleus, whereas after 24 h of pavetamine treatment, however, the mitochondria relocated towards one pole of the cell (Fig. 4.2B) and became more elongated (Fig. 4.2C). The mitochondria of H9c2 cells exposed for 48 h to 20 µM pavetamine (Fig. 4.2D) disintegrated and the fluorescence faded rapidly.

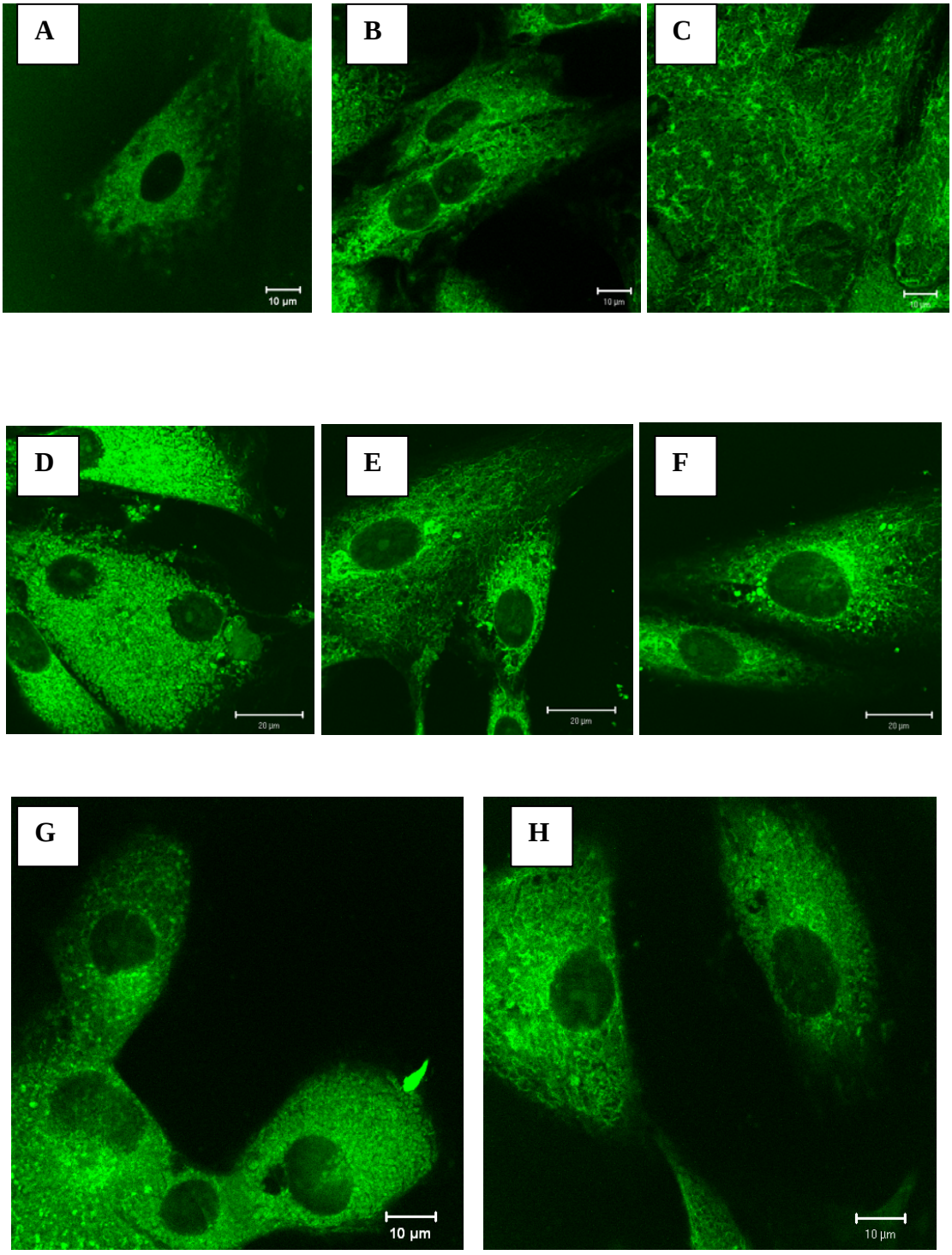

Figure 4.1 H9c2 cells stained with ER Tracker for labeling of sarcoplasmic reticula . A: untreated control cells; B-D: cells treated with 20 µM pavetamine for 24 h; E-F: cells treated with 20 µM pavetamine for 48 h; G-H: cells treated with 3 µM thapsigargin for 24 h.

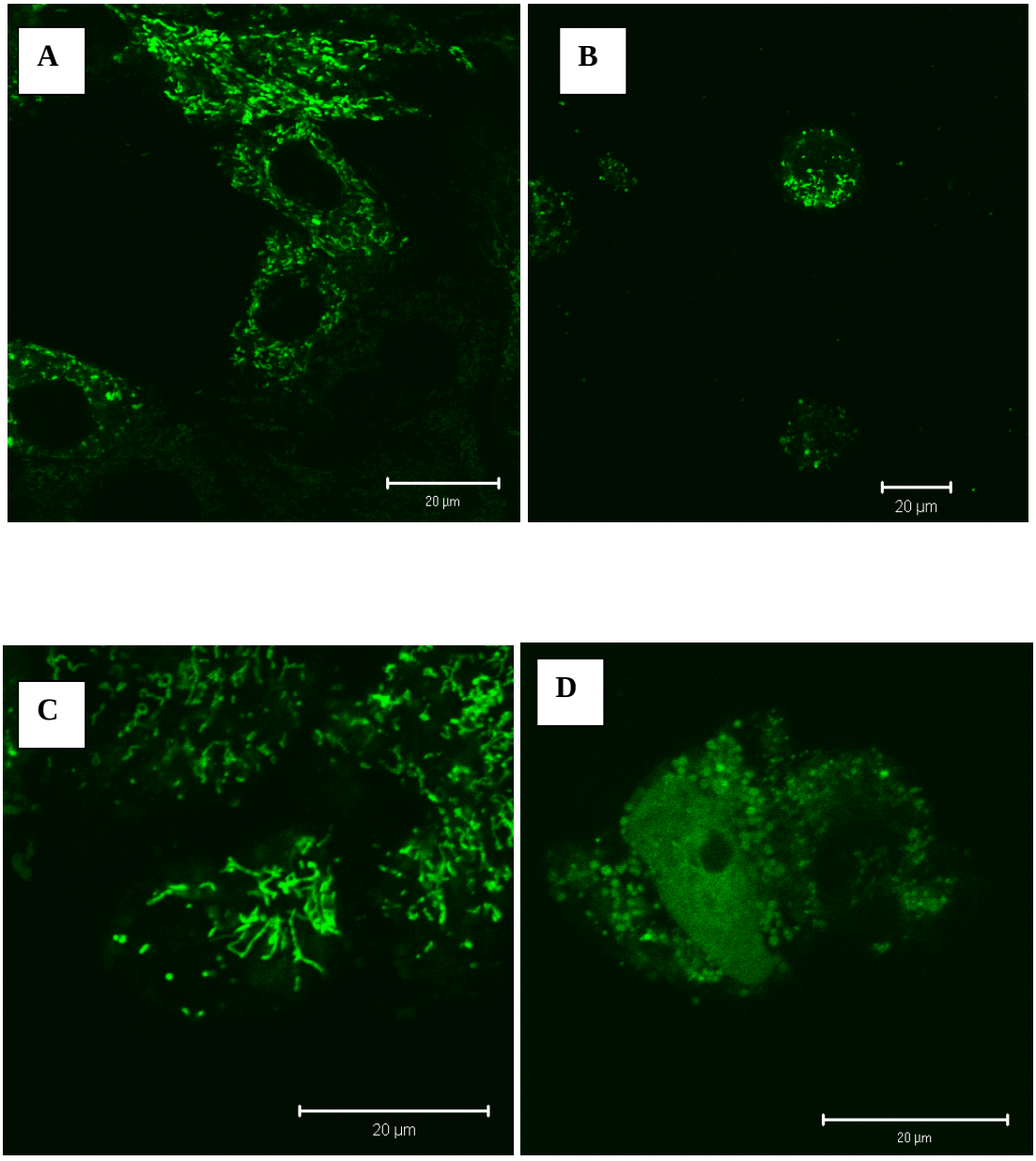

Figure 4.2 H9c2 cells stained with MitoTracker Green for labeling of mitochondria. A: untreated control cells; B-C: cells treated with 20 µM pavetamine for 24 h; D: cells treated with 20 µM pavetamine for 48 h.

Staining of the lysosomes with the LysoSensor probe revealed a number of aberrations in cells treated with pavetamine (Fig. 4.3B-D). An increase in the number and size of lysosomes was noted in H9c2 cells exposed for 48 h to 20 µM pavetamine, (Fig. 4.3B-D), in comparison to untreated control cells (Fig. 4.3A). The lysosomes relocated to the periphery of the cell

(Fig. 4.3B-3D), whilst those in Fig. 4.3C were marketly swollen, with weak fluorescence on the outer edge.

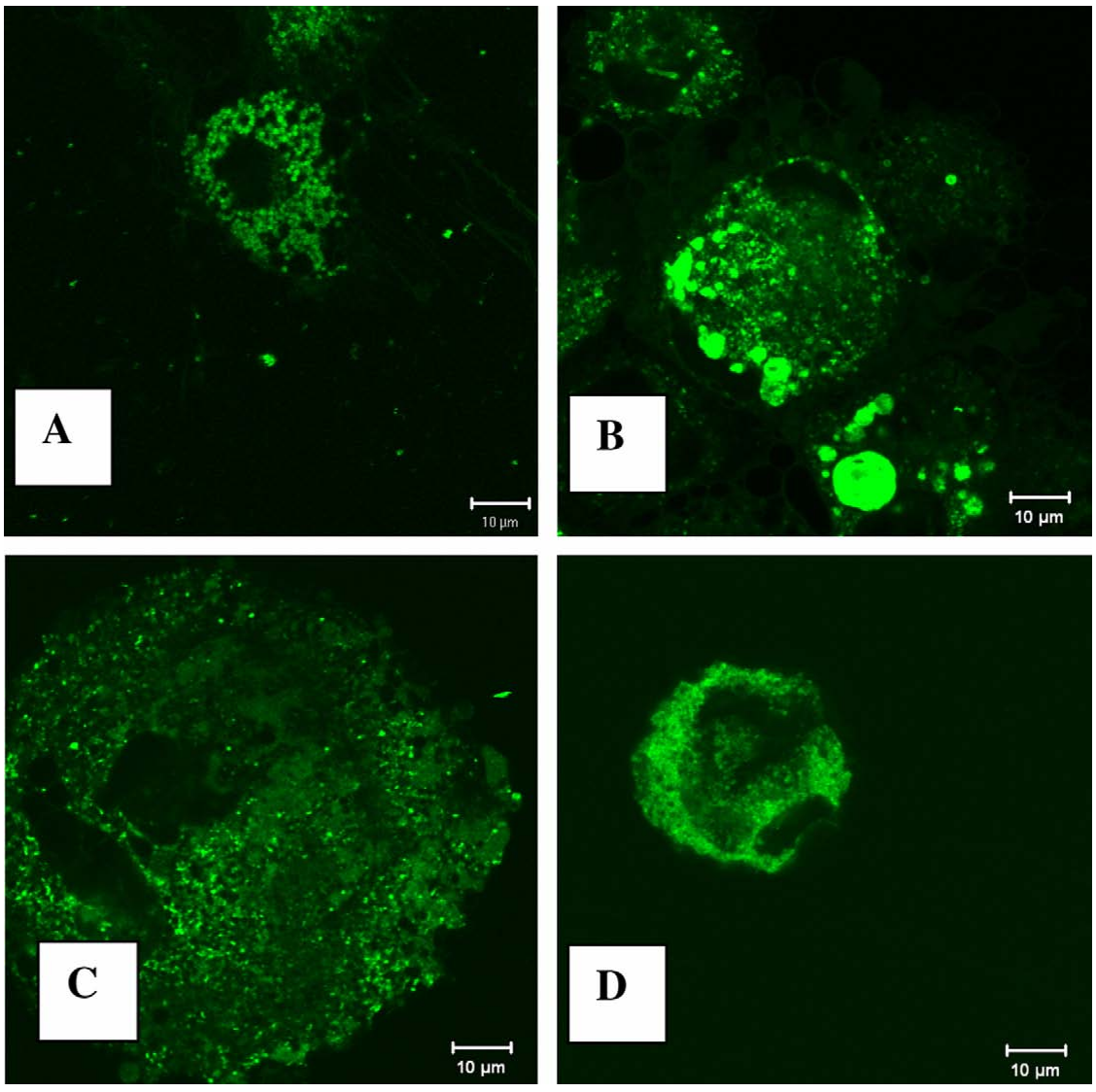

Figure 4.3 H9c2 cells stained with LysoSensor probe, which stains both lysosomes and late endosomes. A: untreated control cells stained with LysoSensor probe; B-D: cells treated with 20 µM pavetamine for 48 h and then stained with Lysosensor probe.

The average activity of hexosaminidase in the treated cells was 635.5 ± 44.2 µM/h/mg protein compared to 243.8 ± 21.4 µM/h/mg protein in the control cells (Fig. 4.4). Digitonin-permeabilized fractions represented the enzyme activity in the cytosol (Theodossiou *et al*., 2006).

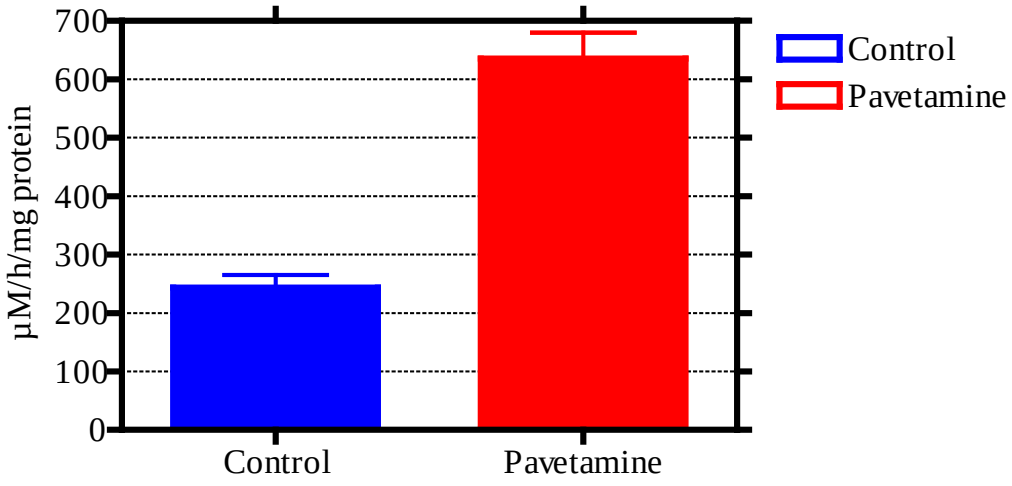

Figure 4.4 Lysosomal hexosaminidase enzyme activity of untreated control and pavetamine-treated H9c2 cells after 48 h exposure. H9c2 cells treated with pavetamine had statistically significant higher hexosaminidase activity than the control cells as analyzed with the Student's *t*-test ($p < 0.05$). The results presented the average of three independent enzyme activity determinations.

H9c2 cells treated with 20 µM pavetamine for 48 h, showed more intense staining with the substrate for acid phosphatase (an enzyme specific for lysosomes) (Fig. 4.5C-D), than the untreated control cells (Fig. 4.5A). There was light pink staining of the lysosomes around the nucleus in control cells, whilst the treated cells were characterized by deep purple staining in all areas of the cytosol, indicating increased enzyme activity.

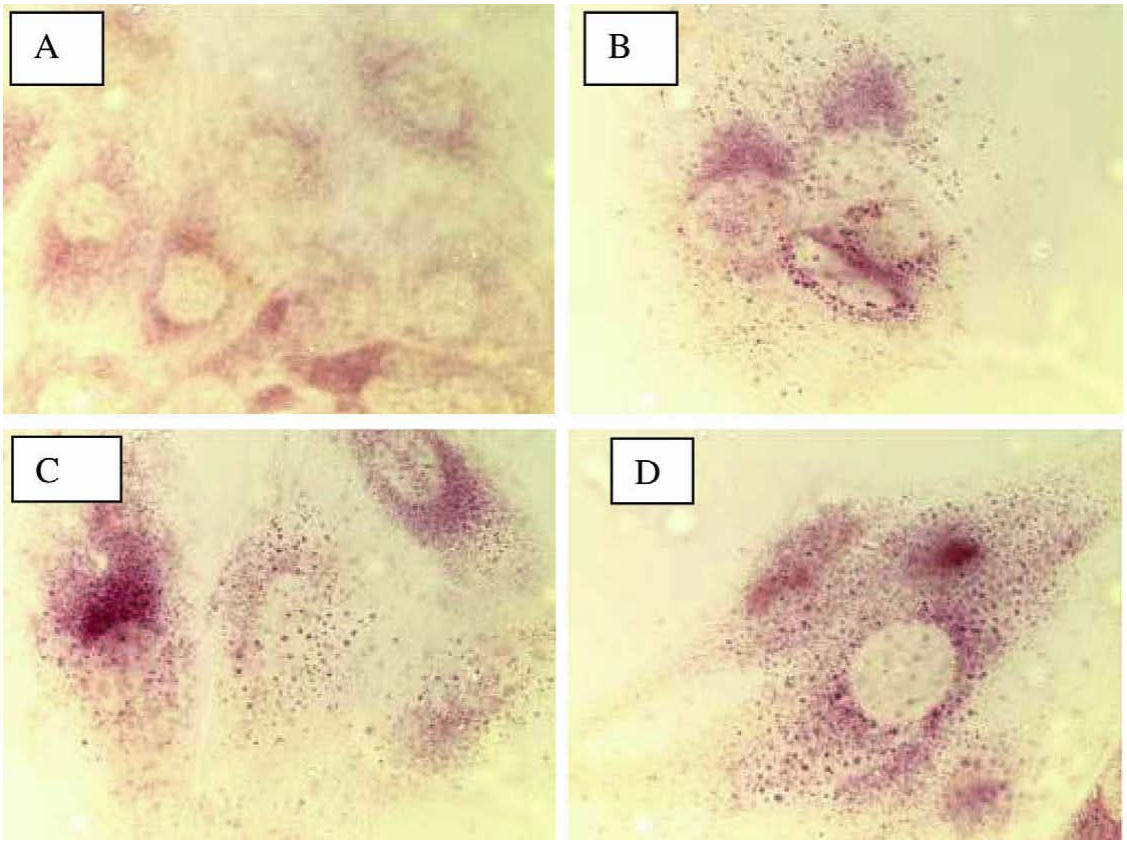

Figure 4.5 Acid phosphatase enzyme activity of untreated control and pavetamine-treated H9c2 cells. A: untreated control cells; B-D: H9c2 cells treated with 20 µM pavetamine after 48 h exposure. The experiments were repeated three times independently with similar results.

The effect of pavetamine on the cytoskeleton of H9c2 cells was investigated using phalloidin-FITC (Fig. 4.6). In the control cells, both thick and thin bundles were stained with phalloidin, with the thicker filaments located at the periphery of the cells (Fig. 4.6A). The filaments appear throughout the cells as a mesh-like network. The H9c2 cells treated with 20 µM pavetamine for 24 h showed differences in cell shape and F-actin patterns, although the intensity of the fluorescent staining was comparable to that of the control cells (Fig. 4.6B and C). The F-actin was ruffled around the nucleus (Fig. 4.6B), or lost its mesh-like appearance and became parallel in orientation (Fig. 4.6C).

Fluorescent staining was much less intense or even absent, with only the nuclei being stained in H9c2 cells treated for 48 h with pavetamine (Fig. 4.6D). Within 10 min exposure of H9c2

cells to 12 µM CytoD, the F-actin network became severely disrupted (Fig. 4.6E). Dissolution of stress fibres and numerous small and highly fluorescent cytoplasmic aggregates, or foci, appeared, with clumping in some areas of the cells.

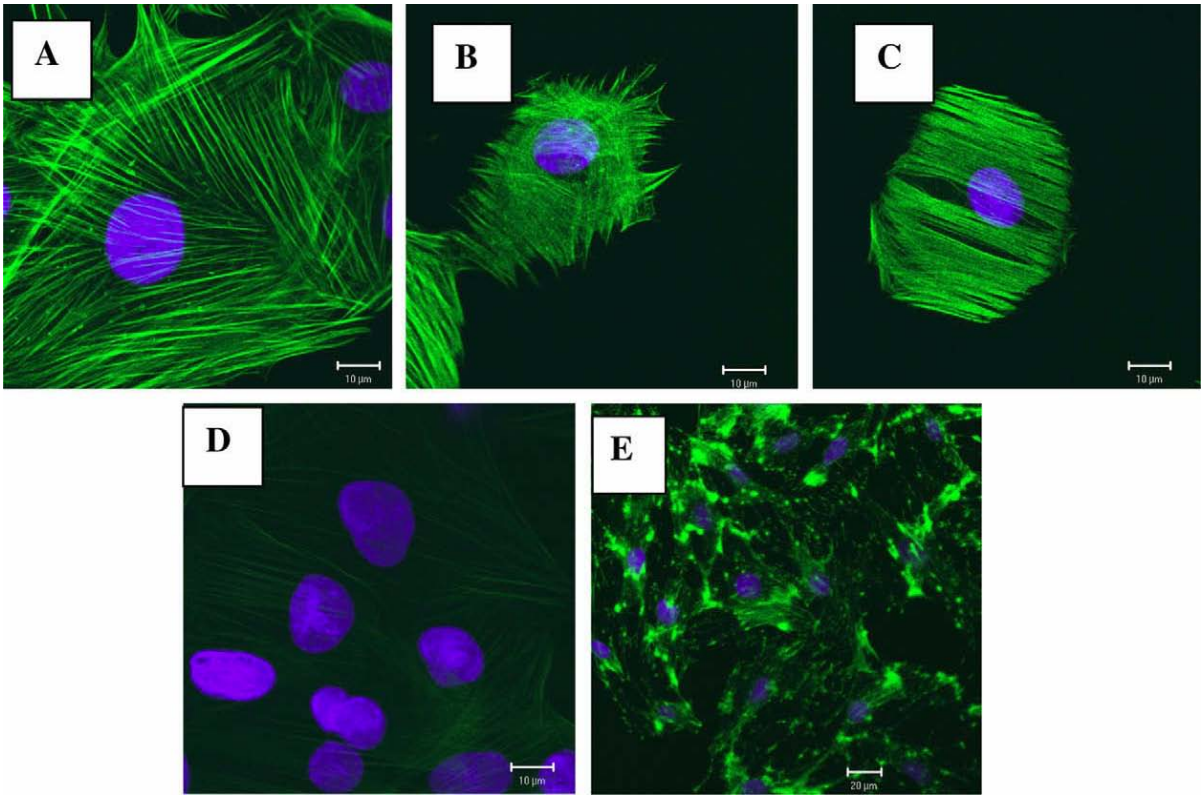

Figure 4.6 H9c2 cells stained with phalloidin-FITC which binds to the F-actin cytoskeleton. A: untreated control cells; B-C: cells treated for 24 h with 20 µM pavetamine; D: cells treated for 48 h with 20 µM pavetamine; E: cells treated with 12 µM cytoD (an inhibitor of actin polymerisation) for 10 min.

4.4 Discussion

This fluorescent subcellular investigation demonstrated that pavetamine caused alterations to the SR, mitochondria, lysosomes and F-actin of H9c2 cells, all of which have important

functions in the cell. These findings concur with the previous TEM study (Ellis *et al*., 2010), where pavetamine was shown to cause damage to the mitochondria and SR of H9c2 cells after 24 h exposure to pavetamine and the appearance of secondary lysosomes after 48 h exposure.

Pretorius *et al*. (1973) reported a depressed uptake of calcium ions by isolated fragments of the SR from sheep dosed with pavetamine-producing *P. pygmaeum* plant material, suggesting that the intracellular Ca^{2+} homeostasis is altered during gousiekte. They concluded that reduced contractility of hearts affected by gousiekte can be directly correlated with altered Ca^{2+} homeostasis. Disturbances in any of these functions will lead to SR-stress, which will alter the efficiency of protein synthesis and protein folding. In this study the SR stained with the ER Tracker probe showed abnormalities in the cells treated with pavetamine, indicating ER stress. Treatment with thapsigargin, a SR stressor, produced similar results. Thapsigargin blocks the SERCA pump and prevents the transport of Ca^{2+} back into the SR, thus causing depletion in the Ca^{2+} stores of the SR, with a resultant rise in cytosolic Ca^{2+} levels (Prasad & Inesi, 2009).

The MitoTracker Green probe diffuses passively across the sarcolemma and accumulates in active mitochondria, irrespective of the $\Delta\Psi_m$. In this study, the morphology of the mitochondria of pavetamine-treated cells was adversely affected and the rapid fading of fluorescent staining indicated that the mitochondria were inactive. A mitochondrion is the power engine of the cell by virtue of generating ATP through oxidative phosphorylation. Snyman *et al*. (1982) investigated the energy production in hearts of sheep dosed with *P. pygmaeum* and found a decreased level of ATP and CrP, with increased lactate levels, reflecting a shift towards anaerobic metabolism. They further demonstrated a reduced uptake of oxygen in isolated mitochondria.

The LysoSensor probe is a dye that is acidotropic and accumulates in acidic organelles, like late endosomes and lysosomes as a result of protonation (Lin *et al*., 2001). Polyamines accumulate in polyamine-sequestering vesicles that co-localize with acidic vesicles of the late endocytic compartment and the *trans* Golgi apparatus (Soulet *et al*., 2004). Amine drugs, such as procaine, nicotine and atropine, cause the formation of multiple, large vacuoles (Morisette *et al*., 2008). These vacuoles are formed by vacuolar (V)-ATPase as a result of the cell's

response to concentrated cationic drugs. Lipophilic weak bases, such as monoamines and diamines, are used to study vacuolar acidification (Millot *et al*., 1997). Lysosomotropism is a term used to describe the accumulation of basic compounds inside acidic organelles. Basic compounds reaching the acidic milieu of lysosomes, become protonated and membrane-impermeable, resulting in their accumulation inside the lysosomes (Lemieux *et al*., 2004). According to the results obtained in this study, pavetamine caused an increase in the amount and size of lysosomes. To further investigate the lysosomes, two enzymatic assays were performed. There was an increase in the activity of cytosolic hexosaminidase in cells treated with pavetamine, indicating that the lysosomal membranes became more permeable. Acid phosphatase activity in the treated cells was also increased, compared to the control cells. There are three proteolytic systems in cells: proteasomes, calpains and the lysosomal hydrolases (Bartoli & Richard, 2005). If the lysosomal hydrolases escape from the lysosomes, they can have a devastating effect on cellular- and extracellular matter (Bechet *et al*., 2005). The lysosomal endopeptidases, called cathepsins, can hydrolyse myofibrillar proteins, like troponin T, myosin heavy chain, troponin I and tropomyosin (Bechet *et al*., 2005). Calpain degrades the cytoskeleton and myofibril proteins such as troponin I, troponin T, desmin, fodrin, filamin, C-protein, nebulin, gelsolin, vinculin and vimentin, leading to impairment of the actin-myosin interaction (Lim *et al*., 2004). The lysosomal damage observed in the current study might explain the typical ultrastructural feature of gousiekte in hearts, namely degeneration of the myofibrils (Prozesky *et al*., 2005). It is possible that the lysosomal endopeptidases may play a part in the degradation of the myofibrils.

Phalloidin, a toxin from the mushroom *Amanita phalloides*, is an actin filament stabilizing compound (Kustermans *et al*., 2008). Therefore, coupling of phalloidin to fluorescent dyes renders it a useful tool to study the cytoskeleton. Phalloidin stains only filamentous actin with seven or more monomeric actin molecules (Visegrady *et al*., 2005). In this study treatment of cells with pavetamine caused alterations in the F-actin cytoskeleton. The F-actin became ruffled around the nuclei and lost its mesh-like appearance. In some cells, F-actin was absent with only the nuclei being stained. CytoD caused severe disruption of the F-actin network. The effect of pavetamine on F-actin was different to that of CytoD. Changes to the F-actin after pavetamine treatment, occurred much later than the CytoD-induced alterations. Owing to the complexity of the cytoskeleton, many other proteins, like the actin-binding, actin-

severing and actin-capping proteins, may be involved in the cytotoxicity caused by pavetamine. Two possible consequences of disruption of the cytoskeleton by pavetamine may include altered protein synthesis (by interfering with transcription) and changes to the L-type calcium channels. Disruption of F-actin decreases calcium current (Lader *et al*., 1999).

In conclusion, the cytotoxicity of pavetamine is exerted through mitochondrial damage, SR stress, increased activity of the lysosomes and damage to the F-actin network. All of these cell components play crucial roles in cell homeostasis. Despite these serious alterations, the target animal survives for four to eight weeks after ingestion of the pavetamine-containing plants. In future studies, some of the cardiac contractile proteins in rat neonatal cardiomyocytes will be immunolabeled, to identify which proteins are degraded during gousiekte. The activity of non-lysosomal enzymes, the proteasome and calpains, will also be investigated to clarify their role in the degradation of the myofibres seen in gousiekte.

CHAPTER 5
DAMAGE TO SOME CONTRACTILE AND CYTOSKELETON PROTEINS OF THE SARCOMERE IN RAT NEONATAL CARDIOMYOCYTES AFTER EXPOSURE TO PAVETAMINE

5.1 Introduction

Gousiekte ("quick disease") is a disease of ruminants characterized by acute heart failure without any premonitory signs four to eight weeks after ingestion of certain rubiaceous plants (Theiler *et al*., 1923; Pretorius & Terblanche, 1967). The compound that causes gousiekte was isolated from *Pavetta harborii* and called pavetamine, which is a cationic polyamine (Fourie *et al*., 1995). Ultrastructural changes observed in sheep, intoxicated with extracts of *Pachystigma pygmaeum* were, amongst others, a loss of cardiac myofilaments. The myofibres became disintegrated and had a frayed appearance, which was accompanied by replacement fibrosis (Schutte *et al*., 1984; Kellerman *et al*., 2005; Prozesky *et al*., 2005). The mitochondria varied in shape and size, and demonstrated swollen, ruptured cristae. The SR were dilated and proliferated (Prozesky *et al*., 2005). Schultz and co-workers (2001) reported that pavetamine, administered intraperitoneally to rats, inhibits protein synthesis in the heart, but not in the liver, kidney, spleen, intestine or skeletal muscle. TEM of sections of the heart of treated rats revealed myofibrillar lysis. Hay *et al*., (2001) used dried, crude extracts of *P. harborii* to inject rats and monitored certain cardiodynamic performances. The contractility (dP/dt_{max}) of the treated group was reduced by more than 50 % and the cardiac work (CW) by about 40 %. The systolic function of rats treated with pavetamine was reduced, when compared to control rats (Hay *et al*., 2008).

In another study, the effect of pavetamine in H9c2 cells, a rat embryonic heart cell line, was investigated at a subcellular level with fluorescent probes. The SR and mitochondria showed abnormalities compared to the control cells, as measured with an ER Tracker and MitoTracker probe. The lysosomes of treated cells were more abundant and enlarged, compared to control cells. The presence of abundant secondary lysosomes, which contained cellular debris, and vacuoles were observed with TEM in H9c2(2-1) cells treated with

pavetamine for 48 h (Ellis, *et al*., 2010). The cytosolic hexosaminidase and acid phosphatase showed increased activity, which was indicative of increased lysosomal membrane permeability. Pavetamine also caused alterations in the organization of F-actin, which could have an influence on gene transcription and chromatin remodeling (Ye *et al*., 2008). Eventual cell death after exposure of H9c2(2-1) cells to pavetamine for 72 h was attributed to necrosis, with membrane blebbing and LDH release (Ellis *et al*., 2010).

During cardiac contraction the thick myosin and thin actin filaments of the sarcomeres slide past each other (Huxley & Peachey, 1961). Titin, the largest macromolecule known, functions as a molecular ruler for myosin assembly and acts as a molecular spring that modulates the intrinsic elastic properties of cardiomyocytes (Cox *et al*., 2008; LeWinter *et al*., 2007). The elastic property of titin is afforded by three elements: tandem immunoglobulin-like (Ig)-repeats, a PEVK domain (rich in Pro-Glu-Val-Lys) and a N2B element (Granzier & Labeit, 2002). Two titin isoforms exist in the heart: a shorter, stiffer N2B isoform and a longer N2BA isoform (Wu *et al*., 2002). Titin is also an integrator of sarcomeric mechanosensory function (Krüger & Linke, 2009). The cytoskeleton, consisting mainly of tubulin (microtubules), desmin (intermediate filaments) and F-actin, anchors subcellular structures and transmits mechanical, and chemical stimuli within, as well as between cells (Hein *et al*., 2000). Actin is also a regulator for transcription, chromatin remodeling and transcription factor acitivity (Miralles & Visa, 2006; Vartiainen *et al*., 2007).

Three proteolytic systems exist in the cell for protein degradation: lysosomal enzymes, Ca^{2+}-dependent calpains and the ubiquitin-proteasome (Bartoli & Richard, 2005). The caspase family, activated during apoptosis, can also degrade proteins. Caspase-3 can degrade small myofilament proteins, but not titin (Lim *et al*., 2004). Intact myofibrils cannot be degraded by the proteasome and contractile proteins like actin and myosin, are removed from the sarcomere by calpains before degradation by the proteasome (Koohmaraie, 1992; Willis *et al*., 2009). In cardiomyocytes, muscle-specific ring finger proteins (MURF1 and MURF3) act as E3 ubiquitin ligases to mediate the degradation of β/slow myosin heavy chain (MHC) and MHCIIa (Fielitz *et al*., 2007). Calpain degrades the cytoskeleton and myofibril proteins such as troponin I, troponin T, desmin, fodrin, filamin, C-protein, nebulin, gelsolin, vinculin and vimentin, leading to impairment of the actin-myosin interaction (Lim *et al*., 2004; Galvez, *et*

al., 2007; Razeghi *et al*., 2007; Ke *et al*., 2008). Titin is also susceptible to calpain proteolysis in a model of anthracycline-induced myofilament injury (Lim *et al*., 2004), while autophagy plays a crucial role in protein quality control (PQC), by bulk degradation of long-lived proteins, multi-protein complexes, oligomers, protein aggregates and organelles (Klionsky & Emr, 2000). Portions of the cytoplasm and/or organelles are sequestered, and delivered to the lysosome for degradation (Wang *et al*., 2008). If the lysosomal hydrolases escape from lysosomes, they can be devastating for cellular and extracellular matter (Bechet *et al*., 2005). The lysosomal endopeptidases, called cathepsins, can hydrolyse myofibrillar proteins, like TNT, MHC, TNI and TPM (Bechet *et al*., 2005).

The purpose of this study was to identify the damage to some of the contractile and cytoskeleton proteins of rat neonatal cardiomyocytes caused by pavetamine by using immunofluorescent staining.

5.2 Materials and Methods

5.2.1 Purification of pavetamine

Pavetamine was extracted and purified from the leaves of *P. harborii* S.Moore according to the method described by Fourie *et al*., 1995.

5.2.2 Preparation of rat neonatal cardiomyocytes (RNCM)

The following chemicals were purchased: NaCl, KCl, glucose and NaH_2PO_4 (Merck, Germany). $MgSO_4$ (Saarchem, South Africa), collagenase (Worthington, USA), pancreatin, Percoll, neonatal calf serum and fibronectin were purchased from Sigma (St. Louis, MO). RNCM were prepared from 1-5 day old Sprague-Dawley rats according to the method of Engelbrecht *et al*. (2004). The animal procedures in this study conformed with the principles outlined in the *Guide for the Care and Use of Laboratory Animals*, NIH Publication No. 85–23, revised 1996. Approval was obtained from the Animal Ethics Committee of the ARC-Onderstepoort Veterinary Institute. Isolated rat hearts were placed into 1x Ads buffer (0.1 M NaCl, 5.4 mM KCl, 5 mM glucose, 1.2 mM NaH_2PO_4, 0.8 mM $MgSO_4$, pH 7.4) in a Petri

dish. The hearts were cut into smaller pieces and transferred to another Petri dish containing 1x Ads buffer. The buffer was removed, the tissue transferred to a flask and 8 ml digestion solution (50 mg Collagenase, 30 mg pancreatin in 1x Ads buffer) added, and incubation was performed at 37 °C with shaking for 20 min. The flask was left standing in a laminar flow hood and the supernatant was removed to a 15 ml conical flask and centrifuged at room temperature for 4 min at 300xg. The supernatant was discarded and the pellet combined with 2 ml neonatal calf serum. Eight ml digestion solution was added to the minced hearts and the digestion was repeated a further three times. The cell suspensions were then combined and centrifuged for 5 min at 300xg. The cell pellet was resuspended in 4 ml 1.082 g/ml Percoll in 1x Ads buffer. An equal volume of 1.062 g/ml Percoll was slowly pipetted on top of the 1.082 g/ml Percoll. Finally, 4 ml of 1.050 g/ml Percoll was pipetted on top of the 1.062 g/ml Percoll layer. The test tube was then centrifuged for 25 min at room temperature at 1000xg. The cardiomyocytes, which formed a layer between the 1.082 and 1.062 g/ml Percoll, were then removed and placed in a new sterile test tube. Fifteen ml of 1x Ads buffer was added and the centrifugation was repeated for 4 min at 300xg. The supernatant was discarded and the cells were resuspended in 4 ml DMEM medium (Sigma, St. Louis, MO) supplemented with 10% foetal calf serum (Sigma, St. Louis, MO), 100 U/ml penicillin, and 100 µg/ml streptomycin sulphate (Sigma, St. Louis, MO). The cells were plated in 6-well plates that were pre-coated with 70 µg/ml fibronectin. Cells were plated at a density of 1 x 10^6 cells/ml.

5.2.3 Treatment of RNCM

RNCM cells were treated with 200 µM pavetamine for 48 h and untreated cells served as controls. TEM of RNCM exposed to 200 µM for 48 h resulted in myofibrillar damage. For this reason, RNCM was exposed to 200 µM pavetamine for 48 h.

5.2.4 Immunofluorescent staining of RNCM

Immunofluorescent staining of RNCM was performed according to the method of BD Biosciences. Cells grown on sterile microscope slide coverslips were rinsed with PBS (2 ml/well) for 5 min with shaking. They were then fixed with 100% acetone for 10 min at -20 °C and rinsed twice with 2 ml PBS/well for 5 min on an orbital shaker, before being blocked

with 1 ml/well 1% BSA/PBS for 30 min at 37 °C. The following dilutions of antibodies were made: monoclonal antibody to sarcomeric actin (Sigma, St. Louis, MO) 1:50, monoclonal antibody to myosin heavy chain (GeneTex, USA) 1:50, rabbit antibody to titin (Prof. S. Labeit, Germany) 1:50 and monoclonal antibody to titin's PEVK region (Prof. S. Labeit, Germany) 1:50. The β-tubulin antibody is a monoclonal antibody conjugated to Cy3 and was diluted 1:100 (Sigma, St. Louis, MO). The diluted antibodies were added and incubation was carried out for 60 min in a humidified chamber at 37 °C. The cells were then washed three times with PBS for 5 min and the secondary antibody conjugates diluted, and added. The secondary antibodies comprised either goat anti-rabbit IgG-FITC conjugate (Sigma, St. Louis, MO) or sheep anti-mouse-Cy3 conjugate (Sigma, St. Louis, MO), each at a concentration of 20 µg/ml. Cells were incubated at 37 °C for 60 min. The PBS washings were repeated and cell nuclei were stained with 1 µg/ml DAPI for 15 min in a humidified chamber at 37 °C. The cells were then washed twice for 5 min with PBS.

5.2.5 Staining of F-actin cytoskeleton

After pavetamine exposure for 48 h, the F-actin of RNCM cells was stained with phalloidin-FITC (Sigma, cat no: P5282, St. Louis, MO). Briefly, the cells were washed with PBS for 5 min, followed by fixing with 100% ice cold acetone at -20 °C for 10 min. The cells were then washed twice with PBS for 5 min, incubated with diluted phalloidin-FITC (1 µg/ml in PBS) for 30 min at 37 °C and washed twice with PBS for 5 min. The nuclei were stained with DAPI at a concentration of 1.3 µg/ml for 15 min at 37 °C and washed twice with PBS for 5 min.

5.2.6 Fluorescence microscopy

After staining and washing, the coverslips were mounted on microscope glass slides using ProLong Gold antifade mounting solution (Invitrogen, Eugene, Oregon, USA). Fluorescence imaging was performed using a confocal laser scanning microscope, model ZEISS LSM 510 (Jena, Germany).

5.2.7 Transmission electron microscopy

Primary rat neonatal cardiomyocytes were prepared for TEM using standard procedures. The TEM studies were conducted after exposure of RNCM to 200 µM pavetamine for 48 h. The cells were fixed in 2.5% glutaraldehyde in Millonig's buffer for 5 min before scraping the cells off the bottom of the flask, removing cells and fixative from flask into an Eppendorf tube and additional fixing for another hour. The cells were post-fixed in 1% osmium tetroxide in Millonig's buffer, washed in buffer and then dehydrated through a series of graded alcohols, infiltrated with a mixture of propylene oxide and an epoxy resin and finally embedded in absolute resin at 60 °C. The cells were pelleted after each step by centrifugation at 3000 rpm for 3 min. After curing overnight, ultra-thin sections were prepared and stained with lead citrate and uranyl acetate and viewed in a Philips CM10 transmission electron microscope operated at 80 kV.

5.3 Results

The myosin of control RNCM, visualized with the monoclonal antibody to cardiac MHC, was highly ordered in a striated pattern with intense red staining that represented the A-band (Fig. 5.1a). The shape of the cells appeared star-like. Cells exposed to pavetamine for 48 h had disassembled sarcomeres (Fig. 5.1b-d). The striated pattern was lost and degraded clumps of myosin were visible (Fig. 5.1b-d, see arrows).

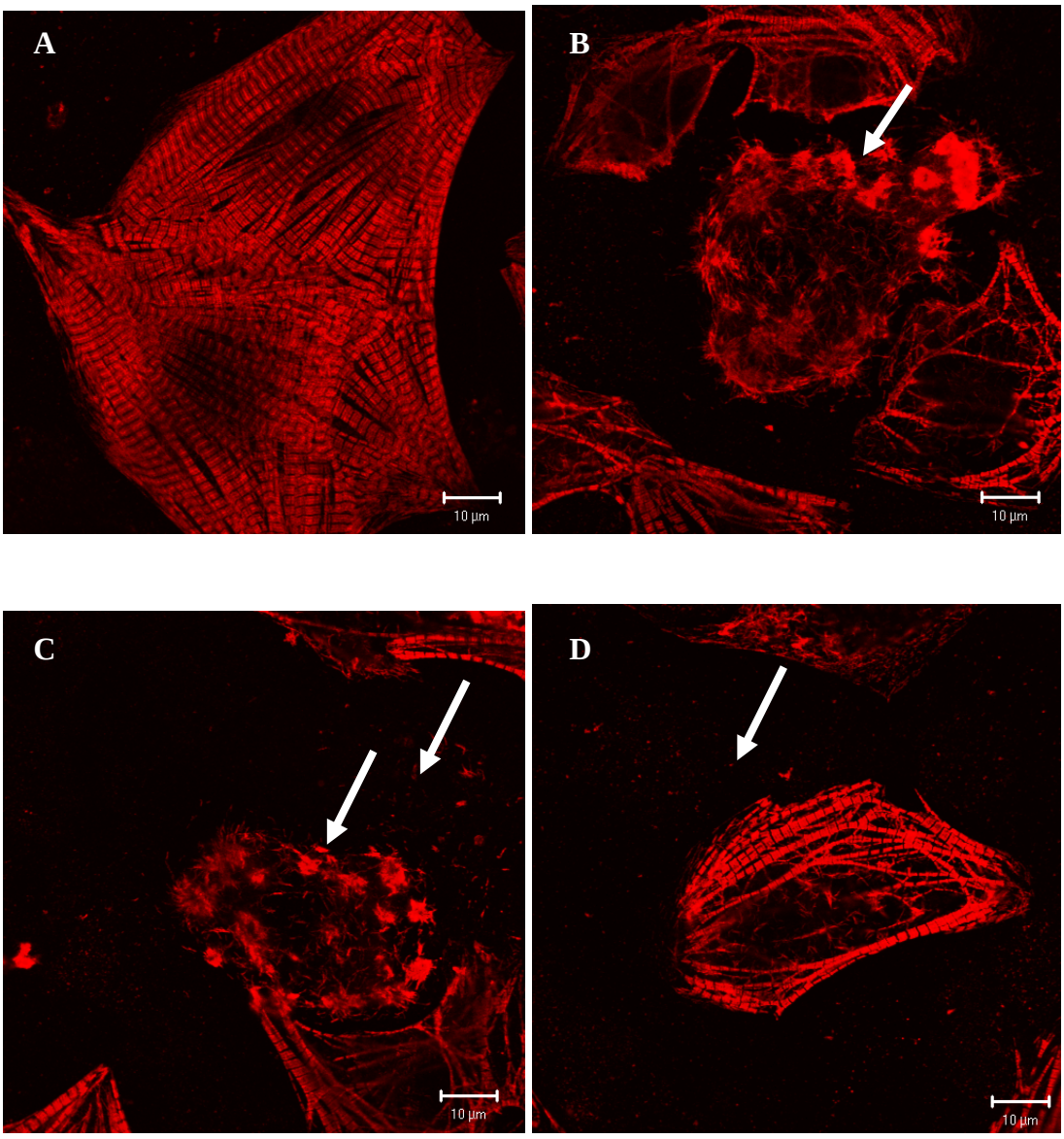

Figure 5.1 Immunofluorescent staining of myosin heavy chain in RNCM cells. A: control rat neonatal cardiomyocytes, B-D: rat neonatal cardiomyocytes treated with 200 µM pavetamine for 48 h.

Staining of titin in control cells with the polyclonal antibody, had a similar striated pattern and organization as the myosin of control cells (Fig. 5.2a). After exposing the RNCM to pavetamine for 48 h, the cells lost their shape and titin became degraded, and lost its striated

pattern (Fig. 5.2b-c). The PEVK region of titin in control cells was clustered around the nuclei, as revealed by staining the cells with a monoclonal antibody to titin's PEVK region (Fig. 5.2d). However, the PEVK region of the exposed cells was spread throughout the cells (Fig. 5.2e-f).

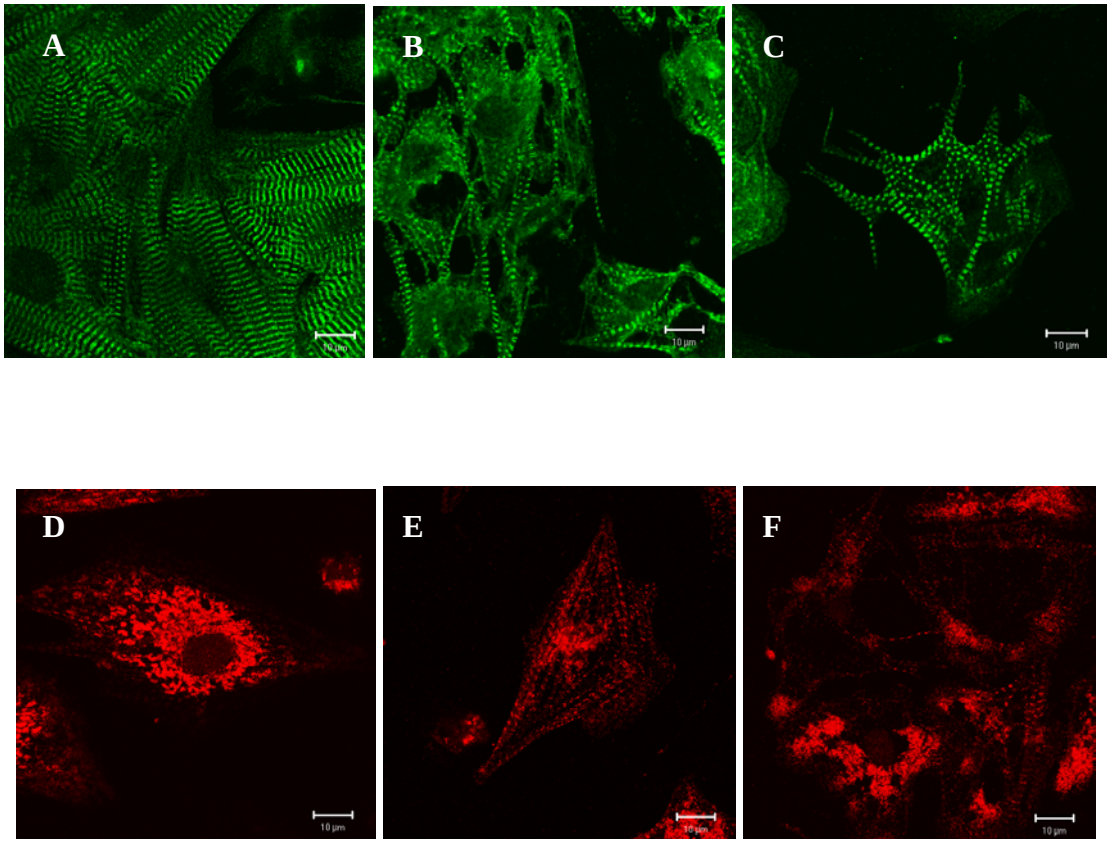

Figure 5.2 Immunofluorescent staining of titin in RNCM cells. A: control rat neonatal cardiomyocytes, B-C: rat neonatal cardiomocytes treated with 200 µM for 48 h, D: control rat neonatal cardiomyocytes stained with an antibody to the PEVK region of titin, E-F: rat cardiomyocytes exposed to 200 µM pavetamine for 48 h and stained with an antibody to the PEVK region of titin.

Sarcomeric alpha-actin in control RNCM was also clustered around the nuclei (Fig. 5.3a). Stained alpha actin of RNCM cells exposed to pavetamine had altered morphology, when compared to the control cells. Margination of alpha actin occurred in pavetamine-exposed

cells (Fig. 5.3b-d, see arrows) and vacuoles were present in some of the exposed cells (Fig. 5.3b-c, see arrow heads).

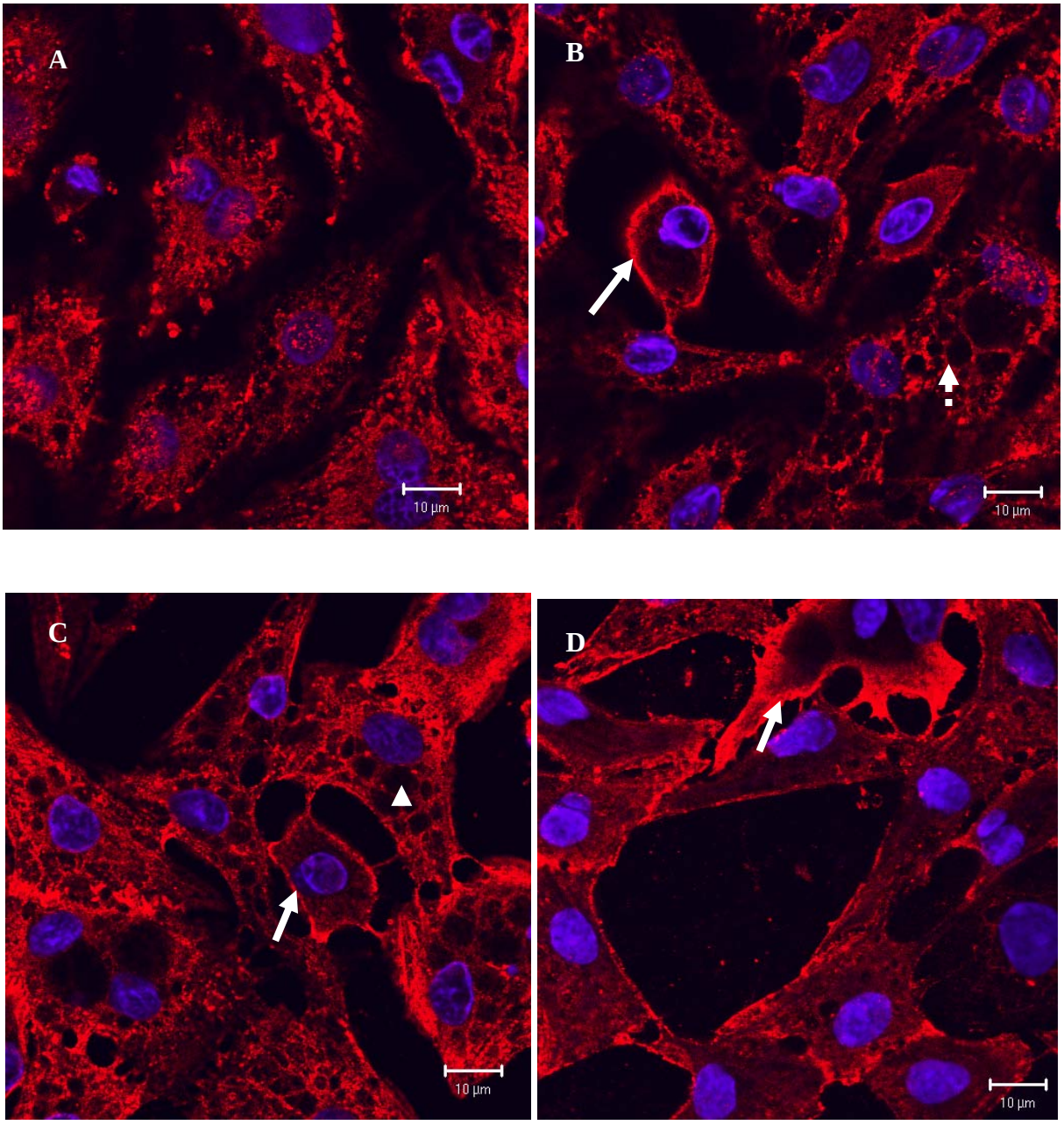

Figure 5.3 Immunostaining of sarcomeric alpha actin (red) in RNCM. The nuclei were stained with DAPI (blue). A: control cells, B-D: cells treated with 200 µM pavetamine for 48 h. Arrow: marginization of alpha actin, arrow head: vacuoles.

Double-labeling of untreated RNCM cells revealed discrete red (myosin heavy chain) and green (titin) staining in a striated pattern (Fig. 5.4a). Cells exposed to pavetamine showed less intense, or no staining for myosin heavy chain (red) (Fig. 5.4b-f). Some cells lost their striated appearance and became rounded (Fig. 5.4c). In Fig. 5.4d, titin appeared at the periphery of the cell with a fragmented nucleus (arrows). Some of the exposed cells had lost the myosin (red) and titin (green), leaving only the nuclei visible (Fig. 5.4e, see arrows). Clumps of degraded titin (green) can be seen in exposed cells (Fig. 5.4f, see arrow).

Staining of F-actin revealed that exposed cells had less intense fluorescent staining (Fig. 5.5b) than untreated cells (Fig. 5.5a). Some of the exposed cells were round with intense fluorescence, possibly representing degraded F-actin (Fig. 5.5b, see arrow). The cytoskeleton of control cells, labeled for F-actin (green) and β-tubulin (red), had a filamentous network (Fig. 5.5c-d), while the F-actin of exposed cells was disrupted or completely absent (Fig. 5.5e-h). The arrow in Fig. 5.5e indicates a cell with intact β-tubulin, but absent F-actin. The mesh-like network of F-actin, as can be seen in Fig. 5.5a and b, disappeared and the F-actin bundles became parallel in orientation (Fig. 5.5f-g). In Fig. 5.5h, the cell indicated with an arrow, had an abnormal β-tubulin appearance ascribed to the disappearance of the tubulin network. This was, however, not a typical feature of most of the exposed cells' tubulin network.

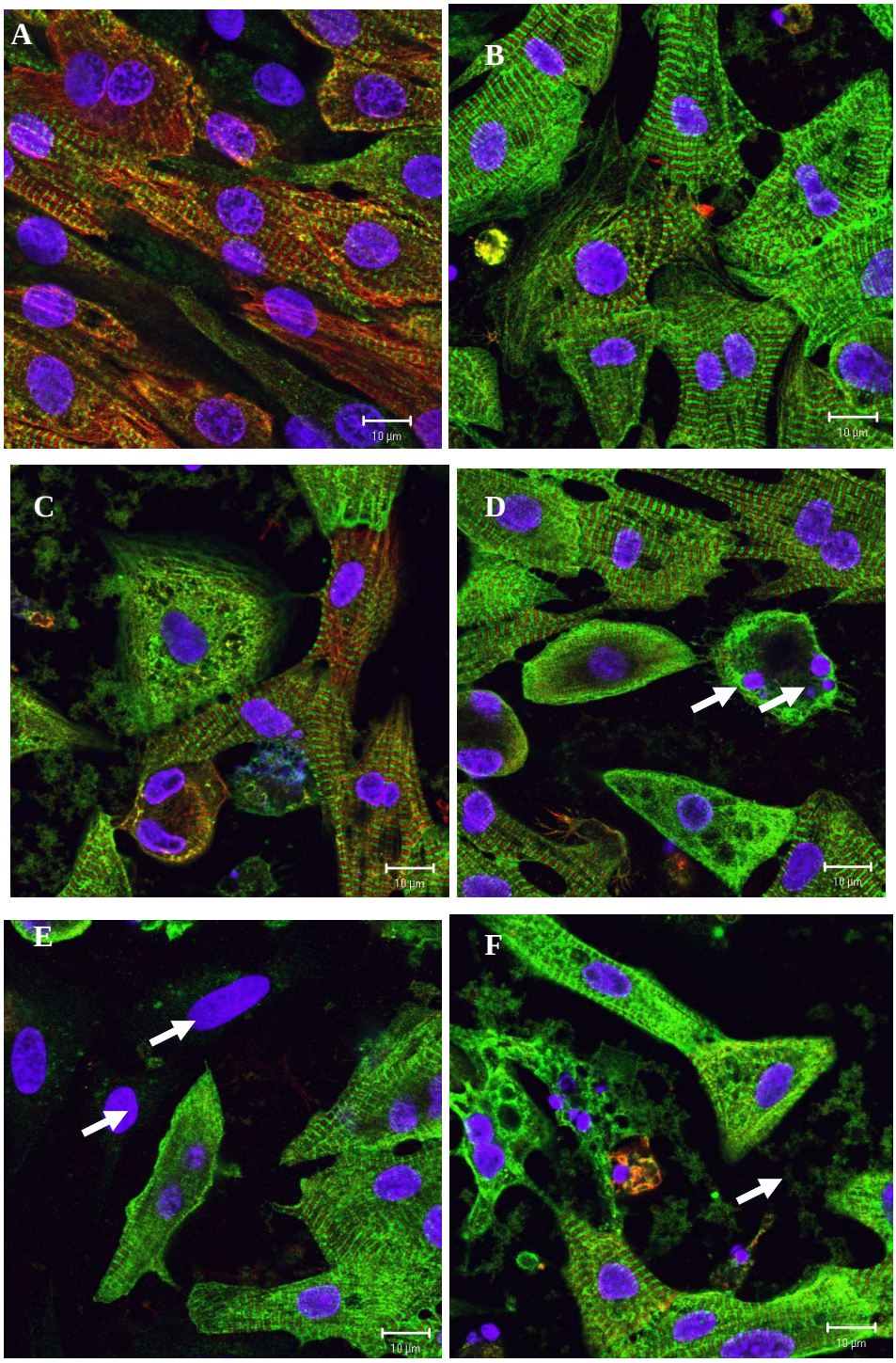

Figure 5.4 Double-immunolabeling of RNCM cells with myosin heavy chain (red) and titin antibodies (green). The nuclei were stained with DAPI (blue) A: control cells, B-F: cells treated with 200 µM pavetamine for 48 h.

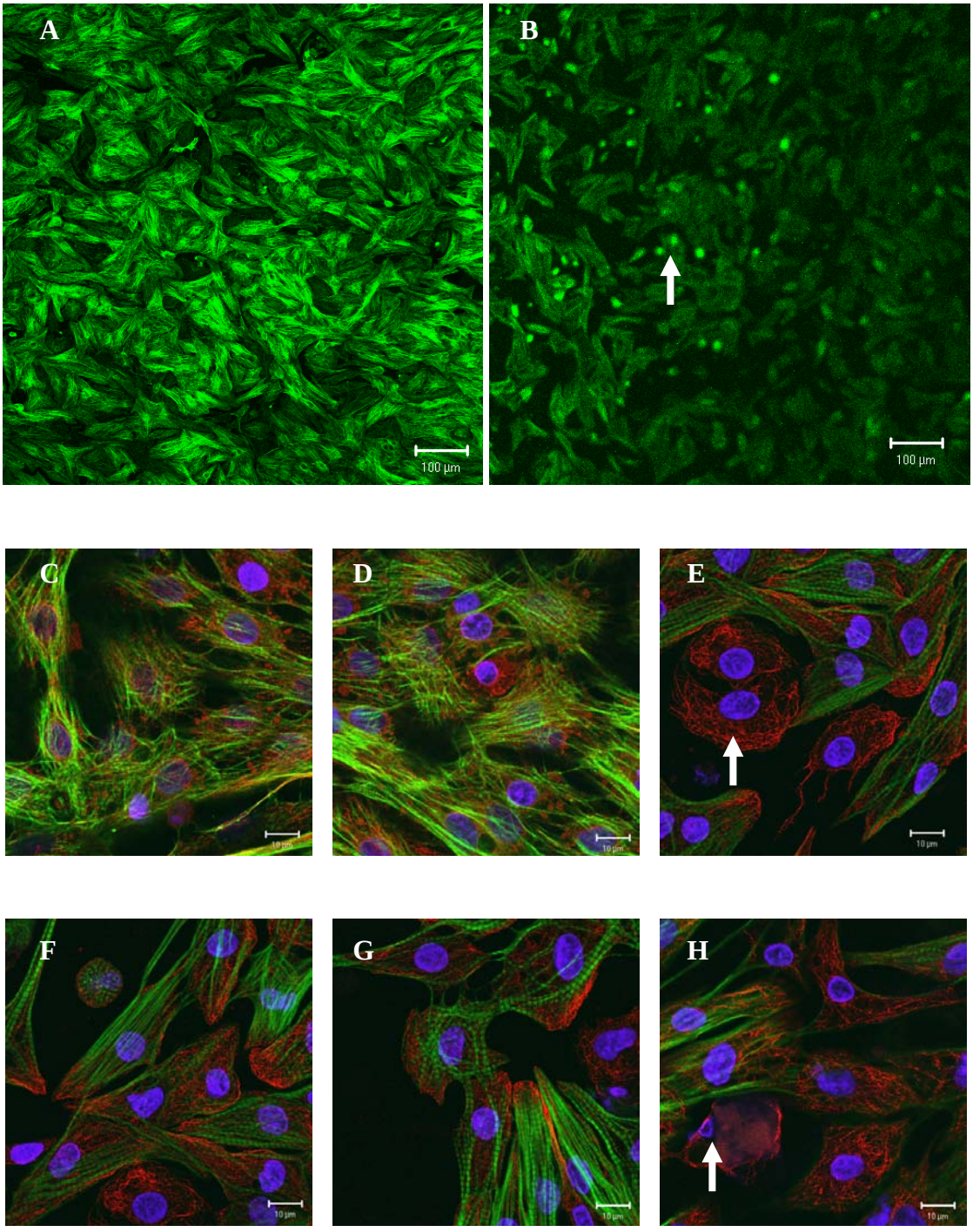

Figure 5.5 Double-immunofluorescent staining of RNCM cells for F-actin (green) and β-tubulin (red). A: control cells stained with phalloidin-FITC for F-actin, B: cells exposed with 200 µM pavetamine for 48 h and stained with phalloidin-FITC for F-actin, C-D: control cells stained for F-actin and tubulin, E-H: Cells exposed to 200 µM pavetamine for 48 h and stained for F-actin and tubulin.

Ultrastructurally, the sarcomeres of untreated cardiomyocytes were neatly organized with electron dense Z-lines (Fig. 5.6a). RNCM exposed to pavetamine (Fig. 5.6b-d) had disorganized sarcomeres and damaged mitochondria. In Fig. 5.6b, the Z-lines were still visible, but were extended, with some of the myofibrils detached from the Z-line.

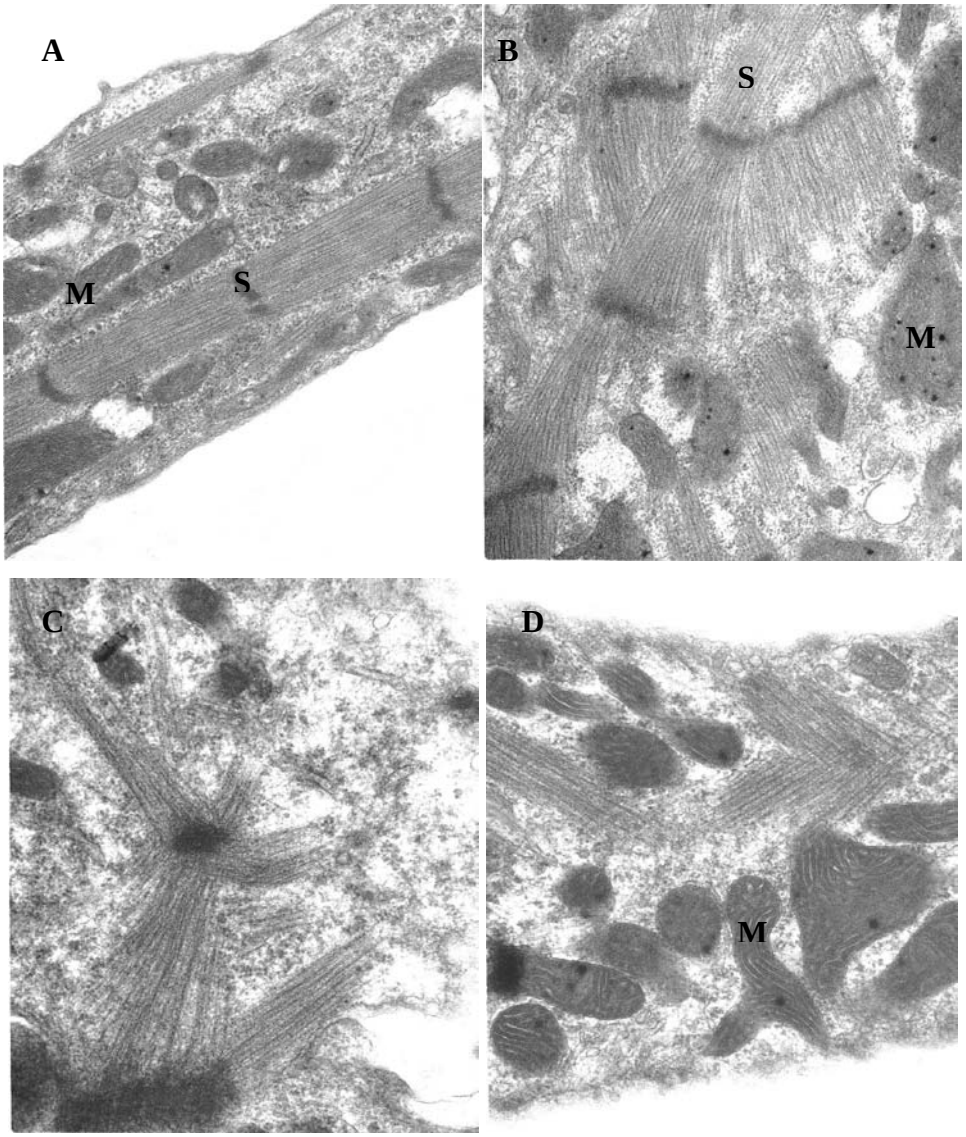

Figure 5.6 Transmission electron micrographs of rat neonatal cardiomyocytes.
A: untreated cells, B-D: cells treated with 200 µM pavetamine for 48 h.
S: sarcomere, M: mitochondria.

In Fig. 5.6c-d, there were few Z-lines present and the myofibrils were scattered in the cells. The mitochondria demonstrated in Fig. 5.6d were enlarged, had an abnormal shape and the cristae were swollen.

5.4 Discussion

This study aimed to immunolabel the contractile cardiac proteins, actin, myosin, and titin, as well as the cytoskeleton proteins (F-actin and β-tubulin) in RNCM treated with pavetamine. The most profound effect induced by pavetamine was myosin degradation. Double-immunolabeling showed that myosin was degraded first, then titin. Of note was the disappearance of the red staining (myosin) from most of the cells, while the majority of the cells still exhibited green fluorescence (titin), albeit with altered morphology. Some of the cells had lost both myosin and titin, and only the nuclei, stained with DAPI, were visible. These findings corroborated earlier ultrastructural reports (Schutte *et al*., 1984; Schultz *et al*., 2001; Prozesky *et al*., 2005). TEM studies of the myocardium of sheep exposed to gousiekte-inducing plants showed a reduction in the number of myofilaments (Schutte *et al*., 1984). These authors speculated that it was especially myosin that was reduced. Changes to titin isoforms have been reported in human hearts with end-stage, dilated cardiomyopathy (Neagoe *et al*., 2002).

In this study, the PEVK region of exposed RNCM showed alterations when compared to the controls. Sarcomeric alpha actin also showed abnormalities such as margination of actin and the appearance of vacuoles. Prozesky *et al.* (2005) performed TEM studies in hearts of sheep with gousiekte and concluded that the degenerative fibrils had a frayed appearance with a preferential loss of thin (actin) filaments.

The cytoskeleton proteins that were stained, demonstrated an altered morphology. F-actin of exposed cardiomyocytes lost its filamentous structure and became parallel in orientation in some cells, while being absent in others. β-tubulin was slightly altered in exposed cardiomyocytes. Sarcomeric and cytoskeleton disarrangement have previously been described

in human dilated cardiomyopathy. In addition to disorganization of myosin and actin, titin was reduced and disorganized, or almost completely absent in diseased cardiac tissue (Hein *et al*., 1994; Morano *et al*., 1994).

The current study revealed that the two major contractile proteins (myosin and actin), titin, (an abundant intra-sarcomeric protein) and the cytoskeleton protein, F-actin, underwent profound changes to their architecture in RNCM exposed to pavetamine. The altered morphology of myosin and titin might be as a consequence of protease degradation. No activation of the proteasome was observed with the three substrates tested (caspase-like, trypsin-like and chymotrypsin-like) in H9c2 cells exposed to pavetamine (results not shown). As described in chapter 4, the lysosomal enzymes hexosaminidase and acid phosphatase exhibited increased activities in treated cells. The degradation of the myofibres could thus be a result of increased lysosomal membrane permeability. Future studies will include determination of the activities of calpain and cathepsin D, to confirm that these proteases are indeed responsible for the degradation of the contractile and F-actin cytoskeleton proteins in cells treated with pavetamine.

In conclusion, pavetamine caused degradation of a number of cardiac proteins that are important in cardiac contractility and cell signalling. Damaged myosin and titin would reduce the contractility of the ruminant heart in animals with gousiekte. Disorganization of F-actin may cause reduced or complete inhibition of protein synthesis. This is corroborated by results of a previous experiment in which Schultz *et al*. (2001) reported inhibition of protein synthesis in the rat heart.

CHAPTER 6
GENERAL DISCUSSION AND CONCLUSION

Pavetamine is the causative agent of gousiekte ("quick disease"), a disease of ruminants characterized by acute heart failure some time after the ingestion of certain rubiaceous plants. The aim of this study was to investigate the mode of action of pavetamine in rat cardiomyocytes.

Two *in vitro* rat cardiomyocyte models were utilized in this study, namely primary rat neonatal cardiomyocytes (RNCM) and the cardiac cell line H9c2 (Kimes & Brandt, 1976). This permanent cell line was used in order to comply with the three R's (replacement, reduction, refinement) for ethical animal experimentation (Russell & Burch, 1959). The H9c2 cell line was derived from embryonic BDIX rat ventricular tissue. This cell line is used as an *in vitro* model for cardiac muscle because it retains many of the biochemical and electrophysiological properties of adult cardiomyocytes (Hescheler *et al*., 1991). This cell line expresses cardiac L-type Ca^{2+} channels and sarcolemmal ATPase splice variants characteristic of the normal heart (Sipido & Marban, 1991). Zordoky and El-Kadi (2007) established that the H9c2 cell line is valuable to study the microsomal drug metabolizing cytochromes P-450 monooxygenase enzyme system (CYPs) in the heart.

The mode of cell death induced by pavetamine was investigated in H9c2 cells. Pavetamine did not induce apoptosis, as the typical features of apoptosis, viz. increased caspase 3 activity and chromatin condensation, were not observed. The cytotoxicity caused by pavetamine is not a consequence of opening of the MPTP. Pavetamine exposure of cells, however, leads to an increase in the mitochondrial membrane potential, in contrast to apoptotic inducers that lead to depolarization of the mitochondrial membrane potential. Features of autophagy were present in cells exposed for two days to pavetamine. This was characterized by the presence of vacuoles in the cytoplasm and numerous secondary lysosomes containing electron dense material. Autophagy is a pro-survival mechanism in the cell to degrade damaged organelles, especially the mitochondria and sarcoplasmic reticula (SR).

Although pavetamine induced autophagy in H9c2 cells, the eventual cell death of H9c2 cells was due to necrosis with the release of LDH into the culture medium. It is accepted that necrosis is characterized by cellular swelling and irreversible plasma membrane damage (Grooten *et al*., 1993), leading to leakage of LDH from the cells. The eventual outcome of the death decision of cells depends on the type and duration of injury, and the intracellular metabolic capacity to maintain the cellular environment (Loos & Engelbrecht, 2009).

It appears that pavetamine targeted the mitochondria of rat cardiomyocytes, as demonstrated by TEM, fluorescence microscopy as well as measurement of the $\Delta\Psi_m$. The heart has a high demand for energy to enable optimal contractile performance where more than 90 % of ATP utilized by cardiomyocytes is synthesized in the mitochondria (Ventura-Clapier *et al*., 2004). During starvation the process of autophagy generates ATP (Loos & Engelbrecht, 2009). ATP can also be replenished from the pool of phosphocreatine (Meininger *et al*., 1999). The cardiac energy metabolism is linked to gene expression and enzyme regulation. ATP is generated in the mitochondria by glycolysis, the Krebs cycle and the electron transport chain, the site for oxidative phosphorylation. Complexes I to V generate the final ATP. During these enzyme cycles, ROS are generated and, if there is an imbalance between production and detoxification, oxidative stress occurs, which has damaging effects on the cell. In the current study pavetamine increased the $\Delta\Psi_m$. The efficiency of oxidative phosphorylation decreases at high $\Delta\Psi_m$ values while ROS are generated above 140 mV (Kadenbach *et al*., 2010). Accumulation of ROS results in DNA damage, protein oxidation and lipid peroxidation (Halliwell & Gutteridge, 1984). Snyman *et al.* (1982) reported a decrease in ATP and CrP in the hearts of sheep with gousiekte and a reduced uptake of O_2 by mitochondria isolated from gousiekte hearts, indicative of the adverse effect of pavetamine on mitochondrial function. This effect is not a consequence of opening of the MPTP, as CsA, an inhibitor of this pore opening, did not reduce the cytotoxicity of pavetamine.

The sarcoplasmic reticula of H9c2 cells exposed to pavetamine were also affected. Rough SR are involved in protein synthesis and thus any damage to these organelles will negatively compromise protein synthesis, protein folding as well as post-translational modifications. This will then activate the UPR and ERAD. Disturbances of the oxidizing environment of the SR will activate the UPS that clears aggregated and misfolded proteins. Pretorius *et al*. (1973)

reported a depressed uptake of Ca^{2+} by isolated fragments of the SR from sheep dosed with pavetamine-producing *P. pygmaeum* plant material, suggesting that the intracellular Ca^{2+} homeostasis is altered during gousiekte. They concluded that reduced contractility of hearts affected by gousiekte can be directly correlated with altered Ca^{2+} homeostasis.

Pavetamine treatment of H9c2 cells also resulted in an increase in the number and size of lysosomes, possibly due to autophagy. The activity of cytosolic hexosaminidase and acid phosphatase was higher in the treated cells compared to the control cells, which suggested increased lysosomal membrane permeability. The acidic pH of lysosomes is maintained by the vacuolar (V)-type ATPase proton pump. Lysosomotropism is the term used to describe the accumulation of cationic compounds inside acidic organelles (De Duve *et al*., 1974). Concentrated amine drugs cause multiple and large vacuoles in several cell types. Pavetamine may behave in the same way as these amine drugs. Many macromolecules contain iron, e.g. ferritin and mitochondrial electron transport complexes, and after autophagic degradation, lysosomes are rich in this element (Sakaida *et al*., 1990). Ferrous iron (Fe^{2+}) can interact with H_2O_2, resulting in the formation of very reactive hydroxyl radicals (Fenton reaction) (Kurz *et al*., 2007). If pavetamine is a lysosomotropic compound, the iron in the lysosomes can contribute to the cytotoxicity induced by pavetamine.

The organization of the cytoskeletal F-actin of H9c2 cells was severely affected by pavetamine. F-actin is involved in chromatin remodelling, transcription, RNA processing and nuclear export (Miralles & Visa, 2006; Vartiainen *et al*., 2007; Farrants, 2008; Vartiainen, 2008; Ye *et al*., 2008; Gieni & Hendzel, 2009). It is surmised that disturbances in F-actin as a result of pavetamine exposure can therefore also inhibit protein synthesis, as has been described by Schultz *et al*. (2001) in rat hearts. Cardiac L-type calcium channels are anchored to F-actin by stabilizing proteins (Lader *et al*., 1999). Any disturbances of the cytoskeleton will thus have a negative influence on the proper functioning of these channels, and directly on contraction.

Rat neonatal cardiomyocytes were labelled with antibodies to the three major contractile proteins (titin, actin and myosin) and cytoskeletal proteins (F-actin and β-tubulin). Cells treated with pavetamine had degraded myosin and titin, with altered morphology of

sarcomeric actin. F-actin was severely disrupted in cardiomyocytes treated with pavetamine by being degraded or even absent. The β-tubulin network seemed to be intact or only marginally affected. Ultrastructurally, the sarcomeres of rat neonatal cardiomyocytes exposed to pavetamine were disorganized and disengaged from the Z-lines. This lesion is also present in the hearts of the ruminants that have contracted gousiekte (Schutte *et al*., 1984; Kellerman *et al*., 2005; Prozesky *et al*., 2005; Prozesky, 2008).

It is proposed that the major contractile proteins and cytoskeleton in cardiomyocytes exposed to pavetamine are degraded by a protease, possibly due to lysosomal permeabilization. Three proteolytic systems are found in cells: calpains, lysosomal enzymes and the proteasome. Any of these systems can be the source for the degradation of the contractile and cytoskeleton proteins. The mitochondria, sarcoplasmic reticula and F-actin are involved in calcium homeostasis. Any damage to these organelles will have a profound influence on calcium flux in the heart and will further contribute to contractile dysfunction reported in gousiekte (Pretorius *et al*., 1973a; Van der Walt & Van Rooyen, 1977; Fourie *et al*., 1989; Hay *et al*., 2001; Hay *et al*., 2008).

In conclusion, there is inhibition of protein synthesis, corroborating the results of Schultz *et al*. (2001) and increased degradation of the cardiac proteins, myosin, titin, sarcomeric actin and F-actin. Although this study was designed to investigate the subcellular damage caused by pavetamine, there are still major gaps in our understanding of the direct mode of action of pavetamine, owing to the complex biology of heart cells.

Proposed Future Research Activities

- Based on this subcellular study, it is hypothesized that some protease(s) is activated during exposure of cardiac cells to pavetamine. Three major proteases are present in cells namely calpains, the lysosomal enzymes and the proteasome. Lysosomal enzymes include acid phosphatase, collagenase, cathepsins, nucleases and carbohydrate- and lipid-digesting enzymes. Studies can be undertaken to test the

activation of these proteases in cardiac cells by means of enzyme activity assays or immunolabelling with antibodies to these major enzymes. A study to investigate the influence of pavetamine on polyubiquitination of cardiac proteins can also be undertaken. In cardiac I/R injury, the proteasome is inhibited with accumulation of ubiquitinated proteins (Powell *et al*., 2005).

- Investigation of oxidative stress induction in cardiomyocytes by pavetamine. 8-Oxo-2'-deoxyguanosine is an oxidized derivative of deoxyguanosine, one of the major products of DNA oxidation. Determination of the latter concentration is an indicator of oxidative stress. The function of the superoxide dismutases (SOD) is the removal of damaging ROS from the intracellular environment. The reduced form of glutathione plays a role in antioxidant defence. By determining the concentration of glutathione reductase, glutathione and glutathione peroxidase, it will be possible to clarify the antioxidative status of the cell. Protein carbonyl content can also be measured to determine ROS as an indicator of oxidative stress. The mitogen-activated protein kinases (MAPKs) are redox-sensitive. c-Jun NH_2 terminal protein kinase (JNK) transmits and converts stress signalling into apoptosis. Extracellular signal-regulated kinase (ERK) seems to have an anti-apoptotic role and may be involved in cell growth processes. The mRNA levels of these kinases can also be quantified as an indicator of oxidative stress. Significant elevation of nitric oxide levels may react with superoxide to produce peroxynitrite, in itself a potent ROS. The influence of pavetamine on the expression of nuclear factor kappa-light-chain-enhancer of activated-B cells (NF-κB), can also be investigated, as this is also a redox-sensitive inducible transcription factor that can promote or inhibit transcription (Hayden & Ghosh, 2008).
- Owing to the very important role of calcium homeostasis in cardiac function, the influence of pavetamine on the intracellular concentration of calcium can be studied to determine its role in the pathogenesis of gousiekte.
- The complex interactive cell signalling pathways can be investigated as well to determine the influence of pavetamine on these pathways. The MAP kinases, mTOR, G-protein coupled receptors, PI3/Akt, tumour necrosis factor and lipid signalling are important pathways. A good approach will be to make use of antibody microarrays.

- Study the influence of pavetamine on the ion channels (voltage-dependent calcium channel, potassium voltage-gated channel, solute carrier, chloride channel and sodium channel) in the heart.
- Study compounds that can reduce or alleviate the effects of pavetamine in the heart, eg. antioxidants like gallic acid, hesperidin, resveratrol and iron chelators like deferoxamine and 2-pyridylcarboxaldehyde 2-thiophenecarboxyl hydrazone.

CHAPTER 7
REFERENCES

ABELIOVICH, H. 2004. Regulation of autophagy by the target of rapamycin (TOR) proteins. In*: Autophagy* (Klionsky, D.J., ed). Georgetown TX: Landes Bioscience, pp. 60-69.

AGARKOVA, I.R. & PERRIARD, J.C. 1995. The M-band: an elastic web that crosslinks thick filaments in the center of the sarcomere. *Trends in Cell Biology*, 15: 477-485.

AGARKOVA, I., SCHOENAUER, R., EHLER, E., CARLSSON, L., CARLSSON, E., THORNELL, E.L. & PERRIARD, J-C. 2004. The molecular composition of the sarcomeric M-band correlates with muscle fiber type. *European Journal of Cell Biology*, 83: 193-204.

AGGELI, I-K. S., BEIS, I. & GAITANAKI, C. 2008. Oxidative stress and calpain inhibition induce alpha B-crystallin phosphorylation via p38-MAPK and calcium signalling pathways in H9c2 cells. *Cellular Signalling*, 20: 1292-1302.

ALEXANDRE, A. & LEHNINGER, A.L. 1984. Bypasses of the antimycin A block of mitochondrial electron transport in relation to ubisemiquinone function. *Biochimica et Biophysica Acta*, 767: 120-129.

ARIMOTO, T., TAKEISHI, Y., TAKAHASHI, H., SHISHIDO, T., TSUNODA, Y., NIIZEKI, T., KOYAMA, Y., SHIGA, R., NOZAKI, N., NAKAJIMA, O., NISHIMARU, K., ABE, J., ENDOH, M., WALSH, R.A., GOTO, K. & KUBOTA, I.. 2006. Cardiac-specific overexpression of diacylglycerol kinase (zeta) prevents Gq protein-coupled receptor agonist-induced cardiac hypertrophy in transgenic mice. *Circulation*, 113: 60-66.

ASNAGHI, L., BRUNO, P., PRIULLA, M. & NICOLIN, A. 2004. mTOR: a protein kinase switching between life and death. *Pharmacological Research*, 50: 545-549.

BAGNATO, P., BARONE, V., GIACOMELLO, E., ROSSI, D. & SORRENTINO, V. 2003. Binding of an ankyrin-1 isoform to obscurin suggests a molecular link between the sarcoplasmic reticulum and myofibrils in striated muscles. *Journal of Cell Biology*, 160: 245-253.

BAINES, C.P. & MOLKENTIN, J.D. 2005. Stress signaling pathways that modulate cardiac myocyte apoptosis. *Journal of Molecular and Cellular Cardiology*, 38: 47-62.

BALASUBRAMANIAN, S., MANI, S., SHIRAISHI, H., JOHNSTON, R.K., YAMANE, K., WILLEY, C.D., COOPER, G., TUXWORTH, W.J. & KUPPUSWAMY, D. 2006. Enhanced ubiquitination of cytoskeletal proteins in pressure overloaded myocardium is accompanied by changes in specific E3 ligases. *Journal of Molecular and Cellular Cardiology*, 41: 669-679.

BANG, M.L., MUDRY, R.E., MCELHINNY, A.S., TROMBITÁS, K., GEACH A.J., YAMASAKI, R., SORIMACHI, H., GRANZIER, H., GREGORIO, C.C. & LABEIT, S. 2001. Myopalladin, a novel 145-kDa sarcomeric protein with multiple roles in Z-disc and I-band protein assemblies. *Journal of Cell Biology*, 153: 413-427.

BARRY, S.P., DAVIDSON, S.M. & TOWNSEND, P.A. 2008. Molecular regulation of cardiac hypertrophy. *International Journal of Biochemistry and Cell Biology*, 40: 2023-2039.

BARTOLI, M. & RICHARD, I. 2005. Calpains in muscle wasting. *International Journal of Biochemistry and Cell Biology*, 37: 2115-2133.

BASSI, R., HEADS, R., MARBER, M.S. & CLARK, J.E. 2008. Targeting p38-MAPK in the ischaemic heart: kill or cure? *Current Opinion in Pharmacology*, 8: 141-146.

BECHET, D., TASSA, A., TAILLANDIER, D., COMBARET, L. & ATTAIX, D. 2005. Lysosomal proteolysis in skeletal muscle. *International Journal of Biochemistry & Cell Biology*, 37: 2098-2114.

BERNUZZI, F., RECALCATI, S., ALBERGHINI, A. & CAIRO, G. 2009. Reactive oxygen species-independent apoptosis in doxorubicin-treated H9c2 cardiomyocytes: role for heme oxygenase-1 down-modulation. *Chemico-Biological Interactions*, 177: 12-90.

BERRIDGE, M.V., TAN, A.S., MCCOY, K.D. & WANG, R., 1996. The biochemical and cellular basis of cell proliferation assays that use tetrazoleum salts. *Biochemica*, 4: 14-19.

BERS, D.M. 2002. Cardiac excitation-contraction coupling. *Nature*, 415: 198-205.

BERSHADSKY, A.D., BALABAN, N.Q. & GEIGER, B. 2003 Adhesion-dependent cell mechanosensitivity. *Annual Review of Cell and Developmental Biology*, 19: 677-695.

BERTOLOTTI, A., ZHANG, Y., HENDERSHOT, L.M., HARDING, H.P. & RON, D. 2000. Dynamic interaction of BiP and ER stress transducers in the unfolded-protein response. *Nature Cell Biology*, 2: 326-332.

BEYER, E.C., PAUL, D.L. & GOODENOUGH, D.A. 1987. Connexin43: a protein from rat heart homologous to a gap junction protein from liver. *Journal of Cell Biology*, 105: 2621-2629.

BLOBEL, G. 2000. Protein targeting. *Bioscience Reports*, 20: 303-344.

BOCKAERT, J., FAGNI, L., DUMUIS, A. & MARIN, P. 2004. GPCR interacting proteins (GIP). *Pharmacology & Therapeutics*, 103: 203-221.

BODE, M.L., GATES, P.J., GEBRETNSAE, S.Y. & VLEGGAAR, R. 2010. Structure elucidation and stereoselective total synthesis of pavettamine, the causal agent of gousiekte. *Tetrahedron*, 66: 2026-2036.

BOGOYEVITCH, M.A., GILLESPIE-BROWN, J., KETTERMAN, A.J., FULLER, S.J., BEN-LEVY, R., ASHWORTH, A., MARSHALL, C.J. & SUGDEN, P.H. 1996. Stimulation of the stress-activated mitogen-activated protein kinase subfamilies in perfused heart: p38/RK mitogen-activated protein kinases and c-Jun N-terminal kinases are activated by ischemia/reperfusion. *Circulation Research*, 79: 162-173.

BONIFACINO, J.S. & TRAUB, L.M. 2003. Signals for sorting of transmembrane proteins to endosomes and lysosomes. *Annual Review of Biochemistry*, 72: 395-447.

BONZO, J.R., NORRIS, A.A., ESHAM, M. & MONCMAN, C.L. 2008. The nebulette repeat domain is necessary for proper maintenance of tropomyosin with the cardiac sarcomere. *Experimental Cell Research*, 314: 3519-3530.

BOX, V.G.S. 2007. The intercalation of DNA double helices with doxorubicin and nagalomycin. *Journal of Molecular Graphics and Modelling*, 26: 14-19.

BOYER, P.D. 2002. A research journey with ATP synthase. *Journal of Biological Chemistry*, 277: 39045-39061.

BRANCACCIO, M., GUAZZONE, S., MENINI, N., SIBONA, E., HIRSCH, E., DE ANDREA, M., ROCCHI, M., ALTRUDA, F., TARONE, G. & SILENGO, L. 1999. Melusin is a new muscle-specific interactor for beta(1) integrin cytoplasmic domain. *Journal of Biolocigal Chemistry*, 274: 29282–29288.

BRUNET, A., BONNI, A., ZIGMOND, M.J., LIN, M.Z., JUO, P., HU, L.S., ANDERSON, M.J., ARDEN, K.C., BLENIS, J. & GREENBERG, M.E. 1999. Akt promotes cell survival by phosphorylating and inhibiting a Forkhead transcription factor. *Cell*, 96: 857-868.

BUEB, J.L., DA SILVA, A., MOUSLI, M. & LANDRY, Y. 1992. Natural polyamines stimulate G-proteins. *Biochemistry Journal*, 282: 545-550.

BUJA, L.M. & VELA, D. 2008. Cardiomyocyte death and renewal in the normal and diseased heart. *Cardiovascular Pathology*, 17: 349-374.

BURSCH, W. 2001. The autophagosomal-lysosomal compartment in programmed cell death. *Cell Death and Differentiation*, 8: 69-81.

CALFON, M., ZENG, H., URANO, F., TILL, J.H., HUBBARD, S.R., HARDING, H.P., CLARK, S.G. & RON, D. 2002. IRE1 couples endoplasmic reticulum load to secretory capacity by processing the XBP-1 mRNA. *Nature*, 415: 92-96.

CAPETANAKI, Y., BLOCH, R.J., KOULOUMENTA, A., MAVROIDIS, M. & PSARRAS, S. 2007. Muscle intermediate filaments and their links to membranes and membranous organelles. *Experimental Cell Research*, 313: 2062-2076.

CARLSSON, L. & THORNELL, L.E. 2001. Desmin-related myopathies in mice and man. *Acta Physiologica Scandinavica*, 171: 341-348.

CHANG, S.C., WOODEN, S.K., NAKAKI, T., KIM, Y.K., LIN, A.Y., KUNG, L., ATTENELLO, J.W. & LEE, A.S. 1987. Rat gene encoding the 78-kDa glucose-regulated protein GRP78: its regulatory sequences and the effect of protein glycosylation on its expression. *Proceedings of the National Academy of Science (USA)*, 84: 680-684.

CHEN, J. & FANG, Y. 2002. A novel pathway regulating the mammalian target of rapamycin (mTOR) signaling. *Biochemical Pharmacology*, 64: 1071-1077.

CLERK, A., COLE, S.M., CULLINGFORD, T.E., HARRISON, J.G., JORMAKKA, M., & VALKS, D.M. 2003. Regulation of cardiac myocyte cell death. *Pharmacology & Therapeutics*, 97: 223-261.

CLERK, A. & SUGDEN, P.H. 2006. Inflame my heart (by p38-MAPK). *Circulation Research*, 99: 455-458.

COHEN, S.S. 1998. A Guide to Polyamines. New York: Oxford University Press.

CONOVER, G.M., HENDERSON, S.N. & GREGORIA, C.C. 2009. A myopathy-linked desmin mutation perturbs striated muscle actin filament architecture. *Molecular Biology of the Cell*, 20: 834-845.

COULIS, G., BECILA, S., HERRERA-MENDEZ, C.H., SENTANDREU, M.A., RAYNAUD, F., RICHARD, I., BENYAMIN, Y. & OUALI, A. 2008. Calpain 1 binding capacities of the N1-line region of titin are significantly enhanced by physiological concentrations of calcium. *Biochemistry*, 47: 9174-9183.

COX, L., UMANS, L., CORNELIS, F., HUYLEBROECK, D. & ZWIJSEN, A. 2008. A broken heart: a stretch too far. An overview of mouse models with mutations in stretch-sensor components. *International Journal of Cardiology*, 131: 33-44.

CROMPTON, M., ELLINGER, H. & COSTI, A. 1988. Inhibition by cyclosporin A of a Ca^{2+}-dependent pore in heart mitochondria activated by inorganic phosphate and oxidative stress. *Biochemical Journal*, 255: 357-360.

CROMPTON, M. 1999. The mitochondrial permeability transition pore and its role in cell death. *Biochemical Journal*, 341: 233-249.

CULLIS, P.M., GREEN, R.E., MERSON-DAVIES, L. & TRAVIS, N. 1999. Probing the mechanism of transport and compartmentalization of polyamines in mammalian cells. *Chemistry and Biology*, 6: 717-729.

DE DUVE, C., DE BARSY, T., POOLE, B., TROUET, A., TULKENS, P. & VAN HOOF, F. 1974. Lysosomotropic agents. *Biochemical Pharmacology*, 23: 2495-2531.

DE MEYER, G.R.Y. & MARTINET, W. 2009. Autophagy in the cardiovascular system. *Biochimica et Biophysica Acta*, 1793: 1485-1495.

DEPRE, C., WANG, Q., YAN, L., HEDHLI, N., PETER, P., CHEN, L., HONG, C., HITTINGER, L., GHALEH, B., SADOSHIMA, J., VATNER, D.E., VATNER,

S.F. & MADURA, K. 2006. Activation of the cardiac proteasome during pressure overload promotes ventricular hypertrophy. *Circulation*, 114: 1796-1798.

DIEZ, J., FORTUNO, M.A. & RAVASSA, S. 1998. Apoptosis in hypertensive heart disease. *Current Opinion in Cardiology*, 13: 317-325.

DIVALD, A. & POWELL, S.R. 2006. Proteasome mediates the removal of proteins oxidized during myocardial ischemia. *Free Radical & Medicine*, 40: 156-164.

DJINOVIC-CARUGO, K., YOUNG, P., GAUTEL, M. & SARASTE, M. 1999. Structure of the alpha-actinin rod: molecular basis for cross-linking of actin filaments. *Cell*, 98: 537-546.

EBASHI, S. & EBASHI, F. 1964. A new protein component participating in the super precipitation of myosin B. *Journal of Biochemistry*, 55: 604-613.

EHLER, E., HOROWITS, R., ZUPPINGER, C., PRICE, R.L., PERRIARD, E., LEU, M., CARONI, P., SUSSMAN, M., EPPENBERGER, H.M. & PERRIARD, J-C. 2001. Alterations at the intercalated disk associated with the absence of muscle LIM protein. *Journal of Cell Biology*, 153: 763-772.

ELFGANG, C., ECKERT, R., LICHTENBERG-FRATE, H., BUTTERWECK, A., TRAUB, O., KLEIN, R.A., HULSER, D.F. & WILLECKE, K. 1995. Specific permeability and selective formation of gap junction channels in connexin-transfected HeLa cells. *Journal of Cell Biology*, 129: 805-817.

ELLIS, C.E., NAICKER, D., BASSON, K.M., BOTHA, C.J., MEINTJES, R.A. & SCHULTZ, R.A. 2010. Cytotoxicity and ultrastructural changes in H9c2(2-1) cells treated with pavetamine, a novel polyamine. *Toxicon*, 55: 12-19.

ELMORE, S.P., QIAN, T., GRISSOM, S.F. & LEMASTERS, J.J. 2001. The mitochondrial permeability transition inititates autophagy in rat hepatocytes. *Federation of American Societies for Experimental Biology Journal*, 15: 2286-2287.

ELSÄSSER, A., VOGT, A., NEF, H., KOSTIN, S., MÖLLMANN, H., SKWARA, W., BODE, C., HAMM, C. & SCHAPER, J. 2004. Human hibernating myocardium is jeopardized by apoptotic and autophagic cell death. *Journal of the American College of Cardiology*, 43: 2191-2199.

ENGEL, F.B. 2005. Cardiomyocyte proliferation: a platform for mammalian cardiac repair. *Cell Cycle*, 4: 1360-1363.

ENGELBRECHT, A-M., NIESLER, C., PAGE, C. & LOCHNER, A. 2004. p38 and JNK have distinct regulating functions in the development of apoptosis during simulated ischemia and reperfusion of neonatal cardiomyocytes. *Basic Research in Cardiology*, 99: 338-350.

ERVASTI, J.M. 2003. Costameres: the Archilles' heel of Herculean muscle. *Journal of Biological Chemistry*, 278: 13591-13594.

FARRANTS, A-K.O. 2008. Chromatin remodelling and actin organization. *FEBS Letters*, 582: 2041-2050.

FESTJENS, N., VANDEN BERGHE, T. & VANDENABEELE, P. 2006. Necrosis, a well-orchestrated form of cell demise: signalling cascades, important mediators and concomitant immune response. *Biochimica et Biophysica Acta*, 1757: 1371-1387.

FIELITZ, J., VAN ROOIJ, E., SPENCER, J.A., SHELTON, J.M., LATIF, S., VAN DER NAGEL, R., BEZPROZVANNAYA, S., DE WINDT, L., RICHARDSON, J.A., BASSEL-DUBY, R. & OLSON, E.N. 2007a. Loss of muscle-specific RING-finger 3 predisposes the heart to cardiac rupture after myocardial infarction. *The Proceedings of the National Academy of Sciences (USA)*, 104: 4377-4382.

FIELITZ, J., KIM, M-S., SHELTON, J.M., LATIF, S., SPENCER, J.A., GLASS, D.J., RICHARDSON, J.A., BASSEL-DUBY, R. & OLSON, E.N. 2007b. Myosin accumulation and striated muscle myopathy result from the loss of muscle RING finger 1 and 3. *Journal of Clinical Investigation*, 117: 2486-2495.

FOMPROIX, N. & PERCIPALLE, P. 2004. An actin-myosin complex on actively transcribing genes. *Experimental Cell Research*, 294: 140-148.

FOUKAS, L.C. & OKKENHAUG, K. 2003. Gene-targeting reveals physiological roles and complex regulation of the phosphoinositide 3-kinases. *Archives of Biochemistry and Biophysics*, 414: 13-18.

FOURIE, N., SCHULTZ, R.A., PROZESKY, L., KELLERMAN, T.S.& LABUSCAGNE, L. 1989. Clinical pathological changes in gousiekte, a plant-

induced cardiotoxicosis of ruminants. *Onderstepoort Journal of Veterinary Research*, 56: 73-80.

FOURIE, N., ERASMUS, G. L., SCHULTZ, R.A. & PROZESKY, L. 1995. Isolation of the toxin responsible for gousiekte, a plant-induced cardiomyopathy of ruminants in southern Africa. *Onderstepoort Journal of Veterinary Research*, 62: 77-87.

FRANKE, W.W., BORRMANN, C.M., GRUND, C. & PIEPERHOFF, S. 2006. The area composita of adhering junctions connecting the heart muscle cells of vertebrates. I. Molecular definition in intercalated disks of cardiomyocytes by immunoelectron microscopy of desmosomal proteins. *European Journal of Cell Biology*, 85: 69-82.

FREY, N., RICHARDSON, J.A. & OLSON, E.N. 2000. Calsarcins, a novel family of sarcomeric calcineurin-binding proteins. *Proceedings of the National Acadamy of Sciences (USA)*, 97: 14632-14637.

FUJIO, Y., NGUYEN, T., WENCKER, D., KITSIS, R.N. & WALSH, K. 2000. Akt promotes survival of cardiomyocytes in vitro and protects against ischemia-reperfusion injury in mouse heart. *Circulation*, 101: 660-667.

FURLONG, I.J., LOPEZ MEDIAVILLA, C., ASCASO, R., LOPEZ RIVAS, A. & COLLINS, M.K. 1998. Induction of apoptosis by valinomycin: mitochondrial permeability transition causes intracellular acidification. *Cell Death and Differentiation*, 5: 214-221.

FÜRST, D.O., OSBORN, M., NAVE, R. & WEBER, K. 1988. The organization of titin filaments in the half-sarcomere revealed by monoclonal antibodies in immunoelectron microscopy: a map of ten nonrepetitive epitopes starting at the Z-line extends close to the M line. *Journal of Cell Biology*, 106: 1563-1572.

FURUKAWA, T., ONO, Y., TSUCHIYA, H., KATAYAMA, Y., BANG, M.L., LABEIT, D., LABEIT, S., INAGAKI, N. & GREGORIO, C.C. 2001. Specific interaction of the potassium channel beta-subunit mink with the sarcomeric protein T-cap suggests a T-tubule-myofibril linking system. *Journal of Molecular Biology*, 313: 775-784.

FYRBERG, C., KETCHUM, A., BALL, E. & FURBERG, E. 1998. Characterization of lethal *Drosophila melanogaster* alpha-actinin mutants. *Biochemical Genetics*, 36: 299-310.

GALVEZ, A.S., DIWAN, A., ODLEY, A.M., HAHN, H.S., OSINSKA, H., MELENDEZ, J.G., ROBBINS, J., LYNCH, R.A., MARREEZ, Y. & DORN, G.W. 2nd. 2007. Cardiomyocyte degeneration with calpain deficiency reveals a critical role in protein homeostasis. *Circulation Research*, 100: 1071-1078.

GARDNER, D.G. 2003. Brain natriuretic peptide: a marker for subclinical cardiovascular disease? *American Journal of Medicine*, 114: 329-330.

GARDNER, D.G., CHEN, S., GLENN, D.J. & GRIGSBY, C.L. 2007. Molecular biology of the natriuretic peptide system: implications for physiology and hypertension. *Hypertension*, 49: 419-426.

GARROD, D. & CHIDGEY, M. 2008. Desmosome structure, composition and function. *Biochimica et Biophysica Acta*, 1778: 572-587.

GHANI, R.A., PALMER, A.J., KAUR, N., PHANSTIEL, O. & WALLACE, H.M. 2009. The polyamine transport system: a means of selective delivery of potentially toxic agents to cancer cells. *Toxicology*, 262: 13.

GIENI, R.S. & HENDZEL, M.J. 2009. Actin dynamics and functions in the interphase nucleus: moving toward an understanding of nuclear polymeric actin. *Biochemistry and Cell Biology*, 87: 283-306.

GLEMBOTSKI, C.C. 2007. Endoplasmic reticulum stress in the heart. *Circulation Research*, 101: 975-984.

GLEMBOTSKI, C.C. 2008. The role of the unfolded protein response in the heart. *Journal of Molecular and Cellular Cardiology*, 44: 453-459.

GLICKMAN, M.H. & CIECHANOVER, A. 2002. The ubiquitin-proteasome proteolytic pathway: destruction for the sake of construction. *Physiology Reviews*, 82: 373-428.

GOA, W.D., ATAR, D., LIU, Y., PEREZ, N.G., MURPHY, A.M. & MARBAN, E. 1997. Role of troponin I proteolysis in the pathogenesis of stunned myocardium. *Circulation Research*, 80: 393-399.

GOLDSTEIN, P. & KROEMER, G. 2006. Cell death by necrosis: towards a molecular definition. *Trends in Biochemical Sciences*, 32: 37-43.

GÓMEZ, A.M., KERFANT, B.G. & VASSORT, G. 1999. Microtubule disruption modulates Ca^{2+} signaling in rat cardiac myocytes. *Circulation Research*, 86: 30-36.

GOOSSENS, V., GROOTEN, J., DE VOS, K. & FIERS, W. 1995. Direct evidence for tumor necrosis factor-induced mitochondrial reactive oxygen intermediates and their involvement in cytotoxicity. *Proceedings of the National Acadamy of Sciences (USA)*, 92: 8115-8119.

GOZUACIK, D. & KIMSHI, A. 2004. Autophagy as a cell death and tumor suppression mechanism. *Oncogene*, 23: 2891-2906.

GRANZIER, H.L. & LABEIT, S. 2002. Cardiac titin: an adjustable multi-functional spring. *Journal of Physiology*, 541: 335-342.

GRANZIER, H.L. & LABEIT, S. 2004. The giant protein titin: a major player in myocardial mechanics, signaling, and disease. *Circulation Research*, 94: 284-295.

GREASER, M. & GERGELY, J. 1971. Reconstruction of troponin activity from three protein components. *Journal of Biological Chemistry*, 246: 4226-4233.

GREEN, P.S. & LEEUWENBURGH, C. 2002. Mitochondrial dysfunction is an early indicator of doxorubicin-induced apoptosis. *Biochimica et Biophysica Acta*, 1588: 94-101.

GREGORIO, C.C., Trombitás, K., Centner, T., Kolmerer, B., Stier, G., Kunke, K., Suzuki, K., Obermayr, F., Herrmann, B., Granzier, H., Sorimachi, H. & Labeit, S. 1998. The NH2 terminus of titin spans the Z-disk: its interaction with a novel 19-kD ligand (T-cap) is required for sarcomeric integrity. *Journal of Cell Biology*, 143: 1013-1027.

GREGORIO, C.C., PERRY, C.N. & MCELHINNY, A.S. 2005. Functional properties of the titin/connectin-associated proteins, the muscle-specific RING finger proteins (MURFs), in striated muscle. *Journal of Muscle Research and Cell Motility*, 26: 389-400.

GROOTEN, J., GOOSSENS, V., VANHAESEBROECK, B. & FIERS, W. 1993. Cell membrane permeabilization and cellular collapse, followed by loss of

dehydrogenase activity: early events in tumour necrosis factor-induced cytotoxicity. *Cytokine*, 5: 546-555.

GROSS, G.J., KERSTEN, J.R. & WARLTIER, D.C. 1999. Mechanism of postischemic contractile dysfunction. *Annals of Thoracic Surgery*, 68: 1898-1904.

GUEVARA-BALCÁZAR, G., QUEREJETA-VILLAGÓMEZ, E., NUEVO-ADALLA, O., OROZCO-GUILLEN, A., RUBIO-GAYOSSO, I., HERNÁNDEZ-CASTILLO, J.R., ZAMORA-GARZA, M. & CEBALLOS-REYES, G. 2003. Spermine-induced negative inotropic effect in isolated rat heart, is mediated through the release of ATP. *Biochemical Pharmacology*, 66: 157-161.

GUY, P.M., KENNY, D.A. & GILL, G.N. 1999. The PDZ domain of the LIM protein enigma binds to beta-tropomyosin. *Molecular Biology of the Cell*, 10: 1973-1984.

HALESTRAP, A.P. & PASDOIS, P. 2009. The role of the mitochondrial permeability transition pore in heart disease. *Biochimica et Biophysica Acta - Bioenergetics*, 1787: 1402-1415.

HALLIWELL, B. & GUTTERIDGE, J.M.C. 1984. Oxygen toxicity, oxygen radicals, transition metals and disease. *Biochemical Journal*, 219: 1-14.

HANDKLOGTEN, M.E., SHIRAISHI, N., AWATA, H., HUANG, C. & MILLER, R.T. 2000. Extracellular Ca^{2+}-sensing receptor is a promiscouos divalent cation sensing that responds to lead. *American Journal Physiology - Renal Physiology*, 279: F1083-F1091.

HANNAN, R.D., JENKINS, A.K. & BRANDENBURGER, Y. 2003. Cardiac hypertrophy: a matter of translation. *Clinical and Experimental Pharmacology and Physiology*, 30: 517-527.

HANNIGAN, G.E., LEUNG-HAGESTEIJN, C., FITZ-GIBBON, L., COPPOLINO, M.G., RADEVA, G., FILMUS, J., BELL, J.C. & DEDHAR, S. 1996. Regulation of cell adhesion and anchorage-dependent growth by a new beta 1-integrin-linked protein kinase. *Nature*, 379: 91-96.

HARRIS, S.P., PATEL, J.R., MARTON, L.J. & MOSS, R.L. 2000. Polyamines decrease Ca^{2+} sensitivity of tension and increase rates of activation in skinned cardiac myocytes. *American Journal of Physiology - Heart and Circulatory Physiology*, 279: H1383-H1391.

HART, M.C. & COOPER, J.A. 1999. Vertebrate isoforms of actin capping protein beta have distinct functions *in vivo*. *Journal of Cell Biology*, 147: 1287-1298.

HATEFI, Y., LEST, R.L., CRANE, F.L. & WIDMER, C. 1959. Studies on the electron transport system. XVI. Enzymatic oxidoreduction reactions of coenzyme Q. *Biochimica et Biophysical Acta* 31: 490-501.

HAY, L., PIPEDI, M., SCHUTTE, P. J., TURNER, M. L. & SMITH, K. A. 2001. The effect of *Pavetta harborii* extracts on cardiac function in rats. *South African Journal of Science*, 97: 481-484.

HAY, L., SCHULTZ, R.A. & SCHUTTE, P.J. 2008. Cardiotoxic effects of pavetamine extracted from *Pavetta harborii* in the rat. *Onderstepoort Journal of Veterinary Research*, 75: 249-253.

HAYATA, N., FUJIO, Y., YAMAMOTO, Y., IWAKURA, T., OBANA, M., TAKAI, M., MOHRI, T., NONEN, S., MAEDA, M. & AZUMA, J. 2008. Connective tissue growth factor induces cardiac hypertrophy through Akt signaling. *Biochemical and Biophysical Research Communications*, 370: 274-278.

HAYDEN, M.S. & GHOSH, S. 2008. Shared principles in NF-kappaB signaling. *Cell*, 132: 344-62.

HEIN, S., SCHOLZ, D., FUJITANI, N., RENNOLLET, H., BRAND, T., FRIEDL, A. & SCHAPER, J. 1994. Altered expression of titin and contractile proteins in failing human myocardium. *Journal of Molecular and Cellular Cardiology*, 26: 1291-1306.

HEIN, S., SCHEFFOLD, T. & SCHAPER, J. 1995. Ischemia induces early changes to cytoskeletal and contractile proteins in diseased human myocardium. *Journal of Thoracic Cardiovascular Surgery*, 110: 89-94.

HEIN, S., KOSTIN, S., HELING, A., MAENO, Y & SCHAPER, J. 2000. The role of the cytoskeleton in heart failure. *Cardiovascular Research*, 45: 273-278.

HEIN, S., ARNON, E., KOSTIN, S., SCHÖNBURG, M., ELSÄSSER, A., POLYAKOVA, V., BAUER, E.P., KLÖVEKORN, W-P. & SCHAPER, J. 2003. Progression from compensated hypertrophy to failure in the pressure-overloaded human heart: structural deterioration and compensatory mechanisms. *Circulation*, 107: 984-991.

HELING, A., ZIMMERMANN, R., KOSTIN, S., MAENO, Y., HEIN, S., DEVAUX, B., BAUER, E., KLOVEKORN, W.P., SCHLEPPER, M., SCHAPER, W. & SCHAPER, J. 2000. Increased expression of cytoskeletal, linkage, and extracellular proteins in failing human myocardium. *Circulation Research*, 86: 846-853.

HERRERA, F., MARTIN, V., CARRERA, P., GARCIA-SANTOS, G., RODRIGUEZ-BLANCO, J., RODRIGUEZ, C. & ANTOLIN, I. 2006. Tryptamine induces cell death with ultrastructural features of autophagy in neurons and glia: possible relevance for neurodegenerative disorders. *Anatomical Record. Part A. Discoveries in Molecular, Cellular and Evolutionary Biology*, 288: 1026-1030.

HESCHELER, J., MEYER, R., PLANT, S., KRAUTWURST, D., ROSENTHAL, W. & SCHULTZ, G. 1991. Morphological, biochemical and electrophysiological characterization of a clonal cell (H9c2) line from rat heart. *Circulation Research*, 69: 1476–1486.

HICKE, L. 2001. A new ticket for entry into budding vesicles-ubiquitin. *Cell*, 106: 527-530.

HITOMI, J., CHRISTOFFERSON, D.E., NG, A., YAO, J., DEGTEREV, A., XAVIER, R.J. & YUAN, J. 2008. Identification of a molecular signaling network that regulates a cellular necrotic cell death pathway. *Cell*, 135: 1311-1323.

HOCHSTRASSER, M. 1995. Ubiquitin, proteasomes, and the regulation of intracellular protein degradation. *Current Opinion in Cell Biology*, 7: 215-223.

HOFMANN, W.A., STOJILJKOVIC, L., FUCHSOVA, B., VARGAS, G.M., MAVROMMATIS, E., PHILIMONENKO, V., KYSELA, K., GOODRICH, J.A., LESSARD, J.L., HOPE, T.J., HOZAK, P. & DE LANEROLLE, P. 2004. Actin is part of pre-initiation complexes and is necessary for transcription by RNA polymerase II. *Nature Cell Biology*, 6: 1094-1101.

HOLLER, N., ZARU, R., MICHEAU, O., THOME, M., ATTINGER, A., VALITUTTI, S., BODMER, J.L., SCHNEIDER, P., SEED, B. & TSCHOPP, J. 2000. Fas triggers an alternative, caspase-8-independent cell death pathway using the kinase RIP as effector molecule. *Nature Immunology*, 1: 489-495.

HORENSTEIN, M.S., VANDER HEIDE, R.S. & L'ECUYER, T.J. 2000. Molecular basis of anthracycline-induced cardiotoxicity and its prevention. *Molecular Genetics and Metabolism*, 71: 436-444.

HORNEMANN, T., KEMPA, S., HIMMEL, M., HAYESS, K., FÜRST, D.O. & WALLIMANN, T. 2003. Muscle-type creatine kinase interacts with central domains of the M-band proteins myomesin and M-protein. *Journal of Molecular Biology*, 332: 877-887.

HOSHIJIMA, M. 2006. Mechanical stress-strain sensors embedded in cardiac cytoskeleton: Z disk, titin, and associated structures. *American Journal of Physiology - Heart and Circulatory Physiology*, 290: H1313-H1325.

HU, P., WU, S. & HERNANDEZ, N. 2004. A role for beta-actin in RNA polymerase III transcription. *Genes and Development*, 18: 3010-3015.

HUXLEY, A.F. & PEACHEY, A.L. 1961. The maximum length for contraction in vertebrate striated muscle. *Journal of Physiology*, 156: 150-165.

IGARASHI, K. & KASHIWAGI, K. 2000. Polyamines: mysterious modulators of cellular functions. *Biochemical and Biophysical Research Communications*, 271: 559-564.

IGARASHI, K. & KASHIWAGI, K. 2010. Modulation of cellular functions by polyamines. *The International Journal of Biochemistry and Cell Biology*, 42: 39-51.

ISHIBASHI, Y., TAKAHASHI, M., ISOMATSU, Y., QIAE, F., IIJIMA, Y., SHIRAISHI, H., SIMSIC, J.M., BAICU, C.F., ROBBINS, J., ZILE, M.R. & COOPER, G., IV. 2003. Role of microtubules versus myosin heavy chain isoforms in contractile dysfunction of hypertrophied murine cardiocytes. *American Journal of Physiology - Heart and Circulatory Physiology*, 285: H1270-H1285.

JAFFE, A.B. & HALL, A. 2005. Rho GTPases: biochemistry and biology. *Annual Review of Cell and Developmental Biology*, 21: 247-269.

JANNE, J., ALHONEN, L. & LEINONEN, P. 1991. Polyamines: from molecular biology to clinical applications. *Annals of Medicine*, 23: 241-259.

JEON, H.B., CHOI, E.S., YOON, J.H., HWANG, J.H., CHANG, J.W., LEE, E.K., CHOI, H.W., PARK, Z.Y. & YOO, Y.J. 2007. A proteomics approach to identify the ubiquitinated proteins in mouse heart. *Biochemical and Biophysical Research Communications*, 357: 731-736.

JEYASEELAN, R., POIZAT, C., BAKER, R.K., ABDISHOO, S., ISTERABADI, L.B., LYONS, G.E. & KEDES, L. 1997. A novel cardiac-restricted target for doxorubicin. CARP, a nuclear modulator of gene expression in cardiac progenitor cells and cardiomyocytes. *Journal of Biological Chemistry*, 272: 22800-22808.

JOHNSTON, H.B., THOMAS, S.M. & ATTERWILL, C.K. 1993. Aluminium and iron induced metabolic changes in neuroblastoma cell lines and rat primary neural cultures. *Toxicology in Vitro*, 1: 229-233.

KADENBACH, B., RAMZAN, R., WEN, L. & VOGT, S. 2010. New extension of the Mitchell theory for oxidative phosphorylation in mitochondria of living organisms. *Biochimica et Biophysica Acta*, 1800: 205-212.

KE, Y., WANG, L., PYLE, W.G., DE TOMBE,P.P. & SOLARO, R.J. 2004. Intracellular localization and functional effects of p21-activated kinase 1 (Pak1) in cardiac myocytes. *Circulation Research*, 94: 194-200.

KE, L., QI, X.Y., DIJKHUIS, A.J., CHARTIER, D., NATTEL, S., HENNING, R.H., KAMPINGA, H.H. & BRUNDEL, B.J. 2008. Calpain mediates cardiac troponin degradation and contractile dysfunction in atrial fibrillation. *Journal of Molecular and Cellular Cardiology*, 45: 685-693.

KELLERMAN, T.S., NAUDÉ, T.W. & FOURIE, N. 1996. The distribution, diagnosis and estimated economic impact of plant poisonings and mycotoxicosis in South Africa. *Onderstepoort Journal of Veterinary Research*, 63: 65-90.

KELLERMAN, T.S., COETZER, J.A.W., NAUDÉ, T.W. & BOTHA, C.J. 2005. *Plant poisonings and mycotoxicoses of livestock in southern Africa.* 2nd ed. Cape Town: Oxford University Press. South Africa, pp. 154-164.

KERKELÄ, R. 2003. p38 mitogen-activated kinases. In: Koskinen, P., Kähäri, V.M. (ed). *Signaling pathways in myocyte hypertrophy, role of GATA4, mitogen-activated protein kinases and protein kinase C*. Oulu University Press. Finland, pp. 32-65.

KEYSE, S.M. 1999. The role of protein phosphatases in the regulation of mitogen and stress-activated protein kinases. *Free Radical Research*, 31: 341-349.

KIM, J-T., KIM, K.D., SONG, E.Y., LEE, H.G., KIM, J.W., KIM, J.W., CHAE, S-K., KIM, E., LEE, M-S., YANG, Y. & LIM, J-S. 2006. Apoptosis-inducing factor (AIF) inhibits protein synthesis by interacting with the eukaryotic translation initiation factor 3 subunit p44 (eIF3g). *FEBS Letters*, 580: 6375-6383.

KIMES, B.W. & BRANDT, B.L. 1976. Properties of a clonal muscle cell line from rat heart. *Experimental Cell Research*, 98: 367-381.

KINCAID, M.M. & COOPER, A.A. 2007. ERADicate ER stress or die trying. *Antioxidant Redox Signaling*, 9: 2373-2387.

KIRSCHKE, H. & BARRETT, A.J. 1987. Chemistry of lysosomal proteases. In*:* Glaumann, H. & Ballard, F.J. (eds), *Lysosomes: Their role in protein breakdown.* New York: Academic Press, pp. 193-238.

KLIONSKY, D.J. & EMR, S.D. 2000. Autophagy as a regulated pathway of cellular degradation. *Science*, 290: 1717-1720.

KNAAPEN, M.W., DAVIES, M.J., DE BIE, M., HAVEN, A.J., MARTINET, W. & KOCKX, M.M. 2001. Apoptotic versus autophagic cell death in heart failure. *Cardiovascular Research*, 51: 304-312.

KNIGHT, R.J. & BUXTON, D.B. 1996. Stimulation of c-Jun kinase and mitogen-activated protein kinase by ischemia and reperfusion in the perfused rat heart. *Biochemical and Biophysical Research Communications*, 218: 83-88.

KNÖLL, R., HOSHIJIMA, M. & CHIEN, K.R. 2002. Z-line proteins: implications for additional functions. *European Heart Journal Supplements*, 4: 113-117.

KOBAYASHI, T. & MATSUOKA, H. 2002. Critical role of Rho-kinase pathway for cardiac performance and remodeling in failing rat hearts. *Cardiovascular Research*, 55: 757-767.

KOJIC., S., MEDEOT, E., GUCCIONE, E., KRMAC, H., ZARA, I., MARTINELLI, V., VALLE, G. & FAULKNER, G. 2004. The Ankrd2 protein, a link between the sarcomere and the nucleus in skeletal muscle. *Journal of Molecular Biology*, 339: 313-325.

KONHILAS, J.P., IRVING, T.C., WOLSKA, B.M., JWEIED, E.E., MARTIN, A.F., SOLARO, R.J., & DE TOMBE, P.P. 2003. Troponin I in the murine heart: influence on length-dependent activation and inter-filament spacing. *Journal of Physiology*, 547: 951-961.

KONTROGIANNI-KONSTANTOPOULOS, A. & BLOCH, R.J. 2003. The hydrophilic domain of small ankyrin-1 interacts with the two N-terminal immunoglobulin domains of titin. *Journal of Biological Chemistry*, 278: 3985-3991.

KOOHMARAIE, M. 1992. Ovine skeleton muscle multicatalytic proteinase complex (proteasome): purification, characterization, and comparison of its effects on myofibrils with mu-calpains. *Journal of Animal Science*, 70: 3697-3708.

KOOPMAN, W.J.H., VERKAART, S., VISCH, H.J., VAN DER WESTHUIZEN, F.H., MURPHY, M.P., VAN DEN HEUVEL, L.W.P.J., SMEITINK, J.A.M. & WILLEMS, P.H.G.M. 2005. Inhibition of complex I of the electron transport chain causes oxygen radical-mediated mitochondrial outgrowth. *American Journal of Physiology - Cellular Physiology*, 288: C1440-C1450.

KOSTIN, S., POOL, L., ELSÄSSER, A., HEIN, S., DREXLER, H.C.A., ARNON, E., HAYAKAWA, Y., ZIMMERMANN, R., BAUER, E., KLÖVEKORN, W-P. & SCHAPER, J. 2003. Myocytes die by multiple mechanisms in failing human hearts. *Circulation Research*, 92: 715-724.

KOVACIC-MILIVOJEVIĆ, B., ROEDIGER, F., ALMEIDA, E.A,, DAMSKY, C.H., GARDNER, D.G. & ILIĆ, D. 2001. Focal adhesion kinase and p130C as mediate both sarcomeric organization and activation of genes associated with cardiac myocyte hypertrophy. *Molecular Biology of the Cell*,12: 2290-2307.

KOZUTSUMI, Y., SEGAL, M., NORMINGTON, K., GETHING, M.J. & SAMBROOK, J. 1988. The presence of malfolded proteins in the endoplasmic reticulum signals the induction of glucose-related proteins. *Nature*, 332: 462-464.

KROEMER, G. & REED, J.C. 2000. Mitochondrial control of cell death. *Nature Medicine*, 6: 513-519.

KROEMER, G., GALLUZZI, I. & BRENNER, C. 2007. Mitochondrial membrane permeabilization in cell death. *Physiological Reviews*, 87: 99-163.

KRÜGER, M. & LINKE, W.A. 2009. Titin-based mechanical signalling in normal and failing myocardium. *Journal of Molecular and Cellular Cardiology*, 46: 490-498.

KUBISTA, M., AAKERMAN, B. & NORDEN, B. 1987. Characterization of interaction between DNA and 4',6-diamidino-2-phenylindole by optical spectroscopy. *Biochemistry*, 26: 4545-4553.

KUMARAPELI, A.R., HORAK, K.M., GLASFORD, J.W., LI, J., CHEN, Q., LIU, J., ZHENG, H. & WANG, X. 2005. A novel transgenic mouse model reveals deregulation of the ubiquitin-proteasome system in the heart by doxorubicin. *Journal of the Federation of American Societies for Experimental Biology*, 19: 2051-2053.

KUNAPULI, S., ROSANIA, S. & SCHWARZ, E.R. 2006. "How Do Cardiomyocytes Die?" Apoptosis and autophagic cell death in cardiac myocytes. *Journal of Cardiac Failure*, 12: 381-391.

KURZ, T., TERMAN, A. & BRUNK, U.T. 2007. Autophagy, ageing and apoptosis: the role of oxidative stress and lysosomal iron. *Achives of Biochemistry and Biophysics*, 462: 220-230.

KUSTERMANS, G., PIETTE, J. & LEGRAND-POELS, S. 2008. Actin-targeting natural compounds as tools to study the role of actin cytoskeleton in signal transduction. *Biochemical Pharmacology*, 76: 1310-1322.

KUWAHARA, K., BARRIENTOS, T., PIPES, G.C., LI, S. & OLSON, E.N. 2005. Muscle-specific signaling mechanism that links actin dynamics to serum response factor. *Molecular and Cellular Biology*, 25: 3173-3181.

LABAJOVA, A., VOJTISKOVA, A., KRIVAKOVA, P., KOFRANEK, J., DRAHOTA, Z. & HOUSTEK, J. 2006. Evaluation of mitochondrial membrane potential using a computerized device with a tetraphenylphosphonium-selective electrode. *Analytical Biochemistry*, 353: 37-42.

LABEIT, S. & KOLMERER, B. 1995. Titins: giant proteins in charge of muscle ultrastructure and elasticity. *Science*, 270: 293-296.

LADER, A.S., KWIATKOWSKI, D.J. & CANTIELLO, H.F. 1999. Role of gelsolin in the actin filament regulation of cardiac L-type calcium channels. *American Journal of Physiology - Cell Physiology*, 46: C1277-C1283.

LAHMERS, S., WU, Y., CALL, D., LABEIT, S. & GRANZIER, H. 2004. Developmental control of titin isoform expression and passive stiffness in fetal and neonatal myocardium. *Circulation Research*, 94: 505-513.

LANGE, S., AUERBACH, D., MCLOUGHLIN, P., PERRIARD, E., SCHÄFER, B.W., PERRIARD, J-C. & EHLER, E. 2002. Subcellular targeting of metabolic enzymes to titin in heart muscle may be mediated by DRAL/FHL-2. *Journal of Cell Science*, 115: 4925-4936.

LANZETTI, L. 2007. Actin in membrane trafficking. *Current Opinion in Cell Biology*, 19: 453-458.

LAPIDUS, R.G. & SOKOLOVE, P.M. 1992. Inhibition by spermine of the inner membrane permeability transition of isolated rat heart mitochondria. *FEBS Letters*, 313: 314-318.

LEE, A.S. 2001. The glucose-regulated proteins: stress induction and clinical applications. *Trends in Biochemical Science*, 26: 504-510.

LEIST, M., SINGLE, B., CASTOLDI, A.F., KÜHNLE, S. & NICOTERA, P. 1997. Intracellular adenosine triphosphate (ATP) concentration: a switch in the decision between apoptosis and necrosis. *Journal of Experimental Medicine*, 185: 1481-1486.

LEMIEUX, B., PERCIVAL, M.D. & FALGUEYRET, J-P. 2004. Quantification of the lysosomotropic character of cationic amphiphilic drugs using the fluorescent basic amine Red DND-99. *Analytical Biochemistry*, 327: 247-251.

LESSARD, J. 1988. Two monoclonal antibodies to actin: one muscle selective and one generally reactive. *Cell Motility Cytoskeleton*, 10: 349-362.

LEUNG, G.P.H., TSE, C-M. & MAN, R.Y.K. 2007. Characterization of adenosine transport in H9c2 cardiomyoblasts. *International Journal of Cardiology*, 116: 186-193.

LEUNG, A.W.C. & HALESTRAP, A.P. 2008. Recent progress in elucidating the molecular mechanism of the mitochondrial permeability transition pore. *Biochimica et Biophysica Acta*, 1777: 946-952.

LEVINE, B. & KLIONSKY, D.J. 2004. Development by self-digestion: molecular mechanisms and biological functions of autophagy. *Developmental Cell*, 6:463-477.

LEVINE, B. & YUAN, J. 2005. Autophagy in cell death: an innocent convict? *Journal of Clinical Investigation*, 115: 2679-2688.

LE WINTER, M.M., WU, Y., LABEIT, S. & GRANZIER, H. 2007. Cardiac titin: structure, functions and role in disease. *Clinica Chimica Acta*, 375: 1-9.

LI, T.B., LIU, X.H., FENG, S., HU, Y., YANG, W.X., HAN, Y., WANG, Y.G. & GONG, L.M. 2004. Characterization of MR-1, a novel myofibrillogenesis regulator in human muscle. *Acta Biochimica et Biophysica Sinica*, 36: 412-418.

LIANG, Q. & MOLKENTIN, J.D. 2003. Redefining the roles of p38 and JNK signaling in cardiac hypertrophy: dichotomy between cultured myocytes and animal models. *Journal of Molecular and Cellular Cardiology*, 35: 1385-1394.

LIM, C.C., ZUPPINGER, C., GUO, X., KUSTER, G.M., HELMES, M., EPPENBERGER, H.M., SUTER, T.M., LIAO, R. & SAWYER, D.B. 2004. Anthracyclines induce calpain-dependent titin proteolysis and necrosis in cardiomyocytes. *Journal of Biological Chemistry*, 279: 8290-8299.

LIN, H-J., HERMAN, P., KANG, J.S. & LAKOWICS, J.R. 2001. Fluorescence lifetime characterization of novel low-pH probes. *Analytical Biochemistry*, 294: 118-125.

LINDAHL, P.E. & OBERG, K.E. 1961. The effect of rotenone on respiration and its point of attack. *Experimental Cell Research*, 23: 228-237.

LIU, Y.H., WANG, D., RHALEB, N.E., YANG, X.P., YU, J., SANKEY, S.S., RUDOLPH, A.E. & CARRETERO, O.A. 2005. Inhibition of p38 mitogen-activated protein kinase protects the heart against cardiac remodeling in mice with heart failure resulting from myocardial infarction. *Journal of Cardiac Failure*, 11: 74-81.

LOCKSHIN, R.A. & ZAKERI, Z. 2004. Apoptosis, autophagy and more. The *International Journal of Biochemistry and Cell Biology*, 36: 2405-2419.

LOOS, B. & ENGELBRECHT, A-M. 2009. Cell death. A dynamic response concept. *Autophagy*, 5: 1-14.

LOPICCOLO, J., BLUMENTHAL, G.M., BERNSTEIN, W.B. & DENNIS, P.A. 2008. Targeting the PI3K/Akt/mTOR pathway: effective combinations and clinical considerations. *Drug Resistance Updates*, 11: 32-50.

LORELL, B.H. & CARABELLO, B.A. 2000. Left ventricular hypertrophy: pathogenesis, detection, and prognosis. *Circulation*, 102: 470-479.

LOWESS, B.D., MINOBE, W., ABRAHAM, W.T., RIZEQ, M.N., BOHLMEYER, T.J. & QUAIEFE, R.A. 1997. Changes in gene expression in the intact human heart. Downregulation of alpha-myosin heavy chain in hypertrophied, failing ventricular myocardium. *Journal of Clinical Investigations*, 100: 2315-2324.

LUO, G., HERRERA, A.H. & HOROWITS, R. 1999. Molecular interactions of N-RAP, a nebulin-related protein of striated muscle myotendon junctions and intercalated disks. *Biochemistry*, 38: 6135-6143.

MACCARRONE, M., BARI, M., BATTISTA, N., DI RIENZO, M., FALCIGLIA, K. & AGR, F. 2001. Oxidation products of polyamines induce mitochondrial uncoupling and cytochrome *c* release. *FEBS Letters*, 507: 30-34.

MACO, B., MANDINOVA, A., DÜRRENBERGER, M.B., SCHÄFER, B.W., UHRÍK, B. & HEIZMANN, C.W. 2001. Ultrastructural distribution of the S100A1 Ca^{2+}-binding proteins in the human heart. *Physiology Research*, 50: 567-574.

MÄKITIE, L.T., KANERVA, L. & ANDERSSON, L.C. 2009. Ornithine decarboxylase regulates the activity and localization of rhoA via polyamination. *Experimental Cell Research*, 315: 1008-1014.

MALAGOLI, D., MARCHESINI, E. & OTTAVIANI, E. 2006. Lysosomes as the target of yessotoxin in invertebrate and vertebrate cell lines. *Toxicology Letters*, 167: 75-83.

MANSER, E., & LIM, L. 1999. Roles of PAK family kinases. *Progress in Molecular and Subcellular Biology*, 22: 115-133.

MARIAN AJ. 2006. Beta-adrenergic receptors signaling and heart failure in mice, rabbits and humans. *Journal of Molecular and Cellular Cardiology*, 41: 11-13.

MARTINET, W., KNAAPEN, M.W.M., KOCKX, M.M. & DE MEYER, G.R.Y. 2007. Autophagy in cardiovascular disease. *Trends in Molecular Medicine*, 13: 482-491.

MARX, J., PRETORIUS, E. & BORNMAN, M.S. 2006. The neorotoxic effects of prenatal cardiac glycoside exposure: a hypothesis. *Neurotoxicology and Teratology*, 28: 135-143.

MATSUI, T. & ROSENZWEIG, A. 2005. Convergent signal transduction pathways controlling cardiomyocyte survival and function: the role of PI 3-kinase and Akt. *Journal of Molecular and Cellular Cardiology*, 38: 63-71.

MATSUKURA, U., OKITANI, A., NISHIMURO, T. & KATO, H. 1981. Mode of degradation of myofibrillar proteins by an endogenous protease, cathepsin L. *Biochimica et Biophysica Acta*, 662: 41-47.

MAYANS, O., VAN DER VEN, P.F., WILM, M., MUES, A., YOUNG, P., FURST, D.O., WILMANNS, M. & GAUTEL, M. 1998. Structural basis for activation of the titin kinase domain during myofibrillogenesis. *Nature*, 395: 863-869.

MAYER, J.B. 2001. SH3 domains: complexity in moderation. *Journal of Cell Science*, 114: 1253-1263.

MCELHINNY, A.S., KAKINUMA, K., SORIMACHI, H., LABEIT, S. & GREGORIO, C.C. 2002. Muscle-specific RING finger-1 interacts with titin to regulate sarcomeric M-line and thick filament structure and may have nuclear functions via its interaction with glucocorticoid modulatory element binding protein-1. *Journal of Cell Biology*, 157: 125-136.

MCKOY, G., PROTONOTARIOS, N., CROSBY, A., TSATSOPOULOU, A., ANASTASAKIS, A., COONAR, A., NORMAN, M., BABOONIAN, C., JEFFERY, S. & MCKENNA, W.J. 2000. Identification of a deletion in plakoglobin in arythmogenic right ventricular cardiomyopathy with palmoplantar keratoderma and woolly hair (Naxos disease). *Lancet*, 355: 2119-2124.

MCMILLAN, D.R., GETHING, M.J. & SAMBROOK, J. 1994. The cellular response to unfolded proteins: intercompartmental signaling. *Current Opinion in Biotechnology*, 5: 540-545.

MEIJER, A.J. & DUBBELHUIS, P.F. 2004. Amino acid signaling and the integration of metabolism. *Biochemical and Biophysical Research Communication*, 313: 397-403.

MEININGER, M., LANDSCHUTZ, W., BEER, M., SEYFARTH, T., HORN, M., PABST, T., HAASE, A., HAHN, D., NEUBAUER, S. & KIENLIN, V.M. 1999. Concentrations of human cardiac phosphorus metabolites determined by SLOOP31P NMR spectroscopy. *Magnetic Resonance in Medicine*, 41: 657-663.

MILLER, M.K., BANG, M.L., WITT, C.C., LABEIT, D., TROMBITAS, C., WATANABE, K., GRANZIER, H., MCELHINNY, A.S., GREGORIO, C.C. & LABEIT, S. 2003. The muscle ankyrin repeat proteins: CARP, ankrd2/Arpp and DARP as a family of titin filament-based stress response molecules. *Journal of Molecular Biology*, 333: 951-964.

MILLER, M.K., GRANZIER, H., EHLER, E. & GREGORIO, C.C. 2004. The sensitive giant: the role of titin-based stretch sensing complexes in the heart. *Trends in Cell Biology*, 14: 119-126.

MILLOT, C., MILLOT, J-M., MORJANI, H., DESPLACES, A. & MANFAIT, M. 1997. Characterization of acidic vesicles in multidrug-resistant and sensitive cancer cells by acridine orange staining and confocal microspectrofluorometry. *Journal of Histochemistry and Cytochemistry*, 45: 1255-1264.

MILNER, D.J., MAVROIDIS, M., WEISLEDER, N. & DAPETANAKI, Y. 2000. Desmin cytoskeleton linked to muscle mitochondrial distribution and respiratory function. *Journal of Cell Biology*, 150: 1283-1298.

MIRALLES, F. & VISA, N. 2006. Actin in transcription and transcription regulation. *Current Opinion in Cell Biology*, 18: 261-266.

MITHCELL, J.L., JUDD, G.G., BAREYAL-LEYSER, A. & LING, S.Y. 1994. Feedback repression of polyamine transport is mediated by antizyme in mammalian tissue-culture cells. *Biochemical Journal*, 299: 19-22.

MOLKENTIN, J.D., LU, J.R., ANTOS, C.L., MARKHAM, B., RICHARDSON, J., ROBBINS, J., GRANT, S.R. & OLSON, E.N. 1998. A calcineurin-dependent transcriptional pathway for cardiac hypertrophy. *Cell*, 93: 215-228.

MONCMAN, C.L., & WANG, K. 1999. Functional dissection of nebulette demonstrates actin binding of nebulin-like repeats and Z-line targeting of SH3 and linker domains. *Cell Motility Cytoskeleton*, 44: 1-22.

MONCMAN, C.L. & WANG, K. 2002. Targeted disruption of nebulette protein expression alters cardiac myofibril assembly and function. *Experimental Cell Research*, 273: 204-218.

MONTELL. C. 2005. The latest waves in calcium signaling. *Cell*, 122: 157-163.

MORANO, I., HÄDICKE, K., GROM, S., KOCH, A., SCHWINGER, R.H., BÖHM, M., BARTEL, S., ERDMANN, E., & KRAUSE, E.G. 1994. Titin, myosin light chains and C-protein in the developing and failing human heart. *Journal of Molecular and Cellular Cardiology*, 26: 361-368.

MORGAN, H. E., GORDON, E. E., KIRA Y., CHUA, B. H. L., RUSSO, L. A., PETERSON, C. J., MCDERMOTT, P. J., & WATSON, P. A. 1987. Biochemical mechanisms of cardiac hypertrophy. *Annual Review of Physiology*, 49: 533-543.

MORI, K., MA, W., GETHING, M.J. & SAMBROOK, J.A. 1993. A transmembrane protein with a cdc2+/CDC28-related kinase activity is required for signaling from the ER to the nucleus. *Cell*, 74: 743-756.

MORISETTE, G., MOREAU, E., GAUDREAULT, R.C. & MARCEAU, F. 2004. Massive cell vacuolization induced by organic amines such as procainamide. *Journal of Pharmacology and Experimental Therapeutics*, 310: 395-406.

MORISETTE, G., LODGE, R. & MARCEAU, F. 2008. Intense pseudotransport of a cationic drug mediated by vacuolar ATPase: procainamide-induced autophagic cell vacuolization. *Toxicology and Applied Pharmacology*, 228: 364-377.

MOSS, D.K. & LANE, J.D. 2006. Microtubules: forgotten players in the apoptotic execution phase. *Trends in Cell Biology*, 16: 330-338.

MOSMANN, T. 1983. Rapid colorimetric assay for cellular growth and survival: application to proliferation and cytotoxicity assays. *Journal of Immunological Methods*, 65: 55-63.

MOZA, M., MOLOGNI, L., TROKOVIC, R., FAULKNER, G., PARTANEN, J. & CARPÉN, O. 2007. Targeted deletion of the muscular dystrophy gene myotilin does not perturb muscle structure or function in mice. *Molecular and Cellular Biology*, 27: 244-252.

MÜLLER, J.M., ISELE, U., METZGER, E., REMPEL,A., MOSER, M., PSCHERER, A., BREYER, T., HOLUBARSCH, C., BUETTNER, R. & SCHÜLE, R. 2000.

FHL2, a novel tissue-specific coactivator of the androgen receptor. *EMBO Journal*, 19: 359-369.

NAGUEH, S.F., SHAH, G., WU, Y., TORRE-AMIONE, G., KING, N.M.P., LAHMERS, S., WITT, C.C., NECKER, K., LABEIT, S. & GRANZIER, L. 2004. Altered titin expression, myocardial stiffness, and left ventricular function in patients with dilated cardiomyopathy. *Circulation*, 110: 155-162.

NAVE, B.T., OUWENS, M., WITHERS, D.J., ALESSI, D.R. & SHEPHERD, P.R. 1999. Mammalian target of rapamycin is a direct target for protein kinase B: identification of a convergence point for opposing effects of insulin and amino acid deficiency on protein translation. *Biochemical Journal*, 344: 427-431.

NEAGOE, C., KULKE, M., DEL MONTE, F., GWATHMEY, J.K., DE TOMBE, P.P., HAJJAR, R.J. & LINKE, W.A. 2002. Titin isoform switch in ischemic human heart disease. *Circulation*, 106: 1333-1341.

NEARING, J., BETKA, M., QUINN, S., HENTSCHEL, H., ELGER, M., BAUM, M., BAI, M., CHATTOPADYHAY, N., BROWN, E.M., HEBERT, S.C. & HARRIS, H.W. 2002. Polyvalent cation receptor proteins (CaRs) are salinity sensors in fish. *Proceedings of the National Acadamy of Sciences (USA)*, 99: 9231-9236.

NIESSEN, C.M. 2007. Tight junctions/adherens junctions: basic structure and function. *Journal of Investigation Dermatology*, 127: 2525-2532.

NOBES, C.D. & HALL, A. 1995. Rho, rac, and cdc42 GTPases regulate the assembly of multimolecular focal complexes associated with actin stress fibers, lamellipodia, and filopodia. *Cell*, 81: 53-62.

NOORMAN, M., VAN DER HEYDEN, M.A.G., VAN VEEN, T.A.B., COX, M.G.P.J., HAUER, R.N.W., DE BAKKER, J.M.T. & VAN RIJEN, H.V.M. 2009. Cardiac cell-cell junctions in health and disease: electrical versus mechanical coupling. *Journal of Molecular and Cellular Cardiology*, 47: 23-31.

OBERMANN, W.M., GAUTEL, M., STEINER, F., VAN DER VEN, P.F., WEBER, K. & FÜRST, D.O. 1996. The structure of the sarcomeric M band: localization of defined domains of myomesin, M-protein, and the 250-kD carboxy-terminal region of titin by immunoelectron microscopy. *Journal of Cell Biology*, 134: 1441-1453.

OBERMANN, W.M., GAUTEL, M., WEBER, K. & FÜRST, D.O. 1997. Molecular structure of the sarcomeric M band: mapping of titin and myosin binding domains in myomesin and the identification of a potential regulatory phosphorylation site in myomesin. *EMBO Journal*, 16: 211-220.

OHNO, Y., YAGI, H., NAKAMURA, M., MASUKO, K., HASHIMOTO, Y. & MASUKO, T. 2008. Simultaneous induction of apoptotic, autophagic, and necrosis-like cell death by monoclonal antibodies recognizing chicken transferrin receptor. *Biochemical and Biophysical Research Communications*, 367: 775-781.

ORIOL-AUDIT, C. 1978. Polyamine-induced actin polymerization. *European Journal of Biochemistry*, 87: 371-376.

OTEY, C.A., RACHLIN, A., MOZA, M., ARNEMAN, D. & CARPEN, O. 2005. The palladin/myotilin/myopalladin family of actin-associated scaffolds. *International Review of Cytology*, 246: 31-58.

PALMER, B.M. 2005. Thick filaments and performance in human heart failure. *Heart Failure Reviews*, 10: 187-197.

PARENT, N., WINSTALL, E., BEAUCHEMIN, M., PAQUET, C., POIRIERG.G. & BERTRANDA, R. 2009. Proteomic analysis of enriched lysosomes at early phase of camptothecin-induced apoptosis in human U-937 cells. *Journal of Proteomics*, 72: 960-973.

PARK., Y., KANEKAL,S. & KEHRER, J.P. 1991. Oxidative changes in hypoxic rat heart tissue. *American Journal of Physiology – Heart and Circulatory Physiology*, 260: H1395-H1405.

PASHMFOROUSH, M., POMIES, P., PETERSON, K. L., KUBALAK, S., ROSS, J., JR., HEFTI, A., AEBI, U., BECKERLE, M. C. & CHIEN, K. R. 2001. Adult mice deficient in actinin-associated LIM-domain protein reveal a developmental pathway for right ventricular cardiomyopathy. *Nature Medicine*, 7: 591-597.

PATTINGRE, S., TASSA, A., QU, X., GARUTI, R., HUAN LIANG, X., MIZUSHIMA, N., PACKER, M., SCHNEIDER, D. & LEVINE, B. 2005. Bcl-2 antiapoptotic proteins inhibit beclin-1-dependent autophagy. *Cell*, 122: 927-939.

PEARSON, G., ROBINSON, F., GIBSON, T.B., XU, B.E., KARANDIKAR, M., BERMAN, K. & COBB, M.H. 2001. Mitogen-activated protein (MAP) kinase

pathways: regulation and physiological functions. *Endocrine Reviews*, 22: 153-183.

PEDREÑO, E., LÓPEZ-CONTRERAS, A.J., CREMADES, A. & PEÑAFIEL, R. 2005. Protecting or promoting effects of spermine on DNA strand breakage induced by iron or copper ions as a function of metal concentration. *Journal of Inorganic Biochemistry*, 99: 2074-2080.

PERIASAMY, M. & HUKE, S. 2001. SERCA pump level is a critical determinant of Ca^{2+} homeostasis and cardiac contractility. *Journal of Molecular Cell Cardiology*, 33: 1053-1063.

PHANSTIEL, O., PRICE, H.L., WANG, L., JUUSOLA, J., KLINE, M. & SHAH, S.M. 2000. The effect of polyamine homologation on the transport and cytotoxicity properties of polyamine-(DNA-intercalator) conjugates. *Journal of Organic Chemistry*, 65: 5590-5599.

POWELL, S.R., WANG, P., KATZEFF, H., SHRINGARPURE, R., TEOH, C., KHALIULIN, I., DAS, D.K., DAVIES, K.J. & SCHWALB, H. 2005. Oxidized and ubiquitinated proteins may predict recovery of postischemic cardiac function: essential role of the proteasome. *Antioxidants and Redox Signaling*, 7: 538-546.

PRASAD, A.M. & INESI, G. 2009. Effect of thapsigargin and phenylephrine on calcineurin and protein kinase C signaling functions in cardiomyocytes. *American Journal of Physiology – Cell Physiology*, 296: C992-C1002.

PRETORIUS, P.J. & TERBLANCHE, M., 1967. A preliminary study on the symptomatology and cardiodynamics of gousiekte in sheep and goats. *Journal of South African Veterinary Medical Association*, 38: 29-52.

PRETORIUS, P.J., TERBLANCHE, M., VAN DER WALT, J.D. & VAN RYSSEN, J.C.J. 1973a. Cardiac failure in ruminants caused by gousiekte. Recent advances in cardiac structure and metabolism. University Park Press, Baltimore. pp. 385-397.

PRETORIUS, P.J., TERBLANCHE, M., VAN DER WALT, J.D. & VAN RYSSEN, J.C.J. 1973. Cardiac failure in ruminants caused by gousiekte. International symposium on cardiomyopathies, Tiervlei, 1971. In: BAJUSZ, E. & RONA, G.

with BRINK, A.J. & LOCHNER, A. (eds). *Cardiomyopathies*, 2, Baltimore: University Park Press, pp. 384-624.

PROZESKY, L., BASTIANELLO, S.S., FOURIE, N. & SCHULTZ, R.A. 2005. A study of the pathology and pathogenesis of the myocardial lesions in gousiekte, a plant-induced cardiotoxicosis of ruminants. *Onderstepoort Journal of Veterinary Research*, 72: 219-230.

PROZESKY, L. 2008. A study of the pathology and pathogenesis of myocardial lesions in gousiekte, a cardiotoxicosis of ruminants. PhD Dissertation, University of Pretoria.

PURCEL, H., TANG, G., YU, C., MERCURIO, F., DIDONATO, J.A. & LIN, A. 2001. Activation of NF-κB is required for hypertrophic growth of primary rat neonatal ventricular cardiomyocytes. *Proceedings of the National Acadamy of Sciences (USA)*, 98: 6668-6673.

PYLE, W.G. & SOLARO, R.J. 2004. At the crossroads of myocardial signaling: the role of Z-discs in intracellular signaling and cardiac function. *Circulation Research*, 94: 296-305.

QUACH, N.L. & RANDO, T.A. 2006. Focal adhesion kinase is essential for costamerogenesis in cultured skeletal muscle cells. *Developmental Biology*, 293: 38-52.

QUINN, S.J., YE, C-P., DIAZ, R., KIFOR, O., BAI, M., VASSILEV, P. & BROWN, E. 1997. The Ca^{2+}-sensing receptor: a target for polyamines. *American Journal of Physiology - Cell Physiology*, 273: C1315-C1323.

RAINAUD, J., WHITMARSCH, A., BARRETT, T., DERIJARD, B. & DAVIS, R. 1996. MKK3-and MKK6-regulated gene expression is mediated by the p38 mitogen-activated protein kinase signal transduction pathway. *Molecular Cell Biology*, 16: 1247-1255.

RAHIMTOOLA, S. 1989. The hibernating myocardium. *American Heart Journal*, 117: 211-221.

RAZEGHI, P., VOLPINI, K.C., WANG, M-E., YOUKER, K.A., STEPKOWSKI, S. & TAEGTMEYER, H. 2007. Mechanical unloading of the heart activates the calpain system. *Journal of Molecular and Cellular Cardiology*, 42: 449-452.

REGULA, K.M., ENS, K. & KIRSHENBAUM, L.A. 2003. Mitochondria-assisted cell suicide: a license to kill. *Journal of Molecular and Cellular Cardiology*, 35: 559-567.

REN, X., LI, Y., MA, X., ZHENG, L., XU, Y. & WANG, J. 2007. Activation of p38/MEF2 pathway by all-trans retinoic acid in cardiac myocytes. *Life Sciences*, 81: 89-96.

REVENU, C., ATHMAN, R., ROBINE, S. & LOUVARD, D. 2004. The co-workers of actin-filaments: from cell structures to signals. *Nature Reviews Molecular Cell Biology*, 5: 635-646.

RIDLEY, A.J. & HALL, A. 1992. The small GTP-binding protein Rho regulates the assembly of focal adhesions and actin stress fibers in response to growth factors. *Cell*, 70: 389-399.

ROGERS, S.L. & GELFAND, V.I. 2000. Membrane trafficking, organelle transport, and the cytoskeleton. *Current Opinion in Cellular Biology*, 12: 57-62.

ROTTENBERG, H. & WU, S. 1998. Quantitative assay by flow cytometry of the mitochondrial membrane potential in intact cells. *Biochimica et Biophysica Acta*, 1404: 393-404.

RUBINSZTEIN, D.C. 2006. The roles of intracellular protein-degradation pathways in neurodegeneration. *Nature*, 443: 780-786.

RUBIOLO, J.A. & VEGA, F.V. 2008. Resveratrol protects primary rat hepatocytes against necrosis induced by reactive oxygen species. *Biomedicine and Pharmacotherapy*, 62: 606-612.

RUECKSCHLOSS, U. & ISENBERG, G. 2001. Cytochalasin D reduces Ca^{2+} currents via cofilin-activated depolymerization of F-actin in guinea pig cardiomyocytes. *Journal of Physiology*, 537: 363-370.

RUMYANTSEV, P.P. 1977. Interrelations of the proliferation and differentiation processes during cardiac myogenesis and regeneration. *International Review of Cell and Molecular Biology*, 51: 186-273.

RUSSELL, W.M.S. & BURCH, R.L. 1959. *The Principles of Humane Experimental Technique*. London, UK: Methuen, pp. 238.

SAKAIDA, I., KYLE, M.E. & FARBER, J.L. 1990. Autophagic degradation of protein generates a pool of ferric iron required for the killing of cultured hepatocytes by an oxidative stress. *Molecular Pharmacology*, 37: 435-442.

SALVI, M. & TONINELLO, A. 2004. Effects of polyamines on mitochondrial Ca^{2+} transport. *Biochimica et Biophysical Acta*, 1661: 113-124.

SAMAREL, A.M. & ENGELMANN, G.L. 1991. Contractile activity modulates myosin heavy chain-β expression in neonatal rat heart cells. *American Journal of Physiology – Heart and Circulatory Physiology*, 261: H1067-H1077.

SARBASSOV, D.D., ALI, S.M. & SABATINI, D.M. 2005. Growing roles for the mTOR pathway. *Current Opinion in Cell Biology*, 17: 596-603.

SCHAUB, M.C., HEFTI, M., ZUELLIG, R.A. & MORANO, I. 1998. Modulation of contractility in human cardiac hypertrophy by myosin essential light chain isoforms. *Cardiovascular Research*, 37: 381-404.

SCHAUB, M.C. & HEIZMANN, C.W. 2008. Calcium, troponin, S100 proteins: from myocardial basics to new therapeutic strategies. *Biochemical and Biophysical Research Communications*, 369: 247-264.

SCHOLL., F.A., MCLOGHLIN, P., EHLER, E., DE GIOVANNI, C. & SCHÄFER, B.W. 2000. DRAL is a p53-responsive gene whose four and a half LIM domain protein product induces apoptosis. *Journal of Cell Biology*, 151: 495-506.

SCHULTZ, R.A., FOURIE, N., BASSON, K.M., LABUSCHAGNE, L. & PROZESKY, L. 2001. Effect of pavetamine on protein synthesis in rat tissue. *Onderstepoort Journal of Veterinary Research*, 68: 325-330.

SCHUTTE, P.J., ELS, H.J. & BOOYENS, J. 1984. Ultrastructure of myocardial cells in sheep with congestive heart failure induced by *Pachystigma pygmaeum*. *South African Journal of Science*, 80: 378-380.

SCHLIWA, M. 1982. Action of cytochalasin D on cytoskeletal networks. *Journal of Cell Biology*, 92: 79-91.

SEGLEN, P.O. & GORDON, P.B. 1982. 3-Methyladenine: specific inhibitor of autophagic/lysosomal protein degradation in isolated rat hepatocytes. *Proceedings of the National Academy of Sciences (USA)*, 79: 1889-1892.

SHEEHAN, K.A., KE, Y. & SOLARO, R.J. 2007. p21-Activated kinase-1 and its role in integrated regulation of cardiac contractility. *American Journal of Physiology - Regulatory, Integrative and Comparative Physiology*, 293: R963-R973.

SHEIKH, F., RASKIN, A., CHU, P.H., LANGE, S., DOMENIGHETTI, A.A., ZHENG, M., LIANG, M.X., ZHANG, T., YAJIMA, T., GU, Y., DALTON, N.D., MAHATA1, S.K., DORN, G.W., HELLER-BROWN, J., PETERSON, K.L., OMENS, J.H., MCCULLOCH, A.D., & CHEN, J.U. 2008. An FHL1-containing complex within the cardiomyocyte sarcomere mediates hypertrophic biomechanical stress responses in mice. *Journal of Clinical Investigation*, 118: 3870-3880.

SHI, Y., VATTEM, K.M., SOOD, R., AN, J., LIANG, J., STRAMM, L. & WEK, R.C. 1998. Identification and characterization of pancreatic eukaryotic initiation factor 2 alpha-subunit kinase, PEK, involved in translation control. *Molecular Cell Biology*, 18: 7499-7509.

SINGH, R.B., CHOHAN, P.K., DHALLA, N.S. & NETTICADAN, T. 2004. The sarcoplasmic reticulum proteins are targets for calpain action in the ischemic-reperfused heart. *Journal of Molecular and Cellular Cardiology*, 37: 101-110.

SIPIDO, K.R. & MARBAN, E. 1991. L-type calcium channels, potassium channels, and novel non-specific cation channels in a clonal muscle cell line derived from embryonic rat heart. *Circulation Research*, 69: 1487-1499.

SKOMMER, J., WLODKOWIC, D. & DEPTALA, A. 2007. Larger than life: mitochondria and the Bcl-2 family. *Leukemia Research*, 31: 277-286.

SNYMAN, L.D., VAN DER WALT, J.J. & PRETORIUS, P.J. 1982. A study on the function on some subcellular systems of the sheep myocardium during gousiekte. I. The energy production system. *Onderstepoort Journal of Veterinary Research*, 49: 215-220.

SOLOMON, V. & GOLDBERG, A.L. 1996. Importance of the ATP-ubiquitin-proteasome pathway in the degradation of soluble and myofibrillar proteins in rabbit muscle extracts. *Journal of Biological Chemistry*, 271: 26690-26697.

SOLARO, R.J. 2001. Modulation of cardiac myofilament activity by protein phosphorylation. In: PAGE, E., FOZZARD, H., SOLARO, R.J., (eds). *Handbook*

of Physiology, Section 2: The Cardiovascular System. The Heart. New York, Oxford University Press, pp 264-327.

SONG, Y., HOANG, B.Q. & CHANG, D.D. 2002. ROCK-II-induced membrane blebbing and chromatin condensation require actin cytoskeleton. *Experimental Cell Research*, 278: 45-52.

SOTIROPOULOS, A., GINEITIS, D., COPELAND, J. & TREISMAN, R. 1999. Signal-regulated activation of serum response factor is mediated by changes in actin dynamics. *Cell*, 98: 159-169.

SOULET, D., GAGNON, B., RIVEST, S., AUDETTE, M. & POULIN, R. 2004. A fluorescent probe of polyamine transport accumulated into intracellular acidic vesicles via a two-step mechanism. *Journal of Biological Chemistry*, 279: 49355-49366.

SPECTOR, I., SHOCHET, N.R., KASHMAN, Y. & GROWEISS, A. 1983. Latrunculins: novel marine toxins that disrupt microfilament organization in cultured cells. *Science*, 219: 493-495.

SPENCER, J.A., ELIAZER, S., ILARIA, R.L., Jr., RICHARDSON, J.A. & OLSON, E.N. 2000. Regulation of microtubule dynamics and myogenic differentiation by MURF, a striated muscle RING-finger protein. *Journal of Cell Biology*, 150: 771-784.

SRIVASTAVA, D. & YU, S. 2006. Stretching to meet needs: integrin-linked kinase and the cardiac pump. *Genes and Development*, 20: 2327-2330.

STAPULIONIST, R., KOLLI, A. & DEUTSCHER, M.P. 1997. Efficient mammalian protein synthesis requires an intact F-actin. *Journal of Biological Chemistry*, 272: 24980-24986.

STEFANELLI, C., STANIC, I., ZINI, M., BONAVITA, F., FLAMIGNI, F., ZAMBONIN, L., LANDI, L., PIGNATTI, C., GUARNIERI, C. & CALDARERA, C.M. 2000. Polyamines directly induce release of cytochrome *c* from heart mitochondria. *Biochemical Journal*, 347: 875-880.

SUN, X.M., BUTTERWORTH, M., MACFARLANE, M., DUBIEL, W., CIECHANOVER, A. & COHEN, G.M. 2004. Caspase activation inhibits proteasome function during apoptosis. *Molecular Cell*, 14: 81-93.

TAKEISHI, Y., PING, P., BOLLI, R., KIRKPATRICK, D.L., HOIT, B.D. & WALSH, R.A. 2000. Transgenic overexpression of constitutively active protein kinase C epsilon causes concentric cardiac hypertrophy. *Circulation Research*, 86: 1218-1223.

TAM, S.K., GU, W., MAHDAVI, V. & NADAL-GINARD, B. 1995. Cardiac myocyte terminal differentiation. *Annals of the New York Academy of Sciences*, 752: 72-79.

TANTINI., B., FIUMANA, E., CETRULLO, S., PIGNATTI, C., BONAVITA, F., SHANTZ, L.M., GIORDANO, E., MUSCARI, C., FLAMIGNI, F., GUARNIERI, C., STEFANELLI, C. & CALDARERA, C.M. 2006. Involvement of polyamines in apoptosis of cardiac myoblasts in a model of simulated ischemia. *Journal of Molecular and Cellular Cardiology*, 40: 775-782.

TEMSAH, R.M., NETTICADAN, T., CHAPMAN, D., TAKEDA, S., MOCHIZUKI, S. & DHALLA, N.S. 1999. Alterations in sarcoplasmic reticulum function and gene expression in ischemic-reperfused rat heart. *American Journal of Physiology – Heart and Circulatory Physiology*, 277: H584-H594.

TFELT-HANSEN, J. 2003. Calcium-sensing receptor stimulates PTHrP release by pathways dependent on PKC, p38-MAPK, JNK, and ERK1/2 in H-500 cells. *American Journal of Physiology – Endocrinology and Metabolism*, 285: E329-E337.

THEILER, A., DU TOIT, P.J. & MITCHELL, D.T. 1923. Gousiekte in sheep. *In*: 9th and 10th reports of the Director of Veterinary Education and Research, Onderstepoort, Pretoria: The Government Printing and Stationary Office, pp 1-106.

THEODOSSIOU, T.A., NORONHA-DUTRA, A. & HOTHERSALL, J.S. 2006. Mitochondria are a primary target of hypericin phototoxicity: synergy of intracellular calcium mobilisation in cell killing. *International Journal of Biochemistry and Cell Biology*, 38: 1946-1956.

TOLSTONOG, G.V., SABASCH, M. & TRAUB, P. 2002. Cytoplasmic intermediate filaments are stably associated with nuclear matrices and potentially modulate their DNA-binding function. *DNA Cell Biology*, 21: 213-239.

TONINELLO, A., SALVI, M. & MONDOVI, B. 2004. Interaction of biologically active amines with mitochondria and their role in the mitochondrial-mediated pathway of apoptosis. *Current Medicinal Chemistry*, 11: 2349-2374.

TSUTSUI, H., ISHIHARA, K. & COOPER, G, 4th. 1993. Cytoskeletal role in the contractile dysfunction of hypertrophied myocardium. *Science*, 260: 682-687.

TURNER, C.E. 2000. Paxillin interactions. *Journal of Cell Science*, 23: 4139-4140.

TWIG, G., HYDE, B. & SHIRIHAI, O.S. 2008. Mitochondrial fusion, fission and autophagy as a quality control axis: the bioenergetic view. *Biochimica et Biophysical Acta - Bioenergetics*, 1777: 1092-1097.

UEHARA, A., FILL, M., VÉLEZ, P., YASUKOCHI, M. & IMANAGA, I. 1996. Rectification of rabbit cardiac ryanodine receptor current by endogenous polyamines. *Biophysical Journal*, 71: 769-777.

VAHEBI, S., KOBAYASHI, T., WARREN, C.M., DE TOMBE, P.P. & SOLARO, R.J. 2005. Functional effects of Rho-kinase-dependent phosphorylation of specific sites on cardiac troponin. *Circulation Research*, 96: 740-747.

VAN DER HEIJDEN, M., VERSTEILEN, A.M., SIPKEMA, P., VAN NIEUW AMERONGEN, G.P., MUSTERS, R.J. & GROENEVELD, A.B. 2008. Rho-kinase-dependent F-actin rearrangement is involved in the inhibition of PI3-kinase/Akt during ischemia-reperfusion-induced endothelial cell apoptosis. *Apoptosis*, 13: 404-412.

VAN DER WALT, J.J. & VAN ROOYEN, J.M. 1977. Use of technetium-99 m to determine haemodynamic changes during the development of ventricular failure with gousiekte. *South African Medical Journal*, 52: 375.

VAN DER WALT, J.J., VAN ROOYEN, J.M., CILLIERS, G.D., VAN RYSSEN, C.J. & VAN AARDE, M.N. 1981. Ratio of cardiopulmonary blood volume to stroke volume as an index of cardiac function in animals and in man. *Cardiovascular Research*, 15: 580-587.

VAN EYK, J.E., POWERS, F., LAW, W., LARUE, C., HODGES, R.S. & SOLARO, R.J. 1997. Breakdown and release of myofilament proteins during ischemia and ischemia/reperfusion in rat hearts. Identification of degradation products and effects on the pCa-force relation. *Circulation Research*, 82: 261-271.

VAN WIJK, S.J.L & HAGEMAN, G.J. 2005. Poly(ADP-ribose) polymerase-1 mediated caspase-independent cell death after ischemia/reperfusion. *Free Radical Biology and Medicine*, 39: 81-90.

VARTIAINEN, M.K., GUETTLER, S., LARIJANI, B. & TREISMAN, R. 2007. Nuclear actin regulates dynamic subcellular localization and activity of the SRF cofactor MAL. *Science*, 316: 1749-1752.

VARTIAINEN, M.K. 2008. Nuclear actin dynamics-from form to function. *FEBS Letters* 582: 2033-2040.

VENTURA-CLAPIER, R., GARNIER, A. & VEKSLER, V. 2004. Energy metabolism in heart failure. *Journal of Physiology*, 555: 1-13.

VIOLA, H.M., ARTHUR, P.G. & HOOL, L.C. 2009. Evidence for regulation of mitochondrial function by the L-type Ca^{2+} channel in ventricular myocytes. *Journal of Molecular and Cellular Cardiology*, 46: 1016-1026.

VISEGRADY, B., LORINCZY, D., HILD, G., SOMOGYI, B. & NYITRAI, M. 2005. A simple model for the cooperative stabilization of actin filaments by phalloidin and jasplakinolide. *FEBS Letters*, 579: 6-10.

VOGT, P.K. 2001. PI 3-kinase, mTOR, protein synthesis and cancer. *Trends in Molecular Medicine*, 11: 482-484.

WALLIMANN, T., WYSS, M., BRDICZKA, D., NICOLAY, K. & EPPENBERGER, H.M. 1992. Intracellular compartmentation, structure and function of creatine kinase isoenzymes in tissues with high and fluctuating energy demands: the 'phosphocreatine circuit' for cellular energy homeostasis. *Biochemical Journal*, 281: 21-40.

WANG, R., XU, C., ZHAO, W., ZHANG, J., CAO, K., YANG, B. & WU, L. 2003. Calcium and polyamine regulated calcium-sensing receptors in cardiac tissue. *European Journal of Biochemistry*, 270: 2680-2688.

WANG, X & PROUD, C.G. 2006. The mTOR pathway in the control of protein synthesis. *Physiology*, 21: 362-369.

WANG, X. & ROBBINS, J. 2006. Heart failure and protein quality control. *Circulation Research*, 99: 1315-1328.

WANG, J-W., SUN, L., HU, J-S., LI, Y-B. & ZHANG, G-J. 2006. Effects of phospholipase A_2 on the lysosomal ion permeability and osmotic sensitivity. *Chemistry and Physics of Lipids*, 144: 117-126.

WANG, X., SU, H. & RANEK, M.J. 2008. Protein quality control and degradation in cardiomyocytes. *Journal of Molecular and Cellular Cardiology*, 45: 11-27.

WARBURG, O. 1926. Wirkung des CO auf den Stoffwechsel der Hefe. *Biochem. Z.* 177.

WILDENTHAL, K., DECKER, R.S., POOLE, A.R., GRIFFIN, E.E. & DINGLE, J.T. 1978. Sequential lysosomal alterations during cardiac ischemia. I. Biochemical and immunohistochemical changes. *Laboratory Investigation*, 38: 656-661.

WILLIS, M.S. & PATTERSON, C. 2006. Into the heart: the emerging role of the ubiquitin-proteasome system. *Journal of Molecular and Cellular Cardiology*, 41: 567-579.

WILLIS, M.S., SCHISLER, J.C., PORTBUTY, A.L. & PATTERSON, C. 2009. Build it up - tear it down: protein quality control in the cardiac sarcomere. *Cardiovascular Research*, 81: 439-448.

WITT, S.H., GRANZIER, H., WITT, C.C. & LABEIT, S. 2005. MURF-1 and MURF-2 target a specific subset of myofibrillar proteins redundantly: towards understanding MURF-dependent muscle ubiquitination. *Journal of Molecular Biology*, 350: 713-722.

WOLSKA, B.M., VIJAYAN, K., ARTEAGA, G.M., KONHILAS, J.P., PHILLIPS, R.M., KIM, R., NAYA, T., LEIDEN, J.M., MARTIN, A.F., PIETER P DE TOMBEND ,P.P. & SOLARO, R.J. 2001. Expression of slow skeletal troponin I in adult heart muscle prevents force decline during acidic conditions. *Journal of Physiology*, 536: 863-870.

WU, Y., BELL, S.P., TROMBITAS, K., WITT, C.C., LABEIT, S., LEWINTER, M.M. & GRANZIER, H. 2002. Changes in titin isoform expression in pacing-induced cardiac failure give rise to increased passive muscle stiffness. *Circulation*, 106: 1384-1389.

XIAO, W. 2004. Advances in NF-kB signaling transduction and transcription. *Cellular and Molecular Immunology*, 1: 425-435.

XIE, B., HUANG, R., HUANG, L., ZHOU, G. & GONG, Z. 2003. The functional domains of human ventricular myosin light chain 1. *Biophysical Chemistry*, 106: 57-66.

XING, J., CHINNARAJ, M., ZHANG, Z., CHEUNG, H.C. & DONG, W.J. 2008. Structural studies of interactions between cardiac troponin I and actin in regulated thin filament using Förster resonance energy transfer. *Biochemistry*, 47: 13383-13393.

YAMASAKI, R., BERRI, M., WU, Y., TROMBITÁS, K., MCNABB, M., KELLERMAYER, M.S.Z., WITT, C., LABEIT, D., LABEIT, S., GREASER, M. & GRANZIER, H. 2001. Titin-actin interaction in mouse myocardium: passive tension modulation and its regulation by calcium/S100A1. *Biophysical Journal,* 81: 2297-2313.

YAMASAKI, R., WU, Y., MCNABB, M., GREASER, M., LABEIT, S. & GRANZIER, H. 2002. Protein kinase A phosphorylates titin's cardiac-specific N2B domain and reduces passive tension in rat cardiac myocytes. *Circulation Research,* 90: 1181-1188.

YAMASHIMA, T. 2000. Implication of cysteine proteases calpain, cathepsin and caspase in ischemic neuronal death of primates. *Progress in Neurobiology*, 62: 273-295.

YAN, L., VATNER, D.E., KIM, S-J., GE, H., MASUREKAR, M., MASSOVER, W.H., YANG, G., MATSUI, Y., SADOSHIMA, J. & VATNER, S.F. 2005. Autophagy in chronically ischemic myocardium. *Proceedings of the National Academy of Science (USA)*, 102: 13807-13812.

YE, J., RAWSON, R.B., KOMURO, R., CHEN, X., DAVE, U.P. & PRYWES, R. 2000. ER stress induces cleavage of membrane-bound ATF6 by the same proteases that process SREBPs. *Molecular Cell*, 6: 1355-1364.

YE, J., ZHAO, J., HOFFMANN-ROHRER, U. & GRUMMT, I. 2008. Nuclear myosin I acts in concert with polymeric actin to drive RNA polymerase I transcription. *Genes and Development,* 22: 322-330.

YOKOGAMI, K., WAKISAKA, S., AVRUCH, J. & REEVES, S.A. 2000. Serine phosphorylation and maximal activation of STAT3 during CNTF signaling is mediated by the rapamycin target mTOR. *Current Biology*, 10: 47-50.

YOON, Y-S., BYUN, H-O., CHO, H., KIM, B-K & YOON, G. 2003. Complex II defect via down-regulation of iron-sulfur subunit induces mitochondrial dysfunction and cell cycle delay in iron chelation-induced senescence-associated growth arrest. *Journal of Biological Chemistry,* 278: 51577-51586.

YOSHIDA, M., TOMITORI, H., MACHI, Y., HAGIHARA, M., HIGASHI, K., GODA, H., OHYA, T., NIITSU, M., KASHIWAGI, K. & IGARASHI, K. 2009. Acrolein toxicity: comparison with reactive oxygen species. *Biochemical and Biophysical Research Communications,* 378: 313-318.

YOUNG, P., EHLER, E. & GAUTEL, M. 2001. Obscurin, a giant sarcomeric Rho guanine nucleotide exchange factor protein involved in sarcomere assembly. *Journal of Cell Biology,* 154: 123-126.

YUE, T-L., WANG, C., ROMANIC, A.M., KIKLY, K., KELLER, P., DEWOLF, W.E. Jr., HART, T.K., THOMAS, H.C., STORER, B., GU, J-L., WANG, X. & FEUERSTEIN, G.Z. 1998. Staurosporine-induced apoptosis in cardiomyocytes: a potential role of caspase-3. *Journal of Molecular and Cell Cardiology,* 30: 495-507.

ZHANG, W. & XU, C. 2009. Calcium sensing receptor and heart diseases. *Pathophysiology*, 16: 317-323.

ZHU, C., JOHANSEN, F.E. & PRYWES, R. 1997. Interaction of ATF6 and serum response factor. *Molecular Cell Biology*, 17: 4957-4966.

ZIEGLER, D.M. & DOEG, K.A. 1962. Studies on the electron transport system. XLIII. The isolation of a succinic-coenzyme Q reductase from beef heart mitochondria. *Archives of Biochemistry and Biophysics*, 97: 41-50.

ZORATTI, M. & SZABO, I. 1995. The mitochondrial permeability transition. *Biochemistry and Biophysical Acta*, 1241: 139-176.

ZORDOKY, B.N.M. & EL-KADI, A.O.S. 2007. H9c2 cell line is a valuable *in vitro* model to study the drug metabolizing enzymes in the heart. *Journal of Pharmacology and Toxicology*, 56: 317-322.

ZOU, Y., EVANS, S., CHEN, J., KUO, H.C., HARVEY, R.P. & CHIEN, K.R. 1997. CARP, a cardiac ankyrin repeat protein, is downstream in the Nkx2-5 homeobox gene pathway. *Development*, 124: 793-804.

Contents lists available at ScienceDirect

Toxicon

journal homepage: www.elsevier.com/locate/toxicon

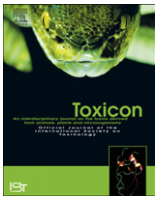

Cytotoxicity and ultrastructural changes in H9c2(2-1) cells treated with pavetamine, a novel polyamine

C.E. Ellis [a,b,*], D. Naicker [a,b], K.M. Basson [a], C.J. Botha [b], R.A. Meintjes [c], R.A. Schultz [a]

[a] Food, Feed and Veterinary Public Health Programme, Agriculture Research Council-Onderstepoort Veterinary Institute, Private Bag X5, Onderstepoort, Pretoria, Gauteng 0110, South Africa
[b] Department of Paraclinical Sciences, Faculty of Veterinary Science, University of Pretoria, Onderstepoort 0110, South Africa
[c] Department of Anatomy and Physiology, Faculty of Veterinary Science, University of Pretoria, Onderstepoort 0110, South Africa

ARTICLE INFO

Article history:
Received 2 September 2008
Received in revised form 22 November 2008
Accepted 25 November 2008
Available online 6 December 2008

Keywords:
Cardiotoxicity
Gousiekte
H9c2(2-1) cell line
Mitochondria
Pavetamine
Polyamine

ABSTRACT

Intake of pavetamine, a novel polyamine, synthesized by certain rubiaceous plants, is the cause of gousiekte ("Quick disease") in ruminants. The disease is characterized by a latent period of 4–8 weeks, followed by heart failure. The aim of this study was to firstly investigate the cytotoxicity in H9c2(2-1) cells using the MTT (3-(4,5-dimethyl-2-thiazolyl)-2,5-diphenyl-2H-tetrazolium bromide) and LDH (lactate dehydrogenase) release assays. Maximum cell death occurred after pavetamine exposure of cells for 72 h at a concentration of 200 μM (55% ± 9.84), as measured by the MTT assay. LDH release was only observed after 72 h exposure to pavetamine. Secondly, the ultrastructural changes induced by pavetamine in H9c2(2-1) cells were investigated. Changes in the mitochondria and sarcoplasmic reticula were observed. The nucleus was not affected during the first 48 h exposure of cells to pavetamine and no chromatin condensation occurred. However, after 72 h exposure to pavetamine, the nucleus became fragmented and membrane blebbing occurred. It was concluded that the ultimate cell death of H9c2(2-1) cells treated with pavetamine, was through necrosis and not apoptosis. Thirdly, the effect of pavetamine on the mitochondrial membrane potential ($\Delta\Psi$) was evaluated by using the JC-1 (5,5′,6,6′-Tetrachloro-1,1′,3,3′-tetraethyl-imidacarbocyanine iodide) and TMRM (tetramethylrhodamine methyl ester perchlorate) probes. Pavetamine treatment led to significant hyperpolarization of the mitochondrial membrane potential. Cyclosporin A (CsA), an inhibitor of the mitochondrial permeability transition pore, did not reduce the cytotoxicity of pavetamine significantly, indicating that the MPTP (mitochondrial permeability transition pore) plays no role in the cytotoxicity of pavetamine.

1. Introduction

Gousiekte, a cardiotoxicosis of ruminants, is characterized by acute heart failure without any premonitory signs four to eight weeks after the initial ingestion of certain rubiaceous plants (Theiler et al., 1923; Pretorius and Terblanche, 1967; Kellerman et al., 2005). The causative plants include *Pachystigma pygmaeum* Schltr., *Pachystigma thamnus*

Abbreviations: ATP, adenosine triphosphate; Ca^{2+}, calcium; CsA, cyclosporin A; DMEM, Dulbecco's Modified Eagle's Medium; EC_{50}, half maximal effective concentration; FCS, fetal calf serum; DMSO, dimethyl sulfoxide; JC-1, 5,5′,6,6′-Tetrachloro-1,1′,3,3′-tetraethyl-imidacarbocyanine iodide; LDH, lactate dehydrogenase; LSCM, laser scanning confocal microscopy; $\Delta\Psi m$, mitochondrial membrane potential; MPTP, mitochondrial permeability transition pore; MTT, 3-(4,5-dimethyl-2-thiazolyl)-2,5-diphenyl-2H-tetrazolium bromide; NAD^+, nicotinamide adenine dinucleotide; ROS, reactive oxygen species; SR, sarcoplasmic reticulum; TEM, transmission electron microscopy; TMRM, tetramethylrhodamine methyl ester perchlorate; UPR, unfolded protein response.

* Corresponding author at: Food, Feed and Veterinary Public Health Programme, Agriculture Research Council-Onderstepoort Veterinary Institute, Private Bag X5, Onderstepoort, Pretoria, Gauteng 0110, South Africa. Tel.: +27 12 5299254; fax: +27 12 5299249.
E-mail address: ellisc@arc.agric.za (C.E. Ellis).

0041-0101/$ – see front matter © 2008 Elsevier Ltd. All rights reserved.
doi:10.1016/j.toxicon.2008.11.017

Robyns, *Pavetta harborii* S. Moore, *Pavetta schumaniana* F. Hoffm and *Fadogia homblei* Robyns (Kellerman et al., 2005). Electron micrographs of the myocardium of sheep intoxicated with *P. pygmaeum*, showed the myofibrils became disintegrated and had a frayed appearance accompanied by replacement fibrosis (Schutte et al., 1984; Kellerman et al., 2005; Prozesky et al., 2005). Transmission electron microscopy (TEM) of the hearts of sheep dosed with gousiekte-inducing plants, showed abnormalities of the mitochondria and sarcoplasmic reticula (Prozesky et al., 2005).

Rats were susceptible to *P. harborii* extracts when administered subcutaneously (Hay et al., 2001). Cardiac contractility was reduced by more than 50% and the cardiac output (heart rate × stroke volume), an indication of the myocardial oxygen requirement, by 40% when compared to control rats (Hay et al., 2001). The novel toxin that causes gousiekte was isolated from *P. harborii* and called pavetamine (Fourie et al., 1995). The structure of pavetamine was elucidated and was identified to belong to the polyamine group, similar to spermidine, spermine and putrescine (R. Vleggaar, unpublished data 1997). Polyamines are essential for normal cell growth, proliferation and differentiation but can also cause neoplastic transformation and cell death (Janne et al., 1991). Schultz and co-workers (2001) reported that pavetamine, administered intraperitoneally to rats, inhibits protein synthesis in the heart. Synthesis of proteins in the liver and kidney were initially also reduced, but returned to normal after 48 h. Other muscle tissue was not affected. Purified pavetamine from *Pavetta harboiri* also caused significantly reduced systolic function in rats (Hay et al., 2008).

Cardiac cells are post-mitotic and changes to the workload of the heart, cause altered expression of the contractile proteins, as a compensatory mechanism (Samarel and Engelmann, 1991). In addition, damaged proteins and organelles are eliminated by pathways like autophagy, but can also cause cell death. Three pathways exist for cell death *viz.* apoptosis (programmed cell death I), autophagy (programmed cell death II) and necrosis (programmed cell death III). Apoptotic cell death is characterized by pre-lytic DNA fragmentation (ladder pattern on gel electrophoresis), chromatin condensation, cytochrome c release from the mitochondria into the cytoplasm and activation of the caspase family of proteases (Kunapuli et al., 2006). Apoptotic signals cause opening of the MPTP with influx of H^+ ions and loss of the mitochondrial membrane potential (Regula et al., 2003). Autophagy is responsible for organelle turnover (Klionsky and Emr, 2000) and occurs in four distinct steps: induction, formation of an autophagosome, autophagosome docking and fusion with the lysosome and autophagic body breakdown (Kunapuli et al., 2006). Excessive autophagy can destroy major portions of the cytoplasm and organelles, especially the mitochondria and endoplasmic reticula, leading to cell death. Necrosis causes disruption of the plasma membrane (Rubiolo and Vega, 2008), leading to lactate dehydrogenase leakage (LDH) from the cells.

The clonal cell line H9c2(2-1), a permanent cell line, was derived from embryonic BDIX rat ventricular heart tissue and retained some of the properties of cardiac muscle (Kimes and Brandt, 1976). This cell line is being used as an *in vitro* model for cardiac muscle, as it resembles the biochemical and electrophysiological properties of adult cardiomyocytes (Hescheler et al., 1991; Green and Leeuwenburgh, 2002; Zordoky and El-Kadi, 2007; Aggeli et al., 2008).

The purpose of this study was to characterize the cytotoxicity of pavetamine in a rat embryonic H9c2(2-1) cell line. Cytotoxicity of pavetamine was determined with the MTT (3-(4,5-dimethyl-2-thiazolyl)-2,5-diphenyl-2H-tetrazolium bromide) assay and the LDH (lactate dehydrogenase) release assay. Ultrastructural changes caused by pavetamine treatment of cells were evaluated with transmission electron microscopy (TEM). Changes in the mitochondrial membrane potential, caused by pavetamine, were investigated utilizing two fluorescent probes, JC-1 (5,5′,6,6′-Tetrachloro-1,1′,3,3′-tetraethyl-imidacarbocyanine iodide) and TMRM (tetramethylrhodamine methyl ester perchlorate).

2. Materials and methods

2.1. H9c2(2-1) cell line

The H9c2(2-1) cell line (Kimes and Brandt, 1976) was obtained from American Type Culture Collection (cat no: CRL-1446™, Manassas, USA). The cells were placed in Dulbecco's Modified Eagle's Medium (DMEM) (Sigma, cat no: D6429, St Louis) supplemented with 10% fetal calf serum (Gibco cat no: 10106-169, Carlsbad, California), and 100 U/ml penicillin, and 100 μg/ml streptomycin sulphate (Gibco cat no: 15070-063, Carlsbad, California). The cells were incubated in a humidified atmosphere of 5% CO_2 at 37 °C.

2.2. Purification of pavetamine

Pavetamine was extracted and purified from the leaves of *P. harborii* S. Moore according to the method described by Fourie et al. (1995).

2.3. Cytotoxicity of pavetamine

Twelve well plates were incubated overnight until 80% confluent. Fifty microliters of ten-fold serial dilutions of pavetamine (0.02; 0.2; 2; 20 and 200 μM) was added to each well, in duplicate. Untreated cells were used as controls. The cells were exposed for 24, 48 and 72 h. The results represent the average of three independent experiments.

2.3.1. MTT assay

The MTT assay (Sigma, cat no: M2128, St Louis, MO) was used to measure the cytotoxicity of pavetamine in H9c2(2-1) cells (Mosmann, 1983). This is a colorimetric assay for the quantification of cell toxicity, based on the conversion of yellow MTT to the water-insoluble purple formazan crystals by dehydrogenases of viable cells, which is impermeable to cell membranes. The crystals are solubilised by the addition of detergents and read in a spectrophotometer. The number of surviving cells is directly proportional to the amount of formazan formed. In this study, cells were exposed for the indicated times to the above-mentioned concentrations of

pavetamine, after which the medium was replaced with fresh medium, containing 0.6 mM MTT (3-(4,5-dimethyl-2-thiazolyl)-2,5-diphenyltetrazolium bromide). The plates were incubated in a 5% CO_2 incubator at 37 °C for 4 h. Five hundred microliters DMSO was added to each well. After incubation at 37 °C for 1 h in a 5% CO_2 incubator, 100 μl were transferred to a 96-well plate and the absorbance was read at 570 nm.

2.3.2. LDH assay

The LDH cytotoxicity detection kit (Roche Diagnostics GmbH, cat no: 11644793001, Mannheim, Germany) is a colorimetric assay for the quantification of cell death and cell lysis, based on the determination of LDH activity released from the cytosol of damaged cells into the medium, thus indicating cell membrane damage. After the end of a cell culture experiment, 200 μl cell culture medium was removed and added to a 96 well plate. Hundred microliters of the reaction mixture (250 μl of Diaphorase/NAD^+ mixture premixed with 11.25 ml of iodotetrazolium chloride/sodium lactate) was added to each well and the plate was incubated for 30 min at room temperature, protected from light. The absorbance was then measured at 492 nm.

2.4. Transmission electron microscopy (TEM)

The TEM studies were conducted after exposure of H9c2(2-1) cells to 20 μM pavetamine for 24, 48 and 72 h. Staurosporine (Roche Applied Science, cat no: 1055682) was used as a positive inducer of apoptosis (Yue et al., 1998). The cells were fixed in 2.5% glutaraldehyde in Millonig's buffer for 5 min before scraping the cells off the bottom of the flask, removing cells and fixative from flask into an Eppendorf tube and additional fixing for another hour. The cells were post-fixed in 1% osmium tetroxide in Millonig's buffer, washed in buffer and then dehydrated through a series of graded alcohols, infiltrated with a mixture of propylene oxide and an epoxy resin and finally embedded in absolute resin at 60 °C. The cells were pelleted after each step by centrifugation at 3000 rpm for 3 min. After curing overnight ultra-thin sections were prepared and stained with lead citrate and uranyl acetate and viewed in a Philips CM10 transmission electron microscope operated at 80 kV.

2.5. Mitochondrial analyses

2.5.1. Measurement of the electrochemical proton gradient (ΔΨm) of the inner mitochondrial membrane with JC-1 and TMRM.

The mitochondrial membrane potential was measured according to the manufacturer's instruction with JC-1 (Sigma, cat no: MITOISO1, St Louis, MO). The fluorescence was measured at an excitation: emission of 485/538 for green monomers and at an excitation: emission of 485/590 for red aggregates with a Fluoroscan Ascent FL fluorometer (Thermo Electron Corporation, Waltham, MA). Valinomycin, a potassium ionophore, was used at a concentration of 0.1 μM (Sigma, cat no: V-0627, St Louis, MO) as a positive control for depolarization of the ΔΨm. Tetramethylrhodamine methyl ester perchlorate (TMRM) (Sigma, cat no: T5428, St Louis, MO), another ΔΨm-dependent fluorescence dye (Yoon et al., 2003), was used at a concentration of 1 μM to stain H9c2 cells that had been exposed to 20 μM pavetamine for 24 h, followed by laser scanning confocal microscopy. The microscope that was used for the LSCM was a model ZEISS LSM 510 (Jena, Germany).

2.5.2. Inhibition of mitochondrial permeability transition pore (MPTP). The mitochondrial permeability transition pore is sensitive for CsA, by blocking opening of this pore. As pavetamine causes swelling of the mitochondria, CsA was tested as a potential antagonist of pavetamine-induced mitochondrial damage. Cyclosporin A (Sigma, cat no: 30024, St Louis, MO) at a concentration of 1 μM was used to pre-treat cells for 30 min to inhibit the MPTP, before cells were exposed to 20 μM pavetamine for 48 h. Cell viability was determined with the MTT assay.

2.5.3. Statistical analysis. The results were expressed as the mean ± sem. The Student's *t*-test was used for statistical analysis of the data, with p values of <0.05 considered as significant.

3. Results

3.1. Cytotoxicity of pavetamine in H9c2(2-1) cell culture

Death of H9c2 cells exposed to pavetamine was time- and concentration-dependent. Exposure of H9c2(2-1) cells to the highest concentration of pavetamine, 200 μM, induced 27.47% ± 5.59 cell death after 24 h, as measured by the MTT assay. Exposure of the H9c2(2-1) cells for longer periods (48–72 h) at a dose of 200 μM, led to about 50% cell death (Fig. 1a). The percentage of non-viable cells almost doubled from 24 to 48 h at concentrations of 2 μM, 20 μM and 200 μM. In contrast, cell death increased by only about 5% after exposing the cells for another 24–72 h. Staurosporine at a concentration of 0.6 μM caused 85% ± 0.002 cell death in 24 h. Pavetamine is thus a slower acting toxin than staurosporine, with a much higher EC_{50}. The percentage cell death of the cells exposed to pavetamine for 72 h correlated with the release of LDH (Fig. 1b). Maximum release of LDH (absorbance values between 2 and 2.25) was measured at concentrations of 20 μM and 200 μM pavetamine respectively, which caused between 40 and 50% cell death. No release of LDH into the medium was observed after exposing the cells for 24 h or 48 h at the above-mentioned concentrations of pavetamine (results not shown).

3.2. Ultrastructural changes of H9c2(2-1) cells induced by pavetamine

H9c2 cells exposed for 24 h, showed abnormal mitochondria (Fig. 2b), compared to the untreated cells (Fig. 2a). The cristae of the mitochondria were swollen and in some instances lysed, however, the nucleus appeared normal (Fig. 2c). Exposure of H9c2(2-1) cells to pavetamine

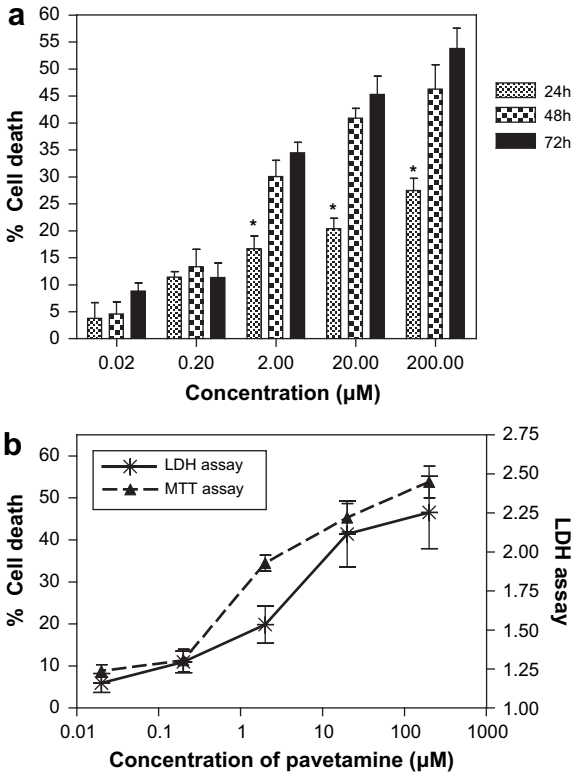

Fig 1. (a) The cytotoxicity of pavetamine was measured in H9c2(2-1) cells over a period of 3 days, and the percentage cell death, compared to the untreated cells, was measured with the MTT assay. The Student's *t*-test (unpaired, two-tailed) was used to analyze the data $^{*}p < 0.05$, significant difference between 24 h *vs.* 48 h and 24 h *vs.* 72 h. No significant difference between 48 h *vs.* 72 h. The results represent the average of three independent experiments. (b) Comparison of the percentage cell death and LDH release into the medium in H9c2(2-1) cells exposed for 72 h to pavetamine at a concentration of ten-fold serial dilutions. The results represent the average of three independent experiments.

for 48 h caused formation of vacuoles (Fig. 2d). Lysosomes were present and contained cellular matter, most likely secondary lysosomes. The nuclear membranes were indented and chromatin marginization also occurred (Fig. 2e). H9c2(2-1) cells exposed to pavetamine for 72 h had numerous empty vacuoles, nucleus fragmentation and abnormal mitochondria (Fig. 2f). Membrane blebbing and externalization of cell contents also occurred after 72 h (Fig. 2f). Untreated H9c2(2-1) cells grown for 72 h had none of these features (Fig. 2a). H9c2(2-1) cells exposed to 0.6 µM staurosporine for 6 h, resulted in the typical crescent moon-shaped chromatin condensation, typical of apoptotic cell death, and swollen rough sarcoplasmic reticula (Fig. 2g).

3.3. Mitochondrial analyses

3.3.1. Measurement of the electrochemical proton gradient ($\Delta\Psi m$) of the inner mitochondrial membrane with JC-1 and TMRM

Exposure of H9c2(2-1) cells to 20 µM pavetamine for 24 h caused significant hyperpolarization of the mitochondrial $\Delta\Psi m$, as measured with the JC-1 probe, with an average ratio of red to green fluorescence of 17.12 ± 0.976, compared to untreated cells, which had a ratio of 12.4 ± 0.403 (Fig. 3a). Valinomycin caused significant depolarization or collapse of the mitochondrial membrane potential, as compared to untreated cells. The average red to green fluorescence for cells treated with valinomycin was 0.52 ± 0.130. As can be seen in Fig. 3b, pavetamine caused an increase in the intensity of stained mitochondria with TMRM, compared to untreated H9c2(2-1) cells, thus confirming that pavetamine causes hyperpolarization of the mitochondrial membrane potential, irrespective of the plasma membrane potential.

3.3.2. Cytotoxicity of pavetamine in the presence of cyclosporin A, an inhibitor of the mitochondrial permeability transition pore (MPTP)

The mean percentage cell survival of cells exposed to pavetamine was $70.24\% \pm 1.842$ ($n = 12$), compared to the untreated cells, while the mean percentage survival of cells treated with pavetamine and cyclosporine A was $73.05\% \pm 1.827$ ($n = 12$) (Fig. 4). This difference was not significant.

4. Discussion

An interesting feature of gousiekte is the long latent period following ingestion of the causative rubiaceous plants, before ruminants eventually succumb due to heart failure. In the cardiac cell line H9c2(2-1), used as an *in vitro* model in this study, maximal cell death occurred 72 h after exposure of the cells to 20 µM and 200 µM pavetamine, as

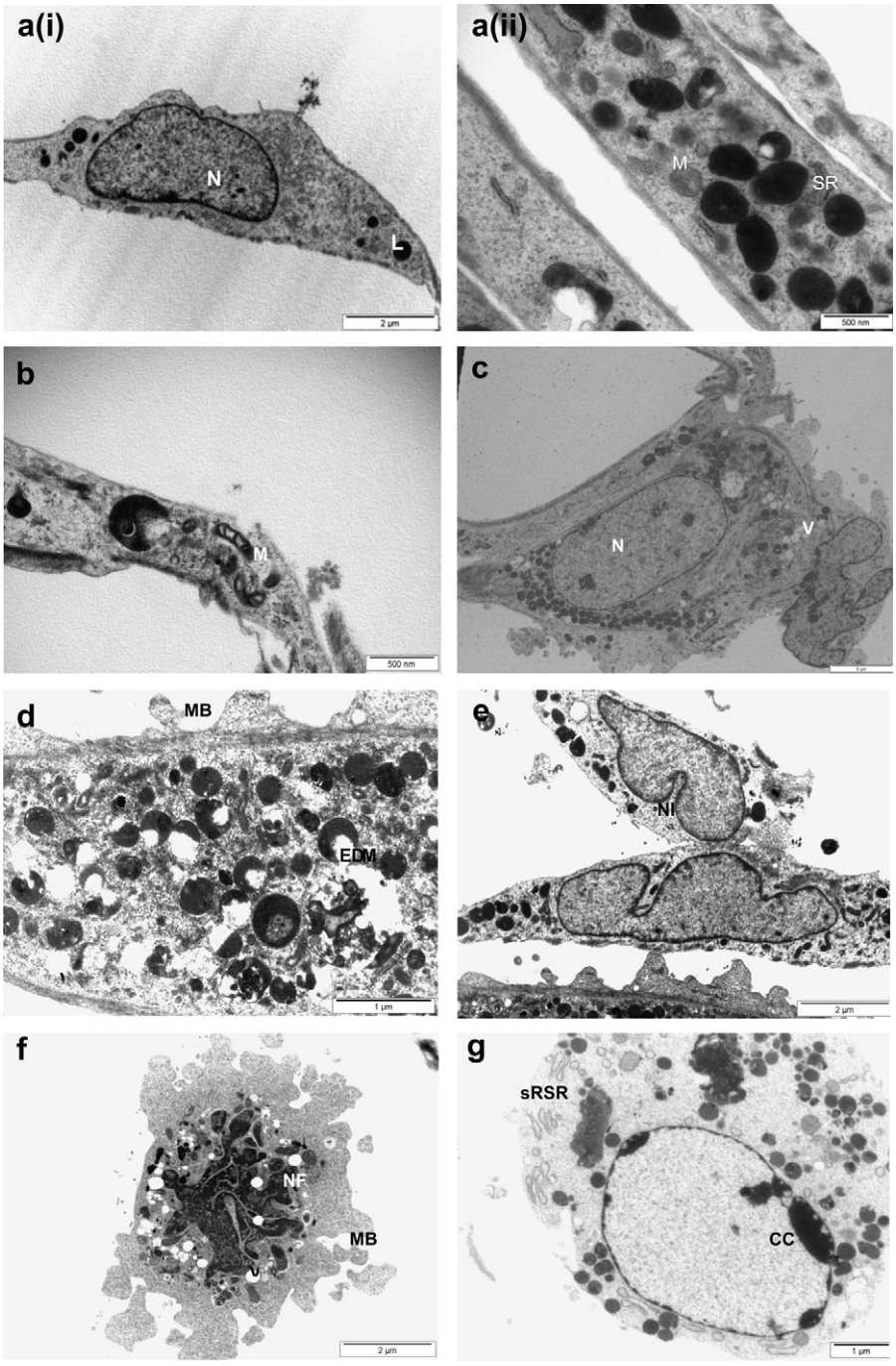

Fig 2. (a) Transmission electron micrograph of control H9c2(2-1) cells. SR: sarcoplasmic reticulum. M: mitochondria. L: lysosome. N: nucleus. (b) Transmission electron micrograph of H9c2(2-1) cells treated for 24 h with 20 μM pavetamine. The mitochondria (M) appeared abnormal in shape; the cristae were grossly swollen and lysed. (c) Transmission electron micrograph of the nucleus of H9c2(2-1) cells treated for 24 h with 20 μM pavetamine. The nucleus (N) appeared normal. Some vacuoles (V) appeared. (d) Transmission electron micrograph of H9c2(2-1) cells treated for 48 h with 20 μM pavetamine. Vacuoles (V) had formed, some containing electron dense material (EDM). Membrane blebbing (MB) also occurred. (e) Transmission electron micrograph of H9c2(2-1) cells exposed for 48 h to 20 μM pavetamine. The nuclear membrane was indented (NI), but no chromatin condensation occurred. (f) Transmission electron micrograph of H9c2(2-1) cells treated for 72 h with 20 μM pavetamine. Numerous vacuoles (V) were formed, the nucleus became fragmented. (NF) membrane blebbing (MB) occurred. (g) Transmission electron micrograph of H9c2(2-1) cell exposed to 0.6 μM staurosporine for 6 h. Staurosporine caused chromatin condensation (CC) and the sarcoplasmic reticula became swollen (sRSR).

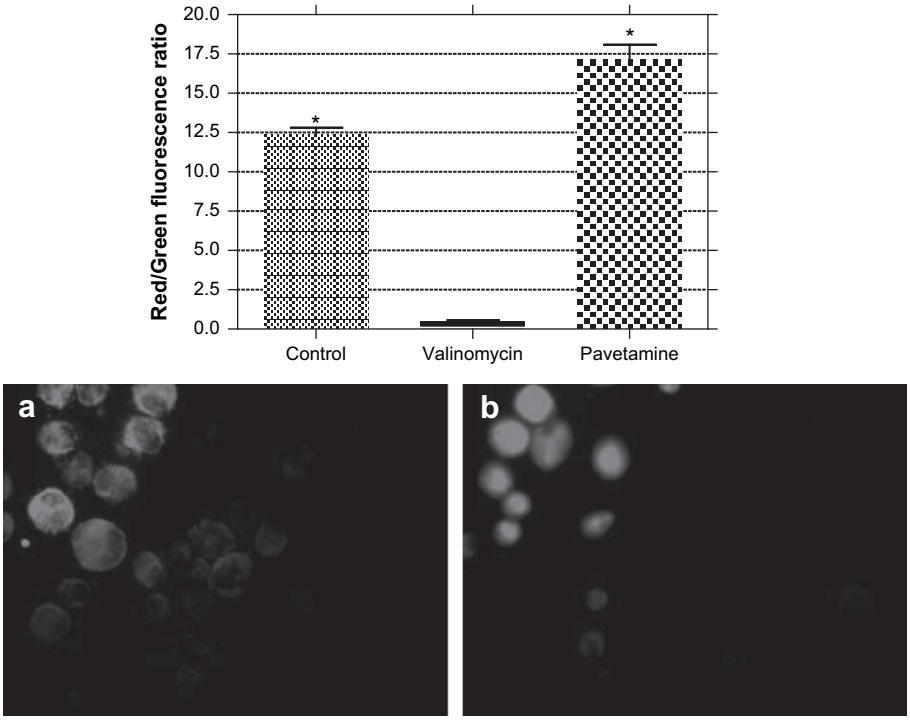

Fig 3. (a) Mitochondrial membrane potential of H9c2(2-1) cells exposed to 20 μM pavetamine for 24 h. The mitochondrial membrane potential was determined with the fluorescent probe JC-1. The results represent the average of three independent experiments. The difference between the control and pavetamine-treated cells were significant with the unpaired, two-tailed Student's *t*-test (*$p < 0.05$). (b) Measurement of mitochondrial membrane potential with tetramethylrhodamine methyl ester perchlorate (TMRM). A: Untreated cells that served as control; B: H9c2(2-1) cells 24 h post-exposure to 20 μM pavetamine.

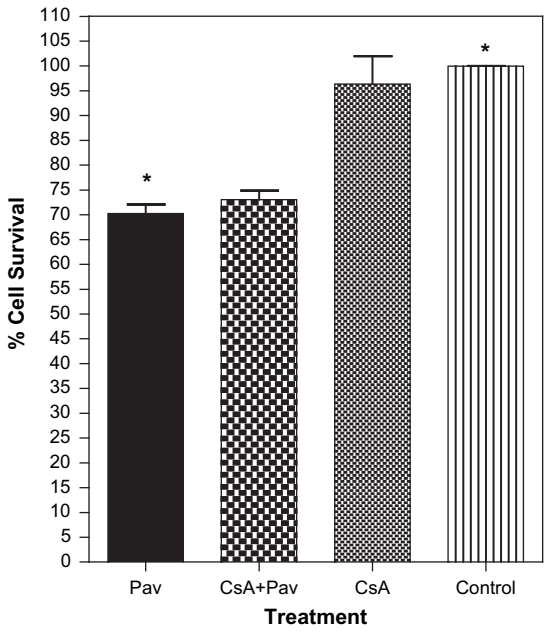

Fig 4. Cytotoxicity of 20 μM pavetamine in the presence or absence of 1 μM CsA. The cells were exposed for 48 h to 20 μM pavetamine. No significant difference was observed between pavetamine-treated cells and pavetamine-treated cells in the presence of CsA. Significant differences (*$p < 0.05$) with the Student's *t*-test were observed between cells treated with pavetamine and untreated cells that served as controls. Pav: Pavetamine; CsA: Cyclosporin A.

determined by the MTT and LDH assays. The cause of death of these H9c2(2-1) cells 72 h after exposure to pavetamine, is necrosis, as maximal release of LDH (a hallmark of necrotic cell death) into the medium occurred at this time.

Pavetamine caused damage to mitochondria in H9c2(2-1) cells exposed to it for 24 h. It caused hyperpolarization of the mitochondrial membrane potential, swollen cristae and in some instances lysis of cristae. Although mitochondrial uptake of JC-1 can be limited by the plasma membrane potential ($\Delta\Psi p$) (Rottenberg and Wu, 1998), the TMRM is a sensitive probe for measuring the mitochondrial membrane potential and the uptake of this dye is independent of the plasma membrane potential. For this reason TMRM was also employed to verify the increase in the mitochondrial membrane potential. Opening of the MPTP leads to depolarization of the mitochondrial membrane potential, with an influx of H^+ ions, release of cytochrome c and apoptotic cell death (Leung and Halestrap, 2008). Cyclosporin A binds to cyclophilin D, part of the MPTP, causing inhibition of the MPTP and prevents apoptosis (Crompton et al., 1988). The addition of CsA did not contribute significantly to a reduction in the cytotoxicity of pavetamine, thus eliminating the MPTP opening as a mechanism of cell toxicity.

Pavetamine-containing plants (*P. pygmaeum*, *F. homblei*, and *P. harborii*) induced dilatation and proliferation of the sarcoplasmic reticulum (SR) in sheep (Prozesky et al., 2005). Pretorius and colleagues (1973) reported reduced uptake of Ca^{2+} by the SR of sheep treated with pavetamine-containing plants (*P. pygmaeum* and *P. harborii*). It was originally

thought that the MTT assay measures enzyme activities in the mitochondria, but it was recently shown that enzymes in the endoplasmic reticulum are responsible for the reduction of MTT (Berridge et al., 1996). The MTT cytotoxicity assay for pavetamine in the H9c2(2-1) cells thus measured the activity of the SR enzymes. The cytosolic free ribosomes are the site where protein synthesis occurs, but depending on cell type, up to 35% of it can occur in the endoplasmic reticulum (Glembotski, 2008). After proteins are synthesized, they must be correctly folded. Any disturbances in this folding process, will lead to accumulation of misfolded proteins, which in turn will activate the ubiquitin–proteasome pathway (Glembotski, 2007). The unfolded protein response (UPR) is the SR-associated protein quality control in the cell, together with the cytosolic protein quality control system (Glembotski, 2008). It is now known that pavetamine caused inhibition of protein synthesis in rat hearts as early as 4 h after administration of pavetamine intraperitoneally at a concentration of 8–10 mg/kg live mass (Schultz et al., 2001). It is also possible that there is increased degradation of cardiac proteins by the ubiquitin–proteasome pathway, as speculated by these authors.

Two systems exist in the cell for protein and organelle turnover, namely autophagy for damaged organelle turnover, especially the mitochondria and the SR (Klionsky and Emr, 2000), and the ubiquitin–proteasome pathway for oxidized and misfolded proteins (Glembotski, 2007). The late-endosomes, autophagosomes and molecular chaperones fuse with the lysosome where degradation of damaged constituents occurs (Buja and Vela, 2008). Autophagy is characterized by the formation of vacuoles in the absence of nuclear chromatin condensation with mitochondrial and endoplasmic reticular swelling as studied with TEM (Gozuacik and Kimshi, 2004; Martinet et al., 2007). H9c2(2-1) cells, treated for 48 h, had numerous vacuoles, possibly indicative of autophagy.

In conclusion, pavetamine caused damage to the mitochondria and SR aberrations in H9c2(2-1) cells. It is surmised that this could either be by inhibition of one or more enzymes of Complex I–V or by the production of ROS and/or interference with Ca^{2+} homeostasis. Damaged organelles were degraded, possibly by autophagy and misfolded or oxidized proteins degraded by the ubiquitin–proteasome pathway, followed by necrosis as the eventual cell death pathway.

Acknowledgements

We would like to thank Mr. A. Hall (Laboratory for Microscopy and Microanalysis, University of Pretoria) for the LCSM work, Mmes. E. van Wilpe and L. du Plessis (Electron microscopy unit, Faculty of Veterinary Science, University of Pretoria) for the TEM work. This investigation was funded by the North-West Province, Gauteng Province and the Faculty of Veterinary Science, University of Pretoria.

Conflict of interest

The authors have no conflict of interest.

References

Aggeli, I.-K.S., Beis, I., Gaitanaki, C., 2008. Oxidative stress and calpain inhibition induce alpha B-crystallin phosphorylation via p38-MAPK and calcium signalling pathways in H9c2 cells. Cell. Signal. 20, 1292–1302.
Berridge, M.V., Tan, A.S., McCoy, K.D., Wang, R., 1996. The biochemical and cellular basis of cell proliferation assays that use tetrazoleum salts. Biochemica 4, 14–19.
Buja, L.M., Vela, D., 2008. Cardiomyocyte death and renewal in the normal and diseased heart. Cardiovas. Pathol. 17, 349–374.
Crompton, M., Ellinger, H., Costi, A., 1988. Inhibition by cyclosporin A of a Ca^{2+}-dependent pore in heart mitochondria activated by inorganic phosphate and oxidative stress. Biochem. J. 255, 357–360.
Fourie, N., Erasmus, G.L., Schultz, R.A., Prozesky, L., 1995. Isolation of the toxin responsible for gousiekte, a plant-induced cardiomyopathy of ruminants in southern Africa. Onderstepoort J. Vet. Res. 62, 77–87.
Glembotski, C.C., 2007. Endoplasmic reticulum stress in the heart. Circ. Res. 101, 975–984.
Glembotski, C.C., 2008. The role of the unfolded protein response in the heart. J. Mol. Cell. Cardiol. 44, 453–459.
Gozuacik, D., Kimshi, A., 2004. Autophagy as a cell death and tumor suppression mechanism. Oncogene 23, 2891–2906.
Green, P.S., Leeuwenburgh, C., 2002. Mitochondrial dysfunction is an early indicator of doxorubicin-induced apoptosis. Biochim. Biophys. Acta 1588, 94–101.
Hay, L., Pipedi, M., Schutte, P.J., Turner, M.L., Smith, K.A., 2001. The effect of *Pavetta harborii* extracts on cardiac function in rats. S. Afr. J. Sci. 97, 481–484.
Hay, L., Schultz, R.A., Schutte, P.J., 2008. Cardiotoxic effects of pavetamine extracted from *Pavetta harborii* in the rat. Onderstepoort J. Vet. Res. 75, 249–253.
Hescheler, J., Meyer, R., Plant, S., Krautwurst, D., Rosenthal, W., Schultz, G., 1991. Morphological, biochemical and electrophysiological characterization of a clonal cell (H9c2) line from rat heart. Circ. Res. 69, 1476–1486.
Janne, J., Alhonen, L., Leinonen, P., 1991. Polyamines: from molecular biology to clinical applications. Ann. Med 23, 241–259.
Kellerman, T.S., Coetzer, J.A.W., Naudé, T.W., Botha, C.J., 2005. Plant Poisonings and Mycotoxicoses of Livestock in Southern Africa. Oxford University Press, Southern Africa, pp. 154–164.
Kimes, B.W., Brandt, B.L., 1976. Properties of a clonal muscle cell line from rat heart. Exp. Cell Res. 98, 367–381.
Klionsky, D.J., Emr, S.D., 2000. Autophagy as a regulated pathway of cellular degradation. Science 290, 1717–1720.
Kunapuli, S., Rosania, S., Schwarz, E.R., 2006. "How do cardiomyocytes die?" Apoptosis and autophagic cell death in cardiac myocytes. J. Card. Fail. 12, 381–391.
Leung, A.W.C., Halestrap, A.P., 2008. Recent progress in elucidating the molecular mechanism of the mitochondrial permeability transition pore. Biochim. Biophys. Acta 1777, 946–952.
Martinet, W., Knaapen, M.W.M., Kockx, M.M., De Meyer, G.R.Y., 2007. Autophagy in cardiovascular disease. Trends Mol. Med. 13, 482–491.
Mosmann, T., 1983. Rapid colorimetric assay for cellular growth and survival: application to proliferation and cytotoxicity assays. J. Imm. Methods 65, 55–63.
Pretorius, P.J., Terblanche, M., 1967. A preliminary study on the symptomatology and cardiodynamics of gousiekte in sheep and goats. J. S. Afr. Vet. Med. Assoc. 38, 29–52.
Pretorius, P.J., Terblanche, M., Van der Walt, J.D., Van Ryssen, J.C.J., 1973. Cardiac Failure in Ruminants Caused by Gousiekte. Recent Advances in Cardiac Structure and Metabolism. University Park Press, Baltimore, pp. 385–397.
Prozesky, L., Bastianello, S.S., Fourie, N., Schultz, R.A., 2005. A study of the pathology and pathogenesis of the myocardial lesions in gousiekte, a plant-induced cardiotoxicosis of ruminants. Onderstepoort J. Vet. Res. 72, 219–230.
Regula, K.M., Ens, K., Kirshenbaum, L.A., 2003. Mitochondria-assisted cell suicide: a license to kill. J. Mol. Cell. Cardiol. 35, 559–567.
Rottenberg, H., Wu, S., 1998. Quantitative assay by flow cytometry of the mitochondrial membrane potential in intact cells. Biochim. Biophys. Acta 1404, 393–404.
Rubiolo, J.A., Vega, F.V., 2008. Resveratrol protects primary rat hepatocytes against necrosis induced by reactive oxygen species. Biomed. Pharmacother. 62, 606–612.
Samarel, A.M., Engelmann, G.L., 1991. Contractile activity modulates myosin heavy-chain-β expression in neonatal rat heart cells. Am. Physiol. Soc. 261, H1067–H1077.
Schultz, R.A., Fourie, N., Basson, K.M., Labuschagne, L., Prozesky, L., 2001. Effect of pavetamine on protein synthesis in rat tissue. Onderstepoort J. Vet. Res. 68, 325–330.

Schutte, P.J., Els, H.J., Booyens, J., 1984. Ultrastructure of myocardial cells in sheep with congestive heart failure induced by *Pachystigma pygmaeum*. S. Afr. J. Sci. 80, 378–380.

Theiler, A., Du Toit, P.J., Mitchell, D.T., 1923. Gousiekte in sheep. In: 9th and 10th Reports of the Director of Veterinary Education and Research, Onderstepoort, Pretoria. The Government Printing and Stationary Office, pp. 1–106.

Yoon, Y.-S., Byun, H.-O., Cho, H., Kim, B.-K., Yoon, G., 2003. Complex II defect via down-regulation of iron–sulfur subunit induces mitochondrial dysfunction and cell cycle delay in iron chelation-induced senescence-associated growth arrest. J. Biol. Chem. 278, 51577–51586.

Yue, T.-L., Wang, C., Romanic, A.M., Kikly, K., Keller, P., DeWolf Jr., W.E., Hart, T.K., Thomas, H.C., Storer, B., Gu, J.-L., Wang, X., Feuerstein, G.Z., 1998. Staurosporine-induced apoptosis in cardiomyocytes: a potential role of caspase-3. J. Mol. Cell. Cardiol. 30, 495–507.

Zordoky, B.N.M., El-Kadi, A.O.S., 2007. H9c2 cell line is a valuable *in vitro* model to study the drug metabolizing enzymes in the heart. J. Pharmacol. Toxicol. 56, 317–322.

Toxicology in Vitro 24 (2010) 1258–1265

Contents lists available at ScienceDirect

Toxicology in Vitro

journal homepage: www.elsevier.com/locate/toxinvit

A fluorescent investigation of subcellular damage in H9c2 cells caused by pavetamine, a novel polyamine

C.E. Ellis [a,b,*], D. Naicker [a,b], K.M. Basson [a], C.J. Botha [b], R.A. Meintjes [c], R.A. Schultz [a]

[a] Food, Feed and Veterinary Public Health Programme, Agricultural Research Council-Onderstepoort Veterinary Institute, Private Bag X5, Onderstepoort 0110, South Africa
[b] Department of Paraclinical Sciences, Faculty of Veterinary Science, University of Pretoria, Onderstepoort 0110, South Africa
[c] Department of Anatomy and Physiology, Faculty of Veterinary Science, University of Pretoria, Onderstepoort 0110, South Africa

ARTICLE INFO

Article history:
Received 18 July 2009
Accepted 4 February 2010
Available online 8 February 2010

Keywords:
Acidic vesicles
Cardiotoxicity
Cytoskeleton
Fluorescent staining
Gousiekte
H9c2 cell line
Mitochondria
Pavetamine
Polyamine
Sarcoplasmic reticula

ABSTRACT

Gousiekte, which can be translated literally as "quick disease", is one of the six most important plant toxicoses that affect livestock in South Africa. It is a plant-induced cardiomyopathy of domestic ruminants characterised by the sudden death of animals within a period of 4–8 weeks after the initial ingestion of the toxic plant. The main ultrastructural change in sheep hearts is degradation of myofibres. In this study, fluorescent probes were used to investigate subcellular changes induced by pavetamine, the toxic compound that causes gousiekte, in H9c2 cells. The sarcoplasmic reticula (SR) and mitochondria showed abnormalities that were not present in the control cells. The lysosomes of treated cells were more abundant and enlarged than those of the control cells. There was increased activity of cytosolic hexosaminidase and acid phosphatase, indicating increased lysosomal membrane permeability. Lysosomes play an important role in both necrosis and apoptosis. The degradation of the myofibres may be a consequence of the increased lysosomal membrane permeability. Pavetamine was also found to cause alterations in the organisation of F-actin. F-actin in the nucleus is a transcription regulator and can therefore influence protein synthesis. Actin filament organisation also regulates the cardiac L-type Ca^{2+} channels. Fluorescent staining demonstrated that pavetamine may damage a number of organelles, all of which can influence the proper functioning of the heart.

1. Introduction

Gousiekte ("quick disease") is a disease of ruminants characterised by acute heart failure without any premonitory signs 4–8 weeks after the initial ingestion of certain rubiaceous plants (Theiler et al., 1923; Pretorius and Terblanche, 1967). The toxic compound pavetamine that causes gousiekte was isolated from *Pavetta harborii* (Fourie et al., 1995). Ultrastructural changes observed in sheep hearts, intoxicated with extracts of *Pachystigma pygmaeum* and dried plants known to cause gousiekte included a loss of cardiac myofilaments. Disintegration of the myofibres, which appeared frayed, was accompanied by replacement fibrosis (Schutte et al., 1984; Kellerman et al., 2005; Prozesky et al., 2005). In addition, mitochondria varied in shape and size, with ruptured swollen cristae, and the sarcoplasmic reticula (SR) were dilated and proliferated (Prozesky et al., 2005). Schultz et al., (2001) reported that pavetamine, administered intraperitoneally to rats, inhibits protein synthesis in the heart, but not in the liver, kidney, spleen, intestine and muscle. Exposure of H9c2 cells (derived from embryonic rat cardiac cells) to pavetamine caused damage to mitochondria and SR, as demonstrated by transmission electron microscopy (TEM) (Ellis et al., 2010). Eventual death of H9c2 cells after exposure to 20 μM pavetamine for 72 h was attributed to necrosis, with membrane blebbing and lactate dehydrogenase (LDH) release into the medium (Ellis et al., 2010).

Cardiomyocytes, performing vigorous mechanical work for an entire lifetime, have elegant mechanisms for protein quality

Abbreviations: ATP, adenosine triphosphate; Ca^{2+}, calcium; CICR, Ca^{2+}-induced Ca^{2+} release; CLSM, confocal laser scanning microscope; CytoD, cytochalasin D; DAPI, 4′,6-diamidino-2-phenylindole; DMEM, Dulbecco's modified Eagle's medium; ER, endoplasmic reticulum; ERAD, endoplasmic reticulum-associated protein degradation; FCS, fetal calf serum; FITC, fluorescein isothiocyanate; H9c2 cells, a clonal myogenic cell line derived from embryonic rat ventricle; HBSS, Hank's balanced salt solution; LDH, lactate dehydrogenase; MHC, myosin heavy chain; $\Delta\Psi_m$, mitochondrial membrane potential; NCX, Na^+/Ca^{2+} exchanger; PBS, phosphate-buffered saline; PQC, protein quality control; RyR, ryanodine receptor; SERCA, sarcoplasmic reticulum Ca^{2+} ATPase; SR, sarcoplasmic reticulum; TEM, transmission electron microscopy; UPR, unfolded protein response; UPS, ubiquitin–proteasome system.

* Corresponding author. Address: Food, Feed and Veterinary Public Health Programme, Agricultural Research Council-Onderstepoort Veterinary Institute, Private Bag X5, Onderstepoort 0110, South Africa. Tel.: +27 125299254; fax: +27 125299249.
E-mail address: ellisc@arc.agric.za (C.E. Ellis).

0887-2333/$ - see front matter © 2010 Elsevier Ltd. All rights reserved.
doi:10.1016/j.tiv.2010.02.002

control (PQC) (Wang et al., 2008). Protein synthesis occurs on cytosolic free ribosomes and, depending on cell type, in the rough SR (Blobel, 2000). In the SR, numerous chaperones, other proteins and factors ensure efficient protein folding as part of the SR-associated PQC. For efficient protein folding during protein synthesis, the correct redox status is required for protein disulphide bond formation (Glembotski, 2008). Endoplasmic reticulum (ER) stressors, namely dithiothreitol, thapsigargin and calcium levels, impair proper folding of proteins and lead to the accumulation of misfolded and dysfunctional proteins, thereby triggering the unfolded protein response (UPR) (Kozutsumi et al., 1988). Cardiomyocytes, in which the myofibrillar proteins occupy more than 80% of the cell volume, have an SR-independent PQC, namely the ubiquitin–proteasome system (UPS) (Wang et al., 2008). Target proteins are ubiquitinated by ubiquitin E3 ligases and degradation occurs on the 26S proteasome. Proteolysis in cardiomyocytes can also occur via calpains and caspases.

The cytoskeleton of cardiomyocytes consists of actin microfilaments, microtubules and intermediate filaments (Kustermans et al., 2008). Actin has several essential roles, namely cell motility, membrane dynamics, endocytosis, exocytosis, vesicular trafficking and cytokinesis (Lanzetti, 2007; Kustermans et al., 2008). G-actin (globular-actin) exists as a monomer and is bound to ATP, whereas F-actin (filamentous actin) is a linear polymer (Kustermans et al., 2008). Many actin-binding proteins regulate the dynamics of actin polymerization (the coordinated assembly and disassembly of actin filaments in response to cellular signaling) (Kustermans et al., 2008). Actin is also found in the nucleus and is an important regulator of transcription, chromatin remodelling and transcription factor activity (Vartiainen, 2008). Furthermore, cardiac L-type calcium channel regulation is tightly controlled by actin filament organization (Lader et al., 1999; Rueckschloss and Isenberg, 2001).

The purpose of this study was to determine the effect of pavetamine on the structure of the mitochondria, sarcoplasmic reticula, lysosomes and the F-actin cytoskeleton in the H9c2 cell line, a subclone derived from embryonic rat heart tissue, using fluorescent probes.

2. Materials and methods

2.1. Chemicals

Cytochalasin D (CytoD), digitonin, Dulbecco's modified Eagle's medium (DMEM), fast red violet LB, magnesium chloride ($MnCl_2$), naphthol phosphate AS-BI, phalloidin-FITC, *p*-nitrophenyl-*N*-acetyl-β-D-glucosaminide and thapsigargin were purchased from Sigma–Aldrich (St. Louis, MO, USA). Foetal calf serum (FCS) and penicillin–streptomycin were purchased from Gibco (Grand island, NY, USA). ER-Tracker Green dye, MitoTracker Green FM dye, Lysosensor Green DND-189 probe and ProLong Gold antifade reagent were purchased from Invitrogen (Eugene, OR, USA). DAPI (4′,6-diamidino-2-phenylindole) was purchased from Roche Diagnostics (Mannheim, Germany) and *N*′-*N*′-dimethylformamide was obtained from BDH Chemicals Ltd (Poole, England).

2.2. H9c2 cell line

The H9c2 cell line (Kimes and Brandt, 1976) was obtained from the American Type Culture Collection (cat no: CRL-1446™, Manassas, USA). The cells were grown on sterile glass coverslips in DMEM, supplemented with 10% FCS and 100 U/ml penicillin-100 μg/ml streptomycin sulphate.

2.3. Purification of pavetamine

Pavetamine was extracted and purified from the leaves of *P. harborii* S. Moore, collected near Ellisras (23°32′S, 27°42′E) in the Limpopo province, South Africa, by staff of the ARC-OVI Toxicology department according to the method described by Fourie et al., 1995. The yield during 2007 to 2008 was 2.7 mg pavetamine per kg dried material.

2.4. Treatment of H9c2 cells

H9c2 cells were treated with 20 μM pavetamine and untreated cells served as controls. In addition, they were also exposed to 3 μM thapsigargin, an ER stressor. In a previous study using TEM, pavetamine was shown to cause damage to the mitochondria and SR of H9c2 cells after 24 h of exposure, and secondary lysosomes only appeared after 48 h of exposure to pavetamine (Ellis et al., 2010). For this reason, the H9c2 cells were stained after exposure for 24 and 48 h to detect organelle damage, and only stained after 48 h to determine lysosomal defects. Cells were incubated in a humidified atmosphere of 5% CO_2 at 37 °C.

2.5. Fluorescent staining

Labeling of H9c2 cells was done with probes to stain subcellular organelles. The images in the figures are derived from three independent experiments and the aim being to study qualitative differences between control cells and H9c2 cells treated with pavetamine.

2.5.1. Staining of the sarcoplasmic reticulum

After a 24 h exposure period, the cells were washed twice for 5 min at a time with Hank's balanced salt solution (HBSS), containing 1% FCS. They were then fixed in 100% acetone for 10 min at −20 °C, followed by staining with 20 μM ER-Tracker Green dye for 30 min at 37 °C and two final 5 min washes with HBSS/1% FCS.

2.5.2. Staining of mitochondria

After a 24 h exposure period, the cells were washed twice for 5 min at a time with DMEM/1% FCS, stained with 0.2 μM MitoTracker Green FM dye for 45 min at 37 °C and washed twice for 5 min with DMEM/1% FCS.

2.5.3. Staining of lysosomes

After a 48 h exposure period, the cells were washed twice for 5 min each time with PBS/1% FCS, stained with 1 μM Lysosensor Green DND-189 probe for 30 min at 37 °C, followed by two final washes for 5 min each time with PBS/1% FCS.

2.5.4. Staining of F-actin cytoskeleton

After exposure to pavetamine for 24 or 48 h, the F-actin of H9c2 cells was stained with phalloidin-FITC. Cytochalasin D (CytoD), a cell-permeable mycotoxin and an inhibitor of actin polymerization, was included as a positive control. H9c2 cells were exposed to 12 μM CytoD for 10 min. Briefly, the cells were washed with PBS for 5 min, followed by fixation in 100% ice-cold acetone at −20 °C for 10 min. They were then washed twice with PBS for 5 min and stained with phalloidin-FITC (diluted to 1 μg/ml in PBS) for 30 min at 37 °C. The washing was repeated and the nuclei were then stained with 1.3 μg/ml 4′,6-diamidino-2-phenylindole (DAPI) for 15 min at 37 °C, followed by two 5 min washes in PBS.

2.5.5. Fluorescence microscopy

After staining and washing, the coverslips were mounted on microscopy glass slides using ProLong Gold antifade reagent.

Fluorescence imaging was performed using a confocal laser scanning microscope (CLSM) (Model LSM 510, ZEISS, Germany).

2.6. Determination of lysosomal hexosaminidase activity

The hexosaminidase activity was determined according to the method described by Theodossiou et al., 2006, with few modifications. Untreated H9c2 cells and H9c2 cells exposed for 48 h to 20 μM pavetamine were harvested by trypsinization. Cells were washed with PBS and resuspended in 1200 μl PBS. Thereafter, 500 μl of the cell suspensions were transferred to 1.5 ml microcentrifuge tubes and centrifuged for 1 min at 720*g*. The supernatants were removed and the cell pellets resuspended in 500 μl of 5 μM digitonin in 0.1 M citric acid (pH 4.5), and incubated for 20 min at room temperature. The cells were then centrifuged at 5000*g* for 1 min and the supernatants were collected. An amount of 500 μl of each supernatant was added to 500 μl of 3.75 mM *p*-nitrophenyl-*N*-acetyl-β-D-glucosaminide in 0.1 M citric acid (pH 4.5) and incubated at 37 °C for 2 h. The reaction was stopped by the addition of 500 μl of 0.1 M carbonate buffer, pH 10.0. The absorbance values were measured at a wavelength of 404 nm in a UV-160A UV/visible spectrophotometer (Shimadzu, North America). The protein content was determined with a Bio-Rad protein assay reagent (Bio-Rad Laboratories, California, USA). The results were expressed as the mean ± standard error of the mean (SEM). The Student's *t*-test was used for statistical analysis of the data, with p values of <0.05 considered to be significant.

2.7. Determination of acid phosphatase activity

The activity of acid phosphatase was determined according to the method of Malagoli et al., 2006. Briefly, H9c2 cells cultured on coverslips were treated with 20 μM pavetamine for 48 h in a humidified 5% CO_2 incubator. For the acid phosphatase activity assay, both control and pavetamine-treated cells were incubated for 4 h at 37 °C in a 0.1 N sodium acetate–acetic acid buffer (pH 5.0)

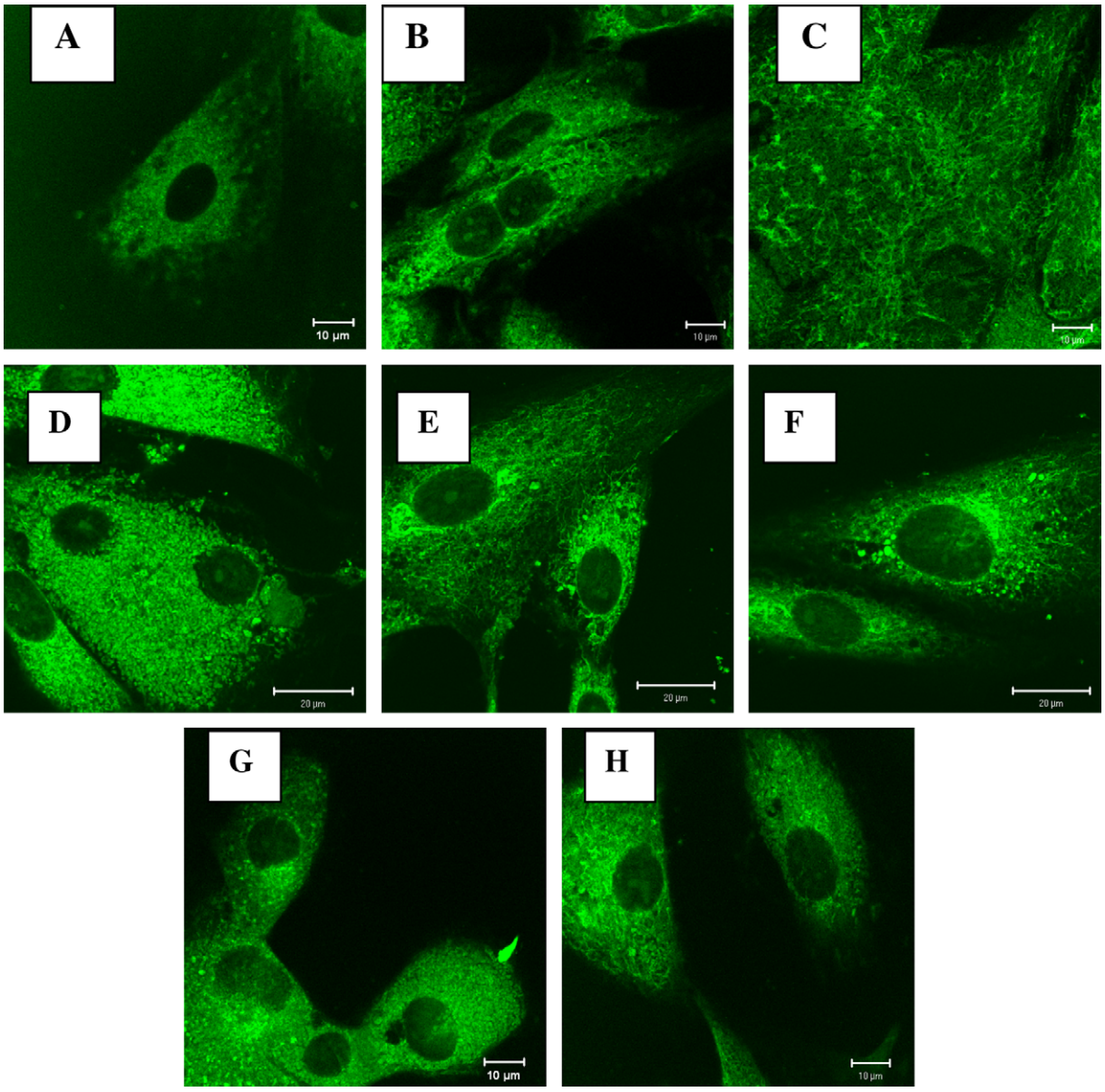

Fig. 1. H9c2 cells stained with ER Tracker for labeling of sarcoplasmic reticula (SR). (A) untreated control cells; (B–D) cells treated with 20 μM pavetamine for 24 h; (E–F) cells treated with 20 μM pavetamine for 48 h; (G–H) cells treated with 3 μM thapsigargin for 24 h.

containing 0.01% naphthol phosphate AS-BI, 2% *N*′-*N*′-dimethylformamide 0.06% fast red violet LB and 0.5 mM $MnCl_2$. Light microscopy images were acquired using a microscope (Leica, Model CTR6000, Germany) fitted with a digital camera system (Leica, DFC490, Germany).

3. Results

The SR of H9c2 cells treated with 20 μM pavetamine (Fig. 1B) differed in appearance from that of the control cells (Fig. 1A). The SR of treated cells were less compact than those of the control cells and appeared more granular (Fig. 1B–F), or even collapsed (Fig. 1C). The SR in Fig. 1D appeared more abundant than those of the control cells Fig. 1A). After exposure to pavetamine for 48 h, the SR accumulated around the nuclei (Fig. 1E and F). In Fig. 1G and H, cells treated with 3 μM thapsigargin demonstrated more numerous and denser SR compared to the control cells (Fig. 1A).

Staining of H9c2 cells exposed to 20 μM pavetamine using MitoTracker Green revealed abnormal mitochondria (Fig. 2B–D). In the control cells (Fig. 2A), the mitochondria were evenly distributed around the nucleus, whereas after 24 h of pavetamine treatment, the mitochondria relocated towards one pole of the cell (Fig. 2B) and became more elongated (Fig. 2C). The mitochondria of H9c2 cells exposed for 48 h to 20 μM pavetamine (Fig. 2D) disintegrated and the fluorescence faded rapidly.

Staining of the lysosomes with the LysoSensor probe revealed a number of aberrations in cells treated with pavetamine (Fig. 3). An increase in the number and size of lysosomes was noted in H9c2 cells exposed for 48 h to 20 μM pavetamine (Fig. 3B–D), in comparison to untreated control cells (Fig. 3A). The lysosomes relocated to the periphery of the cell (Fig. 3B–D), whilst those in Fig. 3C were markedly swollen, with weak fluorescence on the outer edge. The average activity of hexosaminidase in the treated cells was 635.5 ± 44.2 μM/h/mg protein compared to 243.8 ± 21.4 μM/h/mg protein in the control cells (Fig. 4). Digitonin-permeabilized fractions represented the enzyme activity in the cytosol (Theodossiou et al., 2006). H9c2 cells treated with 20 μM pavetamine for 48 h showed more intense staining with the substrate for acid phosphatase (an enzyme specific for lysosomes) (Fig. 5C and D) than the untreated control cells (Fig. 5A). There was light pink staining of the lysosomes around the nucleus in the control cells, whilst the treated cells were characterised by deep purple staining in all areas of the cytosol, indicating increased enzyme activity.

The effect of pavetamine on the cytoskeleton of H9c2 cells was investigated using phalloidin-FITC (Fig. 6). In the control cells, both

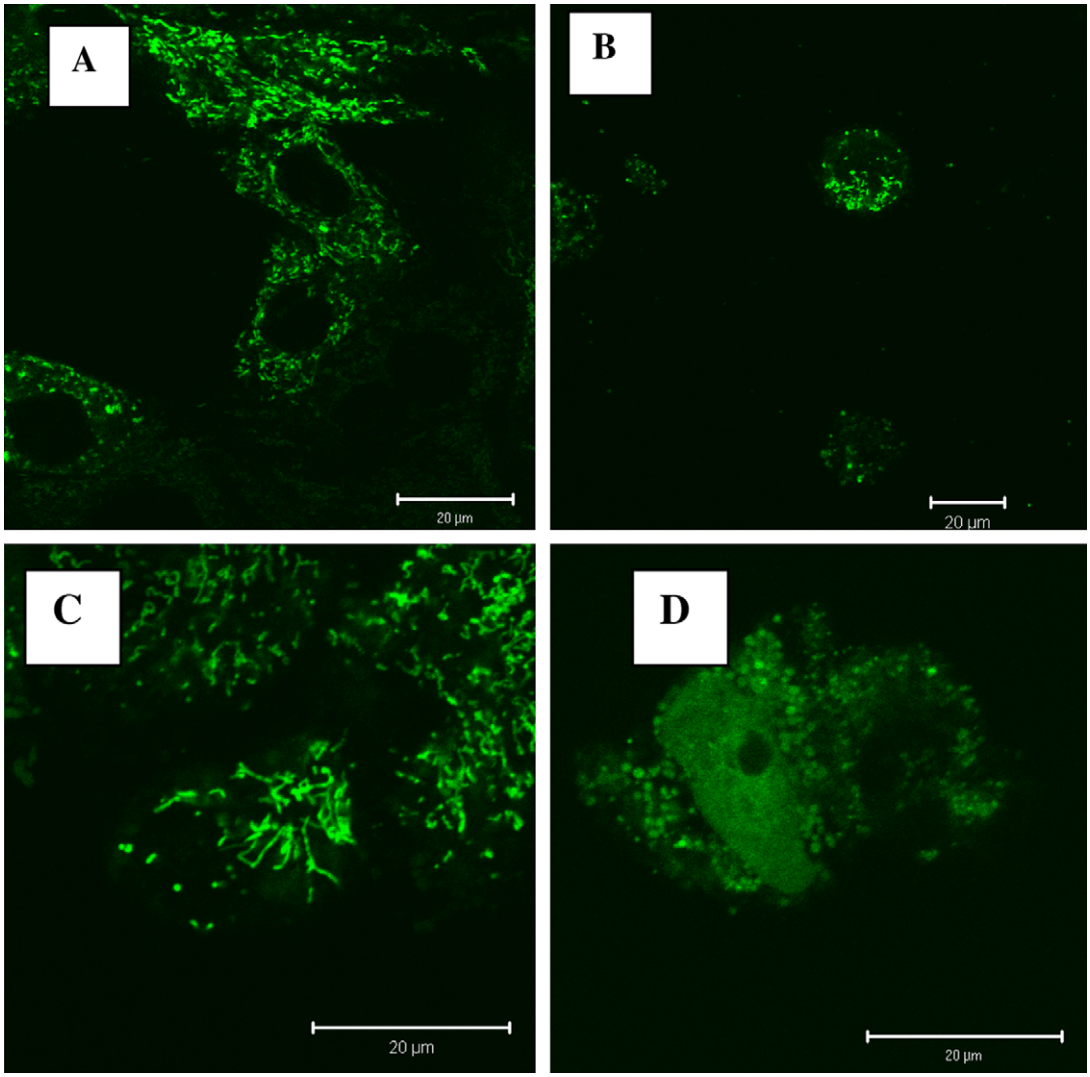

Fig. 2. H9c2 cells stained with MitoTracker Green for labeling of mitochondria. (A) Untreated control cells; (B–C) cells treated with 20 μM pavetamine for 24 h; (D) cells treated with 20 μM pavetamine for 48 h.

thick and thin bundles were stained with phalloidin, with the thicker filaments located at the periphery of the cells (Fig. 6A). The filaments appeared throughout the cells as a mesh-like network. The H9c2 cells treated with 20 μM pavetamine for 24 h showed differences in cell shape and F-actin patterns, although the intensity of the fluorescent staining was comparable to that of the control cells (Fig. 6B and C). The F-actin was ruffled around the nucleus (Fig. 6B), or lost its mesh-like appearance and became parallel in orientation (Fig. 6C). Fluorescent staining was much less intense or even absent, with only the nuclei being stained, in the H9c2 cells treated for 48 h with pavetamine (Fig. 6D). Within 5 min of exposure of H9c2 cells to 12 μM CytoD, the F-actin network became severely disrupted (Fig. 6E). Dissolution of stress fibres and numerous small and highly fluorescent cytoplasmic aggregates, or foci, appeared, with clumping in some areas of the cells.

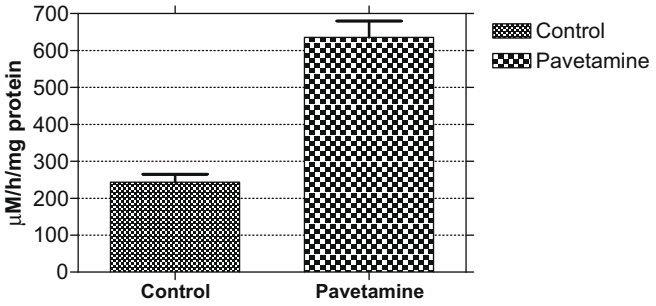

Fig. 4. Lysosomal hexosaminidase enzyme activity of untreated control and pavetamine-treated H9c2 cells after 48 h exposure. H9c2 cells treated with pavetamine had statistically significant higher hexosaminidase activity than the control cells as analyzed with the Student's *t*-test ($p < 0.05$). The results presented the average of three independent enzyme activity determinations.

4. Discussion

This fluorescent subcellular investigation demonstrated that pavetamine caused alterations to the SR, mitochondria, lysosomes and F-actin of H9c2 cells, all of which have important functions in the cell. These findings concur with a previous TEM study (Ellis et al., 2010), in which pavetamine was shown to cause damage to the mitochondria and SR of H9c2 cells after 24 h exposure and the appearance of secondary lysosomes after 48 h exposure.

Pretorius et al. (1973) reported a depressed uptake of calcium ions by isolated fragments of the SR from sheep dosed with pavetamine-producing *P. pygmaeum* plant material, suggesting that the

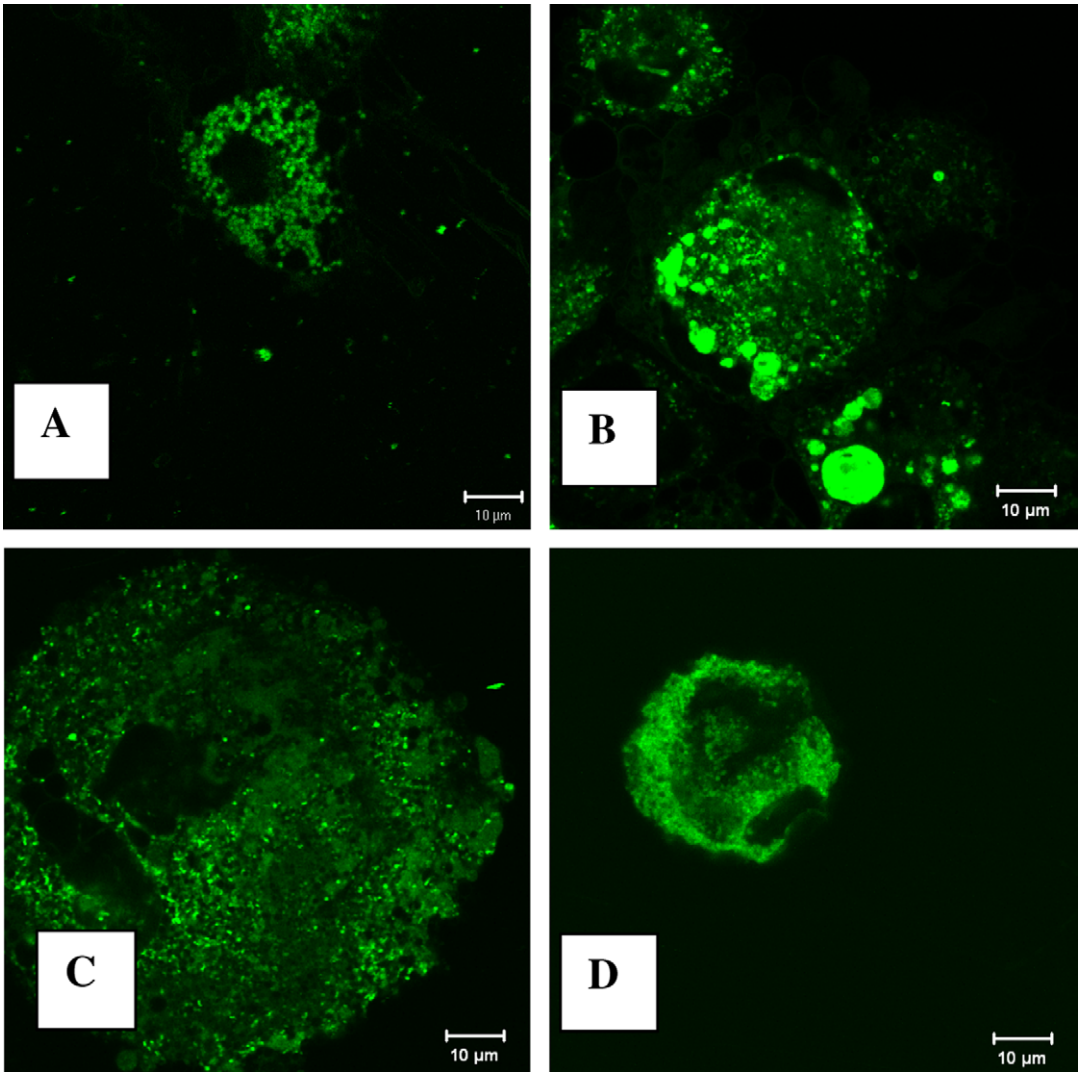

Fig. 3. H9c2 cells stained with Lysosensor probe, which stains both lysosomes and late endosomes. (A) untreated control cells stained with Lysosensor probe; (B–D) cells treated with 20 μM pavetamine for 48 h and then stained with Lysosensor probe.

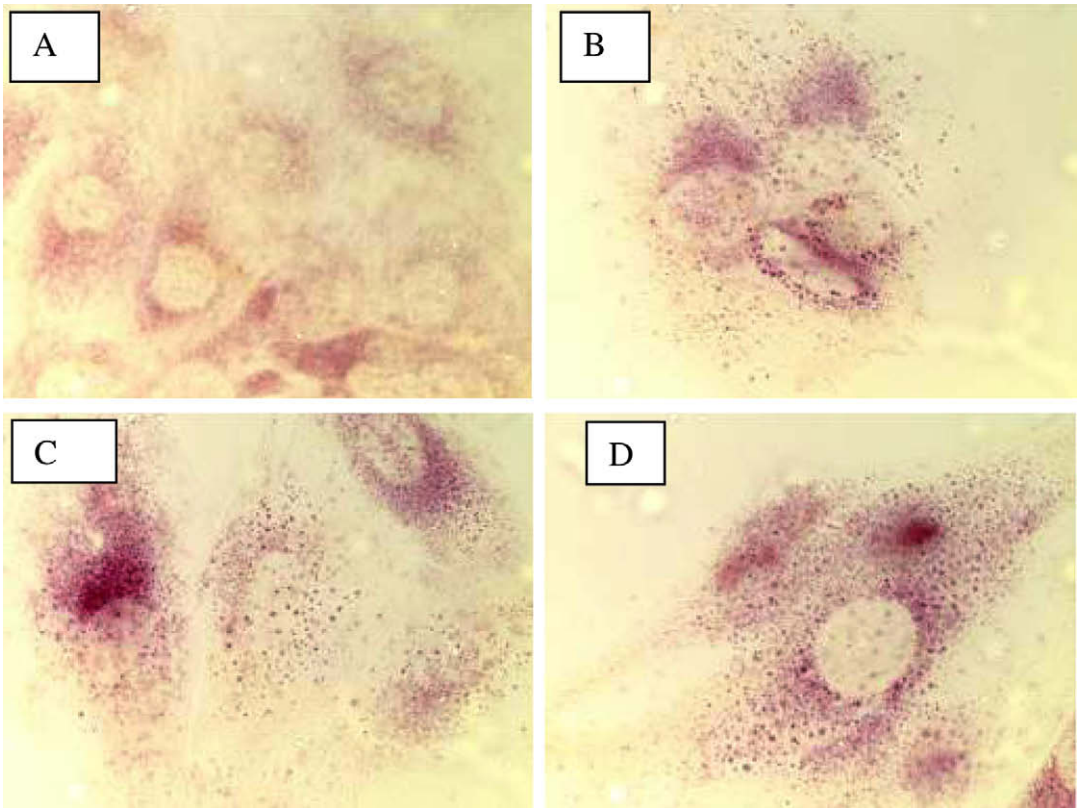

Fig. 5. Acid phosphatase enzyme activity of untreated control and pavetamine-treated H9c2 cells. (A) untreated control cells; (B–D) H9c2 cells treated with 20 μM pavetamine after 48 h exposure. The experiments were repeated three times independently with similar results.

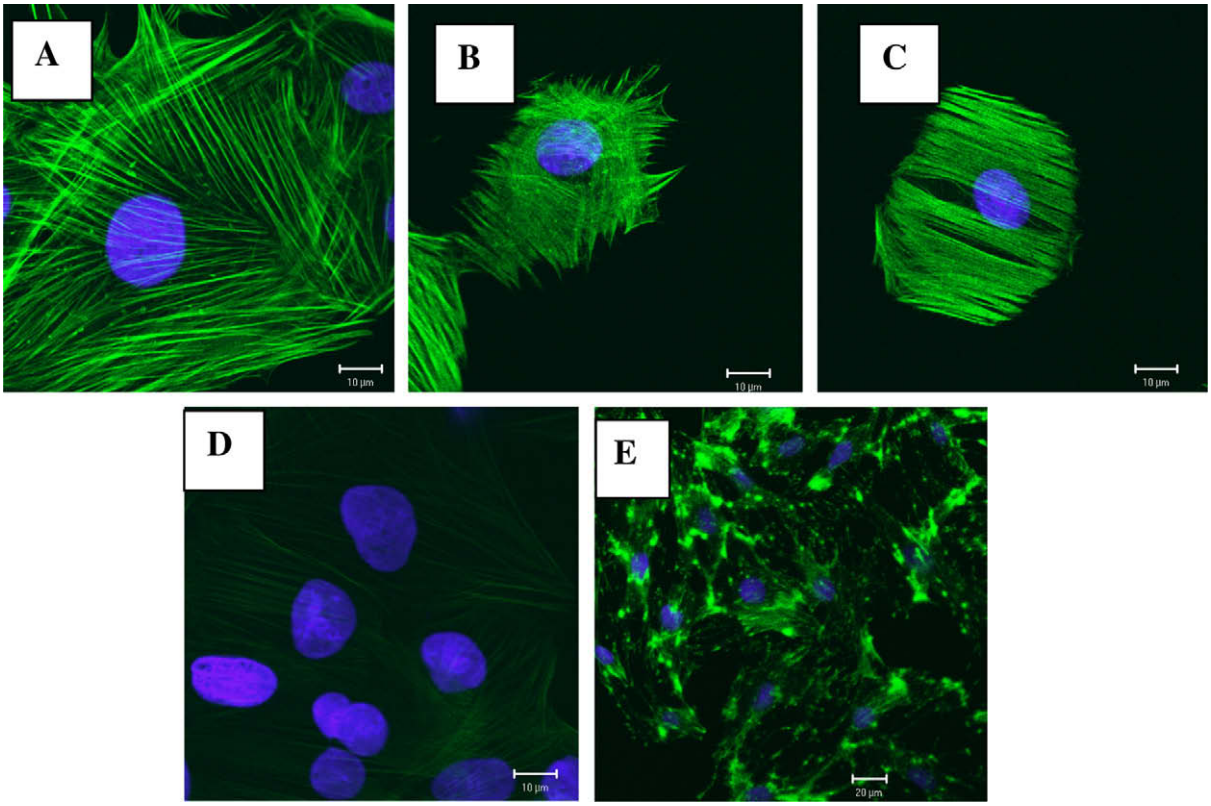

Fig. 6. H9c2 cells stained with phalloidin-FITC which binds to the F-actin cytoskeleton. (A) untreated control cells; (B–C) cells treated for 24 h with 20 μM pavetamine; (D) cells treated for 48 h with 20 μM pavetamine; (E) cells treated with 12 μM cytoD (an inhibitor of actin polymerization) for 5 min.

intracellular Ca^{2+} homeostasis is altered during gousiekte. They concluded that reduced contractility of hearts affected by gousiekte can be directly correlated with the altered Ca^{2+} homeostasis. Disturbances in any of these functions will lead to SR stress, which will alter the efficiency of protein synthesis and protein folding. In this study the SR stained with the ER Tracker probe showed abnormalities in the cells treated with pavetamine, indicating ER stress. Treatment with thapsigargin, a SR stressor, produced similar results. Thapsigargin blocks the SERCA pump and prevents the transport of Ca^{2+} back into the SR, thus causing depletion in the Ca^{2+} stores of the SR, with a resultant rise in cytosolic Ca^{2+} levels (Prasad and Inesi, 2009).

The MitoTracker Green probe diffuses passively across the sarcolemma and accumulates in active mitochondria, irrespective of the mitochondrial membrane potential ($\Delta\Psi_m$). In this study, the morphology of the mitochondria of pavetamine-treated cells was adversely affected and the rapid fading of fluorescent staining indicated that the mitochondria were inactive. The mitochondrion is the power engine of the cell by virtue of generating ATP through oxidative phosphorylation. Snyman et al., (1982) investigated the energy production in hearts of sheep dosed with *P. pygmaeum* and found a decreased level of ATP and creatine phosphate (CrP), with increased lactate levels, reflecting a shift towards anaerobic metabolism. They further demonstrated a reduced uptake of oxygen in isolated mitochondria.

The LysoSensor probe is a dye that is acidotropic and accumulates in acidic organelles like late endosomes and lysosomes as a result of protonation (Lin et al., 2001). Polyamines accumulate in polyamine-sequestering vesicles that co-localize with acidic vesicles of the late endocytic compartment and the *trans* Golgi (Soulet et al., 2004). Amine drugs such as procaine, nicotine and atropine cause multiple large vacuoles to form (Morissette et al., 2008). These vacuoles are formed by vacuolar (V)-ATPase as a result of the cell's response to concentrated cationic drugs. Lipophilic weak bases, such as monoamines and diamines, are used to study vacuolar acidification (Millot et al., 1997). Lysosomotropism is a term used to describe the accumulation of basic compounds inside acidic organelles. Basic compounds reaching the acidic milieu of lysosomes become protonated and membrane-impermeable, resulting in their accumulation inside the lysosomes (Lemieux et al., 2004). According to the results obtained in this study, pavetamine caused an increase in the amount and size of lysosomes. To further investigate the lysosomes, two enzymatic assays were performed. There was an increase in the activity of cytosolic hexosaminidase in cells treated with pavetamine, indicating that the lysosomal membranes became more permeable. Acid phosphatase activity in the treated cells was also increased in comparison to the control cells. There are three proteolytic systems in cells: proteasomes, calpains and the lysosomal hydrolases (Bartoli and Richard, 2005). If the lysosomal hydrolases escape from lysosomes, they can have a devastating effect on cellular and extracellular matter (Bechet et al., 2005). The lysosomal endopeptidases, known as cathepsins, can hydrolyse myofibrillar proteins like troponin T, myosin heavy chain, troponin I and tropomyosin (Bechet et al., 2005). Calpain degrades the cytoskeleton and myofibril proteins such as troponin I, troponin T, desmin, fodrin, filamin, C-protein, nebulin, gelsolin, vinculin and vimentin, leading to impairment of the actin–myosin interaction (Lim et al., 2004). The lysosomal damage observed in the current study might explain the typical ultrastructural feature of gousiekte in hearts, namely degeneration of the myofibrils (Prozesky et al., 2005). It is possible that the lysosomal endopeptidases may play a part in the degradation of the myofibrils.

Phalloidin, a toxin from the mushroom *Amanita phalloides*, is an actin filament stabilizing compound (Kustermans et al., 2008). Coupling of phalloidin to fluorescent dyes therefore renders it a useful tool to study the cytoskeleton. Phalloidin stains only filamentous actin with seven or more monomeric actin molecules (Visegrady et al., 2005). In this study treatment of cells with pavetamine caused alterations in the F-actin cytoskeleton. The F-actin became ruffled around the nuclei and lost its mesh-like appearance. In some cells, F-actin was absent, with only the nuclei being stained. CytoD caused severe disruption of the F-actin network. The effect of pavetamine on F-actin was different to that of CytoD. Changes to the F-actin after pavetamine treatment occurred much later than the CytoD-induced alterations. Owing to the complexity of the cytoskeleton, many other proteins, like the actin-binding, actin-severing and actin-capping proteins, may be involved in the cytotoxicity caused by pavetamine. Two possible consequences of disruption of the cytoskeleton by pavetamine may include altered protein synthesis (by interfering with transcription) and changes to the L-type calcium channels. Disruption of F-actin decreases calcium current (Lader et al., 1999).

In conclusion, the cytotoxicity of pavetamine is exerted through mitochondrial damage, SR stress, increased lysosomal activity and damage to the F-actin network. All of these cell components play crucial roles in cell homeostasis. Despite these serious alterations, the affected animal survives for 4–8 weeks after ingestion of the pavetamine-containing plants. In future studies, some of the cardiac contractile proteins in rat neonatal cardiomyocytes will be immuno-labeled to identify which proteins are degraded during gousiekte. The activity of non-lysosomal enzymes, the proteasome and calpains will also be investigated to clarify their role in the degradation of the myofibres seen in gousiekte.

Conflict of interest

The authors declare that there is no conflict of interest.

Ethical statement

The authors declare that this work has not been published elsewhere and that no animal experiments were carried out in the present study.

Acknowledgements

We would like to thank Mr. A. Hall (Laboratory for Microscopy and Microanalysis, University of Pretoria) for the CLSM work. We would like to thank Prof. Mary-Louise Penrith and Dr. K. Gillingwater for editing this manuscript. This investigation was funded by the North-West and Gauteng Provinces, as well as by the Department of Paraclinical Sciences, University of Pretoria.

References

Bartoli, M., Richard, I., 2005. Calpains in muscle wasting. Int. J. Biochem. Cell Biol. 37, 2115–2133.
Bechet, D., Tassa, A., Taillandier, D., Combaret, L., Attaix, D., 2005. Lysosomal proteolysis in skeletal muscle. Int. J. Biochem. Cell Biol. 37, 2098–2114.
Blobel, G., 2000. Protein targeting. Biosci. Rep. 20, 303–344.
Ellis, C.E., Naicker, D., Basson, K.M., Botha, C.J., Meintjes, R.A., Schultz, R.A., 2010. Cytotoxicity and ultrastructural changes in H9c2(2–1) cells treated with pavetamine, a novel polyamine. Toxicon 55, 12–19.
Fourie, N., Erasmus, G.L., Schultz, R.A., Prozesky, L., 1995. Isolation of the toxin responsible for gousiekte, a plant-induced cardiomyopathy of ruminants in southern Africa. Onderstepoort J. Vet. Res. 62, 77–87.
Glembotski, C.C., 2008. The role of the unfolded protein response in the heart. J. Mol. Cell. Cardiol. 44, 453–459.
Kellerman, T.S., Coetzer, J.A.W., Naudé, T.W., Botha, C.J., 2005. Plant Poisonings and Mycotoxicoses of Livestock in Southern Africa. Oxford University Press, Southern Africa. pp. 154–164.
Kimes, B.W., Brandt, B.L., 1976. Properties of a clonal muscle cell line from rat heart. Exp. Cell Res. 98, 367–381.

Kozutsumi, Y., Segal, M., Normington, K., Gething, M.J., Sambrook, J., 1988. The presence of malfolded proteins in the endoplasmic reticulum signals the induction of glucose-related proteins. Nature 332, 462–464.

Kustermans, G., Piette, J., Legrand-Poels, S., 2008. Actin-targeting natural compounds as tools to study the role of actin cytoskeleton in signal transduction. Biochem. Pharmacol. 76, 1310–1322.

Lader, A.S., Kwiatkowski, D.J., Cantiello, H.F., 1999. Role of gelsolin in the actin filament regulation of cardiac L-type calcium channels. Am. J. Physiol. 277, C1277–83.

Lanzetti, L., 2007. Actin in membrane trafficking. Curr. Opin. Cell Biol. 19, 453–458.

Lemieux, B., Percival, M.D., Falgueyret, J.-P., 2004. Quantification of the lysosomotropic character of cationic amphiphilic drugs using the fluorescent basic amine Red DND-99. Anal. Biochem. 327, 247–251.

Lim, C.C., Zuppinger, C., Guo, X., Kuster, G.M., Helmes, M., Eppenberger, H.M., Suter, T.M., Liao, R., Sawyer, D.B., 2004. Anthracyclines induce calpain-dependent titin proteolysis and necrosis in cardiomyocytes. J. Biol. Chem. 279, 8290–8299.

Lin, H.-J., Herman, P., Kang, J.S., Lakowics, J.R., 2001. Fluorescence lifetime characterization of novel low-pH probes. Anal. Biochem. 294, 118–125.

Malagoli, D., Marchesini, E., Ottaviani, E., 2006. Lysosomes as the target of yessotoxin in invertebrate and vertebrate cell lines. Toxicol. Lett. 167, 75–83.

Millot, C., Millot, J.-M., Morjani, H., Desplaces, A., Manfait, M., 1997. Characterization of acidic vesicles in multi-drug resistant and sensitive cancer cells by acridine orange staining and confocal microspectrofluorometry. J. Histochem. Cytochem. 45, 1255–1264.

Morissette, G., Lodge, R., Marceau, F., 2008. Intense pseudotransport of a cationic drug mediated by vacuolar ATPase: procainamide-induced autophagic cell vacuolization. Toxicol. Appl. Pharmacol. 229, 320–331.

Prasad, A.M., Inesi, G., 2009. Effect of thapsigargin and phenylephrine on calcineurin and protein kinase C signaling functions in cardiomyocytes. Am. J. Cell Physiol.. doi:10.1152/ajpcell.00474.2008.

Pretorius, P.J., Terblanche, M., 1967. A preliminary study on the symptomatology and cardiodynamics of gousiekte in sheep and goats. J. S. Afr. Vet. Med. Ass. 38, 29–52.

Pretorius, P.J., Terblanché, M., Van der Walt, J.D., Van Ryssen, J.C.J., 1973. Cardiac failure in ruminants caused by gousiekte. International symposium on cardiomyopathies, Tiervlei, 1971. In: Bajusz, E., Rona, G., Brink, A.J., Lochner, A. (Eds.), Cardiomyopathies, vol 2. University Park Press, Baltimore, pp. 384–624.

Prozesky, L., Bastianello, S.S., Fourie, N., Schultz, R.A., 2005. A study of the pathology and pathogenesis of the myocardial lesions in gousiekte, a plant-induced cardiotoxicosis of ruminants. Onderstepoort J. Vet. Res. 72, 219–230.

Rueckschloss, U., Isenberg, G., 2001. Cytochalasin D reduces Ca^{2+} currents via cofilin-activated depolymerization of F-actin in guinea pig cardiomyocytes. J. Physiol. 537, 363–370.

Schultz, R.A., Fourie, N., Basson, K.M., Labuschagne, L., Prozesky, L., 2001. Effect of pavetamine on protein synthesis in rat tissue. Onderstepoort J. Vet. Res. 68, 325–330.

Schutte, P.J., Els, H.J., Booyens, J., 1984. Ultrastructure of myocardial cells in sheep with congestive heart failure induced by *Pachystigma pygmaeum*. S. Afr J. Sci. 80, 378–380.

Snyman, L.D., Van der Walt, J.J., Pretorius, P.J., 1982. A study on the function of some subcellular systems of the sheep myocardium during gousiekte. I. The energy production system. Onderstepoort J. Vet. Res. 49, 215–220.

Soulet, D., Gagnons, B., Rivest, S., Audette, M., Poulin, R., 2004. A fluorescent probe of polyamine transport accumulated into intracellular acidic vesicles via a two-step mechanism. J. Biol. Chem. 249, 49355–49366.

Theiler, A., Du Toit, P.J., Mitchell, D.T. 1923. Gousiekte in sheep. In: 9th and 10th reports of the Director of Veterinary Education and Research, Onderstepoort. The Government Printing and Stationary Office, Pretoria, pp. 1–106.

Theodossiou, T.A., Noronha-Dutra, A., Hothersall, J.S., 2006. Mitochondria are a primary target of hypericin phototoxicity: synergy of intracellular calcium mobilisation in cell killing. Int. J. Biochem. Cell Biol. 38, 1946–1956.

Vartiainen, M.K., 2008. Nuclear actin dynamics-from form to function. FEBS Lett. 582, 2033–2040.

Visegrady, B., Lorinczy, D., Hild, G., Somogyi, B., Nyitrai, M., 2005. A simple model for the cooperative stabilization of actin filaments by phalloidin and jasplakinolide. FEBS Lett. 579, 6–10.

Wang, X., Su, H., Ranek, M.J., 2008. Protein quality control and degradation in cardiomyocytes. J. Mol. Cell. Cardiol. 45, 11–27.

Toxicon 55 (2010) 1071–1079

Contents lists available at ScienceDirect

Toxicon

journal homepage: www.elsevier.com/locate/toxicon

Damage to some contractile and cytoskeleton proteins of the sarcomere in rat neonatal cardiomyocytes after exposure to pavetamine

C.E. Ellis [a,b,*], D. Naicker [a,b], K.M. Basson [a], C.J. Botha [b], R.A. Meintjes [c], R.A. Schultz [a]

[a] Food, Feed and Veterinary Public Health Programme, Agricultural Research Council-Onderstepoort Veterinary Institute, Private Bag X5, Onderstepoort, Pretoria, Gauteng 0110, South Africa
[b] Department of Paraclinical Sciences, Faculty of Veterinary Science, University of Pretoria, Onderstepoort 0110, South Africa
[c] Department of Anatomy and Physiology, Faculty of Veterinary Science, University of Pretoria, Onderstepoort 0110, South Africa

ARTICLE INFO

Article history:
Received 31 August 2009
Received in revised form 9 December 2009
Accepted 10 December 2009
Available online 21 December 2009

Keywords:
Actin
Cardiotoxicity
Cytoskeleton
F-actin
Gousiekte
Myosin
Pavetamine
Polyamine
Rat neonatal cardiomyocytes
Titin

ABSTRACT

Pavetamine, a cationic polyamine, is a cardiotoxin that affects ruminants. The animals die of heart failure after a period of four to eight weeks following ingestion of the plants that contain pavetamine. This immunofluorescent study was undertaken in rat neonatal cardiomyocytes (RNCM) to label some of the contractile and cytoskeleton proteins after exposure to pavetamine for 48 h. Myosin and titin were degraded in the RNCM treated with pavetamine and the morphology of alpha-actin was altered, when compared to the untreated cells, while those of β-tubulin seemed to be unaffected. F-actin was degraded, or even absent, in some of the treated cells. On an ultrastructural level, the sarcomeres were disorganized or disengaged from the Z-lines. Thus, all three contractile proteins of the rat heart were affected by pavetamine treatment, as well as the F-actin of the cytoskeleton. It is possible that these proteins are being degraded by proteases like the calpains and/or cathepsins. The consequence of pavetamine exposure is literally a "broken heart".

1. Introduction

Gousiekte ("quick disease") is a disease of ruminants characterized by acute heart failure without any premonitory signs four to eight weeks after ingestion of certain rubiaceous plants (Theiler et al., 1923; Pretorius and Terblanche, 1967). The compound that causes gousiekte was isolated from *Pavetta harborii* and called pavetamine, which is a cationic polyamine (Fourie et al., 1995). Ultrastructural changes observed in sheep, intoxicated with extracts of *Pachystigma pygmaeum* were, amongst others, a loss of cardiac myofilaments. The myofibres became disintegrated and had a frayed appearance, which was accompanied by replacement fibrosis (Schutte et al., 1984; Kellerman et al., 2005; Prozesky et al., 2005). The mitochondria varied in shape and size, and demonstrated swollen, ruptured cristae. The sarcoplasmic reticula (SR) were dilated and proliferated (Prozesky et al., 2005). Schultz et al. (2001) reported that pavetamine, administered intraperitoneally to rats, inhibits protein synthesis in the heart, but not in the liver, kidney, spleen, intestine or skeletal muscle. Transmission electron microscopy (TEM) of sections of the heart

Abbreviations: BSA, bovine serum albumin; DMEM, Dulbecco's Modified Eagle's Medium; LDH, lactate dehydrogenase; LSCM, laser scanning confocal microscope; MHC, myosin heavy chain; MURF, muscle-specific RING-finger protein; PBS, phosphate saline; PQC, protein quality control; RNCM, rat neonatal cardiomyocytes; SR/ER, sarcoplasmic/endoplasmic reticulum; TEM, transmission electron microscopy.

* Corresponding author. Food, Feed and Veterinary Public Health Programme, Agricultural Research Council-Onderstepoort Veterinary Institute, Biotechnology, Old Soutpan Road, Private Bag X5, Onderstepoort, Pretoria, Gauteng 0110, South Africa. Tel.: +27 12 5299254; fax: +27 12 5299249.
E-mail address: ellisc@arc.agric.za (C.E. Ellis).

0041-0101/$ – see front matter © 2009 Elsevier Ltd. All rights reserved.
doi:10.1016/j.toxicon.2009.12.006

of treated rats revealed myofibrillar lysis. Hay et al. (2001) used dried, crude extracts of *P. harborii* to inject rats and monitored certain cardiodynamic performances. The contractility (dP/dt_{max}) of the treated group was reduced by more than 50% and the cardiac work (CW) by about 40%. The systolic function of rats treated with pavetamine was reduced, when compared to control rats (Hay et al., 2008).

In another study, the effect of pavetamine in H9c2(2-1) cells, a rat embryonic heart cell line, was investigated at a subcellular level with fluorescent probes. The SR and mitochondria showed abnormalities compared to the control cells, as measured with an ER Tracker and Mito-Tracker probe. The lysosomes of treated cells were more abundant and enlarged, compared to control cells. The presence of abundant secondary lysosomes, which contained cellular debri, and vacuoles were observed with TEM in H9c2(2-1) cells treated with pavetamine for 48 h (Ellis et al., 2010). The cytosolic hexosaminidase and acid phosphatase showed increased activity, which was indicative of increased lysosomal membrane permeability. Pavetamine also caused alterations in the organization of F-actin, which could have an influence on gene transcription and chromatin remodeling (Ye et al., 2008). Eventual cell death after exposure of H9c2(2-1) cells to pavetamine for 72 h was attributed to necrosis, with membrane blebbing and LDH release (Ellis et al., 2010).

During cardiac contraction the thick myosin and thin actin filaments of the sarcomeres slide past each other (Huxley and Peachey, 1961). Titin, the largest macromolecule known, functions as a molecular ruler for myosin assembly and acts as a molecular spring that modulates the intrinsic elastic properties of cardiomyocytes (Cox et al., 2008; LeWinter et al., 2007). The elastic property of titin is afforded by three elements: tandem immunoglobulin-like (Ig)-repeats, a PEVK domain (rich in Pro-Glu-Val-Lys) and a N2B element (Granzier and Labeit, 2002). Two titin isoforms exist in the heart: a shorter, stiffer N2B isoform and a longer N2BA isoform (Wu et al., 2002). Titin is also an integrator of sarcomeric mechanosensory function (Krüger and Linke, 2009). The cytoskeleton, consisting mainly of tubulin (microtubules), desmin (intermediate filaments) and F-actin, anchors subcellular structures and transmits mechanical, and chemical stimuli within, and between, cells (Hein et al., 2000). Actin is also a regulator for transcription, chromatin remodeling and transcription factor activity (Miralles and Visa, 2006; Vartiainen et al., 2007).

Three proteolytic systems exist in the cell for protein degradation: lysosomal enzymes, Ca^{2+}-dependent calpains and the ubiquitin-proteasome (Bartoli and Richard, 2005). The caspase family, activated during apoptosis, can also degrade proteins. Caspase-3 can degrade small myofilament proteins, but not titin (Lim et al., 2004). Intact myofibrils cannot be degraded by the proteasome and contractile proteins, like actin and myosin, are removed from the sarcomere by calpains before degradation by the proteasome (Koohmaraie, 1992; Willis et al., 2009). In cardiomyocytes, muscle-specific RING-finger proteins (MuRF1 and MuRF3) act as E3 ubiquitin ligases to mediate the degradation of β/slow myosin heavy chain (MHC) and MHCIIa (Fielitz et al., 2007). Calpain degrades the cytoskeleton and myofibril proteins such as troponin I, troponin T, desmin, fodrin, filamin, C-protein, nebulin, gelsolin, vinculin and vimentin, leading to impairment of the actin–myosin interaction (Lim et al., 2004; Galvez et al., 2007; Razeghi et al., 2007; Ke et al., 2008). Titin is also susceptible to calpain proteolysis in a model of anthracycline-induced myofilament injury (Lim et al., 2004). Autophagy also plays a crucial role in protein quality control (PQC), by bulk degradation of long-lived proteins, multi-protein complexes, oligomers, protein aggregates and organelles (Klionsky and Emr, 2000). Portions of the cytoplasm and/or organelles are sequestered, and delivered to the lysosome for degradation (Wang et al., 2008). If the lysosomal hydrolases escape from lysosomes, they can be devastating for cellular and extracellular matter (Bechet et al., 2005). The lysosomal endopeptidases, called cathepsins, can hydrolyse myofibrillar proteins, like troponin T, MHC, troponin I and tropomyosin (Bechet et al., 2005).

The purpose of this study was to identify the damage to some of the contractile and cytoskeleton proteins of cardiomyocytes caused by pavetamine by using immunofluorescent staining.

2. Materials and methods

2.1. Purification of pavetamine

Pavetamine was extracted and purified from the leaves of *P. harborii* S. Moore according to the method described by Fourie et al. (1995).

2.2. Preparation of rat neonatal cardiomyocytes (RNCM)

The following chemicals were purchased: NaCl, KCl, glucose and NaH_2PO_4 (Merck, Germany). $MgSO_4$ (Saarchem, South Africa), collagenase (Worthington, USA), pancreatin, Percoll, neonatal calf serum and fibronectin were purchased from Sigma (St. Louis, MO). RNCM were prepared from 1 to 5 day old Sprague–Dawley rats according to the method of Engelbrecht et al. (2004). The animal procedures in this study conformed with the principles outlined in the *Guide for the Care and Use of Laboratory Animals*, NIH Publication No. 85–23, revised 1996. Approval was obtained from the Animal Ethics Committee of the ARC-Onderstepoort Veterinary Institute. Isolated rat hearts were placed into 1× Ads buffer (0.1 M NaCl, 5.4 mM KCl, 5 mM glucose, 1.2 mM NaH_2PO_4, 0.8 mM $MgSO_4$, pH 7.4) in a Petri dish. The hearts were cut into smaller pieces and transferred to another Petri dish containing 1× Ads buffer. The buffer was removed, the tissue transferred to a flask and 8 ml digestion solution (50 mg Collagenase, 30 mg pancreatin in 1× Ads buffer) added, and incubation was performed at 37 °C with shaking for 20 min. The flask was left standing in a laminar flow hood and the supernatant was removed to a 15 ml conical flask and centrifuged at room temperature for 4 min at 300 g. The supernatant was discarded and the pellet combined with 2 ml neonatal calf serum. Eight ml digestion solution was added to the minced hearts and the digestion was repeated a further three times. The cell suspensions were then combined and centrifuged for 5 min at 300 g. The cell pellet was resuspended in 4 ml 1.082 g/ml Percoll in 1× Ads

buffer. An equal volume of 1.062 g/ml Percoll was slowly pipetted on top of the 1.082 g/ml Percoll. Finally, 4 ml of 1.050 g/ml Percoll was pipetted on top of the 1.062 g/ml Percoll layer. The test tube was then centrifuged for 25 min at room temperature at 1000 g. The cardiomyocytes, which formed a layer between the 1.082 and 1.062 g/ml Percoll, were then removed and placed in a new sterile test tube. Fifteen ml of 1× Ads buffer was added and the centrifugation was repeated for 4 min at 300 g. The supernatant was discarded and the cells were resuspended in 4 ml DMEM medium (Sigma, St. Louis, MO) supplemented with 10% fetal calf serum (Sigma, St. Louis, MO), 100 U/ml penicillin, and 100 μg/ml streptomycin sulphate (Sigma, St. Louis, MO). The cells were plated in 6-well plates that were pre-coated with 70 μg/ml fibronectin. Cells were plated at a density of 1×10^6 cells/ml.

2.3. Treatment of RNCM

RNCM cells were treated with 200 μM pavetamine for 48 h and untreated cells served as controls. TEM of RNCM exposed to 200 μM for 48 h resulted in myofibrillar damage. All subsequent immunofluorescent labeling of RNCM was done due to this result.

2.4. Immunofluorescent staining of RNCM

Immunofluorescent staining of RNCM was performed according to the method of BD Biosciences. Cells grown on sterile microscope slide coverslips were rinsed with PBS (2 ml/well) for 5 min with shaking. They were then fixed with 100% acetone for 10 min at −20 °C and rinsed twice with 2 ml PBS/well for 5 min on an orbital shaker, before being blocked with 1 ml/well 1% BSA/PBS for 30 min at 37 °C. The following dilutions of antibodies were made: monoclonal antibody to sarcomeric actin (Sigma, St. Louis, MO) 1:50, monoclonal antibody to myosin heavy chain (GeneTex, USA) 1:50, rabbit antibody to titin (Prof. S. Labeit, Germany) 1:50 and monoclonal antibody to titin's PEVK region (Prof. S. Labeit, Germany) 1:50. The β-tubulin antibody is a monoclonal antibody conjugated to Cy3 and was diluted 1:100 (Sigma, St. Louis, MO). The diluted antibodies were

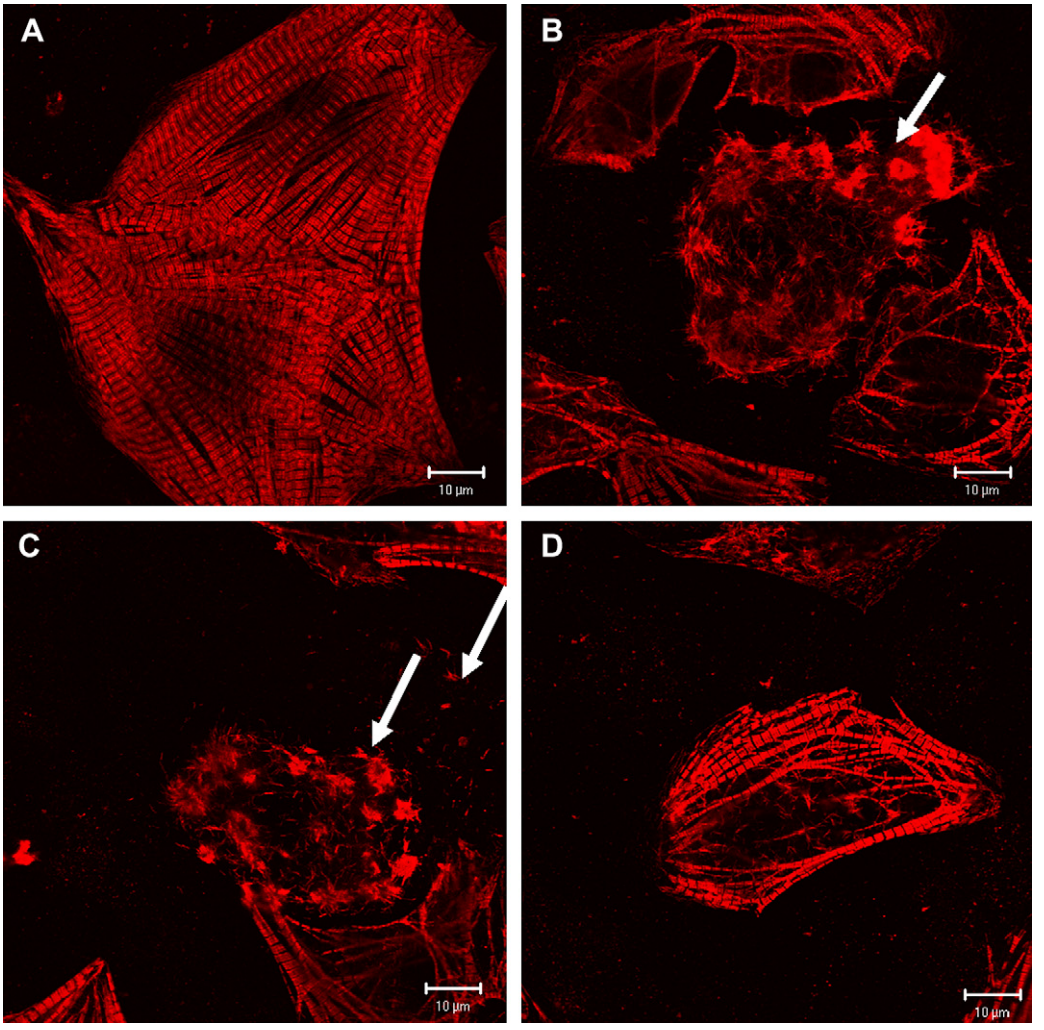

Fig. 1. Immunofluorescent staining of myosin heavy chain in RNCM cells. A: Control rat neonatal cardiomyocytes, B–D: rat neonatal cardiomyocytes treated with 200 μM pavetamine for 48 h.

added and incubation was carried out for 60 min in a humidified chamber at 37 °C. The cells were then washed three times with PBS for 5 min and the secondary antibody conjugates diluted, and added. The secondary antibodies comprised either goat anti-rabbit IgG-FITC conjugate (Sigma, St. Louis, MO) or sheep anti-mouse-Cy3 conjugate (Sigma, St. Louis, MO), each at a concentration of 20 μg/ml. Cells were incubated at 37 °C for 60 min. The PBS washings were repeated and cell nuclei were stained with 1 μg/ml DAPI for 15 min in a humidified chamber at 37 °C. The cells were then washed twice for 5 min with PBS.

2.5. Staining of F-actin cytoskeleton

After pavetamine exposure for 48 h, the F-actin of RNCM cells was stained with phalloidin-FITC (Sigma, cat no: P5282, St. Louis, MO). Briefly, the cells were washed with PBS for 5 min, followed by fixing with 100% ice cold acetone at −20 °C for 10 min. The cells were then washed twice with PBS for 5 min, incubated with diluted phalloidin-FITC (1 μg/ml in PBS) for 30 min at 37 °C and washed twice with PBS for 5 min. The nuclei were stained with DAPI at a concentration of 1.3 μg/ml for 15 min at 37 °C and washed twice with PBS for 5 min.

2.6. Fluorescence microscopy

After staining and washing, the coverslips were mounted on microscope glass slides using ProLong Gold antifade mounting solution (Invitrogen, cat no: P36930, Eugene, Oregon, USA). Fluorescence imaging was performed using a confocal laser scanning microscope, model ZEISS LSM 510 (Jena, Germany).

2.7. Electron microscopy

Primary rat neonatal cardiomyocytes were prepared for TEM using standard procedures. The TEM studies were conducted after exposure of RNCM to 200 μM pavetamine for 48 h. The cells were fixed in 2.5% glutaraldehyde in Millonig's buffer for 5 min before scraping the cells off the bottom of the flask, removing cells and fixative from flask into an Eppendorf tube and additional fixing for another hour. The cells were post-fixed in 1% osmium tetroxide in Millonig's buffer, washed in buffer and then dehydrated through a series of graded alcohols, infiltrated with a mixture of propylene oxide and an epoxy resin and finally embedded in absolute resin at 60 °C. The cells were pelleted after each step by centrifugation at 3000 rpm for 3 min. After curing overnight ultra-thin sections were prepared and stained with lead citrate and uranyl acetate and viewed in a Philips CM10 transmission electron microscope operated at 80 kV.

3. Results

The myosin of control RNCM, visualized with the monoclonal antibody to cardiac MHC, was highly ordered in a striated pattern with intense red staining that represented the A band (Fig. 1A). The shape of the cells appeared

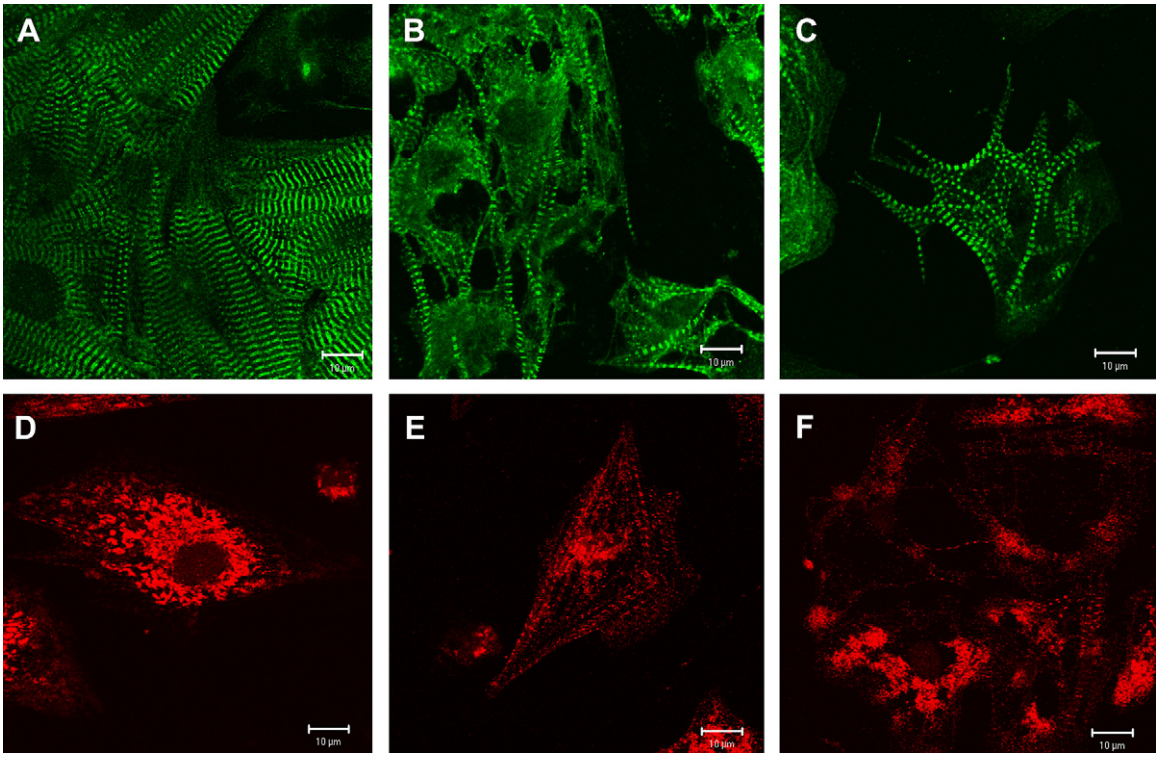

Fig. 2. Immunofluorescent staining of titin in RNCM cells. A: Control rat neonatal cardiomyocytes, B–C: rat neonatal cardiomocytes treated with 200 μM for 48 h, D: control rat neonatal cardiomyocytes stained with an antibody to the PEVK region of titin, E–F: rat cardiomyocytes exposed to 200 μM pavetamine for 48 h and stained with an antibody to the PEVK region of titin.

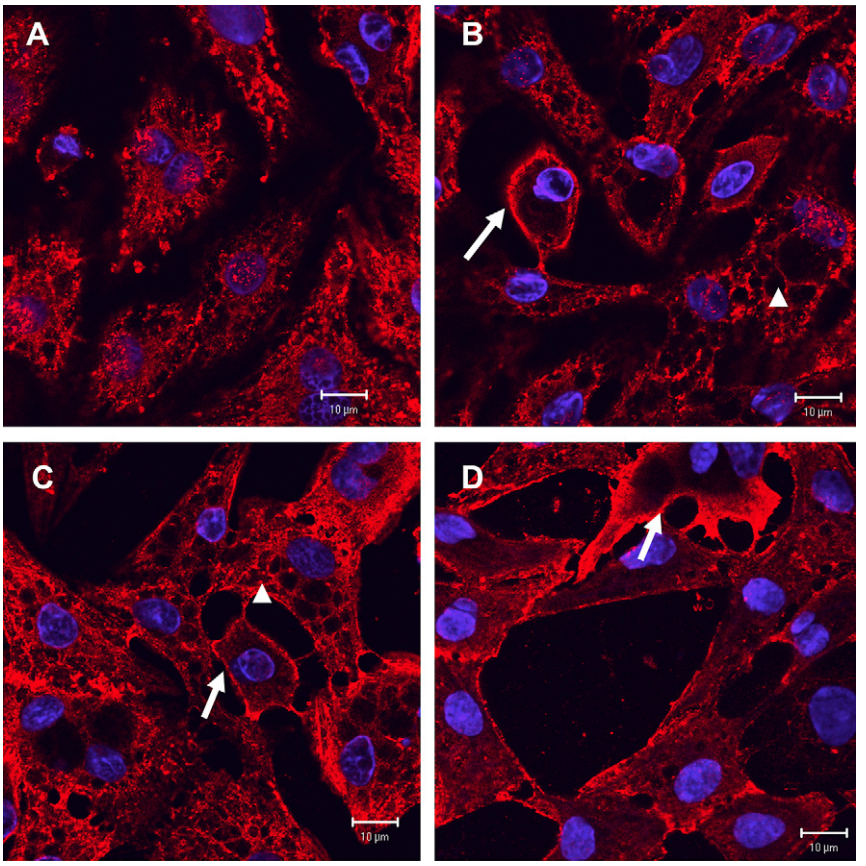

Fig. 3. Immunostaining of sarcomeric alpha-actin (red) in RNCM. The nuclei were stained with DAPI (blue). A: Control cells, B–D: Cells treated with 200 µM pavetamine for 48 h. Arrow: marginization of alpha-actin, arrow head: vacuoles.

star-like. Cells exposed to pavetamine for 48 h had disassembled sarcomeres (Fig. 1B–D). The striated pattern was lost and degraded clumps of myosin were visible (Fig. 1 B and C, see arrows). Staining of titin in control cells with the polyclonal antibody, had a similar striated pattern and organization as the myosin of control cells (Fig. 2A). After exposing the RNCM to pavetamine for 48 h, the cells lost their shape and titin became degraded, and lost its striated pattern (Fig. 2B–C). The PEVK region of titin in control cells was clustered around the nuclei, as revealed by staining the cells with a monoclonal antibody to titin's PEVK region (Fig. 2D). However, the PEVK region of the exposed cells was spread throughout the cells (Fig. 2E–F). Sarcomeric alpha-actin in control RNCM was also clustered around the nuclei (Fig. 3A). Stained alpha-actin of RNCM cells exposed to pavetamine had altered morphology, when compared to the control cells. Margination of alpha-actin occurred in pavetamine-exposed cells (Fig. 3B–D, see arrows) and vacuoles were present in some of the exposed cells (Fig. 3B and C, see arrow heads). Double-labeling of untreated RNCM cells revealed discrete red (myosin heavy chain) and green (titin) staining in a striated pattern (Fig. 4A). Cells exposed to pavetamine showed less intense, or no staining for myosin heavy chain (red) (Fig. 4B–F). Some cells lost their striated appearance and became rounded (Fig. 4C). In Fig. 4D, titin appeared at the periphery of the cell with a fragmented nucleus (arrows). Some of the exposed cells had lost the myosin (red) and titin (green), leaving only the nuclei visible (Fig. 4E, see arrows). Clumps of degraded titin (green) can be seen in exposed cells (Fig. 4F, see arrow). Staining of F-actin revealed that exposed cells had less intense fluorescent staining (Fig. 5B) than untreated cells (Fig. 5A). Some of the exposed cells were round with intense fluorescence, possibly representing degraded F-actin (Fig. 5B, see arrow). The cytoskeleton of control cells, labeled for F-actin (green) and β-tubulin (red), had a filamentous network (Fig. 5C and D), while the F-actin of exposed cells was disrupted or completely absent (Fig. 5E–H). The arrow in Fig. 5E indicates a cell with intact β-tubulin, but absent F-actin. The mesh-like network of F-actin, as can be seen in Fig. 5A and B, disappeared and the F-actin bundles became parallel in orientation (Fig. 5F and G). In Fig. 5H, the cell indicated with an arrow, had an abnormal β-tubulin appearance ascribed to the disappearance of the tubulin network. This was, however, not a typical feature of most of the exposed cells' tubulin network. Ultrastructurally, the sarcomeres of untreated cardiomyocytes were neatly organized with electron dense Z-lines (Fig. 6A). RNCM exposed to pavetamine (Fig. 6B–D) had disorganized sarcomeres and damaged mitochondria.

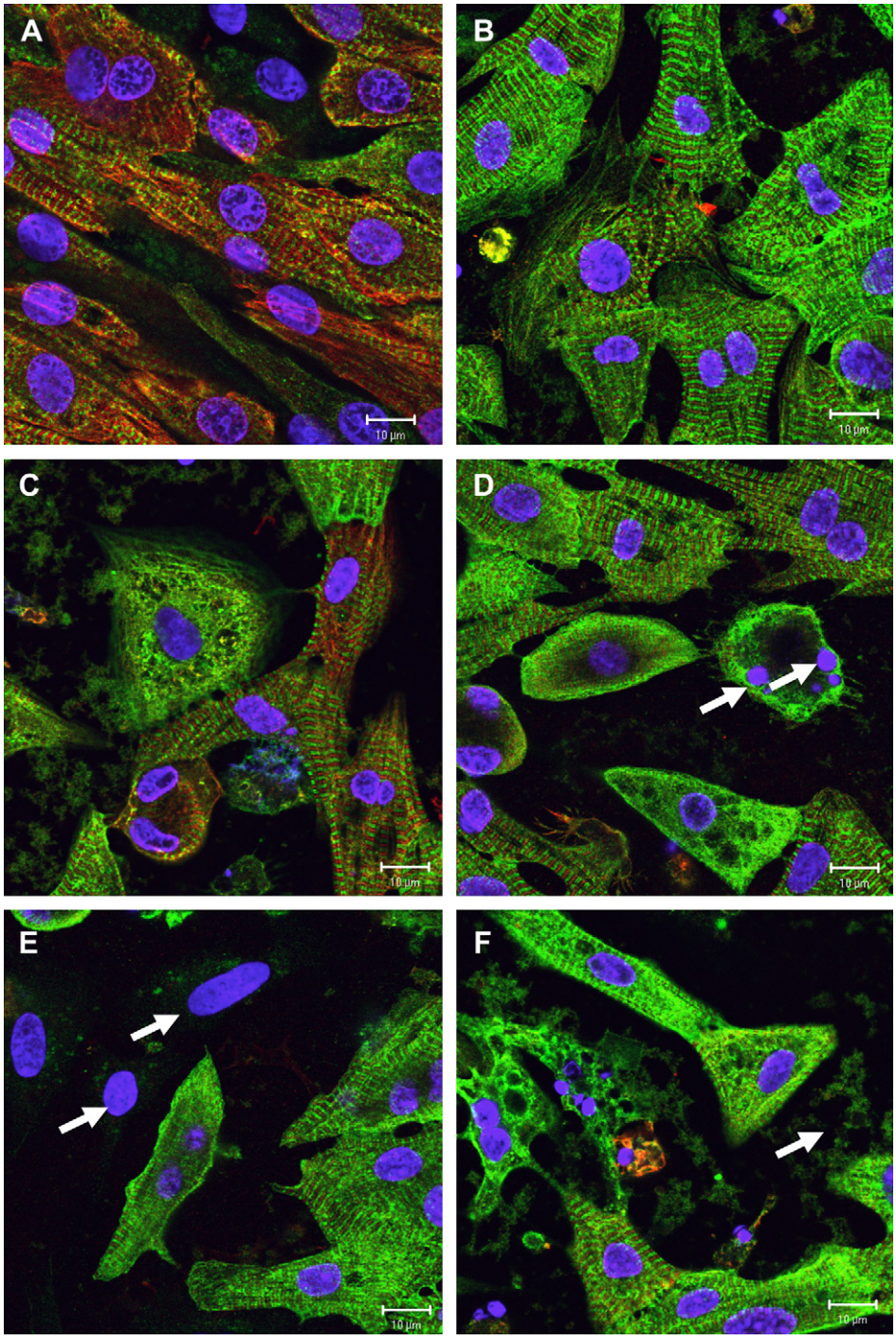

Fig. 4. Double-immunolabeling of RNCM cells with myosin heavy chain (red) and titin antibodies (green). The nuclei were stained with DAPI (blue) A: Control cells, B–F: Cells treated with 200 µM pavetamine for 48 h.

In Fig. 6B, the Z-lines were still visible, but were extended, with some of the myofibrils detached from the Z-line. In Fig. 6C and D, there were few Z-lines present and the myofibrils were scattered in the cells. The mitochondria demonstrated in Fig. 6D were enlarged, had an abnormal shape and the cristae were swollen.

4. Discussion

This study aimed to immunolabel the contractile cardiac proteins, actin, myosin, and titin, as well as the cytoskeleton proteins (F-actin and β-tubulin) in RNCM treated with pavetamine. The most profound effect induced by

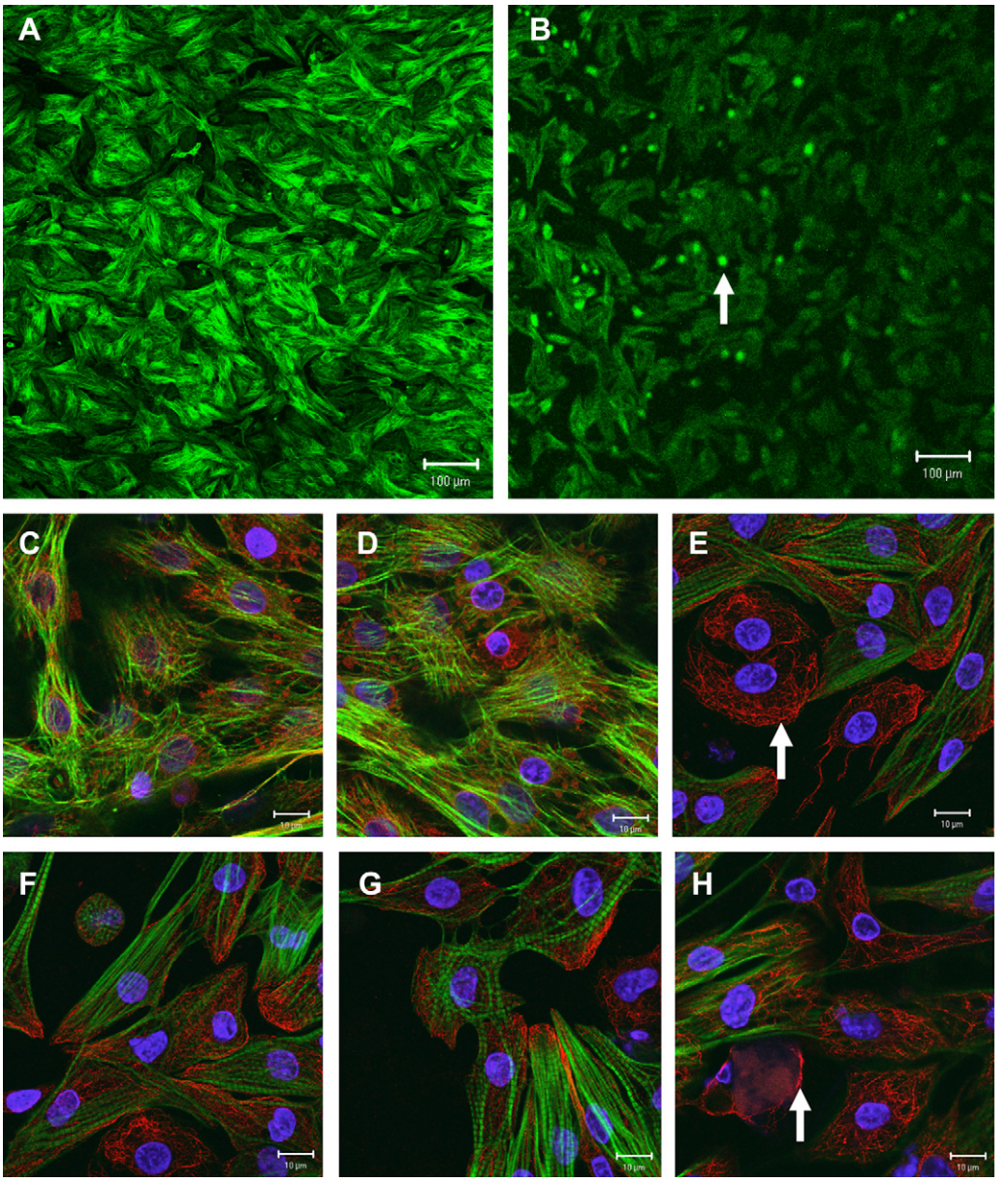

Fig. 5. Double-immunofluorescent staining of RNCM cells for F-actin (green) and β-tubulin (red). A: Control cells stained with phalloidin-FITC for F-actin, B: Cells exposed with 200 μM pavetamine for 48 h and stained with phalloidin-FITC for F-actin, C–D: control cells stained for F-actin and tubulin, E–H: Cells exposed to 200 μM pavetamine for 48 h and stained for F-actin and tubulin.

pavetamine was myosin degradation. Double-immunolabeling showed that myosin was degraded first, then titin. Of note was the disappearance of the red staining (myosin) from most of the cells, while the majority of the cells still exhibited green fluorescence (titin), albeit with altered morphology. Some of the cells had lost both myosin and titin, and only the nuclei, stained with DAPI, were visible. These findings corroborated earlier ultrastructural reports (Schutte et al., 1984; Schultz et al., 2001; Prozesky et al., 2005). TEM studies of the myocardium of sheep exposed to gousiekte-inducing plants showed a reduction in the number of myofilaments (Schutte et al., 1984). These authors speculated that it was especially myosin that was reduced. Changes to titin isoforms have been reported in human hearts with end-stage, dilated cardiomyopathy (Neagoe et al., 2002).

In this study, the PEVK region of exposed RNCM showed alterations when compared to the controls. Sarcomeric alpha-actin also showed abnormalities such as margination of actin and the appearance of vacuoles. Prozesky et al. (2005) also performed TEM studies in hearts of gousiekte sheep and concluded that the degenerative fibrils had a frayed appearance with a preferential loss of thin (actin) filaments.

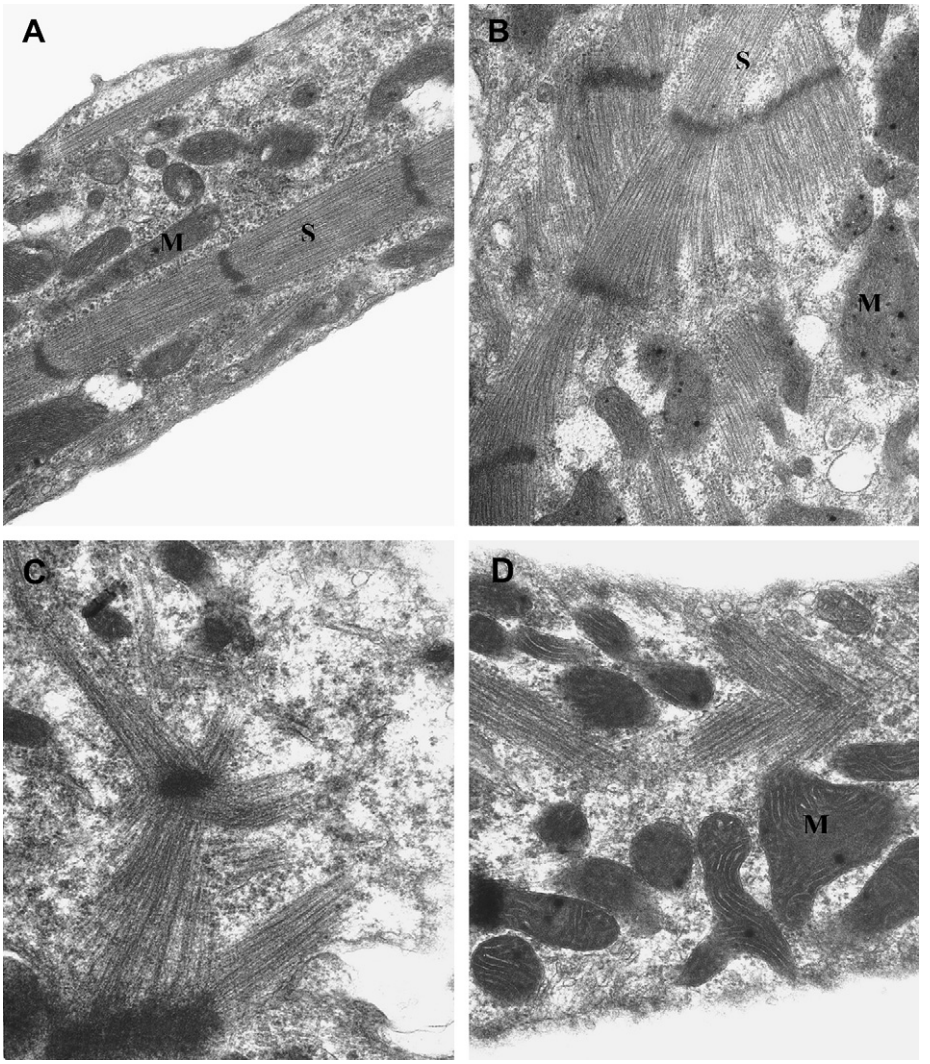

Fig. 6. Transmission electron micrographs of rat neonatal cardiomyocytes. A: Untreated cells, B–D: Cells treated with 200 μM pavetamine for 48 h. S: sarcomere, M: mitochondria.

The cytoskeleton proteins that were stained, also demonstrated an altered morphology. F-actin of exposed cardiomyocytes lost its filamentous structure and became parallel in orientation in some cells, and was absent in others. β-tubulin was slightly altered in exposed cardiomyocytes. Sarcomeric and cytoskeleton disarrangement have also been described in human dilated cardiomyopathy. In addition to disorganization of myosin and actin, titin was reduced and disorganized, or almost completely absent in diseased cardiac tissue (Hein et al., 1994; Morano et al., 1994).

The current study revealed that the two major contractile proteins (myosin and actin), titin, (an abundant intra-sarcomeric protein) and the cytoskeleton protein, F-actin, underwent profound changes to their architecture in RNCM exposed to pavetamine. The altered morphology of myosin and titin might be as a consequence of protease degradation. No activation of the proteasome was observed with the three substrates tested (caspase-like, trypsin-like and chymotrypsin-like) in H9c2 cells exposed to pavetamine (results not shown). On the other hand, the lysosomal enzymes hexosaminidase and acid phosphatase exhibited increased activities in treated cells. The degradation of the myofibres could thus be a result of increased lysosomal membrane permeability. Future studies will include determination of the activities of calpain and cathepsin D, to confirm that these proteases are responsible for the degradation of the contractile and F-actin cytoskeleton proteins in cells treated with pavetamine.

In conclusion, pavetamine caused degradation of a number of cardiac proteins that are important in cardiac contractility and cell signaling. Damaged myosin and titin would reduce the contractility of the ruminant heart in gousiekte animals. Disorganization of F-actin may cause reduced, or complete inhibition of, protein synthesis. This is corroborated by results of a previous experiment in which Schultz et al. (2001) reported inhibition of protein synthesis in the rat heart.

Acknowledgements

We would like to thank Mr. A. Hall (Laboratory for Microscopy and Microanalysis, University of Pretoria) for the CLSM work. We would also like to thank Ms E. van Wilpe and Ms. L. du Plessis from the Electron microscopy unit, University of Pretoria. This investigation was funded by the North-West Department of Agriculture, Conservation, Environment and Tourism and the Gauteng Department of Agriculture, Conservation and Environment (GDACE), as well as by the Department of Paraclinical Sciences, University of Pretoria.

Conflict of interest

The authors have no conflict of interest.

Ethical statement

The authors declare that this work has not been published.

References

Bartoli, M., Richard, I., 2005. Calpains in muscle wasting. Int. J. Biochem. Cell Biol. 37, 2115–2133.
Bechet, D., Tassa, A., Taillandier, D., Combaret, L., Attaix, D., 2005. Lysosomal proteolysis in skeletal muscle. Int. J. Biochem. Cell Biol. 37, 2098–2114.
Cox, L., Umans, L., Cornelis, F., Huylebroeck, D., Zwijsen, A., 2008. A broken heart: a stretch too far. An overview of mouse models with mutations in stretch-sensor components. Int. J. Cardiol. 131, 33–44.
Ellis, C.E., Naicker, D., Basson, K.M., Botha, C.J., Meintjes, R.A., Schultz, R.A., 2010. Cytotoxicity and ultrastructural changes in H9c2(2-1) cells treated with pavetamine, a novel polyamine. Toxicon 55, 12–19.
Engelbrecht, A.-M., Niesler, C., Page, C., Lochner, A., 2004. p38 and JNK have distinct regulating functions in the development of apoptosis during simulated ischemia and reperfusion of neonatal cardiomyocytes. Basic Res. Cardiol. 99, 338--350.
Fielitz, J., Kim, M.-S., Shelton, J.M., Latif, S., Spencer, J.A., Glass, D.J., Richardson, J.A., Bassel-Duby, R., Olson, E.N., 2007. Myosin accumulation and striated muscle myopathy result from the loss of muscle RING finger 1 and 3. J. Clin. Invest. 117, 2486–2495.
Fourie, N., Erasmus, G.L., Schultz, R.A., Prozesky, L., 1995. Isolation of the toxin responsible for gousiekte, a plant-induced cardiomyopathy of ruminants in southern Africa. Onderstepoort J. Vet. Res. 62, 77–87.
Galvez, A.S., Diwan, A., Odley, A.M., Hahn, H.S., Osinska, H., Melemdez, J.G., Robbins, J., Lynch, R.A., Marreez, Y., Dorn II, G.W., 2007. Cardiomyocyte degeneration with calpain deficiency reveals a critical role in protein homeostasis. Circ. Res. 100, 1071–1078.
Granzier, H., Labeit, S., 2002. Cardiac titin: an adjustable multi-functional spring. J. Physiol. 541, 335–342.
Hay, L., Pipedi, M., Schutte, P.J., Turner, M.L., Smith, K.A., 2001. The effect of *Pavatta harborii* extracts on cardiac function in rats. S. Afr. J. Sci. 97, 481–484.
Hay, L., Schultz, R.A., Schutte, P.J., 2008. Cardiotoxic effects of pavetamine extracted from *Pavetta harborii* in the rat. Onderstepoort J. Vet. Res. 75, 249–253.
Hein, S., Scholz, D., Fujitani, N., Rennollet, H., Brand, T., Friedl, A., Schaper, J., 1994. Altered expression of titin and contractile proteins in failing human myocardium. J. Mol. Cell. Cardiol. 26, 1291–1306.
Hein, S., Kostin, S., Heling, A., Maeno, Y., Schaper, J., 2000. The role of the cytoskeleton in heart failure. Cardiovasc. Res. 45, 273–278.
Huxley, A.F., Peachey, A.L., 1961. The maximum length for contraction in vertebrate striated muscle. J. Physiol. 156, 150–165.
Ke, L., Qi, X.Y., Dijkhuis, A.J., Chartier, D., Nattel, S., Henning, R.H., Kampinga, H.H., Brundel, B.J., 2008. Calpain mediates cardiac troponin degradation and contractile dysfunction in atrial fibrillation. J. Mol. Cell. Cardiol. 45, 685–693.
Kellerman, T.S., Coetzer, J.A.W., Naudé, T.W., Botha, C.J., 2005. Plant Poisonings and Mycotoxicoses of Livestock in Southern Africa. Oxford University Press, Southern Africa, pp. 154–164.
Klionsky, D.J., Emr, S.D., 2000. Autophagy as a regulated pathway of cellular degradation. Science 290, 1717–1720.
Koohmaraie, M., 1992. Ovine skeleton muscle multicatalytic proteinase complex (proteasome): purification, characterization, and comparison of its effects on myofibrils with mu-calpains. J. Anim. Sci. 70, 3697–3708.
Krüger, M., Linke, W.A., 2009. Titin-based mechanical signalling in normal and failing myocardium. J. Mol. Cell. Cardiol. 46, 490–498.
LeWinter, M.M., Wu, Y., Labeit, S., Granzier, H., 2007. Cardiac titin: structure, function and role in disease. Clin. Chim. Acta 375, 1–9.
Lim, C.C., Zuppinger, C., Guo, X., Kuster, G.M., Helmes, M., Eppenberger, H.M., Suter, T.M., Liao, R., Sawyer, D.B., 2004. Anthracyclines induce calpain-dependent titin proteolysis and necrosis in cardiomyocytes. J. Biol. Chem. 279, 8290–8299.
Miralles, F., Visa, N., 2006. Actin in transcription and transcription regulation. Curr. Opin. Cell Biol. 18, 261–266.
Morano, I., Hädicke, K., Grom, S., Koch, A., Schwinger, R.H., Böhm, M., Bartel, S., Erdmann, E., Krause, E.G., 1994. Titin, myosin light chains and C-protein in the developing and failing human heart. J. Mol. Cell. Cardiol. 26, 361–368.
Neagoe, C., Kulke, M., del Monte, F., Gwathmey, J.K., de Tombe, P.P., Hajjar, R.J., Linke, W.A., 2002. Titin isoform switch in ischemic human heart disease. Circulation 106, 1333–1341.
Pretorius, P.J., Terblanche, M., 1967. A preliminary study on the symptomatology and cardiodynamics of gousiekte in sheep and goats. J. S Afr. Vet. Med. Assoc. 38, 29–52.
Prozesky, L., Bastianello, S.S., Fourie, N., Schultz, R.A., 2005. A study of the pathology and pathogenesis of the myocardial lesions in gousiekte, a plant-induced cardiotoxicosis of ruminants. Onderstepoort J. Vet. Res. 72, 219–230.
Razeghi, P., Volpini, K.C., Wang, M.-E., Youker, k.A., Stepkowski, S., Taegtmeyer, H., 2007. Mechanical unloading of the heart activates the calpain system. J. Mol. Cell. Cardiol. 42, 449--452.
Schultz, R.A., Fourie, N., Basson, K.M., Labuschagne, L., Prozesky, L., 2001. Effect of pavetamine on protein synthesis in rat tissue. Onderstepoort J. Vet. Res. 68, 325–330.
Schutte, P.J., Els, H.J., Booyens, J., 1984. Ultrastructure of myocardial cells in sheep with congestive heart failure induced by *Pachystigma pygmaeum*. S. Afr. J. Sci. 80, 378–380.
Theiler, A., Du Toit, P.J., Mitchell, D.T., 1923. Gousiekte in sheep. In: 9th and 10th Reports of the Director of Veterinary Education and Research, Onderstepoort. The Government Printing and Stationary Office, Pretoria, pp. 1–106.
Vartiainen, M.K., Guettler, S., Larijani, B., Treisman, R., 2007. Nuclear actin regulates dynamic subcellular localization and activity of the SFR cofactor MAL. Science 316, 1749–1752.
Wang, X., Su, H., Ranek, M.J., 2008. Protein quality control and degradation in cardiomyocytes. J. Mol. Cell. Cardiol. 45, 11–27.
Willis, M.S., Schisler, J.C., Portbury, A.L., Patterson, C., 2009. Build it up-tear it down: protein quality control in the cardiac sarcomere. Cardiovasc. Res. 81, 439–448.
Wu, Y., Bell, S.P., Trombitas, K., Witt, C.C., Labeit, S., LeWinter, M.M., Granzier, H., 2002. Changes in titin isoform expression in pacing-induced cardiac failure give rise to increased passive muscle stiffness. Circulation 106, 1384–1389.
Ye, J., Zhao, J., Hoffmann-Rohrer, U., Grummt, I., 2008. Nuclear myosin I acts in concert with polymeric actin to drive polymerase I transcription. Genes Dev. 22, 322–330.